frontiers | Research Topics

Neuroimaging in early intervention in psychiatry

Edited by
João Valente Duarte, Sandra Vieira and Nuno Madeira

Published in
Frontiers in Psychiatry

ISSN 1664-8714
ISBN 978-2-8325-2476-3
DOI 10.3389/978-2-8325-2476-3

About Frontiers

Frontiers is more than just an open access publisher of scholarly articles: it is a pioneering approach to the world of academia, radically improving the way scholarly research is managed. The grand vision of Frontiers is a world where all people have an equal opportunity to seek, share and generate knowledge. Frontiers provides immediate and permanent online open access to all its publications, but this alone is not enough to realize our grand goals.

Frontiers journal series

The Frontiers journal series is a multi-tier and interdisciplinary set of open-access, online journals, promising a paradigm shift from the current review, selection and dissemination processes in academic publishing. All Frontiers journals are driven by researchers for researchers; therefore, they constitute a service to the scholarly community. At the same time, the *Frontiers journal series* operates on a revolutionary invention, the tiered publishing system, initially addressing specific communities of scholars, and gradually climbing up to broader public understanding, thus serving the interests of the lay society, too.

Dedication to quality

Each Frontiers article is a landmark of the highest quality, thanks to genuinely collaborative interactions between authors and review editors, who include some of the world's best academicians. Research must be certified by peers before entering a stream of knowledge that may eventually reach the public - and shape society; therefore, Frontiers only applies the most rigorous and unbiased reviews. Frontiers revolutionizes research publishing by freely delivering the most outstanding research, evaluated with no bias from both the academic and social point of view. By applying the most advanced information technologies, Frontiers is catapulting scholarly publishing into a new generation.

What are Frontiers Research Topics?

Frontiers Research Topics are very popular trademarks of the *Frontiers journals series*: they are collections of at least ten articles, all centered on a particular subject. With their unique mix of varied contributions from Original Research to Review Articles, Frontiers Research Topics unify the most influential researchers, the latest key findings and historical advances in a hot research area.

Find out more on how to host your own Frontiers Research Topic or contribute to one as an author by contacting the Frontiers editorial office: frontiersin.org/about/contact

Neuroimaging in early intervention in psychiatry

Topic editors

João Valente Duarte — University of Coimbra, Portugal

Sandra Vieira — Institute of Psychiatry, Psychology and Neuroscience, King's College London, United Kingdom

Nuno Madeira — University of Coimbra, Portugal

Citation

Duarte, J. V., Vieira, S., Madeira, N., eds. (2023). *Neuroimaging in early intervention in psychiatry*. Lausanne: Frontiers Media SA. doi: 10.3389/978-2-8325-2476-3

Table of contents

05 Editorial: Neuroimaging in early intervention in psychiatry
João Valente Duarte, Sandra Vieira and Nuno Madeira

07 Aberrant Neural Response to Social Exclusion Without Significantly Greater Distress in Youth With Bipolar Disorder: Preliminary Findings
Donna J. Roybal, Victoria E. Cosgrove, Ryan Kelley, Rachel Smallwood Shoukry, Rose Marie Larios, Blake Novy, Kiki D. Chang and Amy S. Garrett

17 Thalamic Shape Abnormalities Differentially Relate to Cognitive Performance in Early-Onset and Adult-Onset Schizophrenia
Derin Cobia, Chaz Rich, Matthew J. Smith, Pedro Engel Gonzalez, Will Cronenwett, John G. Csernansky and Lei Wang

27 Abnormal Brain Structure Morphology in Early-Onset Schizophrenia
Jia Cai, Wei Wei, Liansheng Zhao, Mingli Li, Xiaojing Li, Sugai Liang, Wei Deng, Xiang Dong Du, Qiang Wang, Wan-jun Guo, Xiaohong Ma, Pak C. Sham and Tao Li

37 The effect of antipsychotics on glutamate levels in the anterior cingulate cortex and clinical response: A ^{1}H-MRS study in first-episode psychosis patients
Uzma Zahid, Robert A. McCutcheon, Faith Borgan, Sameer Jauhar, Fiona Pepper, Matthew M. Nour, Maria Rogdaki, Martin Osugo, Graham K. Murray, Pamela Hathway, Robin M. Murray and Oliver D. Howes

49 The alternations of nucleus accumbent in schizophrenia patients with auditory verbal hallucinations during low-frequency rTMS treatment
Yuanjun Xie, Yun Cai, Muzhen Guan, Zhongheng Wang, Zhujing Ma, Peng Fang and Huaning Wang

60 Brain morphometric abnormalities and their associations with affective symptoms in males with methamphetamine use disorder during abstinence
Xinyue Hu, Ping Jiang, Yingxue Gao, Jiayu Sun, Xiaobo Zhou, Lianqing Zhang, Hui Qiu, Hailong Li, Lingxiao Cao, Jing Liu, Qiyong Gong and Xiaoqi Huang

69 Heschl's gyrus duplication pattern and clinical characteristics in borderline personality disorder: A preliminary study
Tsutomu Takahashi, Daiki Sasabayashi, Dennis Velakoulis, Michio Suzuki, Patrick D. McGorry, Christos Pantelis and Andrew M. Chanen

77 Gross anatomical features of the insular cortex in schizophrenia and schizotypal personality disorder: Potential relationships with vulnerability, illness stages, and clinical subtypes

Tsutomu Takahashi, Daiki Sasabayashi, Yoichiro Takayanagi, Atsushi Furuichi, Haruko Kobayashi, Yusuke Yuasa, Kyo Noguchi and Michio Suzuki

88 Prediction of transition to psychosis from an at-risk mental state using structural neuroimaging, genetic, and environmental data

Vânia Tavares, Evangelos Vassos, Andre Marquand, James Stone, Isabel Valli, Gareth J. Barker, Hugo Ferreira and Diana Prata

frontiers | Frontiers in Psychiatry

TYPE Editorial
PUBLISHED 05 May 2023
DOI 10.3389/fpsyt.2023.1196886

OPEN ACCESS

EDITED AND REVIEWED BY
Stefan Borgwardt,
University of Lübeck, Germany

*CORRESPONDENCE
João Valente Duarte
✉ joao.v.duarte@fmed.uc.pt

RECEIVED 30 March 2023
ACCEPTED 17 April 2023
PUBLISHED 05 May 2023

CITATION
Duarte JV, Vieira S and Madeira N (2023) Editorial: Neuroimaging in early intervention in psychiatry. *Front. Psychiatry* 14:1196886. doi: 10.3389/fpsyt.2023.1196886

Editorial: Neuroimaging in early intervention in psychiatry

João Valente Duarte[1,2]*, Sandra Vieira[3,4,5] and Nuno Madeira[1,6,7]

[1]Coimbra Institute for Biomedical Imaging and Translational Research (CIBIT), Institute for Nuclear Sciences Applied to Health, University of Coimbra, Coimbra, Portugal, [2]Faculty of Medicine, University of Coimbra, Coimbra, Portugal, [3]Department of Psychosis Studies, Institute of Psychiatry, Psychology & Neuroscience, King's College London, London, United Kingdom, [4]Center for Research in Neuropsychology and Cognitive Behavioral Intervention, Faculty of Psychology and Educational Sciences, University of Coimbra, Coimbra, Portugal, [5]Connectomics Lab, Department of Radiology, Lausanne University Hospital and University of Lausanne (CHUV-UNIL), Lausanne, Switzerland, [6]Institute of Psychological Medicine, Faculty of Medicine, University of Coimbra, Coimbra, Portugal, [7]Department of Psychiatry, Centro Hospitalar e Universitário de Coimbra (CHUC), Coimbra, Portugal

KEYWORDS

neuroimaging, mental health, diagnosis, early intervention, prognosis

Editorial on the Research Topic
Neuroimaging in early intervention in psychiatry

In Psychiatry, understanding disease progression and unpredictable treatment response are still a significant clinical challenge, leading to fruitless therapeutic trials. There is an urgent need to develop biomarkers capable of assisting with real world clinical care and its unmet needs (1). In order to prevent chronic disability and promote long-term recovery, there has been a noticeable shift in the past 20 years toward conducting research during the early stages of illness, when there is an opportunity to intervene (2). This Research Topic brings together original psychiatric neuroimaging studies aimed at investigating possible biomarkers that can assist clinical the decision-making process related to diagnosis, prognosis, and monitoring of individuals who exhibit initial symptoms of an illness or even before the onset of the illness.

Taken collectively, this Research Topic includes a wide range of interesting populations, analytical methods and imaging features, including machine learning to predict the transition of individuals at risk of psychosis; MRI-derived anatomical features of the brain in the early stage of schizophrenia, borderline personality disorder patients with minimal treatment exposure, and individuals with methamphetamine use disorder; the effect of treatment with TMS in functional and structural characteristic patterns in schizophrenia; the effect of antipsychotic treatment in the glutamatergic function in people with first-episode psychosis; and the neural correlates of social exclusion in young individuals with bipolar disorder and their impact on functionality.

After utilizing a rigorous predictive modeling approach, Tavares et al. present compelling evidence that urges a re-evaluation of the predictive potential of structural MRI and genome-wide in identifying the risk of transitioning to psychosis among high-risk individuals. Results show that none of the modalities alone could predict psychosis onset statistically better than chance. However, the authors did not train a multimodal classification model, thus the multivariate nature of neuroimaging combined with genetic and environmental data was not explored, yielding further investigation.

Interestingly, studies after illness onset show anatomical variations that correlate with positive symptomatology, suggesting that such abnormalities may not yet be well-established at the individual level in high-risk individuals. For example, Takahashi, Sasabayashi, Takayanagi et al. showed that altered insular morphology was associated with positive symptoms in early stages and clinical subtypes of schizophrenia.

In addition, Cai et al. observed a reduction in gray matter volume in the middle temporal gyrus on both sides and a decrease in cortical thickness in multiple brain regions in individuals with early-onset schizophrenia. In this study, early-onset schizophrenia with genetic risk (first-, second-, or third-degree relatives diagnosed with schizophrenia) showed a different brain structure morphology compared to patients without genetic risk, which indicates that atypical brain structure, particularly in the frontal and temporal lobes, may play a significant role in the pathophysiology of early-onset schizophrenia. This is corroborated by the study of Cobia et al. as it revealed that thalamic shape irregularities were a notable characteristic in both early-onset and late-onset schizophrenia, although more pronounced in the latter group. Additionally, each group displayed distinct brain-behavior patterns (Cobia et al.). Furthermore, the authors proposed that the enduring presence of these irregularities in adult patients with early-onset schizophrenia could signify indicators of disturbed neurodevelopment that are specifically linked to clinical and cognitive aspects of the illness.

Takahashi, Sasabayashi, Velakoulis et al. conducted a second study on this topic, suggesting that neurodevelopmental pathology associated with Heschl's gyrus duplication might be implicated in the neurobiology of early borderline personality disorder patients with minimal treatment exposure, especially for emotional and behavioral control. Interestingly, alterations of gyrification, which are influenced by early neurodevelopment, are further suggested to play a pivotal role in developing mental disorders. Hu et al. showed hypergyrification across multiple brain regions in individuals with methamphetamine use disorder, which was furthermore positively associated with depression and anxiety symptom severity.

While brain structural characteristics in patients with psychiatric illness might constitute biomarkers for early diagnosis, anatomical and functional alterations could also identify target regions for neuromodulation. In one MRI study presented in this Research Topic, Xie et al. investigated the gray matter volume and the seed-based resting-state functional connectivity profile of the nucleus accumbens (Nacc) in individuals with schizophrenia and auditory verbal hallucinations throughout low-frequency repetitive TMS treatment. While the volumetric changes of the NAcc were not impacted, the anomalous functional connectivity patterns of the NAcc in patients before treatment were rectified or reversed after receiving low-frequency repetitive TMS treatment. These FC alterations were linked to symptom and neurocognitive enhancements, indicating that they could serve as a clinical effect biomarker for this treatment approach in individuals with schizophrenia. In a functional study, Roybal et al. investigated brain function with fMRI in youth with bipolar disorder while performing a social exclusion task. Authors found that patients exhibited greater activation in the left fusiform gyrus and significantly decreased functional connectivity of this region with the posterior cingulate/precuneus during social exclusion. Despite having a small sample size, this study proposes that young people with bipolar disorder handle social exclusion by prioritizing basic visual details, while individuals without the disorder rely on prior experiences to comprehend present social interactions. This variance may contribute to the social cognitive challenges faced by those with bipolar disorder, exacerbating symptoms of anxiety and mood disorders.

Lastly, Zahid et al. employed MR spectroscopy in a longitudinal study to examine the impact of antipsychotic therapy on glutamatergic levels in the anterior cingulate cortex (ACC) and to determine whether there was a connection between initial glutamatergic levels and clinical reaction following antipsychotic therapy in individuals experiencing their first episode of psychosis. The authors found no significant impact of antipsychotic treatment on glutamate and glutamate/glutamine levels in the ACC and no correlation between therapeutic outcomes and glutamatergic levels measured prior to antipsychotic administration, indicating null findings. As per this study, it appears that response to treatment is unlikely to be connected to baseline glutamatergic metabolites before antipsychotic therapy, highlighting the need for further investigation of clinically useful biomarkers.

Author contributions

All authors listed have made a substantial, direct, and intellectual contribution to the work and approved it for publication.

Acknowledgments

The authors thank their institutions for providing the time to edit this Research Topic and editorial.

Conflict of interest

The authors declare that the research was conducted in the absence of any commercial or financial relationships that could be construed as a potential conflict of interest.

Publisher's note

References

1. Etkin A. A reckoning and research agenda for neuroimaging in psychiatry. *Am J Psychiatry*. (2019) 176:507–511. doi: 10.1176/appi.ajp.2019.19050521

2. Madeira N, Martins R, Duarte JV, Costa GN, Macedo A, Castelo-Branco M. A fundamental distinction in early neural processing of implicit social interpretation in schizophrenia and bipolar disorder. *NeuroImage Clin.* (2021) 32:2836. doi: 10.1016/j.nicl.2021.102836

frontiers | Frontiers in Psychiatry

ORIGINAL RESEARCH
published: 01 April 2022
doi: 10.3389/fpsyt.2022.687052

Aberrant Neural Response to Social Exclusion Without Significantly Greater Distress in Youth With Bipolar Disorder: Preliminary Findings

Donna J. Roybal[1,2,3,4†], Victoria E. Cosgrove[1], Ryan Kelley[2], Rachel Smallwood Shoukry[3], Rose Marie Larios[3,4], Blake Novy[3,4], Kiki D. Chang[1†] and Amy S. Garrett[2,3,4†]*

[1] Division of Child and Adolescent Psychiatry, Department of Psychiatry and Behavioral Sciences, Stanford University School of Medicine, Stanford, CA, United States, [2] Center for Interdisciplinary Brain Sciences Research, Department of Psychiatry and Behavioral Sciences, Stanford University School of Medicine, Stanford, CA, United States, [3] Research Imaging Institute, University of Texas Health Science Center, San Antonio, TX, United States, [4] Department of Psychiatry and Behavioral Sciences, University of Texas Health Science Center, San Antonio, TX, United States

Background: Little is known about the effects of social exclusion on youth with bipolar disorder (BD). Understanding these effects and the functional neural correlates of social exclusion in youth with BD may establish differences from healthy youth and help identify areas of intervention.

Methods: We investigated brain function in 19 youth with BD and 14 age and gender matched healthy control (HC) participants while performing Cyberball, an fMRI social exclusion task. Whole brain activation, region-of-interest, and functional connectivity were compared between groups and examined with behavioral measures.

Results: Compared with the HC group, youth with BD exhibited greater activation in the left fusiform gyrus (FFG) during social exclusion. Functional connectivity between the left FFG and the posterior cingulate/precuneus was significantly greater in the HC compared with the BD group. For the HC group only, age and subjective distress during Cyberball significantly predicted mean FFG activation. No significant differences in distress during social exclusion were found between groups.

Conclusion: Although preliminary due to small sample size, these data suggest that youth with BD process social exclusion in a manner that focuses on basic visual information while healthy youth make use of past experiences to interpret current social encounters. This difference may account for the social cognitive issues experienced by youth with BD, which can lead to more severe anxiety and mood symptoms.

Keywords: bipolar, social exclusion, neuroimaging, anxiety, cyberball

OPEN ACCESS

Edited by:
Jeffrey Robert Strawn, University of Cincinnati, United States

Reviewed by:
Gemma C. Monté-Rubio, University of Barcelona, Spain
Jennifer Barredo, Providence VA Medical Center, United States

****Correspondence:***
Donna J. Roybal
djwdv31@gmail.com

†Present addresses:
Donna J. Roybal, Division of Child and Adolescent Psychiatry, Department of Psychiatry and Behavioral Sciences, University of Texas Health Science Center, San Antonio, TX, United States; Traditions Behavioral Health, Napa, CA, United States
Amy S. Garrett, Division of Child and Adolescent Psychiatry, Department of Psychiatry and Behavioral Sciences, University of Texas Health Science Center, San Antonio, TX, United States
Kiki D. Chang, Private Practitioner, Palo Alto, CA, United States

Specialty section:
This article was submitted to Neuroimaging and Stimulation, a section of the journal Frontiers in Psychiatry

Received: *08 April 2021*
Accepted: *15 February 2022*
Published: *01 April 2022*

Citation:
Roybal DJ, Cosgrove VE, Kelley R, Smallwood Shoukry R, Larios RM, Novy B, Chang KD and Garrett AS (2022) Aberrant Neural Response to Social Exclusion Without Significantly Greater Distress in Youth With Bipolar Disorder: Preliminary Findings. Front. Psychiatry 13:687052. doi: 10.3389/fpsyt.2022.687052

INTRODUCTION

Bipolar disorder (BD) with comorbid anxiety is associated with poorer response to treatment, more severe depression, rapid cycling, substance abuse, and suicide attempts (1–5). Emerging longitudinal evidence suggests that youth at high-risk for BD that develop any mood disorder experience an anxiety disorder as an early antecedent (2, 5, 6). In fact, the risk of a mood disorder

diagnosis was over two times higher in those with an anxiety disorder than those without, with social anxiety disorder and generalized anxiety disorder the most predictive (5). Anxiety is therefore an important symptom in the developmental trajectory of BD, both as a comorbidity and as a potential risk factor for the development of a mood disorder.

One of the largest sources of anxiety in youth is the quality of social relationships, which greatly influence youth's perceived quality of life (7–9). Youth with BD demonstrate deficits in interpersonal functioning that contribute to anxiety (9, 10) and undermine emotion regulation, potentially leading to mood episodes (10–13). A major source of anxiety for youth is social exclusion (14). Therefore, better understanding of responses to social exclusion in youth with BD could lead to interventions that prevent mood symptom development.

No previous studies have examined the neural underpinnings of social exclusion in youth with BD. For youth with unipolar depression, previous studies of social exclusion have reported abnormal hyperactivation of the anterior insula and subgenual cingulate cortex (sgACC) (11, 12, 15–18), which was correlated with greater feelings of distress compared with healthy controls (HC) (12). Additionally, hyperactivation in the sgACC and medial prefrontal cortex (PFC) during social exclusion was predictive of depressive symptoms one year later (13). FMRI studies also suggest the ventral PFC and ventral striatum regulate areas hyperactivated during social exclusion (12, 15). In fact, a recent coordinate-based meta-analysis found that activation in the right ventral striatum and left ventrolateral prefrontal cortex (VLPFC) is consistently reported in studies of developmental samples during a social exclusion fMRI task called "Cyberball" (19). Taken together, these studies suggest that the neural response to social exclusion involves structures associated with internal perception (anterior insula) and emotional experience (sgACC) regulated by the VLPFC. We therefore hypothesized that youth with BD would exhibit greater activation of this neural circuitry and report significantly greater distress during social exclusion when compared with HC.

MATERIALS AND METHODS

Participants and Assessments

The Stanford University Administrative Panel of Medical Research in Human Subjects approved the protocol. We recruited 19 youth fulfilling DSM-IV-TR criteria for BD I, II, or not otherwise specified (NOS) from a pediatric bipolar disorders clinic and 16 gender and age matched healthy controls (HC) from the surrounding community. We examined the bipolar spectrum of disease owing to the fact that longitudinal studies have shown that within 2.5 years, youth with BD, NOS convert to BD II or I, and youth with BD II convert to BD I (1). All participants were between the ages of 10–18. We obtained written informed consent and assent from the parents and children, respectively. Children were administered the Young Mania Rating Scale (YMRS) (20) and the Children's Depression Rating Scale-Revised Version (CDRS-R) (21) by raters with established inter-rater reliability (ICC $>$ 0.9). Participants were also administered the children's Rejection Sensitivity Questionnaire (RSQ), a validated scale measuring the severity of anxiety and anger that might be experienced with regards to the likelihood of being accepted in various social exclusion scenarios (22). Participants were also administered the Need Threat Scale (NTS), a validated scale used to assess the severity of subjective distress felt during the fMRI social exclusion task (23, 24). Subjective distress, as defined by the NTS, assesses the degree of threat someone feels during social exclusion to their needs for belonging, control, self-esteem, and meaningful existence (23, 24). The NTS is scored such that higher scores indicate lower levels of subjective distress, or threat to need, and lower scores indicate higher subjective distress.

The affective module of the Washington University in St. Louis Kiddie-Schedule for Affective Disorders and Schizophrenia (WASH-U KSADS) (kappa $>$ 0.9 for diagnostic reliability) (25, 26) and the Kiddie–Schedule for Affective Disorders and Schizophrenia, Present and Lifetime (kappa 0.77–1.00 for diagnostic reliability) (27) were administered to parents and children in separate interviews by a trained masters-level clinician and/or board-certified psychiatrist. DSM-IV-TR criteria were used to determine current and lifetime psychiatric diagnoses. BD-NOS criteria was defined as a minimum of either (1) two lifetime episodes of at least four hours duration each of criterion A: either elevated mood plus two associated symptoms or irritable mood plus three associated symptoms, but not meeting threshold BD I or II criteria or (2) 2–3 days of criterion A. Participants taking medications were stable on medications, defined as three weeks at the same dosage if taking a selective serotonin reuptake inhibitor (SSRI), and 2 weeks if taking a mood stabilizer, antipsychotic, and/or stimulant.

Youth were excluded from the BD group if they had diagnoses of pervasive development disorder, intellectual disability, obsessive-compulsive disorder, panic disorder, post-traumatic stress disorder, a history of head trauma with loss of consciousness, or Tourette's syndrome. Participants in the healthy control group were excluded if they were taking psychotropic medications or if they or any of their first-degree relatives had a current or lifetime DSM-IV-TR diagnosis. Further excluded from either group were any children with a neurologic condition (e.g., seizure disorder), substance use disorder, or the presence of metallic implants or braces.

"Cyberball" Task During fMRI

Participants were scanned while playing Cyberball, a computer game used to study the effects of social exclusion that has been adapted for use in the fMRI scanner (23, 24, 28). In this game, the participant played a virtual ball-tossing game with two other players. To enhance the interpersonal nature of the game, the participant was told s/he was playing with two other players and that each player was in a separate scanner. These two other players were shown as cartoon figures on the projection screen viewed by the participant via a mirror attached to the headcoil. The participant was represented by a cartoon hand at the bottom of the screen.

The cyberball task was designed to replicate that used in previous studies (12). The task is a block design containing "inclusion" and "exclusion" blocks. During inclusion blocks, a

cartoon ball was thrown to the participant, who could then throw the ball to one of the two other (cartoon) players by pressing the left or right button on the button box. During exclusion blocks, the ball was thrown to one of the other (cartoon) players, and the participant was excluded from all throws. For all blocks, each throw had a duration of 5–6 s (depending on how quickly the participant threw the ball) with an inter-throw interval of 0.5 s. The order of blocks was inclusion–inclusion–exclusion. The first inclusion block contained 55 throws, the second inclusion block contained 30 throws, and the exclusion block contained 27 throws. Overall, the task duration was 4:29".

After the scan, participants were administered the Need Threat Scale to assess the severity of subjective distress experienced during the game (23, 24).

fMRI Acquisition and Preprocessing

Magnetic resonance imaging scans were conducted at the Stanford University Richard M. Lucas Center for Imaging. Images were acquired using a 3.0T General Electric MR750 scanner (General Electric, Milwaukee, WI, United States) using an 8-channel head coil. The following pulse sequence parameters were used for the fMRI scans: spiral in-out, echo time (TE)/repetition time (TR) = 30/2,000 ms, flip angle = 89° and 1 interleave, matrix size 64 × 64, field of view (FOV) = 240 mm, 31 slices, slice thickness 4 mm, skip 0.5 mm; entire brain and cerebellum. An individually calculated high-order shim for spiral acquisitions was used to reduce field inhomogeneity. A high resolution fast spoiled grass (FSPGR) anatomical scan also was collected to optimize registration of fMRI data to standard space.

fMRI Data Preprocessing

Functional MRI data were analyzed using SPM8 software.[1] Images were realigned to the third volume and motion was corrected using the ArtRepair toolbox (cibsr.stanford.edu/tools/ArtRepair). Volumes with motion artifact (slope > 1.5 mm/volume) were replaced with a volume that was interpolated from the nearest surrounding unaffected volumes. Scans were rejected from further analysis for motion spikes greater than 4 mm translation or if more than 20% of volumes required motion correction. Images were normalized to the MNI152 template using each subject's anatomical scan and resampled to a 2-cubic mm matrix using sinc interpolation, smoothed with a 5 mm FWHM Gaussian filter, and high pass filtered at 120 s.

Group Differences in Ratings of Distress and Rejection Sensitivity

An independent-sample *t*-test performed in IBM SPSS v26.0[2] was used to examine differences between BD and HC group mean NTS scores. Spearman's correlations within each group were used to examine the association between NTS and RSQ scores. RSQ scores comprised two scores, an anger and an anxiety domain. NTS scores for each group were therefore correlated with each domain separately. Thresholds for significance were set at q = 0.05, after FDR correction for multiple comparisons.

Whole Brain Analyses

For each subject, a fixed-effects analysis in SPM8 using the general linear model was performed to calculate voxel-wise statistical maps for each subject, for the contrast of exclusion minus inclusion blocks. Between group voxel-wise comparisons were conducted using an independent groups t-test, while covarying for age.

Inference was conducted using a cluster-forming threshold of $p < 0.005$, combined with family-wise error correction of $p < 0.05$ at the cluster level. While our cluster-forming threshold of $p = 0.005$ is somewhat more liberal than the traditional setting of $p = 0.001$ (29), it is recommended for reducing Type II error in fMRI studies of social and affective processes, which have small effect sizes and weak statistical power due to the complexity of these psychological processes (30,31). In addition, this threshold is similar to previous studies examining the effects of Cyberball in youth (19, 30). Age was covaried given previous findings that brain regions activated by Cyberball were age dependent (19).

Region-of-Interest Analyses

Regions of interest (ROI) were defined using the Automated Anatomic Labeling (AAL) atlas (32) for the anterior insula and the anterior cingulate cortex. For the ventral striatum and ventral PFC, coordinates were taken from a meta-analysis of developmental Cyberball studies and a 5 mm sphere was created for each *a priori* region using MarsBar[3] from which mean activation was extracted (19).

Functional Connectivity

The generalized Psychophysiological Interaction (gPPI) toolbox (33) was used to examine whole brain functional connectivity with seeds placed at each of the significant activation clusters. The resulting voxel-wise connectivity maps were contrasted between the BD and HC groups using independent groups *t*-tests in SPM8. Inference was conducted using a cluster-forming threshold of $p < 0.005$, combined with Family-wise error correction of $p < 0.05$ at the cluster level, as justified in the section "Whole Brain Analyses."

Associations Between Significant Clusters and Self-Reported Distress and Mood Symptomatology

Within each group separately, linear regression in SPSS was used to predict NTS score from mean activation in each significant cluster, adjusted for age. A second model was used to predict RSQ from mean activation in significant clusters.

CDRS-R scores measuring depression symptoms were correlated with each individual's mean activation for each significant cluster using Spearman's rho. Thresholds for significance were set at q = 0.05, after FDR correction for multiple comparisons. The same was performed for mania symptoms using YMRS scores.

[1] http://www.fil.ion.ucl.ac.uk/spm

[2] https://www.ibm.com/products/spss-statistics

[3] http://marsbar.sourceforge.net/

TABLE 1 | Description of participants.

	Bipolar Group (n = 19)	Healthy Control Group (n = 14)	Group comparison p-value
Males	10 (53%)	8 (57%)	0.066
Females	9 (47%)	6 (43%)	0.797
Age (mean ± SD)	14.97 ± 2.00	14.73 ± 2.07	0.740
Body Mass Index (BMI)	24.0 ± 5.0	20.4 ± 1.5	0.086
Motion during MRI scan (absolute displacement in mm)	0.12 ± 0.10	0.14 ± 0.15	0.753
Primary Diagnosis			
Bipolar I	9 (47%)	None	
Bipolar, NOS	10 (53%)		
Comorbid Diagnoses		None	
Generalized Anxiety Disorder	4 (21%)		
ODD[4]	1 (5%)		
% Taking or Exposed to Meds	53%	None	
Medication at Time of Scan		None	
Antidepressants (SSRI)	5%		
Stimulant	16%		
Lithium	11%		
Other mood stabilizers	21%		
Antipsychotics	32%		
Anxiolytics	0%		

NOS, not otherwise specified; ODD, Oppositional Defiant Disorder; SSRI, Selective Serotonin Reuptake Inhibitors.

Whole-brain linear regression was also performed for each group twice using activation and functional connectivity each as dependent variables in separate models in SPM8. Total NTS scores and age were the independent variables in these models. We used a cluster forming threshold of p = 0.005 and thresholds of inference set at $p \leq 0.05$, FWE corrected.

RESULTS

Demographics and Clinical Characteristics

Two HC scans were not usable, one due to artifact during the exclusion run and the second due to incomplete capture of superior portions of the brain. A total of 19 scans in the BD group and 14 scans in the HC group were included in fMRI analysis. There were no group differences in age [t(30) = 0.540, $p = 0.74$] or proportion of females to males ($\chi^2 = 0.07$, $p = 0.80$). Nine youth were diagnosed with BD I and ten with BD, NOS. Four had Generalized Anxiety Disorder and one had Oppositional Defiant Disorder. **Table 1** provides additional demographic and clinical characteristics.

Group Differences in Mood Symptoms and Distress During Exclusion

Table 2 depicts CDRS-R, YMRS, NTS, and RSQ scores for each group. No significant difference was found between the BD and HC groups for mean NTS scores ($p = 0.33$). The BD group had significantly higher scores when compared with HC for the anger domain [t(24) = 2.73, $p = 0.012$] and the anxiety domain [t(28) = 2.15, $p = 0.041$] of the RSQ. As expected, YMRS and CDRS-R scores were significantly higher in the BD group [YMRS: t(21) = 3.04, $p = 0.006$; CDRS-R: t(19) = 7.38, $p < 0.001$]. Within the BD group, NTS score was significantly correlated with RSQ scores in the anger domain (rho = –0.65, $p = 0.012$, q = 0.025, FDR corrected; **Figure 1**) and a near significant correlation was found between NTS and RSQ scores in the anxiety domain (rho = –0.55, $p = 0.041$, q = 0.05, FDR corrected). None of the correlations within the HC group were significant.

fMRI Results

Group Differences in Activation to Exclusion vs Inclusion

For the whole brain voxel-wise analysis, youth with BD showed significantly greater activation than HC in the left fusiform gyrus [FFG, Brodmann's Area (BA) 37, peak X = –42, Y = –56, Z = –12, z = 3.71, cluster size = 270, $p = 0.037$, **Figure 2**]. For the ROI analysis, no significant differences were found between BD and HC for the ventral striatum ROI, ventral PFC ROI, and anterior insula ROI.

Functional Connectivity

The BD group, compared with the HC group, showed significantly lower functional connectivity between the left FFG cluster and two clusters: (1) posterior cingulate (PCC), precuneus, and cuneus (BA 23, 30, 31, 17 and 18; peak X = 6, Y = –66, Z = 18, z = 3.92, cluster size = 1617, $p < 0.001$) and (2) the postcentral gyrus (BA 3, 4; peak X = 24, Y = –32, Z = 64,

TABLE 2 | Symptom severity and behavioral ratings for each group.

	Bipolar group Mean (*SE*)	Healthy group Mean (*SE*)	t (*df*)	Group comparison p-value
Depression (CDRS-R)	40.84 (2.93)	18.93 (0.47)	7.38 (18.94)	0.001*
Mania (YMRS)	7.42 (1.66)	2.14 (0.51)	3.04 (21.32)	0.006*
Subjective Distress (NTS)	2.87 (0.17)	3.16 (0.24)	1.01 (23.45)	0.325
Anger domain of the Rejection Sensitivity scale (RSQ)	9.64 (1.39)	5.40 (0.68)	2.73 (24.21)	0.012*
Anxiety domain of the Rejection Sensitivity scale (RSQ)	12.26 (1.49)	8.44 (0.97)	2.15 (27.92)	0.041*

*SE, standard error; df, degrees of freedom; CDRS-R, Children's Depression Rating Scale-Revised; YMRS, Young Mania Rating Scale; NTS, Need Threat Scale; RSQ, children's Rejection Sensitivity Questionnaire. *Significant differences.*

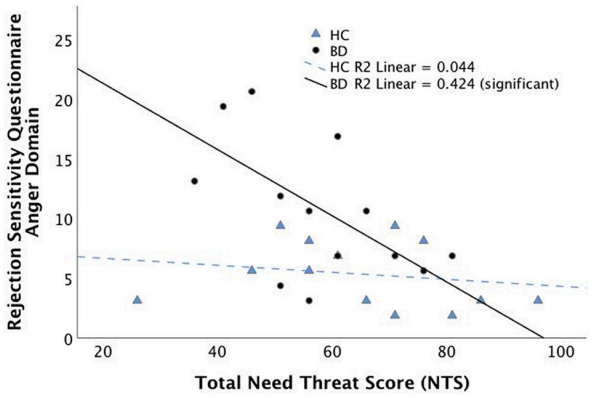

FIGURE 1 | Spearman's correlation between subjective distress during social exclusion (as measured by the Need Threat Scale) and the anger domain of the Rejection Sensitivity Questionnaire (RSQ). Correlation is significant within the Bipolar Disorder group but not the Healthy Control group.

z = 3.60, cluster size = 411, $p = 0.006$). These results are shown in **Figure 3**.

Associations Between Activation and Distress During Exclusion

Within the HC group, fusiform gyrus activation was significantly associated with subjective distress during exclusion (total NTS score), after adjusting for age (model R square = 0.53, $p = 0.020$), such that lower distress during exclusion was associated with higher levels of FFG activation. Within the BD group, the association between subjective distress during exclusion and FFG activation was not significant (R square = 0.006, $p = 0.961$). A scatterplot of these associations is shown in **Figure 4**, for each group separately. No significant correlations were found between FFG activation and CDRS-R or YMRS scores within either group.

Whole Brain Associations Between Functional Connectivity and Distress During Exclusion

Within the BD group, subjective distress during exclusion was not significantly associated with connectivity of the FFG. Within the HC group, greater distress during exclusion was significantly associated with lower connectivity between the left FFG and left posterior cerebellum ($p = 0.004$) and greater connectivity between the left FFG and four regions: (1) left cuneus ($p < 0.001$), (2) left precuneus ($p = 0.008$), (3) right anterior insula ($p = 0.001$), and (4) right premotor cortex ($p = 0.001$). These results are shown in **Figure 5**.

DISCUSSION

During a social exclusion task, youth with BD showed greater activation in the left FFG compared with HC. The HC group had greater functional connectivity over BD between the left FFG and the PCC compared to the BD group. Interestingly, there was no significant difference between the BD and HC groups in severity

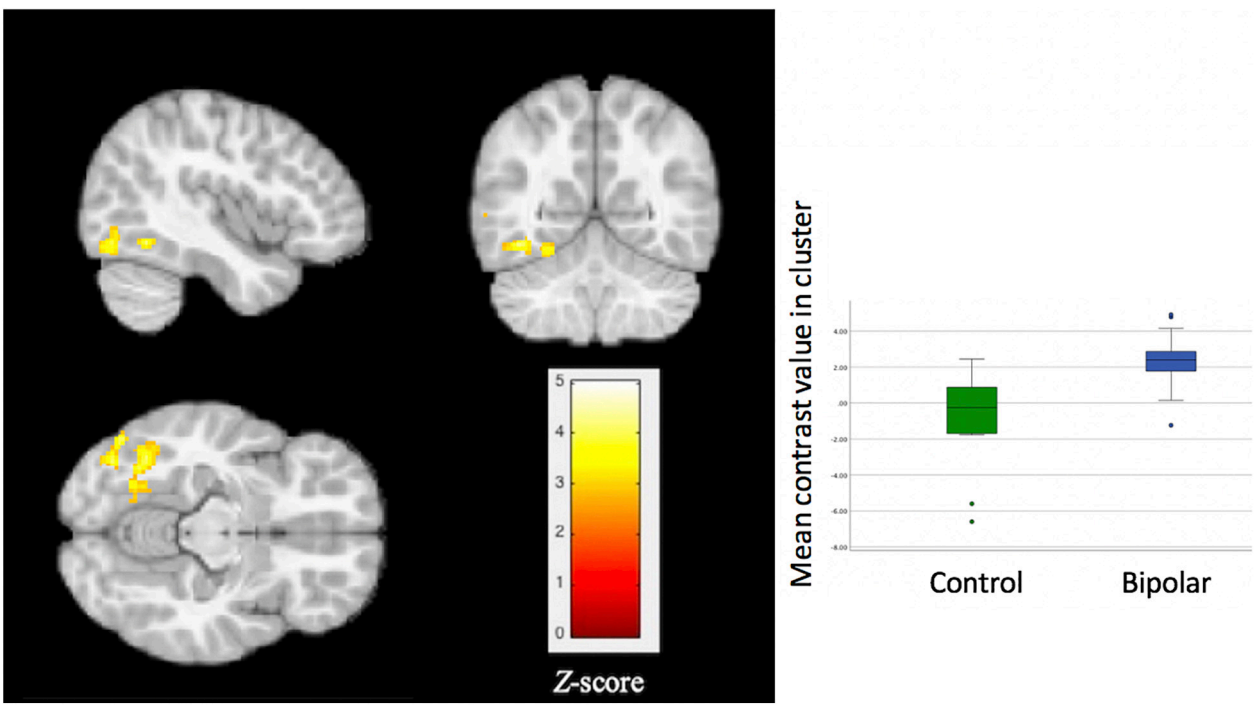

FIGURE 2 | Significant group differences in activation of the left fusiform gyrus during a social exclusion task. Compared to healthy controls, youth with bipolar disorder showed significantly greater activation ($p = 0.037$) for the contrast of exclusion > inclusion. Thresholds for inference were set at $p < 0.05$, FWE corrected at the cluster level.

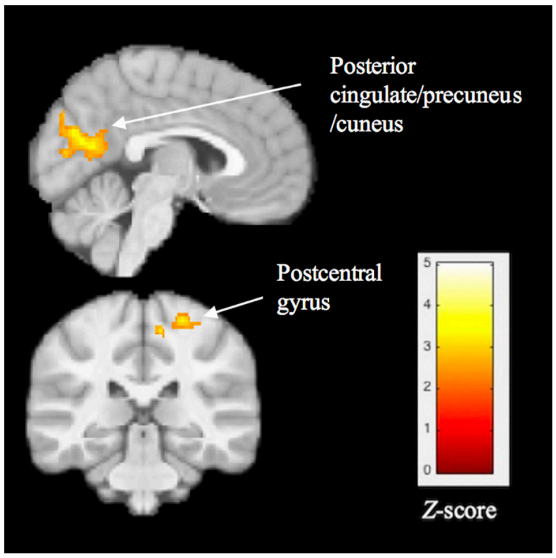

FIGURE 3 | Significant group differences in task-related functional connectivity of the left fusiform gyrus, assessed using psychophysiological interaction analysis. Compared with healthy controls, youth with BD showed lower connectivity between the fusiform cluster and 3 regions: posterior cingulate, precuneus/cuneus, and postcentral gyrus. Thresholds were set at $p < 0.05$, FWE corrected at the cluster level.

of distress during the social exclusion task. We found that distress significantly predicted FFG activation in the HC group but not in the BD group. In functional connectivity analysis for the HC group using the left FFG as the seed, greater connectivity with the right anterior insula, right premotor cortex, and left middle occipital cortex was also significantly correlated with greater feelings of distress. Taken together, these results suggest that youth with BD process social exclusion differently than healthy youth and that distress from social exclusion may correlate with alternate pathways not typically seen in healthy youth. These results are considered preliminary due to small sample size.

To our knowledge, this is the first fMRI study examining social exclusion in youth with BD. While we hypothesized we would see greater activation in the BD group, when compared with HC, in areas previously shown to hyperactivate in adolescent samples experiencing Cyberball, our study did not produce these results using ROI analysis. Regions in the HC group that correlated with greater distress in social exclusion, however, were the same that were hyperactivated in previous studies of Cyberball in healthy developmental samples (19). A recent meta-analysis of 53 cyberball neuroimaging studies including both adult and child samples, reported consistent recruitment of ventral anterior cingulate, posterior cingulate, inferior and superior frontal, insula and occipital cortex (34). These findings overlap with the 2017 meta-analysis (19) that also found consistent recruitment of the posterior cingulate and ventrolateral frontal corticies. While these meta-analyses do not include comparisons between clinical and healthy groups, they are relevant to the present findings of lower connectivity between posterior cingulate and fusiform gyrus in BD versus HC groups, suggesting that the fusiform is relevant to social exclusion through its connectivity to the posterior cingulate. We also note that the current findings of a correlation between subjective distress and functional connectivity of insula with fusiform gyrus within the healthy control group further suggest that the fusiform gyrus is clinically relevant because of its connectivity with regions that are consistently reported across previous studies of the cyberball paradigm.

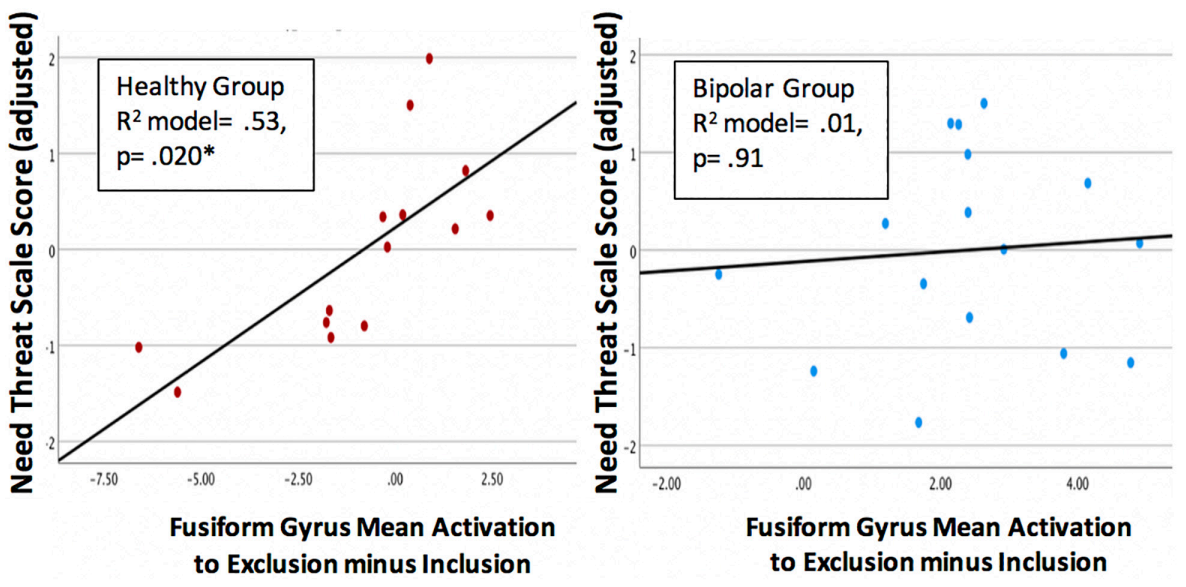

FIGURE 4 | Scatterplots showing the association between activation of the left fusiform gyrus (FFG) and subjective distress during exclusion (Need Threat Scale total score adjusted for age) within the each group. Regression models were significant for the healthy control group ($p = 0.020$, **left**) but not the bipolar group ($p = 0.91$, **right**).

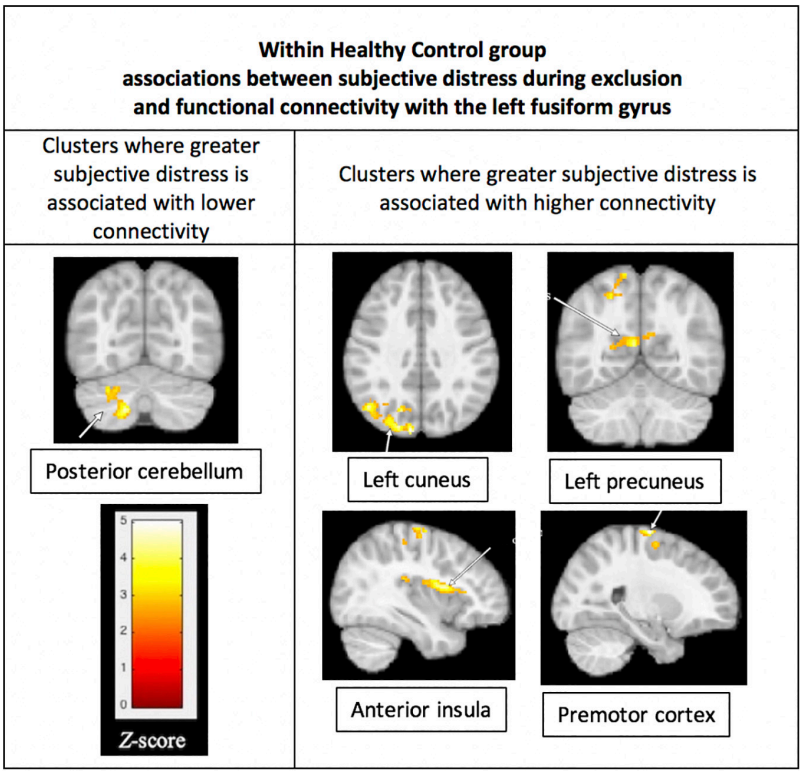

FIGURE 5 | Associations between subjective distress and functional connectivity with the left fusiform gyrus (FFG). Within the HC group, greater distress during social exclusion was associated with lower connectivity between the fusiform gyrus and the left posterior cerebellum ($p = 0.004$), shown in the **(left)** column of the figure. Also for the HC group, greater distress was associated with higher connectivity of the cuneus, precuneus, insula, and premotor cortex, as shown in the **(right)** column. Functional connectivity was performed using the left FFG cluster as the seed in a generalized PPI analysis, with a threshold of $p < 0.05$, FWE corrected at the cluster level. Results were not significant within the Bipolar Disorder group.

To explore whether the BD group's distress from social rejection was correlated with other brain regions, we conducted an exploratory whole brain voxel-wise correlation with NTS scores, but results were not significant. This could suggest the processing of distress after social rejection is not localized to a particular region or regions in the brain, or that our sample size was too small to detect an effect. However, the effect for the HC group was found with a smaller sample than the BD group.

The BD group did report some subjective distress but it was not significantly different than the HC group. However, the BD group had significantly higher ratings of anger and depression than the HC group, which were negatively correlated with subjective distress. This suggests that symptoms of anger and depression experienced by the BD group may have diminished or interfered with reporting subjective distress related to social exclusion in the BD group. If so, higher fusiform activation in BD may reflect an altered way of processing social exclusion that is not on a continuum with the HC group, e.g., not simply a more extreme level of subjective distress from social exclusion, but a different strategy, perhaps involving the visual system.

We hypothesized that the BD group would show greater activation in regions previously implicated in social exclusion in healthy controls (e.g., anterior cingulate cortex, VLPFC, and ventral striatum) but our results showed group differences in the fusiform gyrus. The fusiform gyrus is salient to higher level visual processing and implicated in facial perception, which are important components in the social cognitive circuit (35, 36). While some debate surrounds the function of the FFG, studies agree the area is recruited in the processing of faces (37). The role of facial processing and perception is important to understand the intention and emotions of others and therefore, to social interaction (37). In fact, a recent meta-analysis of the neural network of face processing in healthy adults showed the left posterior FFG was specifically involved in face processing tasks that required emotion evaluation (38). The posterior FFG, where our findings are located, encompasses the fusiform face area. Studies have shown this area to have higher activation when healthy adolescents are viewing fearful compared to neutral faces (39). Perhaps the BD group finds the depiction of cartoon faces in Cyberball emotionally evocative. This finding is consistent with previous literature suggesting adolescents with BD misinterpret neutral faces as fearful with greater hostility (40). Aberrant face emotion processing is well established in bipolar disorder, and so it is perhaps not surprising this marker of illness may be involved in any sort of social evaluative process (41).

Our connectivity analysis using the FFG as the seed showed the HC group had greater functional connectivity between the left FFG and the left PCC, specifically the caudal left PCC,

which is an area associated with autobiographical memory. The left PCC is activated during successful autobiographical memory recollection in healthy adults (42). This may suggest that the HC group recalls social experiences more than the BD group in the context of social exclusion. The PCC is also implicated in tasks of emotional salience. Studies have shown hyperactivation of the PCC in tasks of both positive and negative emotional stimuli (43). These studies have postulated the strength of successful recall of autobiographical memories to be dependent on their emotional importance, and the PCC consistently hyperactivates on successful recall of such memories. This suggests the PCC moderates the interaction between memory and emotion (42). Healthy youth may be able to interpret social exclusion in the larger context of positive autobiographical memories of social experiences. Youth with BD, however, are known to have structural and functional abnormalities in the PCC, which may suggest they do not have the same ability to recall autobiographical experiences in the same way as healthy youth (44, 45).

Lastly, for the HC group only, lower distress during Cyberball was correlated with greater functional connectivity between the posterior cerebellum and the FFG. Studies suggest the posterior cerebellum connects with the limbic system and participates in the limbic related functions of emotion (46). The posterior cerebellum has been shown to have abnormal function and structure in youth with bipolar disorder (47). Lesions in the cerebellum have been implicated in causing manic states (48) and with problems with social interaction (49). It may be, then, that the HC group has a more intact emotional circuit during the social exclusion experience, unlike the BD group. Areas known to have structural and functional abnormalities in BD that overlap with our findings, specifically the PCC and the posterior cerebellum, are therefore associated with aberrant processing of social exclusion when compared with healthy youth.

Limitations of this study include a small sample size. However, this is the only published study to date to examine the functional neuroanatomy of youth with bipolar disorder using a social cognitive paradigm. The fMRI block design which provided only four minutes of game time data also is a limitation of this study. Current Cyberball fMRI studies have extended this model to provide more data points by using an alternating block design and multiple games in one scan (19). We did use FWE for fMRI analysis, which is a stringent thresholding method, but may have missed some relevant between group differences as a result. Future studies should examine whether domains of anxiety, affective lability, and coping skills moderate responses to social exclusion. We did find greater scores in the anger domain for the RSQ to significantly correlate with greater distress in the BD but not the HC group. A similar finding was discovered for the anxiety domain of the RSQ, though this finding did not reach significance. This suggests an emotional and anxious component in youth with BD that may predict the reaction to social exclusion that should be further explored.

In summary, despite aberrant neural processing, the BD group did not show significant differences in distress during social exclusion when compared with the HC group. Youth with BD may therefore process social exclusion in a manner different from the HC group that focuses on visual processes early in the social cognitive circuit while HC uses past social experiences to inform current social encounters. This difference in processing may pose clinical implications for improving social cognition in youth with BD and preventing mood symptoms.

DATA AVAILABILITY STATEMENT

Due to difficulties in de-identifying MRI images of this vulnerable child population, raw data are not available. Processed data are available upon request to the corresponding author, with a data sharing agreement.

ETHICS STATEMENT

This study was reviewed and approved by the Institutional Review Board of Stanford University School of Medicine. Written informed assent and consent were provided by the youth and parent/guardian, respectively.

AUTHOR CONTRIBUTIONS

DR, KC, and AG designed the study. DR wrote the protocol and performed literature searches. DR, RML, and BN conducted the statistical analyses. DR, AG, RS, and RK conducted scans, pre-processed neuroimaging data, and analyzed neuroimaging data. All authors contributed to and approved the final manuscript.

FUNDING

This work was supported by funding awarded to DR from the American Academy of Child and Adolescent Psychiatry/Lilly Pilot Research Award.

ACKNOWLEDGMENTS

We thank Jennifer Pearlstein, Paige Staudemaier, and Sherrie Li for their assistance with recruiting and scanning participants.

REFERENCES

1. Birmaher B, Axelson D, Monk K, Kalas C, Goldstein B, Hickey MB, et al. Lifetime psychiatric disorders in school-aged offspring of parents with bipolar disorder: the pittsburgh bipolar offspring study. *Arch Gen Psychiatry.* (2009) 66:287–96. doi: 10.1001/archgenpsychiatry.2008.546
2. Duffy A. The early natural history of bipolar disorder: what we have learned from longitudinal high-risk research. *Can J Psychiatry.* (2010) 55:477–85. doi: 10.1177/070674371005500802

3. Sala R, Axelson DA, Castro-Fornieles J, Goldstein TR, Ha W, Liao F, et al. Comorbid anxiety in children and adolescents with bipolar spectrum disorders: prevalence and clinical correlates. *J Clin Psychiatry.* (2010) 71:1344–50. doi: 10.4088/JCP.09m05845gre
4. Sala R, Strober MA, Axelson DA, Gill MK, Castro-Fornieles J, Goldstein TR, et al. Effects of comorbid anxiety disorders on the longitudinal course of pediatric bipolar disorders. *J Am Acad Child Adolesc Psychiatry.* (2014) 53:72–81. doi: 10.1016/j.jaac.2013.09.020
5. Duffy A, Horrocks J, Doucette S, Keown-Stoneman C, McCloskey S, Grof P. Childhood anxiety: an early predictor of mood disorders in offspring of bipolar parents. *J Affect Disord.* (2013) 150:363–9. doi: 10.1016/j.jad.2013.04.021
6. Duffy A, Horrocks J, Doucette S, Keown-Stoneman C, McCloskey S, Grof P. The developmental trajectory of bipolar disorder. *Br J Psychiatry.* (2014) 204:122–8.
7. Hecht DB, Inderbitzen HM, Bukowski AL. The relationship between peer status and depressive symptoms in children and adolescents. *J Abnorm Child Psychol.* (1998) 26:153–60. doi: 10.1023/a:1022626023239
8. Nelson EE, Leibenluft E, McClure EB, Pine DS. The social re-orientation of adolescence: a neuroscience perspective on the process and its relation to psychopathology. *Psychol Med.* (2005) 35:163–74. doi: 10.1017/s0033291704003915
9. Siegel RS, Hoeppner B, Yen S, Stout RL, Weinstock LM, Hower HM, et al. Longitudinal associations between interpersonal relationship functioning and mood episode severity in youth with bipolar disorder. *J Nerv Ment Dis.* (2015) 203:194–204. doi: 10.1097/NMD.0000000000000261
10. Goldstein TR, Miklowitz DJ, Mullen KL. Social skills knowledge and performance among adolescents with bipolar disorder. *Bipolar Disord.* (2006) 8:350–61. doi: 10.1111/j.1399-5618.2006.00321.x
11. Sebastian CL, Roiser JP, Tan GCY, Viding E, Wood NW, Blakemore SJ. Effects of age and MAOA genotype on the neural processing of social rejection. *Genes Brain Behav.* (2010) 9:628–37. doi: 10.1111/j.1601-183X.2010.00596.x
12. Masten CL, Eisenberger NI, Borofsky LA, Pfeifer JH, McNealy K, Mazziotta JC, et al. Neural correlates of social exclusion during adolescence: understanding the distress of peer rejection. *Soc Cogn Affect Neurosci.* (2009) 4:143–57. doi: 10.1093/scan/nsp007
13. Masten CL, Eisenberger NI, Borofsky LA, Mcnealy K, Pfeifer JH, Dapretto M. Subgenual anterior cingulate responses to peer rejection: a marker of adolescents' risk for depression. *Dev Psychopathol.* (2011) 23:283–92. doi: 10.1017/S0954579410000799
14. Leary MR. Responses to social exclusion: social anxiety, jealousy, loneliness, depression, and low self-esteem. *J Soc Clin Psychol.* (1990) 9:221–9.
15. Bolling DZ, Pitskel NB, Deen B, Crowley MJ, Mayes LC, Pelphrey KA. Development of neural systems for processing social exclusion from childhood to adolescence. *Dev Sci.* (2011) 14:1431–44. doi: 10.1111/j.1467-7687.2011.01087.x
16. Bolling DZ, Pitskel NB, Deen B, Crowley MJ, McPartland JC, Mayes LC, et al. Dissociable brain mechanisms for processing social exclusion and rule violation. *Neuroimage.* (2011) 54:2462–71. doi: 10.1016/j.neuroimage.2010.10.049
17. Sebastian CL, Blakemore SJ. Understanding the neural response to social rejection in adolescents with autism spectrum disorders: a commentary on Masten et al., McPartland et al. and Bolling et al. *Dev Cogn Neurosci.* (2011) 1:256–9. doi: 10.1016/j.dcn.2011.03.006
18. Sebastian CL, Tan GCY, Roiser JP, Viding E, Dumontheil I, Blakemore SJ. Developmental influences on the neural bases of responses to social rejection: implications of social neuroscience for education. *Neuroimage.* (2011) 57:686–94. doi: 10.1016/j.neuroimage.2010.09.063
19. Vijayakumar N, Cheng TW, Pfeifer JH. Neural correlates of social exclusion across ages: a coordinate-based meta-analysis of functional MRI studies. *Neuroimage.* (2017) 153:359–68. doi: 10.1016/j.neuroimage.2017.02.050
20. Young RC, Biggs JT, Ziegler VE, Meyer DA. A rating scale for mania: reliability, validity and sensitivity. *Br J Psychiatry.* (1978) 133:429–35. doi: 10.1192/bjp.133.5.429
21. Poznanski EO, Grossman JA, Buchsbaum Y, Banegas M, Freeman L, Gibbons R. Preliminary studies of the reliability and validity of the children's depression rating scale. *J Am Acad Child Psychiatry.* (1984) 23:191–7. doi: 10.1097/00004583-198403000-00011
22. Downey G, Lebolt A, Rincón C, Freitas AL. Rejection sensitivity and children's interpersonal difficulties. *Child Dev.* (1998) 69:1074–91.
23. Williams KD, Cheung CKT, Choi W. Cyberostracism: effects of being ignored over the Internet. *J Pers Soc Psychol.* (2000) 79:748–62. doi: 10.1037//0022-3514.79.5.748
24. Williams KD, Govan CL, Croker V, Tynan D, Cruickshank M, Lam A. Investigations into differences between social- and cyberostracism. *Group Dyn.* (2002) 6:65–77.
25. Geller B, Williams M, Zimerman B, Frazier J. *Washington University in St. Louis Kiddie Schedule for Affective Disorders and Schizophrenia (WASH-U-KSADS)*. St. Louis, MO: Washington University (1996).
26. Geller B, Zimerman B, Williams M, Bolhofner K, Craney JL, Delbello MP, et al. Reliability of the Washington University in St. Louis Kiddie schedule for affective disorders and schizophrenia (WASH-U-KSADS) mania and rapid cycling sections. *J Am Acad Child Adolesc Psychiatry.* (2001) 40:450–5. doi: 10.1097/00004583-200104000-00014
27. Kaufman J, Birmaher B, Brent D, Rao UMA, Flynn C, Moreci P, et al. Schedule for affective disorders and schizophrenia for school-age children-present and lifetime version (K-SADS-PL): initial reliability and validity data. *J Am Acad Child Adolesc Psychiatry.* (1997) 36:980–8. doi: 10.1097/00004583-199707000-00021
28. Williams KD, Jarvis B. Cyberball: a program for use in research on interpersonal ostracism and acceptance. *Behav Res Methods.* (2006) 38:174–80. doi: 10.3758/bf03192765
29. Eklund A, Nichols TE, Knutsson H. Cluster failure: why fMRI inferences for spatial extent have inflated false-positive rates. *Proc Natl Acad Sci U S A.* (2016) 113: 7900–905. doi: 10.1073/pnas.1602413113
30. Lieberman MD, Cunningham WA. Type I and type II error concerns in fMRI research: re-balancing the scale. *Soc Cogn Affect Neurosci.* (2009) 4(:423–8. doi: 10.1093/scan/nsp052
31. Poldrack RA, Baker, CI, Durnez J, Gorgolewski KJ, Matthews PM, Munafo MR, et al. Scanning the horizon: towards transparent and reproducible neuroimaging research. *Nat Rev Neurosci.* (2017) 18:115–26. doi: 10.1038/nrn.2016.167
32. Tzourio-Mazoyer N, Landeau B, Papathanassiou D, Crivello F, Etard O, Delcroix N, et al. Automated anatomical labeling of activations in SPM using a macroscopic anatomical parcellation of the MNI MRI single-subject brain. *Neuroimage.* (2002) 15:273–89.
33. McLaren DG, Ries ML, Xu G, Johnson SC. A generalized form of context-dependent psychophysiological interactions (gPPI): a comparison to standard approaches. *Neuroimage.* (2012) 61:1277–86. doi: 10.1016/j.neuroimage.2012.03.068
34. Mwilambwe-Tshilobo L, Spreng RN. Social exclusion reliably engages the default network: a meta-analysis of cyberball. *Neuroimage.* (2021) 227:117666. doi: 10.1016/j.neuroimage.2020.117666
35. Brothers L, Ring B, Kling A. Response of neurons in the macaque amygdala to complex social stimuli. *Behav Brain Res.* (1990) 41:199–213. doi: 10.1016/0166-4328(90)90108-q
36. Frith CD. The social brain? *Philos Trans R Soc B Biol Sci.* (2007) 362: 671–8.
37. Albohn DN, Adams RB. Social vision: at the intersection of vision and person perception. In: Absher JR, Cloutier J editors. *Neuroimaging Personality, Social Cognition, and Character*. San Diego, CA: Academic Press (2016). p. 159–86.
38. Müller VI, Höhner Y, Eickhoff SB. Influence of task instructions and stimuli on the neural network of face processing: an ALE meta-analysis. *Cortex.* (2018) 103:240–55. doi: 10.1016/j.cortex.2018.03.011
39. Guyer AE, Lau JYF, McClure-Tone EB, Parrish J, Shiffrin ND, Reynolds RC, et al. Amygdala and ventrolateral prefrontal cortex function during anticipated peer evaluation in pediatric social anxiety. *Arch Gen Psychiatry.* (2008) 65:1303–12. doi: 10.1001/archpsyc.65.11.1303
40. Rich BA, Vinton DT, Roberson-Nay R, Hommer RE, Berghorst LH, McClure EB, et al. Limbic hyperactivation during processing of neutral facial expressions in children with bipolar disorder. *Proc Natl Acad Sci USA.* (2006) 103:8900–5. doi: 10.1073/pnas.0603246103
41. Kryza-Lacombe M, Brotman MA, Reynolds RC, Towbin K, Pine DS, Leibenluft E, et al. Neural mechanisms of face emotion processing in youths

and adults with bipolar disorder. *Bipolar Disord.* (2019) 21:309–20. doi: 10.1111/bdi.12768
42. Maddock RJ, Garrett AS, Buonocore MH. Remembering familiar people: the posterior cingulate cortex and autobiographical memory retrieval. *Neuroscience.* (2001) 104:667–76. doi: 10.1016/s0306-4522(01)00108-7
43. Pearson JM, Heilbronner SR, Barack DL, Hayden BY, Platt ML. Posterior cingulate cortex: adapting behavior to a changing world. *Trends Cogn Sci.* (2011) 15:143–51. doi: 10.1016/j.tics.2011.02.002
44. Chang K, Garrett A, Kelley R, Howe M, Sanders EM, Acquaye T, et al. Anomalous prefrontal-limbic activation and connectivity in youth at high-risk for bipolar disorder. *J Affect Disord.* (2017) 222:7–13. doi: 10.1016/j.jad.2017.05.051
45. Kaur S, Sassi RB, Axelson D, Nicoletti M, Brambilla P, Monkul ES, et al. Cingulate cortex anatomical abnormalities in children and adolescents with bipolar disorder. *Am J Psychiatry.* (2005) 162:1637–43. doi: 10.1176/appi.ajp.162.9.1637
46. Blatt GJ, Oblak AL, Schmahmann JD. Cerebellar connections with limbic circuits: anatomy and functional implications. In: Manto M, Schmahmann JD, Rossi F, Gruol DL, Koibuchi N editors. *Handbook of the Cerebellum and Cerebellar Disorders*. Berlin: Springer (2013). p. 479–96.
47. Kim D, Byul Cho H, Dager SR, Yurgelun-Todd DA, Yoon S, Lee JH, et al. Posterior cerebellar vermal deficits in bipolar disorder. *J Affect Disord.* (2013) 150:499–506. doi: 10.1016/j.jad.2013.04.050
48. Lupo M, Olivito G, Siciliano L, Masciullo M, Molinari M, Cercignani M, et al. Evidence of cerebellar involvement in the onset of a manic state. *Front Neurol.* (2018) 9:774. doi: 10.3389/fneur.2018.00774
49. Strakowski SM, DelBello MP, Adler CM. The functional neuroanatomy of bipolar disorder: a review of neuroimaging findings. *Mol Psychiatry.* (2005) 10:105–16. doi: 10.1038/sj.mp.4001585

Conflict of Interest: The authors declare that the research was conducted in the absence of any commercial or financial relationships that could be construed as a potential conflict of interest.

Publisher's Note: All claims expressed in this article are solely those of the authors and do not necessarily represent those of their affiliated organizations, or those of the publisher, the editors and the reviewers. Any product that may be evaluated in this article, or claim that may be made by its manufacturer, is not guaranteed or endorsed by the publisher.

frontiers | Frontiers in Psychiatry

ORIGINAL RESEARCH
published: 11 April 2022
doi: 10.3389/fpsyt.2022.803234

Thalamic Shape Abnormalities Differentially Relate to Cognitive Performance in Early-Onset and Adult-Onset Schizophrenia

Derin Cobia[1,2], Chaz Rich[3], Matthew J. Smith[4], Pedro Engel Gonzalez[2], Will Cronenwett[2], John G. Csernansky[2] and Lei Wang[2,5]*

[1] Department of Psychology and Neuroscience Center, Brigham Young University, Provo, UT, United States, [2] Department of Psychiatry and Behavioral Sciences, Northwestern University Feinberg School of Medicine, Chicago, IL, United States, [3] Department of Psychology, University of Notre Dame, Notre Dame, IN, United States, [4] School of Social Work, University of Michigan, Ann Arbor, MI, United States, [5] Department of Psychiatry and Behavioral Health, The Ohio State University Wexner Medical Center, Columbus, OH, United States

OPEN ACCESS

Edited by:
Jihane Homman-Ludiye, Monash University, Australia

Reviewed by:
Michael M. Halassa, Massachusetts Institute of Technology, United States
Wen Qin, Tianjin Medical University General Hospital, China

***Correspondence:**
Derin Cobia
derin_cobia@byu.edu

Specialty section:
This article was submitted to Schizophrenia, a section of the journal Frontiers in Psychiatry

Received: *27 October 2021*
Accepted: *02 March 2022*
Published: *11 April 2022*

Citation:
Cobia D, Rich C, Smith MJ, Engel Gonzalez P, Cronenwett W, Csernansky JG and Wang L (2022) Thalamic Shape Abnormalities Differentially Relate to Cognitive Performance in Early-Onset and Adult-Onset Schizophrenia. Front. Psychiatry 13:803234. doi: 10.3389/fpsyt.2022.803234

Early-onset schizophrenia (EOS) shares many biological and clinical features with adult-onset schizophrenia (AOS), but may represent a unique subgroup with greater susceptibility for disease onset and worsened symptomatology and progression, which could potentially derive from exaggerated neurodevelopmental abnormalities. Neurobiological explanations of schizophrenia have emphasized the involvement of deep-brain structures, particularly alterations of the thalamus, which have been linked to core features of the disorder. The aim of this study was to compare thalamic shape abnormalities between EOS and AOS subjects and determine whether unique behavioral profiles related to these differences. It was hypothesized abnormal thalamic shape would be observed in anterior, mediodorsal and pulvinar regions in both schizophrenia groups relative to control subjects, but exacerbated in EOS. Magnetic resonance T1-weighted images were collected from adult individuals with EOS (n = 28), AOS (n = 33), and healthy control subjects (n = 60), as well as collection of clinical and cognitive measures. Large deformation high-dimensional brain mapping was used to obtain three-dimensional surfaces of the thalamus. General linear models were used to compare groups on surface shape features, and Pearson correlations were used to examine relationships between thalamic shape and behavioral measures. Results revealed both EOS and AOS groups demonstrated significant abnormal shape of anterior, lateral and pulvinar thalamic regions relative to CON (all $p < 0.007$). Relative to AOS, EOS exhibited exacerbated abnormalities in posterior lateral, mediodorsal and lateral geniculate thalamic regions (p = 0.003). Thalamic abnormalities related to worse episodic memory in EOS (p = 0.03) and worse working memory (p = 0.047) and executive functioning (p = 0003) in AOS. Overall, findings suggest thalamic abnormalities

are a prominent feature in both early- and late-onset schizophrenia, but exaggerated in EOS and have different brain-behavior profiles for each. The persistence of these abnormalities in adult EOS patients suggests they may represent markers of disrupted neurodevelopment that uniquely relate to the clinical and cognitive aspects of the illness.

Keywords: psychosis, development, MRI, surface-mapping, neuroimaging

INTRODUCTION

The onset of psychosis during childhood or early adolescence provides a unique research opportunity to explore the etiology of schizophrenia since children and adolescents with early-onset schizophrenia may represent a more homogenous subgroup associated with severe developmental deficits and greater familial susceptibility for the disorder (1). Additionally, given abnormal neural development is thought to contribute to the modulation of schizophrenia, early-onset schizophrenia offers a window to study the well-established neurodevelopmental hypothesis for schizophrenia (2). The anatomical pattern and the timing of the illness is still unclear, hence studies of early-onset schizophrenia could offer further insight into the pathophysiological process of the disease to precisely differentiate between normal brain development and the disease-associated pathological development.

Previously, it was unknown whether early-onset schizophrenia was an earlier extension of adult-onset schizophrenia or if it represented an independent pathophysiological process (3). Examination of early-onset schizophrenia has provided evidence for the continuity between early- and adult-onset groups since both types broadly share many of the same physiological and psychopathological features (4, 5). However, early-onset schizophrenia has been consistently associated with more severe premorbid psychopathology and cognitive impairment (2), which could potentially derive from an exaggeration of the neurodevelopmental abnormalities usually present in schizophrenia. For example, patients with early onset typically present with more severe premorbid language, motor, and social delays than patients with later onset in adolescence (4). Moreover, a study exploring cognitive differences between first-episode adolescents and first-episode adults with schizophrenia found that early-onset patients performed poorly in language and working memory tasks, as well as exhibited greater motor performance deficits compared with adult-onset (6).

Recent theories about the neurobiology of schizophrenia have emphasized the involvement of deep-brain structures, particularly the thalamus (7, 8). Due to the central role the thalamus plays in the coordination of information flow and cognition (9), dysfunction of this region is often implicated in many of the cardinal symptoms of schizophrenia, such as disorganized thought and executive dysfunction among others (10). Developmentally, the thalamus plays a pivotal role in the genesis of the cerebral cortex, with thalamic input being critical for appropriate functional differentiation of the cortex and intercommunicating regions (11), which is consistent with the neurodevelopmental hypothesis of schizophrenia (2). Neuroimaging studies of early-onset schizophrenia have demonstrated similar, and sometimes more pronounced, patterns of structural brain abnormalities with respect to schizophrenia in general (12–14). There is evidence thalamic volume is globally reduced in early-onset subjects (15, 16), with specific volume loss in mediodorsal and pulvinar regions (17).

Most studies to date have examined the features of early-onset schizophrenia in child and adolescent populations (18, 19), with few investigating them later in the course of the illness. Furthermore, there are no studies that have specifically investigated subtle morphological alterations of the thalamus available through shape analytic procedures in early-onset schizophrenia and compared against a matched adult-onset group. The aim of the current study was to utilize high-dimensional surface-mapping to characterize regional abnormalities of the thalamus in well-matched adult groups of early-onset and adult-onset schizophrenia, as well as matched control participants, to assess the persistence of theorized neurobiological exacerbations of altered neurodevelopment in early-onset schizophrenia. Based on previous work (20), it was hypothesized that abnormal shape would be observed in anterior, mediodorsal and pulvinar regions in the schizophrenia groups, but exaggerated in early-onset schizophrenia. Furthermore, it was hypothesized that early-onset-associated shape changes would demonstrate stronger relationships with cognition and psychopathology than those associated with adult-onset schizophrenia.

MATERIALS AND METHODS

Sample

Participants included 28 individuals with early-onset schizophrenia (EOS), 33 individuals with adult-onset schizophrenia (AOS) and 60 healthy control (CON) participants all group-matched (using random selection) with respect to age, gender, and parental SES. Given schizophrenia is associated with progressive gray matter loss (21, 22), AOS and EOS subjects were also group-matched based on duration of illness. Complete recruitment methods have been described previously (23). The project was approved by the IRB at Washington University in St. Louis, and informed consent was obtained from each subject after a complete description of the study was given.

Clinical Measures

Diagnosis of schizophrenia was determined by the consensus of a research psychiatrist and trained research clinicians using the Structured Clinician Interview for DSM-IV Axis I Disorders [SCID, (24)]. The criteria for coding age of illness onset were

adapted from other longitudinal studies of EOS (2) where early-onset was defined as illness onset before 18 years of age, and AOS as onset by 18 years of age or older. Schizophrenia participants were asked to identify the age at which their acute psychotic symptoms first took place, which was provided using self-report during the SCID, as well as cross-referenced with medical records and a research evaluation by a psychiatrist. Duration of illness was computed as years difference between age of illness onset and current age.

The SCID was also used to identify lifetime diagnosis of a substance-use disorder for alcohol, cannabis, cocaine, stimulants, hallucinogens, sedatives, and opioids. Antipsychotic medication for schizophrenia participants was assessed through self-report, with first- and second-generation antipsychotic (FGA and SGA) treatments quantitatively measured based on type, dosage amount, duration of use, and the calculation of chlorpromazine equivalents using published guidelines (25). Nicotine use was estimated using a semi-structured interview adapted from Sullivan et al. (26), and alcohol use *via* the Lifetime Alcohol Consumption Assessment Procedure (27).

Clinical and Cognitive Assessments

A battery of neuropsychological measures assessing key cognitive domains affected in schizophrenia was administered to all participants (28); raw scores were converted into standardized scores then selected measures were factored into three cognitive domains: working memory, episodic memory, and executive functioning. An index of crystallized intelligence was also derived to estimate the generalized cognitive deficit in psychosis. Some missing data was observed for cognitive variables, which included three CON, two EOS, and two AOS individuals, who were not included in the analyses. Three psychopathology clusters (positive, negative, and disorganized symptoms) were assessed and calculated using global ratings from the Scale for the Assessment of Positive Symptoms (29) and the Scale for the Assessment of Negative Symptoms (29). A full description of the specific measures used is reported in previous work (23).

Image Acquisition

Details of the image acquisition, surface mapping and analysis of subjects can be found in previously published reports (20, 30). Briefly, magnetic resonance scans were collected with a standard head coil on a Siemens Magnetom 1.5T (Erlangen, Germany) scanner using a turbo-FLASH sequence (repetition time = 20 ms, echo time = 5.4 ms, flip angle = 30°, 180 slices, FOV = 256 mm, matrix = 356 × 256, time = 13.5 min) that acquired 1 mm^3 isotropic whole-head images. Total brain volume was estimated using an atlas scaling factor (ASF), which is the reciprocal of the determinant of the alignment matrix to Talairach atlas space, and signifies the extent that the brain volume contracts or expands during alignment (31). No between-group differences were observed in the ASF ($F_{2,117} = 1.7$, $p = 0.19$) and thus, was not used as a covariate in statistical analyses.

Surface Mapping

Thalamic surfaces were generated using Large-Deformation High-Dimensional Brain Mapping (HDBM-LD) procedures (32), an atlas-based approach that utilizes diffeomorphic transformations which aligns a template image to a target (i.e., subject) image and allows independent matching of individual surface points to maintain unique morphological features of each subject (33, 34). Validity and reliability for mapping the thalamus were established in previous reports (20, 30). Prior to diffeomorphic transformations, anatomic landmarks were placed by expert raters who were blinded to the group status of the scan being landmarked, detailed landmarking procedures can be found in previous publications (32, 33).

Statistical Analyses

Demographic and clinical characteristics were calculated using chi-squared statistics and analysis of variance (ANOVA) models. Group differences in cognition and psychopathology were also evaluated using ANOVA models.

To examine thalamic volume, a repeated-measures ANOVA was used with hemisphere as the within-subjects effect and group as the between-subjects effect. For thalamic shape, deformation values along each surface were calculated as a contrast from the sample mean based on triangulated surface points for all subjects. Next, a principal components analysis (PCA) was used to reduce the high dimensionality of the surfaces, yielding an orthonormal set of eigenvectors that represented variation in the shape of the structures (33). The first 15 eigenvectors of the PCA accounted for more than 90% of total shape variance (across subjects and hemispheres) and used for subsequent statistical modeling. To evaluate thalamic shape differences across groups, a multivariate analysis of variance (MANOVA) model was utilized with shape variation (using all 15 eigenvectors scores averaged across hemispheres) as the dependent variable, and group status (EOS, AOS, and CON) as a fixed effect. If the overall MANOVA statistic was significant, follow-up MANOVA models were used to identify whether specific significant group contrasts existed (EOS vs. CON and AOS vs. CON). For the EOS vs. AOS contrast, a follow-up multivariate analysis of covariance (MANCOVA) model was used to account for the potentially confounding effects of illness duration, medication, and lifetime presence of a substance use disorder, which were included as covariates.

Visualization of group differences in thalamic shape deformation was accomplished by the construction of vertex-wise studentized-t contrast maps of the composite surfaces for each group. Shape displacements were calculated at each surface point as the difference between the means of the group vectors in magnitude and coded using a colored scale; final maps reflected corrected p-values using a familywise error rate approach based on random field theory with a vertex-wise threshold of $p < 0.05$ and a cluster-wise threshold of $p < 0.01$ (35). Inward and outward displacements, or deformations, of the surface were estimated as representations of localized volume loss or exaggeration at the neurobiological level (36).

To evaluate the relationship between thalamic shape and behavioral measures, a canonical score was first computed as a representation of composite shape based on all left-right averaged eigenvectors scores of the thalamus (37). Bivariate Pearson correlation coefficients were then calculated between the thalamic canonical shape score and measures of cognition

(working memory, episodic memory, and executive functioning) and psychopathology (positive, negative, and disorganized symptoms) separately for EOS and AOS groups.

Sensitivity Power Analysis

Sample sizes for the groups were fixed as data was derived from an archival schizophrenia dataset (8, 38). Sensitivity power analyses were calculated for the proposed models above to determine the smallest possible effect that could be detected from the data considering sample size restrictions. Using G*Power (39), it was determined that at 80% power, with a type I error rate of 0.05, and a combined sample of 121, there was power to detect the following minimal Cohen's f effect sizes (40): ANOVA models for cognition = 0.29, and psychopathology = 0.26; thalamic volume RM-ANOVA = 0.28 (group effect). For the thalamic surface shape models, minimum Critical F-values were identified using G*Power for the main group effect given their multivariate nature: Three-group MANOVA = 1.51; 2-group MANOVAs for EOS vs. CON = 1.81, EOS vs. AOS = 1.89, AOS vs. CON = 1.79. For the correlation analyses, at a type I error rate of 0.05, there was 80% power to detect a correlation as large as: $r = \pm 0.37$ in the EOS group ($n = 28$); and $r = \pm 0.34$ in the AOS group ($n = 33$). The sample appears adequately powered to address the proposed research hypotheses, with the ability to, at a minimum, detect moderate effects (41). Cohen's f values were calculated using criteria from Cohen (40) and Lenhard and Lenhard (42).

RESULTS

Demographic, Clinical, and Confounding Variables

Anti-psychotic medication treatment has known effects on brain structure (43), while nicotine has been associated with reduced gray matter density (44), and a history of substance-use disorder can also affect brain morphometry (45). Given these findings, potential group differences for these confounds were examined; demographic and clinical variables are summarized in **Table 1**. Groups differed with respect to nicotine use, and lifetime histories of substance use disorders for alcohol, cannabis, cocaine, opiates, and sedatives. These variables were subsequently examined as fixed effect covariates in EOS vs. AOS linear models, with an aggregate measure (any lifetime history of a substance use disorder = 1, no lifetime history = 0) used for substance use. The EOS and AOS subjects also differed on mean dose years of first-generation antipsychotic treatment using the chlorpromazine equivalent, which was also included as a fixed effect covariate.

Cognition and Psychopathology

Cognition was compared across all three groups using ANOVA models with group as a fixed factor. Results (see **Table 1**) revealed a significant main effect of group for crystallized intelligence ($F_{2,113} = 13.7$, $p < 0.001$, Cohen's $f = -2.6$), working memory ($F_{2,113} = 29.8$, $p < 0.001$, Cohen's $f = 0.65$), episodic memory ($F_{2,113} = 50.5$, $p < 0.001$, Cohen's $f = 0.77$), and executive functioning ($F_{2,113} = 32.6$, $p < 0.001$, Cohen's $f = 0.62$). For all four cognitive domains, CON scored significantly higher than EOS and AOS (all p-values < 0.001). Contrasts between EOS and AOS did not achieve statistical significance (all p-values > 0.10). Results from ANOVA models evaluating EOS and AOS group differences on positive, negative, and disorganized symptoms were all non-significant.

Thalamic Volume Analyses

For the volume of the thalamus, there was a significant main effect for hemisphere ($F_{1,118} = 13.5$, $p < 0.001$), but not for group ($F_{2,118} = 2.93$, $p = 0.06$, Cohen's $f = 0.173$) or a group-by-hemisphere interaction ($F_{2,118} = 0.83$, $p = 0.44$).

Thalamic Shape Analyses

A MANOVA model of thalamic eigenvectors (averaged across hemispheres) revealed an overall significant main effect of group on shape metrics ($F_{2,118} = 2.4$, $p < 0.001$). *Post hoc* comparisons using two-group MANOVA designs found significant differences between EOS ($F_{1,86} = 2.4$, $p = 0.007$) and AOS ($F_{1,91} = 2.6$, $p = 0.003$) versus CON. In the EOS vs. AOS MANCOVA, there was a significant main effect for group ($F_{15,40} = 2.44$, $p = 0.012$), as well as duration of illness ($F_{15,40} = 4.3$, $p < 0.001$), but not first-generation antipsychotic use, cigarette usage, or lifetime presence of a substance use disorder on the model. Notably, all of the significant F-values surpassed the Critical F thresholds calculated from the sensitivity analyses above.

Visualization of RFT-corrected thalamic shape maps (**Figure 1**) revealed that EOS was characterized by prominent inward deformation, indicative of localized volume loss, in ventral lateral and lateral geniculate nuclei, as well as in anterior (right only) and pulvinar nuclei relative to CON (**Figure 1A**). For AOS, notable inward deformations were also observed in pulvinar nuclei in addition to left-sided anterior and lateral regions relative to CON (**Figure 1B**). Regarding the comparison between EOS and AOS, prominent inward deformations in EOS were observed in posterior ventral and left dorsal regions, as well as in the lateral geniculate nuclei (**Figure 1C**).

Correlation Analyses

Calculation of canonical scores for thalamic shape revealed increases in these values equated to greater shape abnormality (i.e., more disparate from the surface shape of the healthy comparison subjects). An outlier canonical score was observed in a single EOS participant (>3 SD above the mean), which was adjusted in to the 3 SD value using Winsorization procedures. In the EOS group, there was an inverse correlation between episodic memory scores and thalamic shape ($r = -0.43$, $p = 0.03$; **Figure 2A**), such that more abnormal thalamic surface shape related to poorer episodic memory performance. In the AOS group, a similar inverse correlation was observed between thalamic shape and working memory ($r = -0.36$, $p = 0.047$; **Figure 2B**) and executive functioning ($r = -0.52$, $p = 0.003$; **Figure 2C**). No other correlations between cognition or psychopathology and brain structure were significant (all p-values > 0.10).

TABLE 1 | Demographic and clinical characteristics of study sample.

	CON (n = 60)		EOS (n = 28)		AOS (n = 33)		Statistic		
	Mean	**(SD)**	**Mean**	**(SD)**	**Mean**	**(SD)**	***F*-test**	**df**	***p***
Age, mean (SD)	36.2	(13.9)	34.7	(14.0)	40.1	(11.7)	1.40	2,118	0.25
Age of illness onset, mean (SD)	–	–	13.8	(3.0)	22.2	(4.1)	81.73	1,60	**<0.001**
Duration of illness, mean (SD)	–	–	21.0	(14.1)	17.9	(12.5)	0.82	1,60	0.37
Cigarette use (cigarettes per year)*	1,389	(2,892)	4,404	(4,699)	5,065	(5,525)	9.98	2,119	**<0.001**
Antipsychotic medication use									
1st-generation (Dose years)	–	–	0.3	(1.1)	3.0	(5.3)	7.36	1,60	**0.009**
2nd-generation (Dose years)	–	–	3.2	(2.9)	3.7	(3.6)	0.30	1,60	0.58
Cognition									
Crystallized IQ†	0.45	(0.87)	−0.39	(1.0)	−0.44	(0.77)	13.6	2,113	**<0.001**
Working memory†	0.38	(0.63)	−0.61	(0.67)	−0.42	(0.55)	29.8	2,113	**<0.001**
Episodic memory†	0.68	(0.66)	−0.56	(0.74)	−0.61	(0.64)	50.5	2,113	**<0.001**
Executive functioning†	0.41	(0.49)	−0.46	(0.76)	−0.57	(0.77)	32.5	2,113	**<0.001**
Psychopathology									
Positive symptoms	–	–	0.31	(0.82)	0.18	(0.84)	0.38	1,60	0.53
Negative symptoms	–	–	0.35	(0.66)	0.41	(0.64)	0.16	1,60	0.68
Disorganized symptoms	–	–	0.17	(0.67)	0.21	(0.56)	0.08	1,60	0.77
	N	**(%)**	***N***	**(%)**	***N***	**(%)**	**X^2**	**df**	***p***
Gender, No. (% male)	36	(60.0%)	17	(60.7%)	21	(63.6%)	0.12	2	0.94
SES class (Class 3)	25	(42.4%)	9	(40.95)	5	(17.2%)	13.56	8	0.94
Substance use disorder									
Alcohol	9	(15.0%)	13	(46.4%)	13	(39.4%)	11.59	2	**0.003**
Cannabis	2	(3.3%)	15	(53.6%)	7	(21.2%)	30.35	2	**<0.001**
Cocaine	1	(1.7%)	9	(32.1%)	2	(6.1%)	20.60	2	**<0.001**
Opiates	1	(1.7%)	4	(14.3%)	1	(3.0%)	6.81	2	**0.03**
Hallucinogens	1	(1.7%)	4	(14.8%)	1	(3.0%)	7.14	2	0.28
Sedatives	1	(1.7%)	5	(18.5%)	2	(6.1%)	8.52	2	**0.01**
Stimulants	1	(1.7%)	1	(3.7%)	2	(6.1%)	1.29	2	0.52

**EOS > CON ($p = 0.002$); AOS > CON ($p < 0.001$).*
†EOS < CON ($p < 0.001$); AOS < CON ($p < 0.001$). Bold = $p < 0.05$ for the overall omnibus model.

DISCUSSION

Age of onset continues to represent an important factor for understanding and conceptualizing the pathology associated with the development of schizophrenia (46). This study sought to examine whether morphological differences of the thalamus, a highly implicated structure in the pathophysiology of psychosis, exist between early-onset and adult-onset schizophrenia in adulthood. Findings revealed a hemispheric difference in thalamic volume, but only modest differences between the schizophrenia and control groups, and no significant differences between EOS and AOS. However, shape analysis revealed significant thalamic abnormalities in EOS relative to CON in multiple anterior, posterior, and lateral regions; with similar patterns observed in AOS relative to CON. Examination of differences between the psychosis groups revealed exaggerated localized volume loss in EOS relative to AOS in ventral posterior and medial regions. Multivariate eigenvector models were also highly significant and support the observed vertex-wise group differences. Finally, unique relationships between shape and cognition were noted in the psychosis groups, with EOS demonstrating increased episodic memory impairment, and AOS worse working memory and executive functions, as thalamic shape became increasingly abnormal. Overall, these findings reveal the exaggerated effects of early-onset psychosis in adulthood on a brain structure critical to the pathophysiology of schizophrenia.

Early-onset schizophrenia is described as a condition with greater developmental and premorbid departures relative to AOS, likely due to a stronger genetic component to their presentation (2). This exacerbated presentation often leads to poorer clinical and cognitive outcomes (47), which has prompted considerations for focused treatments (48). Furthermore, unique brain abnormalities observed in EOS are generally more neurobiologically severe that in AOS (4). Summarized by Brent et al. (49), the most consistent findings include cortical abnormalities of frontal, temporal, and parietal regions, in addition to reduced global cerebral and cerebellar volumes. Furthermore, there is strong support for reduced thalamic volumes in EOS (50–52), with some evidence for progressive

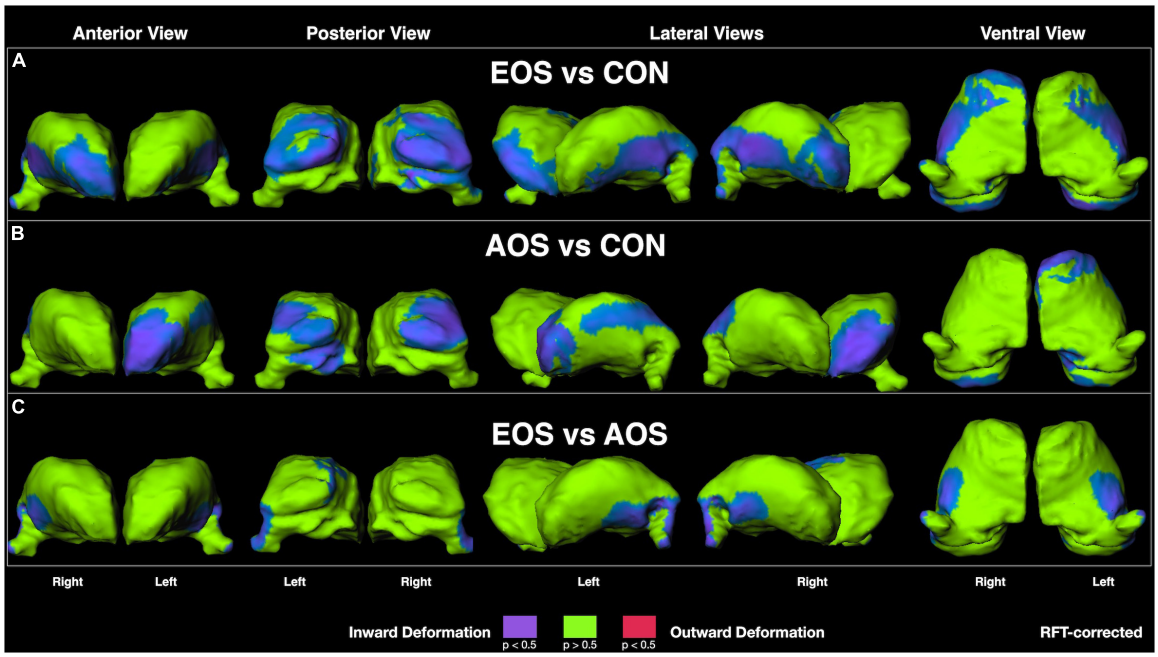

FIGURE 1 | Thalamic surface shape displacement maps between: **(A)** Early-Onset Schizophrenia (EOS) patients and control (CON) participants; **(B)** Adult-Onset Schizophrenia (AOS) patients and CON participants; and **(C)** EOS and AOS patients. Cooler colors indicate significant regions of inward shape differences and warmer colors indicate significant regions of outward shape differences corrected for multiple comparisons using random field theory (RFT).

loss over time (17). While previous work has examined the gross anatomical volumetrics of the thalamus in EOS, the regional specificity of these abnormalities has yet to be characterized. This is especially relevant given the diverse connectivity matrix and unique nuclei specialization contained within the organization of the thalamus (9). Results from the current study revealed distinct patterns of abnormal shape, representative of localized volume loss, in EOS participants relative to AOS and healthy-matched individuals. Specifically, EOS was noted to have widespread inward deformations in ventral lateral regions, lateral geniculate nuclei, and in anterior and pulvinar nuclei relative to CON. The AOS group demonstrated a similar pattern relative to CON, but with more diffuse changes in lateral aspects and relative sparing in right regions. When the schizophrenia groups were compared directly against each other, it was observed EOS showed significant abnormal inward deformation in posterior ventral and dorsal regions, and in the lateral geniculate nucleus. The results suggest a pattern of abnormal thalamic shape in EOS that is similar to, but exacerbated, relative to AOS, which strongly implicates and supports a continuum model for the neurobiology of schizophrenia (53). Our finding is consistent with other neuroimaging work that found cortical gray matter loss in EOS is exaggerated, but mimics that in AOS (54). Furthermore, changes in global gray matter brain volume also support a neurodevelopmental continuum in psychosis as noted in a study examining these features in the offspring of probands with schizophrenia (55). Overall, neuroimaging markers, especially those involved in the pathophysiology of schizophrenia such as the thalamus, appear to be a robust approach for supporting a dimensional model of disease onset in psychosis-spectrum disorders (56).

Our pattern of findings within these onset types are broadly consistent with previous work on thalamic morphology from our group using different derivations of the sample, and include primarily alterations in anterior and posterior extremes in chronic cases (20), and a similar presentation in siblings (30). However, research using different methodology and sample compositions also provide consistent support for our results. For example, a study conducted by Janssen et al. (17) on thalamic volumes in an adolescent sample of male-only early-onset psychosis patients revealed regional volume loss in anterior mediodorsal and pulvinar areas in the right thalamus using a surface-based approach. In addition, using a combined voxel-based morphometry and novel thalamic nuclei segmentation procedure, Huang et al. (57) identified smaller pulvinar volumes in a large sample of youths with psychotic spectrum disorders. And in another recent report, Zhang et al. (58) observed abnormal functional connectivity (both hyper- and hypoconnectivity relative to healthy individuals) in the thalamocortical circuits of an EOS sample that included lateral and mediodorsal nuclei. While there is agreement between the above studies, the absence of anterior and ventral lateral abnormalities which was observed in our work is noted. This discrepancy could reflect the mean age difference in the samples used; as previously noted, our sample consisted of adult-aged EOS subjects while others were of early-onset adolescents. Thus, our findings may reflect an exaggerated pattern of abnormality that occurs as EOS ages into adulthood, which meaningfully

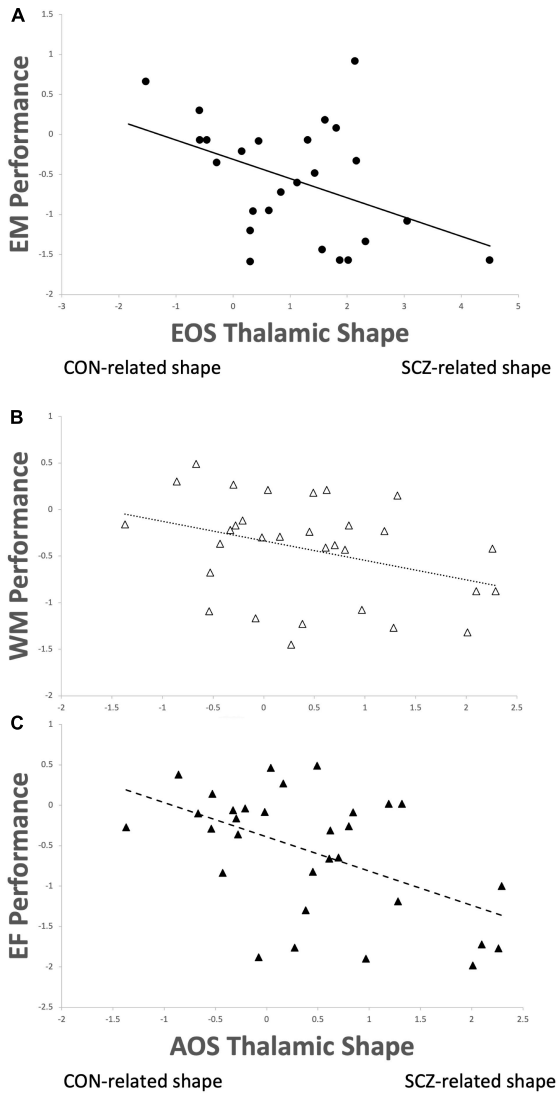

FIGURE 2 | Thalamic shape progressing from healthy control (CON) to schizophrenia (SCZ) correlated with **(A)** poorer episodic memory performance ($r = -0.43$, $p = 0.03$) in early-onset schizophrenia (EOS); **(B)** poorer working memory performance ($r = -0.36$, $p = 0.047$) and **(C)** poorer executive functioning ($r = -0.52$, $p = 0.003$) in adult-onset schizophrenia (AOS).

informs an anticipated trajectory of development for these individuals, particularly in reference to AOS counterparts.

Cognitive dysfunction is a known feature in EOS (59) and has a general profile similar to that observed in AOS (60). We found that across various cognitive domains both EOS and AOS were significantly impaired relative to the healthy control group in crystallized IQ, working memory, episodic memory, and executive functioning, but did not significantly differ from each other in these domains. This is consistent with the known level of impairment observed in previous work on EOS where aspects of working memory, episodic memory and executive functioning are generally impaired to the same degree at AOS (60). The only exception to this literature is we found no difference between groups in crystallized IQ where other studies have found this domain to be more impaired in EOS (60). Again, it is important to note our comparisons were conducted on adult-aged patients, regardless of onset status, the EOS cognitive profiles we examined were ∼20 years post-onset. Work examining the longitudinal course of cognition in EOS as they transition into adulthood observes a broad attenuation of cognitive development relative to peers with no further decline after that (59, 61–63). Thus, it appears cognitive trajectories of EOS mimic that of AOS into adulthood.

Studies of neuroimaging markers for cognitive impairment in AOS are relatively plentiful (64–67), while much fewer have been conducted in EOS (68, 69). The behavioral substrates of affected thalamic nuclei we observed from the unique shape deformation patterns in EOS and AOS suggests these brain features may partially explain their observed cognitive impairment. In particular, higher-order aspects of cognitive control are known to involve the mediodorsal thalamus (70–72), while attentional and memory processes involve the pulvinar (73), and the anterior thalamus is implicated in episodic memory as part of Papez' circuit (74). Clues regarding the relevance of thalamic involvement in cognition are well-detailed in experimental studies of animal mechanisms. For example, interrogations of mediodorsal nuclei in mice has revealed that excitation of this region is critical for sustaining task-related activity of the prefrontal cortex (75), and can also assist in modulating decision-making abnormalities *via* separate pathways between these areas (76). Linking disruption of thalamocortical circuitry with behavioral dysfunction in animal models such as these has yielded new insights into the pathophysiology of schizophrenia (77), and reinforced many findings from human imaging studies such as those described here. As such, abnormalities of the thalamus are increasingly considered putative biomarkers of schizophrenia given their endophenotypic potential with cognitive functioning and predictive ability for functional outcome and disease burden (78). While both EOS and AOS groups in our study demonstrated significant cognitive-thalamic relationships, the nature of these relationships differed. For EOS, it appears thalamic shape abnormalities in combined bilateral pulvinar and ventrolateral, with right anterior regions, strongly related to poorer performance in episodic memory. For AOS it was also bilateral pulvinar, but also left anterior and dorsolateral regions that related to poorer working memory and executive functioning. Given cognitive dysfunction in all these domains is a common feature for both groups, it is interesting to observe that a potential substrate for the impairment was *not* common. The development of brain features in EOS clearly differs from that of AOS, both in pattern and timing (18, 79–81). How these features relate to the maturation of cognitive functioning across childhood, adolescence and eventually adulthood is unclear and not well-studied. Our findings provide some insight into this process insomuch that, at least in adulthood, the possible underlying mechanisms of equivalently observed dysfunction are ultimately separate. This highlights the persistent conversation of heterogeneity in schizophrenia and its relevance to diagnosis, progression, treatment, and outcome (82–85).

One primary limitation to our study was the relatively small sample sizes of each group. To address this we conducted a sensitivity analysis for each model, which revealed sufficient power to detect even small-to-moderate effects in the aforementioned analyses. Given many of the Cohen's *f* effect sizes, critical *F*, and *r* values for the shape MANOVA models and correlations were moderate-to-large, we believe the findings were not likely spurious or underpowered.

CONCLUSION

Our research findings suggest that abnormalities of the thalamus are a prominent feature in both early- and late-onset schizophrenia. Using shape analyses we determined that the region pattern of these abnormalities was relatively similar between the early and late onset groups, occurring primarily in pulvinar, anterior and lateral regions. However, early-onset subjects demonstrated exaggerated abnormalities in ventral, left dorsomedial and lateral geniculate regions relative to adult-onset. Interestingly, abnormal thalamic shape features differentially related to cognition in each group – episodic memory for early-onset and working memory and executive functioning for adult-onset. These differences may be potentially useful as markers to understanding the developmental effects of schizophrenia onset on the neurobiology and cognitive functioning of this condition.

DATA AVAILABILITY STATEMENT

The datasets presented in this study can be found in online repositories. The names of the repository/repositories and accession number(s) can be found below: http://schizconnect.org.

ETHICS STATEMENT

The studies involving human participants were reviewed and approved by the IRB at Washington University in St. Louis, St. Louis, MO, United States. The patients/participants provided their written informed consent to participate in this study.

AUTHOR CONTRIBUTIONS

DC and MS were responsible for study design, data analysis and interpretation, and drafting of the manuscript. CR and PE were responsible for data analysis and manuscript drafting. WC was responsible for manuscript drafting. JC and LW were responsible for study design and data analysis and interpretation. All authors contributed to the article and approved the submitted version.

FUNDING

This work was supported by funding from the National Institutes of Health (R01 MH056584 and P50 MH071616 to JC; R01 MH084803, U01 MH097435, and R01 EB020062 to LW; and NINDS T32 NS047987 to DC) and National Science Foundation (NSF SP0037646 and NSF BCS 1734853 to LW). Funding sources had no further role in study design; collection, analysis, and interpretation of data; writing of the report; and decision to submit the manuscript for publication.

ACKNOWLEDGMENTS

We acknowledge research staff at the Northwestern University Schizophrenia Research Group (NU-SRG) and Conte Center for the Neuroscience of Mental Disorders at Washington University School of Medicine for clinical and neuropsychological assessments, and database management. We also acknowledge the Northwestern University Neuroimaging and Applied Computational Anatomy Laboratory (NIACAL) for image processing.

REFERENCES

1. Douaud G, Mackay C, Andersson J, James S, Quested D, Ray M, et al. Schizophrenia delays and alters maturation of the brain in adolescence. *Brain.* (2009) 132:2437–448. doi: 10.1093/brain/awp126
2. Rapoport JL, Addington AM, Frangou S, Psych MRC. The neurodevelopmental model of schizophrenia: update 2005. *Mol Psychiatr.* (2005) 10:434–49. doi: 10.1038/sj.mp.4001642
3. Watkins JM, Asarnow RF, Tanguay PE. Symptom development in childhood onset schizophrenia. *J Child Psychol Psyc.* (1988) 29:865–78. doi: 10.1111/j.1469-7610.1988.tb00759.x
4. Nicolson R, Lenane M, Hamburger SD, Fernandez T, Bedwell J, Rapoport JL. Lessons from childhood-onset schizophrenia. *Brain Res Rev.* (2000) 31:147–56. doi: 10.1016/s0165-0173(99)00032-6
5. Jacobsen LK, Rapoport JL. Research update: childhood-onset schizophrenia: implications of clinical and neurobiological research. *J Child Psychol Psyc.* (1998) 39:101–13. doi: 10.1111/1469-7610.00305
6. White T, Ho B-C, Ward J, O'Leary D, Andreasen NC. Neuropsychological performance in first-episode adolescents with schizophrenia: a comparison with first-episode adults and adolescent control subjects. *Biol Psychiat.* (2006) 60:463–71. doi: 10.1016/j.biopsych.2006.01.002
7. Andrews J, Wang L, Csernansky JG, Gado MH, Barch DM. Abnormalities of thalamic activation and cognition in schizophrenia. *Am J Psychiat.* (2006) 163:469. doi: 10.1176/appi.ajp.163.3.463
8. Cobia DJ, Smith MJ, Salinas I, Ng C, Gado M, Csernansky JG, et al. Progressive deterioration of thalamic nuclei relates to cortical network decline in schizophrenia. *Schizophr Res.* (2017) 180:27.
9. Halassa MM, Sherman SM. Thalamocortical circuit motifs: a general framework. *Neuron.* (2019) 103:762–70. doi: 10.1016/j.neuron.2019.06.005
10. Byne W, Hazlett EA, Buchsbaum MS, Kemether E. The thalamus and schizophrenia: current status of research. *Acta Neuropathol.* (2009) 117:368. doi: 10.1007/s00401-008-0404-0
11. Deck M, Lokmane L, Chauvet S, Mailhes C, Keita M, Niquille M, et al. Pathfinding of corticothalamic axons relies on a rendezvous with thalamic projections. *Neuron.* (2013) 77:484. doi: 10.1016/j.neuron.2012.11.031
12. Greenstein DK, Lerch J, Shaw P, Clasen L, Giedd J, Gochman P, et al. Childhood onset schizophrenia: cortical brain abnormalities as young adults. *J Child Psychol Psyc.* (2006) 47:1012. doi: 10.1111/j.1469-7610.2006.01658.x

13. Giedd JN, Jeffries NO, Blumenthal J, Castellanos FX, Vaituzis AC, Fernandez T, et al. Childhood-onset schizophrenia: progressive brain changes during adolescence. *Biol Psychiat.* (1999) 46:892–8. doi: 10.1016/s0006-3223(99)00072-4
14. Johnson SLM, Wang L, Alpert KI, Greenstein D, Clasen L, Lalonde F, et al. Hippocampal shape abnormalities of patients with childhood-onset schizophrenia and their unaffected siblings. *J Am Acad Child Adolesc Psychiatry.* (2013) 52:527.e–36.e. doi: 10.1016/j.jaac.2013.02.003
15. Sowell ER, Levitt J, Thompson PM, Holmes CJ, Blanton RE, Kornsand DS, et al. Brain abnormalities in early-onset schizophrenia spectrum disorder observed with statistical parametric mapping of structural magnetic resonance images. *Am J Psychiat.* (2000) 157:1475–84. doi: 10.1176/appi.ajp.157.9.1475
16. Sowell ER, Toga AW, Asarnow R. Brain abnormalities observed in childhood-onset schizophrenia: a review of the structural magnetic resonance imaging literature. *Ment Retard Dev D R.* (2000) 6:180–5. doi: 10.1002/1098-2779(2000)6:3<180::AID-MRDD5>3.0.CO;2-I
17. Janssen J, Alemán-Goméz Y, Reig S, Schnack HG, Parellada M, Graell M, et al. Regional specificity of thalamic volume deficits in male adolescents with early-onset psychosis. *Brit J Psychiat.* (2012) 200:30–6. doi: 10.1192/bjp.bp.111.093732
18. Gurholt TP, Lonning V, Nerland S, Jørgensen KN, Haukvik UK, Alloza C, et al. Intracranial and subcortical volumes in adolescents with early-onset psychosis: a multisite mega-analysis from the ENIGMA consortium. *Hum Brain Mapp.* (2020) 43:373–84. doi: 10.1002/hbm.25212
19. Zhou H, Shi L, Shen Y, Fang Y, He Y, Li H, et al. Altered topographical organization of grey matter structural network in early-onset schizophrenia. *Psychiat Res Neuroimaging.* (2021) 316:111344. doi: 10.1016/j.pscychresns.2021.111344
20. Csernansky JG, Schindler MK, Splinter NR, Wang L, Gado M, Selemon LD, et al. Abnormalities of thalamic volume and shape in schizophrenia. *Am J Psychiat.* (2004) 161:896–902. doi: 10.1176/appi.ajp.161.5.896
21. Cobia DJ, Smith MJ, Wang L, Csernansky JG. Longitudinal progression of frontal and temporal lobe changes in schizophrenia. *Schizophr Res.* (2012) 139:6. doi: 10.1016/j.schres.2012.05.002
22. Haren NEM, van Schnack HG, Cahn W, Heuvel MP, van den Lepage C, Collins L, et al. Changes in cortical thickness during the course of illness in schizophrenia. *Arch Gen Psychiat.* (2011) 68:880. doi: 10.1001/archgenpsychiatry.2011.88
23. Delawalla Z, Barch DM, Eastep JLF, Thomason ES, Hanewinkel MJ, Thompson PA, et al. Factors mediating cognitive deficits and psychopathology among siblings of individuals with schizophrenia. *Schizophrenia Bull.* (2006) 32:537. doi: 10.1093/schbul/sbj082
24. Spitzer M, Robert L, Gibbon M, Williams J. *Structured Clinical Interview for DSM-IV-TR Axis I Disorders, Research Version, Non-patient Edition (SCID-I/NP)*. New York, NY: New York State Psychiatric Institute (2002).
25. Andreasen NC, Pressler M, Nopoulos P, Miller D, Ho B-C. Antipsychotic dose equivalents and dose-years: a standardized method for comparing exposure to different drugs. *Biol Psychiat.* (2010) 67:262. doi: 10.1016/j.biopsych.2009.08.040
26. Sullivan EV, Rosenbloom MJ, Lim KO, Pfefferbaum A. Longitudinal changes in cognition, gait, and balance in abstinent and relapsed alcoholic men: relationships to changes in brain structure. *Neuropsychology.* (2000) 14:188. doi: 10.1037//0894-4105.14.2.178
27. Skinner HA. *Development and Validation of a Lifetime Alcohol Consumption Assessment Procedure*. Toronto, ON: Addiction Research Foundation Substudy (1982).
28. Nuechterlein KH, Barch DM, Gold JM, Goldberg TE, Green MF, Heaton RK. Identification of separable cognitive factors in schizophrenia. *Schizophr Res.* (2004) 72:39. doi: 10.1016/j.schres.2004.09.007
29. Andreasen NC. *Scale for the Assessment of Positive Symptoms*. Iowa City, IA: University of Iowa (1984).
30. Harms MP, Wang L, Mamah D, Barch DM, Thompson PA, Csernansky JG. Thalamic shape abnormalities in individuals with schizophrenia and their nonpsychotic siblings. *J Neurosci.* (2007) 27:13842. doi: 10.1523/jneurosci.2571-07.2007
31. Buckner RL, Head D, Parker J, Fotenos AF, Marcus D, Morris JC, et al. A unified approach for morphometric and functional data analysis in young, old, and demented adults using automated atlas-based head size normalization: reliability and validation against manual measurement of total intracranial volume. *Neuroimage.* (2004) 23:738. doi: 10.1016/j.neuroimage.2004.06.018
32. Csernansky JG, Wang L, Joshi SC, Ratnanather JT, Miller MI. Computational anatomy and neuropsychiatric disease: probabilistic assessment of variation and statistical inference of group difference, hemispheric asymmetry, and time-dependent change. *Neuroimage.* (2004) 23:S5668. doi: 10.1016/j.neuroimage.2004.07.025
33. Beg M, Miller M, Trouvé A, Younes L. Computing large deformation metric mappings *via* geodesic flows of diffeomorphisms. *Int J Comput Vis.* (2005) 61:139–57. doi: 10.1023/b:visi.0000043755.93987.aa
34. Miller MI, Trouvé A, Younes L. On the metrics of euler-lagrange equations of computational anatomy. *Annu Rev Biomed Eng.* (2002) 4:375–405. doi: 10.1146/annurev.bioeng.4.092101.125733
35. Flandin G, Friston KJ. Topological Inference. In: Toga W editor. *Methods and Modeling*. Waltham: Academic Press (2015). p. 495–500. doi: 10.1016/b978-0-12-397025-1.00322-5
36. Hanko V, Apple AC, Alpert KI, Warren KN, Schneider JA, Arfanakis K, et al. In vivo hippocampal subfield shape related to TDP-43, amyloid beta, and tau pathologies. *Neurobiol Aging.* (2019) 74:181. doi: 10.1016/j.neurobiolaging.2018.10.013
37. Wang L, Mamah D, Harms MP, Karnik M, Price JL, Gado MH, et al. Progressive deformation of deep brain nuclei and hippocampal-amygdala formation in schizophrenia. *Biol Psychiat.* (2008) 64:1060–8. doi: 10.1016/j.biopsych.2008.08.007
38. Womer FY, Wang L, Alpert KI, Smith MJ, Csernansky JG, Barch DM, et al. Basal ganglia and thalamic morphology in schizophrenia and bipolar disorder. *Psychiat Res Neuroimaging.* (2014) 223:83. doi: 10.1016/j.pscychresns.2014.05.017
39. Faul F, Erdfelder E, Lang A-G, Buchner A. G*Power 3: a flexible statistical power analysis program for the social, behavioral, and biomedical sciences. *Behav Res Methods.* (2007) 39:175–91. doi: 10.3758/bf03193146
40. Cohen J. *Statistical Power Analysis for the Behavioral Sciences*. Amsterdam: Elsevier Science (2013).
41. Selya AS, Rose JS, Dierker LC, Hedeker D, Mermelstein RJ. A practical guide to calculating cohen's F2, a measure of local effect size, from PROC MIXED. *Front Psychol.* (2012) 3:111. doi: 10.3389/fpsyg.2012.00111
42. Lenhard W, Lenhard A. *Calculation of Effect Sizes*. (2016). Available online at: https://www.psychometrica.de/effect_size.html (accessed July 15, 2020).
43. Voineskos AN, Mulsant BH, Dickie EW, Neufeld NH, Rothschild AJ, Whyte EM, et al. Effects of antipsychotic medication on brain structure in patients with major depressive disorder and psychotic features. *JAMA Psychiat.* (2020) 77:36. doi: 10.1001/jamapsychiatry.2020.0036
44. Swan GE, Lessov-Schlaggar CN. The effects of tobacco smoke and nicotine on cognition and the brain. *Neuropsychol Rev.* (2007) 17:273. doi: 10.1007/s11065-007-9035-9
45. Smith MJ, Cobia DJ, Reilly JL, Gilman JM, Roberts AG, Alpert KI, et al. Cannabis-related episodic memory deficits and hippocampal morphological differences in healthy individuals and schizophrenia subjects. *Hippocampus.* (2015) 25:1042–51. doi: 10.1002/hipo.22427
46. DeLisi LE. The significance of age of onset for schizophrenia. *Schizophrenia Bull.* (1992) 18:209–15. doi: 10.1093/schbul/18.2.209
47. Schimmelmann BG, Conus P, Cotton S, McGorry PD, Lambert M. Pre-treatment, baseline, and outcome differences between early-onset and adult-onset psychosis in an epidemiological cohort of 636 first-episode patients. *Schizophr Res.* (2007) 95:1–8. doi: 10.1016/j.schres.2007.06.004
48. Giannitelli M, Consoli A, Raffin M, Jardri R, Levinson DF, Cohen D, et al. An overview of medical risk factors for childhood psychosis: implications for research and treatment. *Schizophr Res.* (2018) 192:39–49. doi: 10.1016/j.schres.2017.05.011
49. Brent BK, Thermenos HW, Keshavan MS, Seidman LJ. Gray matter alterations in schizophrenia high-risk youth and early-onset schizophrenia a review of structural MRI findings. *Child Adol Psych Cl.* (2013) 22:689–714. doi: 10.1016/j.chc.2013.06.003
50. James AC, James S, Smith DM, Javaloyes A. Cerebellar, prefrontal cortex, and thalamic volumes over two time points in adolescent-onset schizophrenia. *Am J Psychiat.* (2004) 161:1029. doi: 10.1176/appi.ajp.161.6.1023
51. Frazier JA, Giedd JN, Hamburger SD, Albus KE, Kaysen D, Vaituzis AC, et al. Brain anatomic magnetic resonance imaging in childhood-onset

schizophrenia. *Arch Gen Psychiat.* (1996) 53:617. doi: 10.1001/archpsyc.1996.01830070065010
52. Rapoport JL, Giedd J, Kumra S, Jacobsen L, Smith A, Lee P, et al. Childhood-onset schizophrenia: progressive ventricular change during adolescence. *Arch Gen Psychiat.* (1997) 54:897–903. doi: 10.1001/archpsyc.1997.01830220013002
53. DeRosse P, Karlsgodt KH. Examining the psychosis continuum. *Curr Behav Neurosci Rep.* (2015) 2:80–9. doi: 10.1007/s40473-015-0040-7
54. Gogtay N. Cortical brain development in schizophrenia: insights from neuroimaging studies in childhood-onset schizophrenia. *Schizophrenia Bull.* (2008) 34:36. doi: 10.1093/schbul/sbm103
55. Sugranyes G, de la Serna E, Borras R, Sanchez-Gistau V, Pariente JC, Romero S, et al. Clinical, cognitive, and neuroimaging evidence of a neurodevelopmental continuum in offspring of probands with schizophrenia and bipolar disorder. *Schizophrenia Bull.* (2017) 43:1208–19. doi: 10.1093/schbul/sbx002
56. Driver DI, Gogtay N, Rapoport JL. Childhood onset schizophrenia and early onset schizophrenia spectrum disorders. *Child Adol Psych.* (2013) 22:539–55. doi: 10.1016/j.chc.2013.04.001
57. Huang AS, Rogers BP, Sheffield JM, Jalbrzikowski ME, Anticevic A, Blackford JU, et al. Thalamic nuclei volumes in psychotic disorders and in youths with psychosis spectrum symptoms. *Am J Psychiat.* (2020) 177:1159–67. doi: 10.1176/appi.ajp.2020.19101099
58. Zhang M, Palaniyappan L, Deng M, Zhang W, Pan Y, Fan Z, et al. Abnormal thalamocortical circuit in adolescents with early-onset schizophrenia. *J Am Acad Child Adolesc Psychiat.* (2020) 60:903. doi: 10.1016/j.jaac.2020.07.903
59. Frangou S. Neurocognition in early-onset schizophrenia. *Child Adol Psych.* (2013) 22:715–26. doi: 10.1016/j.chc.2013.04.007
60. Harvey PD, Isner EC. Cognition, social cognition, and functional capacity in early-onset schizophrenia. *Child Adol Psych Cl.* (2020) 29:171–82.
61. Frangou S, Hadjulis M, Vourdas A. The maudsley early onset schizophrenia study: cognitive function over a 4-year follow-up period. *Schizophrenia Bull.* (2008) 34:52–9. doi: 10.1093/schbul/sbm124
62. Juuhl-Langseth M, Holmén A, Thormodsen R, Øie M, Rund BR. Relative stability of neurocognitive deficits in early onset schizophrenia spectrum patients. *Schizophr Res.* (2014) 156:241–7. doi: 10.1016/j.schres.2014.04.014
63. Øie MG, Sundet K, Haug E, Zeiner P, Klungsøyr O, Rund BR. Cognitive performance in early-onset schizophrenia and attention-deficit/hyperactivity disorder: a 25-year follow-up study. *Front Psychol.* (2021) 11:606365. doi: 10.3389/fpsyg.2020.606365
64. Glahn DC, Ragland JD, Abramoff A, Barrett J, Laird AR, Bearden CE, et al. Beyond hypofrontality: a quantitative meta-analysis of functional neuroimaging studies of working memory in schizophrenia. *Hum Brain Mapp.* (2005) 25:69. doi: 10.1002/hbm.20138
65. Minzenberg MJ, Laird AR, Thelen S, Carter CS, Glahn DC. Meta-analysis of 41 functional neuroimaging studies of executive function in schizophrenia. *Arch Gen Psychiat.* (2009) 66:822. doi: 10.1001/archgenpsychiatry.2009.91
66. Goghari VM III, Macdonald AW, Sponheim SR. Relationship between prefrontal gray matter volumes and working memory performance in schizophrenia: a family study. *Schizophr Res.* (2014) 153:121. doi: 10.1016/j.schres.2014.01.032
67. Ehrlich S, Brauns S, Yendiki A, Ho B-C, Calhoun V, Schulz SC, et al. Associations of cortical thickness and cognition in patients with schizophrenia and healthy controls. *Schizophrenia Bull.* (2012) 38:1062.
68. Tamnes CK, Agartz I. White matter microstructure in early-onset schizophrenia: a systematic review of diffusion tensor imaging studies. *J Am Acad Child Adolesc Psychiat.* (2016) 55:269–79. doi: 10.1016/j.jaac.2016.01.004
69. Arsalidou M, Yaple Z, Jurcik T, Ushakov V. Cognitive brain signatures of youth with early onset and relatives with schizophrenia: evidence from FMRI meta-analyses. *Schizophrenia Bull.* (2020) 46:857–68. doi: 10.1093/schbul/sbz130
70. Ferguson B, Delevich K. Mediodorsal thalamus and prefrontal cortex: specialized partners in cognitive control. *J Neurosci.* (2020) 40:5515–7. doi: 10.1523/jneurosci.0820-20.2020
71. Halassa MM, Kastner S. Thalamic functions in distributed cognitive control. *Nat Neurosci.* (2017) 20:1679. doi: 10.1038/s41593-017-0020-1
72. Phillips JM, Fish LR, Kambi NA, Redinbaugh MJ, Mohanta S, Kecskemeti SR, et al. Topographic organization of connections between prefrontal cortex and mediodorsal thalamus: evidence for a general principle of indirect thalamic pathways between directly connected cortical areas. *Neuroimage.* (2019) 189:846. doi: 10.1016/j.neuroimage.2019.01.078
73. Guedj C, Vuilleumier P. Functional connectivity fingerprints of the human pulvinar: decoding its role in cognition. *Neuroimage.* (2020) 221:117162. doi: 10.1016/j.neuroimage.2020.117162
74. Nishio Y, Hashimoto M, Ishii K, Ito D, Mugikura S, Takahashi S, et al. Multiple thalamo-cortical disconnections in anterior thalamic infarction: implications for thalamic mechanisms of memory and language. *Neuropsychologia.* (2014) 53:273. doi: 10.1016/j.neuropsychologia.2013.11.025
75. Schmitt LI, Wimmer RD, Nakajima M, Happ M, Mofakham S, Halassa MM. Thalamic amplification of cortical connectivity sustains attentional control. *Nature.* (2017) 545:219–23. doi: 10.1038/nature22073
76. Mukherjee A, Lam NH, Wimmer RD, Halassa MM. Thalamic circuits for independent control of prefrontal signal and noise. *Nature.* (2021) 600:100–4. doi: 10.1038/s41586-021-04056-3
77. Schmitt LI, Halassa MM. Interrogating the mouse thalamus to correct human neurodevelopmental disorders. *Mol Psychiatr.* (2017) 22:183–91. doi: 10.1038/mp.2016.183
78. Steullet P. Thalamus-related anomalies as candidate mechanism-based biomarkers for psychosis. *Schizophr Res.* (2020) 226:147–57. doi: 10.1016/j.schres.2019.05.027
79. Kyriakopoulos M, Frangou S. Pathophysiology of early onset schizophrenia. *Int Rev Psychiatr.* (2009) 19:315–24. doi: 10.1080/09540260701486258
80. Toga AW, Thompson PM, Sowell ER. Mapping brain maturation. *Trends Neurosci.* (2006) 29:148–59. doi: 10.1016/j.tins.2006.01.007
81. Chung Y, Allswede D, Addington J, Bearden CE, Cadenhead K, Cornblatt B, et al. Cortical abnormalities in youth at clinical high-risk for psychosis: findings from the NAPLS2 cohort. *Neuroimage Clin.* (2019) 23:101862. doi: 10.1016/j.nicl.2019.101862
82. Wolfers T, Rokicki J, Alnæs D, Berthet P, Agartz I, Kia SM, et al. Replicating extensive brain structural heterogeneity in individuals with schizophrenia and bipolar disorder. *Hum Brain Mapp.* (2021) 42:2546–55. doi: 10.1002/hbm.25386
83. Mizuno Y, McCutcheon RA, Brugger SP, Howes OD. Heterogeneity and efficacy of antipsychotic treatment for schizophrenia with or without treatment resistance: a meta-analysis. *Neuropsychopharmacol.* (2019) 45:622–31. doi: 10.1038/s41386-019-0577-3
84. Fusar-Poli P, Cappucciati M, Borgwardt S, Woods SW, Addington J, Nelson B, et al. Heterogeneity of psychosis risk within individuals at clinical high risk: a meta-analytical stratification. *JAMA Psychiat.* (2016) 73:120. doi: 10.1001/jamapsychiatry.2015.2324
85. Collado-Torres L, Burke EE, Peterson A, Shin J, Straub RE, Rajpurohit A, et al. Regional heterogeneity in gene expression, regulation, and coherence in the frontal cortex and hippocampus across development and schizophrenia. *Neuron.* (2019) 103:203216.e8. doi: 10.1016/j.neuron.2019.05.013

Conflict of Interest: JC is a consultant for Indivior Pharmaceuticals. DC is a consultant for Sage Pharmaceuticals.

The remaining authors declare that the research was conducted in the absence of any commercial or financial relationships that could be construed as a potential conflict of interest.

Publisher's Note: All claims expressed in this article are solely those of the authors and do not necessarily represent those of their affiliated organizations, or those of the publisher, the editors and the reviewers. Any product that may be evaluated in this article, or claim that may be made by its manufacturer, is not guaranteed or endorsed by the publisher.

frontiers | Frontiers in Psychiatry

ORIGINAL RESEARCH
published: 07 July 2022
doi: 10.3389/fpsyt.2022.925204

Abnormal Brain Structure Morphology in Early-Onset Schizophrenia

Jia Cai[1†], Wei Wei[1†], Liansheng Zhao[1], Mingli Li[1], Xiaojing Li[1], Sugai Liang[2], Wei Deng[2], Xiang Dong Du[3], Qiang Wang[1], Wan-jun Guo[1], Xiaohong Ma[1], Pak C. Sham[4,5,6] and Tao Li[1,2]*

[1] Mental Health Center, West China Hospital of Sichuan University, Chengdu, China, [2] Affiliated Mental Health Center & Hangzhou Seventh People's Hospital, Zhejiang University School of Medicine, Hangzhou, China, [3] Suzhou Psychiatry Hospital, Affiliated Guangji Hospital of Soochow University, Suzhou, China, [4] Department of Psychiatry, Li Ka Shing Faculty of Medicine, The University of Hong Kong, Hong Kong SAR, China, [5] Center for PanorOmic Sciences, The University of Hong Kong, Hong Kong SAR, China, [6] State Key Laboratory of Brain and Cognitive Sciences, The University of Hong Kong, Hong Kong SAR, China

OPEN ACCESS

Edited by:
Roberto Canitano,
Siena University Hospital, Italy

Reviewed by:
Haisan Zhang,
Second Affiliated Hospital of Xinxiang Medical University, China
Francois Maurice Lalonde,
National Institute of Mental Health (NIH), United States

***Correspondence:**
Tao Li
litaozjusc@zju.edu.cn

[†] These authors have contributed equally to this work and share first authorship

Specialty section:
This article was submitted to Child and Adolescent Psychiatry, a section of the journal Frontiers in Psychiatry

Received: 21 April 2022
Accepted: 31 May 2022
Published: 07 July 2022

Citation:
Cai J, Wei W, Zhao L, Li M, Li X, Liang S, Deng W, Du XD, Wang Q, Guo W-j, Ma X, Sham PC and Li T (2022) Abnormal Brain Structure Morphology in Early-Onset Schizophrenia. Front. Psychiatry 13:925204. doi: 10.3389/fpsyt.2022.925204

With less exposure to environmental and medication influences, individuals with early-onset schizophrenia (EOS) may provide valuable evidence to study the pathogenesis and phenotypic pattern of schizophrenia.T1-weighted magnetic resonance images were collected in 60 individuals with EOS and 40 healthy controls. Voxel-based morphometry and surface-based morphometry analyzes were performed. Gray matter volume, cortical thickness and cortical surface area were compared between the EOS and healthy controls and among schizophrenia subgroups (with or without family history of schizophrenia). Compared with healthy controls, the EOS group had reduced gray matter volume in the bilateral middle temporal gyrus and reduced cortical thickness in several brain regions. The sporadic early onset schizophrenia and the familial early onset schizophrenia showed different brain structure morphology. These findings suggest that abnormal brain structure morphology, especially in the temporal and frontal lobes, may be an important pathophysiological feature of EOS.

Keywords: schizophrenia, MRI, early onset, cerebral cortex, gray matter

INTRODUCTION

Schizophrenia is a group of severe psychiatric disorders with unknown etiology. Individuals who are diagnosed with schizophrenia before the age of 18 years are defined as having early-onset schizophrenia (EOS) (1). The prevalence of EOS accounts for approximately 4–5% of all schizophrenia cases (2). EOS shows more severe symptoms, a longer duration of untreated illness, and a poorer response to medication than adult-onset schizophrenia (AOS) (3). With relatively little exposure to the environment and medication, people with EOS may be a source of valuable evidence regarding the pathogenesis and phenotypic pattern of schizophrenia.

In the effort understand the etiology of schizophrenia, there has been increasing focus on structural brain abnormalities in schizophrenia, as evidenced by a large number of magnetic resonance imaging (MRI) studies. There are fewer studies on EOS than on AOS. Previous studies reported decreased grey matter volume (GMV) in the frontal, temporal and parietal lobes in EOS (4, 5). However, some studies found increased GMV in the temporal lobe (6), whereas others did

not find any change (7). Abnormal cortical thickness and cortical surface area in people with EOS were also reported (8–10). A cross-sectional study found that the average cortical thickness of the EOS group was significantly thinner (7.5%) than that of healthy controls (HCs) (11). Later studies showed reduced cortical thickness in the frontal and temporal lobes in the EOS group (12, 13). Reduced cortical thickness in the parietal lobe, corpus callosum, hippocampus and posterior central gyrus has also been reported (14, 15). Healthy siblings of those with EOS also showed a pattern of reduced cortical thickness in the frontal, temporal, and parietal lobes (16). Although these are promising findings, the evidence supporting abnormal brain structure morphology in EOS remains equivocal. There are several possible reasons for this. First, most studies included small sample sizes, which limited the statistical power. Second, the diagnosis categories and the age range of participants varied in the studies. For example, some studies included other mental disorders, such as bipolar disorder or schizoaffective disorder, while some studies included subjects with a wide range of ages or included subjects who developed the disorder before the age of 18 years but were adults when participating in the study (17). Third, a relatively long course of illness and antipsychotic medications may affect the structure of the brain (12, 13). Therefore, brain structure morphology in EOS has yet to be confirmed.

Genetic factors play an important role in the pathogenesis of schizophrenia (18). Individuals with familial schizophrenia (FSP) and those with sporadic schizophrenia (SSP) showed different brain structure/functional connectivity, although the findings were inconsistent (19–22). No studies thus far have explored whether the presence of a family history of schizophrenia causes differences in brain structure in EOS. In the study, we conducted an exploratory analysis of this possibility.

To address the above questions, we included a relatively large sample of people with EOS whose average age was 14 years; most of them had received low-dose antipsychotics for less than a week and had a short disease duration, i.e., less than 6 months. Voxel-based morphometry (VBM) is the most commonly used algorithm in the study of GMV (23). As an alternative method, surface-based morphometry (SBM) can detect changes in the cerebral grey matter (GM), and it can also provide an independent definition of GM thinning and regional surface area change (24). In this study, we combined VBM and SBM analyzes to explore the macrostructural changes in the EOS group in a Han Chinese population and to further conduct an exploratory analysis on whether a family history of psychiatric disorder was related to the severity of abnormalities in brain structure morphology.

MATERIALS AND METHODS

Participants

Sixty-six participants with EOS were recruited from inpatient and outpatient psychiatric units at West China Hospital, Sichuan University. Diagnosis was made according to DSM-IV criteria. All participants were interviewed using the Structured Clinical Interview for the DSM-IV (SCID-P). Subjects also underwent further clinical evaluation by using the Positive and Negative Syndrome Scale (PANSS) (25). Six subjects were excluded due to poor-quality MRI scans. The psychiatric history of each subject was reviewed to exclude those with a previous history of any major psychiatric disorder, including psychotic, affective and schizoaffective disorders; head trauma; substance use disorder; or neurological disorders. All participants were followed up for at least 6 months to ensure the diagnosis. Twenty-one out of 60 participants with EOS were naive to drug treatment at the time of MRI scanning, and the remaining 39 had been treated with second-generation antipsychotics at a low dosage (average daily dose equivalent of 5.32 mg olanzapine). Of the 39 treated individuals, 27 had taken drugs for less than a week, 9 for a week to a month, and 3 for one to three months.

Healthy controls ($n = 44$) were recruited from ordinary primary/secondary schools in Chengdu. They were screened by the Mini International Neuropsychiatric Interview for Children and Adolescents (MINI-Kid) to exclude psychiatric disorders. Subjects were excluded if a first/second/third-degree relative suffered from any mental disorders. Four HCs were excluded due to poor-quality MRI. All participants were right-handed (Annett Handedness Scale (26)).

A family history of schizophrenia was obtained by interviewing each participant, both parents, and other first-degree relatives where possible; all interviewees provided detailed information on family history during the clinical interview. This study adopted the definition of family history as described by Xu et al. (27). Familial early-onset schizophrenia (FEOS) was defined as having at least one relative with schizophrenia among their first-, second- or third-degree relatives; otherwise, they were defined as sporadic early-onset schizophrenia (SEOS). Within the FEOS group ($n = 11$), 5 had first-degree relatives, 5 had second-degree relatives, and the other had third-degree relatives with a history of schizophrenia.

Written informed consent was obtained from the parents and the subjects with consenting capacity. This study complied with the content and requirements of the Helsinki Declaration and was reviewed and approved by the Medical Ethics Committee of West China Hospital of Sichuan University.

MRI Scans

All participants underwent MRI scanning in the Department of Radiology at West China Hospital using a Signa 3.0 T scanner (Achieva, Philips, Netherlands). Foam padding and earplugs were used to reduce head movement and scanner noise. A number of pulse sequences [T2-weighted and two-dimensional (2D), fluid-attenuated inversion recovery (FLAIR)] and image contrasts were collected for clinical review. T1w images were acquired by a magnetization-prepared rapid-acquisition gradient-echo (MPRAGE) sequence: repetition time (TR): 8.1 ms, echo time (TE): 3.7 ms, inversion time (TI): 1072.4 ms, flip angle: 7°, slice thickness: 1 mm (no slice gap), 188 axial slices, matrix size: 256 × 256, field of view (FOV): 256 × 256 mm, and voxel size: 1 × 1 × 1 mm. Slice orientation:sagittal, the phase encode directions:anterior to posterior.T2w images were acquired by a turbo spin-echo sequence: TR: 2500 ms, TE: 261 ms, f lip angle: 90°, slice thickness: 1 mm (no slice gap), 180 axial slices, matrix

size: 256 × 256, FOV: 256 × 256 mm, voxel size: 1 × 1 × 1 mm, with strong fat suppression.

Image Processing: Voxel-Based Morphometry

Image files in DICOM format were transformed to NIfTI format using MRI Convert software[1]. The 3D T1-weighted images were processed using voxel-based morphometry-diffeomorphic anatomical registration through exponentiated Lie algebra (VBM-DARTEL) in SPM12[2] software and run on the MATLAB (R2017a) platform. The preprocessing steps were as follows: (1) Coordinates: The position of the slice passing through the anterior commissure and posterior commissure was defined as zero; (2) New segment: GM was automatically segmented using tissue signal intensity values or tissue priors for the distribution of brain tissue type (such as gray matter, white matter and cerebrospinal fluid), and GM/white matter images were averaged automatically; (3) Run DARTEL (Create Templates): using the average image as the initial template, the GM images of the subjects were registered with the template, and then the images were averaged to obtain the template for the next iteration. This process was repeated until an optimal template was obtained; (4) Normalize to Montreal Neurological Institute (MNI) space: performing an affine transformation of segmented brain maps into the MNI space(modulation was performed); and (5) Smooth: images were smoothed with an 8 mm × 8 mm × 8 mm full width at half maximum (FWHM) Gaussian kernel.

Image Processing: FreeSurfer

FreeSurfer's (v6.0)[3] standard automatic reconstruction algorithm was used to segment GM/white matter (WM) and reconstruct cortical surfaces. The preprocessing steps included normalization of tissue intensity heterogeneity, removal of non-brain tissue, and segmentation of GM/WM tissue. Each image was carefully inspected, and any segmentation errors were manually corrected by a trained investigator who was blinded to the subject groups. Then, the segmentation calculation was performed again, and the cortex was reorganized by registration with a standard brain template. After reconstruction, it was registered on the sphere template (Fsaverage template) and smoothed with a 10 mm × 10 mm × 10 mm FWHM Gaussian kernel. The Fsaverage Template was used because previous work has found it is suitable for the age range of young samples (28, 29).

Statistical Analyzes

Statistical analysis was performed with the Statistical Package for the Social Sciences (SPSS 22.0 for Windows, IBM Corp., Armonk, NY, United States). Chi-square tests, Student's *t*-tests and analysis of variance (ANOVA) were used to compare the distribution and differences of categorical and continuous data, respectively. Mann-Whitney U test was used to compare the difference of disease course, medication time, equal effective dose of olanzapine between FEOS and SEOS group.

First, the comparison of GMV between the EOS and HCs was performed by using two-sample *t*-tests on the statistical parametric maps with sex, age, and total brain volume as covariates. Then, GMV was compared among the FEOS, SEOS, and HC groups by using the analysis of ANOVA, with sex, age, and total brain volume as covariates. Each individual cluster that showed significant differences among groups was defined as a region of interest (ROI). The ROI then was used as explicit mask to compared between groups by using two-sample *t*-tests. We set the significant differences at the threshold of $p < 0.001$ at the voxel level and l$p < 0.05$ at a FDR corrected cluster level.

Second, we used FreeSurfer's general linear model to compare cortical thickness and surface area between people with EOS and HCs, with sex and age as covariates. Then cortical thickness and surface area were compared among the FEOS, SEOS, and HC groups by using the analysis of ANOVA, with sex, and age as covariates. The difference was statistically significant when $p < 0.001$ at the vertex level and $p < 0.05$ at the cluster level after family wise error (FWE) correction.

Each individual cluster that showed significant differences between groups was defined as a region of interest (ROI). The GMV/cortical thickness of individual ROIs was extracted from each subject. We used Spearman's rho to explore the association between symptoms (i.e., PANSS subscores) and the values of ROIs. Given that we conducted 3 groups comparisons for each hemisphere ($0.005 < 0.05/6$), we employed the $p < 0.005$ threshold for the correlational analyzes to control for type II errors in these analyzes (12 tests in 2 groups for each hemisphere).

RESULTS

Demographic Characteristics

The demographic characteristics of the participants are shown in **Table 1** (EOS and HCs) and **Table 2** (FEOS, SEOS, and HCs). There were no significant differences in age (range = 10–16 years; $T = 1.862$, $p = 0.067$), sex ($x^2 = 2.232$, $p = 0.135$) or education ($T = 1.24$, $p = 0.219$) between people with EOS and HCs. Significant differences were found in education among the FEOS, SEOS and control groups ($F = 3.726$, $p = 0.02$). *Post hoc* analysis found that the SEOS group had significantly higher education than the control group; no significant differences were found in age ($F = 2.085$, $p = 0.13$) or sex ($x^2 = 4.36$, $p = 0.113$) among these groups. No significant difference was found in age of onset, disease course, medication time, olanzapine equivalent dose or PANSS score between the FEOS and SEOS groups.

Comparison Between the Early-Onset Schizophrenia and Healthy Control Groups

Figure 1 and **Table 3** show that GMV in the EOS group, compared to the control group, was decreased in the left middle temporal gyrus (MTG) ($T = -5.62$, cluster size = 631) and right MTG ($T = -4.29$, cluster size = 31). **Figures 2**, **3** and **Table 4** show that reduced cortical thickness was found in the EOS group in the left inferior temporal gyrus (ITG) ($p = 0.026$, $T = -3.91$),

[1]https://lcni.uoregon.edu/downloads

[2]http://www.fil.ion.ucl.ac.uk/spm

[3]https://surfer.nmr.mgh.harvard.edu/fswiki/FreeSurferWiki

TABLE 1 | Demographic profile of early-onset schizophrenia (EOS) and healthy controls (HCs) [values are mean (S.D.)].

	EOS ($n = 60$)	HCs ($n = 40$)	T/χ 2	*P*
Age, year	14.27 ± 1.471	13.60 ± 1.191	1.862	0.067[a]
Sex (male/female)	21/39	20/20	2.232	0.135[b]
Educational attainment, year	8.13 ± 1.523	7.68 ± 1.979	1.24	0.219[a]
Handedness (left/right)	0/60	0/40	/	/
Age of onset, year	13.75 ± 1.612	/	/	/
Disease course, month	5.433 ± 7.883	/	/	/
Medication time, day	8.45 ± 19	/	/	/
Equal effective dose of olanzapine, mg	5.32 ± 5.94	/	/	/
Score of positive symptoms scale	21.43 ± 6.07	/	/	/
Score of negative symptoms scale	19.92 ± 8.12	/	/	/
General Psychopathology Scale	37.83 ± 12.51	/	/	/
PANSS	79.18 ± 23.98	/	/	/

EOS: Early-onset schizophrenia; HCs: Healthy controls.
[a]*Two sample T test.*
[b]*Chi-square test.*
$p < 0.05$.

TABLE 2 | Demographic profile of familial early-onset schizophrenia (FEOS), sporadic early-onset schizophrenia (SEOS) and healthy controls (HCs) [values are mean (S.D.)].

	FEOS ($n = 11$)	SEOS ($n = 49$)	HCs ($n = 40$)	T/F	*P*
Age, year	14 ± 1.265	14.33 ± 1.519	13.6 ± 1.919	2.085	0.13[a]
Sex (male/female)	6/5	15/34	20/20	4.36	0.113[a]
Education, year	7.91 ± 1.375	8.67 ± 1.625	7.68 ± 1.979	3.726	0.02[a]
Handness (left/right)	0/11	0/49	0/40	/	/
Age of onset, year	13.73 ± 1.191	13.76 ± 1.702	/	−0.51	0.959[b]
Disease course, month	3.91 ± 5.108	5.78 ± 8.385	/	/	0.677[c]
Medication time, day	4.18 ± 8.931	9.4 ± 20.758	/	/	0.183[c]
Equal effective dose of olanzapine, mg	4.51 ± 5.76	5.49 ± 6.02	/	/	0.584[c]
Score of positive symptoms scale	21.27 ± 4.45	21.47 ± 6.42	/	−0.09	0.924[b]
Score of negative symptoms scale	22.9 ± 7.73	19.24 ± 8.11	/	1.407	0.18[b]
General Psychopathology Scale	40.27 ± 13.09	37.28 ± 12.44	/	0.69	0.501[b]
PANSS	84.45 ± 23.22	78 ± 23	/	0.834	0.417[b]

FEOS: Familial early-onset schizophrenia; SEOS: Sporadic early-onset schizophrenia; HCs: Healthy controls.
[a]*Chi-square test.*
[b]*Two sample T test.*
[c]*Mann-Whitney U.*
$P < 0.05$.

left superior temporal gyrus (STG) ($p = 0.03$, $T = -3.99$), left middle frontal gyrus (MFG) ($p = 0.03$, $T = -4.07$), right MFG ($p = 0.003$, $T = -3.83$), and right inferior frontal gyrus (IFG) ($p = 0.009$, $T = -3.91$). No significant differences in cortical surface area were found between the two groups.

Comparison Between the Familial Early-Onset Schizophrenia, Sporadic Early-Onset Schizophrenia and Control Groups

Figure 4 and **Table 3** show that compared with the HC group, decreased GMV was found in the SEOS group in the left MTG ($T = -5.97$, cluster size = 282) ($p < 0.05$, FDR corrected). No significant difference of cortical thickness nor surface area was found among the three groups.

Correlation Between the Region of Interest and Clinical Measures

There was no significant correlation between values of ROIs and PANSS total/subscale scores in the EOS group. There was no significant correlation between values of ROIs and PANSS total/subscale scores in the FEOS nor SEOS group.

DISCUSSION

The combined VBM and SBM analysis revealed significantly decreased GMV in the bilateral MTG and reduced cortical thickness in the left ITG, STG, MFG and right MFG, IFG in the EOS group. The analysis of the impact of family history showed that the FEOS and SEOS group showed different brain structure morphology.

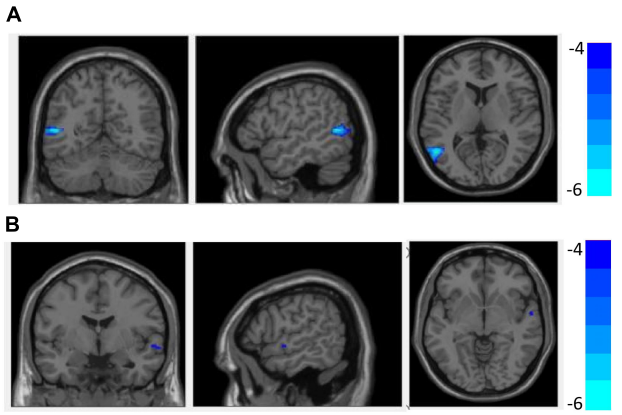

FIGURE 1 | Compared with healthy controls (HCs), grey matter volume (GMV) was decreased in the left middle temporal gyrus **(A)** and right middle temporal gyrus **(B)** in early-onset schizophrenia (EOS) group ($p < 0.05$, FDR corrected).

Comparison of Grey Matter Volume, Cortical Thickness and Surface Area Between the Early-Onset Schizophrenia and Healthy Control Groups

In line with previous studies, this study supports the finding that individuals with EOS showed decreased GMV in the bilateral MTG (30, 31). Some studies also found decreased GMV in the bilateral MTG in young first-degree relatives of people with schizophrenia (32). A similar pattern was found in both AOS and their healthy siblings (33, 34). The MTG is associated with cognitive functions such as semantic memory encoding, observational movement, deductive reasoning and advanced sensory processing (35, 36). As one of the key regions in the social brain network, the MTG has been widely reported to be associated with schizophrenia and other childhood-onset mental disorders, such as autism spectrum disorder (37–39). Decreased GMV in the MTG among individuals with EOS is consistent with schizophrenia being a disorder of neurodevelopment. This is because the MTG is reported to be a phylogenetically late-developing region, and it has no homolog in non-human primates (40, 41). Therefore, the MTG can express a high degree of interindividual variability in morphology, which is caused by differences in neurodevelopmental processes such as intra- and interareal connections of nerve cells, synaptic development, neuronal migration and differentiation, and cytoarchitectonic formation (38). Decreased GMV observed in the EOS extends the observations from adults, which suggests that the reduction in GMV in the bilateral MTG may be a stable biomarker in both early-onset and adult-onset schizophrenia.

Consistent with previous research, we found reduced cortical thickness in the left ITG, STG, MFG, right MFG, and IFG in the EOS group (42, 43). Although some studies did not find regions with greater/less cortical thickness in EOS (44, 45), there have been a large number of consistent reports on cortical thinning in the EOS group (13, 46, 47). Brain regions such as the frontal and temporal lobes were most commonly reported.

The frontal and temporal lobes are thought to be associated with cognitive functions such as visual processing, language, emotional processing, executive function and decision-making in people with schizophrenia (48). Cortical thickness changes in these brain areas may be associated with abnormal behavior in schizophrenia (49). Two meta-regression analyzes showed that a common pattern of thinning of GM in the left lateral temporal lobe in schizophrenia was significantly associated with positive symptoms and aggression (50). The frontal and temporal lobes are related to higher functions such as cognition, speech, thinking and emotion and are relatively late to mature (40). The brain undergoes dramatic changes during adolescence, with the elimination of millions of synapses and their associated neuronal processes (dendrites and axon terminals) (51). Changes in GMV and cortical thickness in the frontal and temporal lobes in individuals with EOS may be associated with abnormal synaptic pruning in these areas. It has been suggested that schizophrenia occurs with the dysfunction of healthy brain maturation during adolescence (52), which may be due to abnormalities in the genes coding for these trophic factors (53). This may explain the finding of structural brain abnormalities in the EOS group. Compared with AOS, EOS show more problems with thinking disorder, emotional poverty, and cognitive dysfunction. Brain structure changes mainly in the frontal and temporal lobes in the study may be consistent with such prominent symptoms in EOS. Reduced cortical thickness in the frontal and temporal lobes may be considered to be a fundamental pathological feature of EOS.

However, we found no significant differences in surface area between the two groups. Using FreeSurfer, Janssen et al. also reported that there were no significant differences in brain surface area between the EOS and HC groups (13). Cortical surface area is formed by symmetrical division of cortical progenitor cells in ventricular and subventricular regions and increases rapidly due to the curling and folding of the cortex. Unlike cortical thickness, which is associated with changes in neuronal dendrites, dendritic spines, and myelin sheaths in specific brain regions, cortical surface area is related only to the size of neurons and is not affected by brain maturity (54). The results indicated that

TABLE 3 | Abnormal grey matter volume (GMV) between the comparison of the groups.

	Cluster size	T	MNI coordinates (X,Y,Z)	Anatomical regions
EOS < HCs				
	31	−4.29	58.5, −3, −4.5	Right middle temporal gyrus
	631	−5.62	−52.5, −58.5, 7.5	Left middle temporal gyrus
SEOS < HCs				
	282	−5.97	−48, −57, 6	Left middle temporal gyrus

MNI: The Montreal Neurological Institute; EOS: Early-onset schizophrenia; SEOS: Sporadic early-onset schizophrenia; HCs: Healthy controls.
$p < 0.05$, FDR corrected.

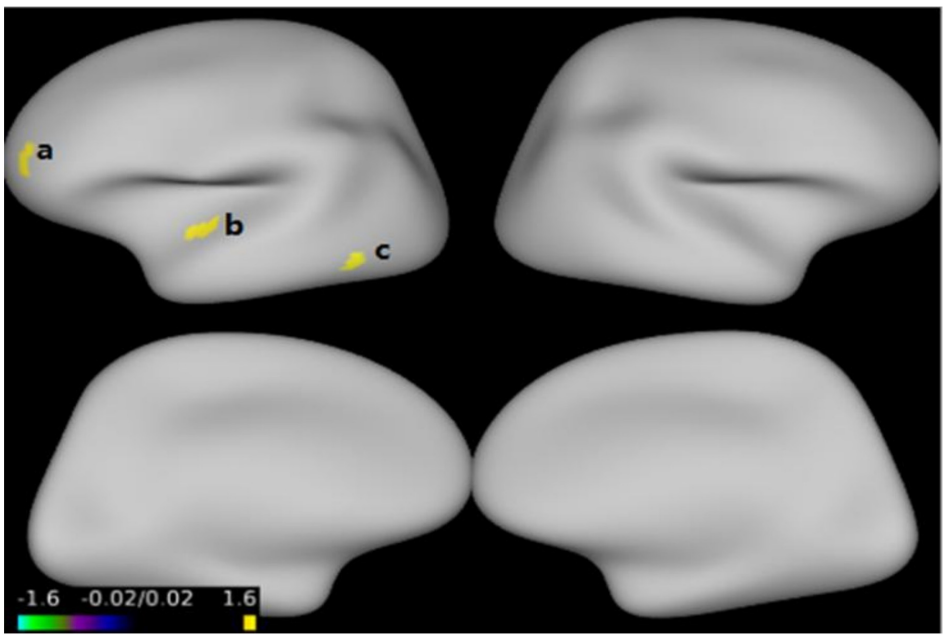

FIGURE 2 | Compared with healthy control (HC) group, cortical thickness was thinner in the left inferior temporal gyrus **(a)**, left superior temporal gyrus **(b)**, left middle frontal gyrus **(c)** in early-onset schizophrenia (EOS) group ($p < 0.05$, FWE corrected).

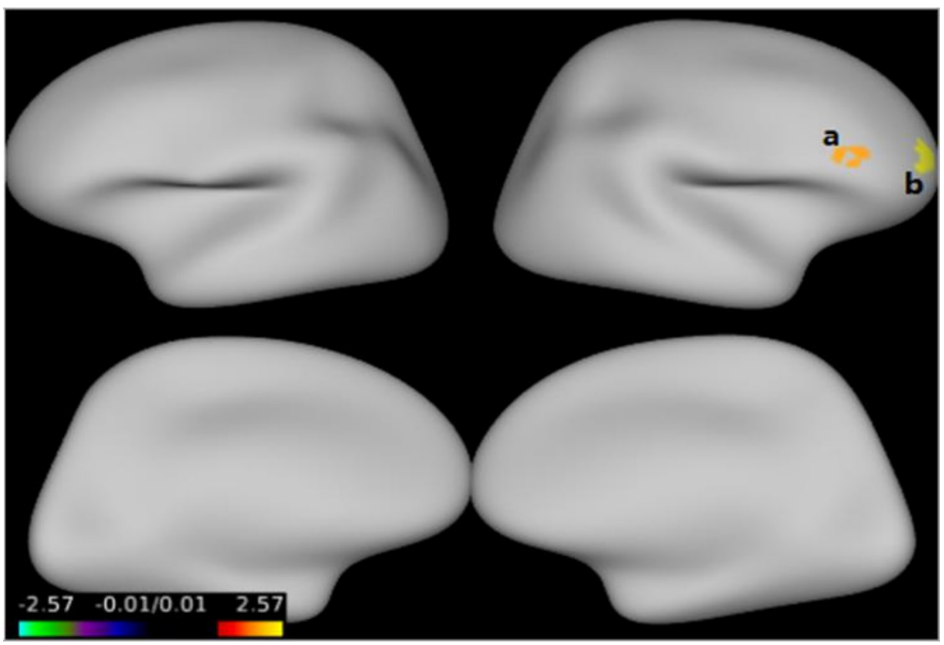

FIGURE 3 | Compared with the healthy controls (HCs), cortical thickness was thinner in the right middle frontal gyrus **(a)**, right inferior frontal gyrus **(b)** in early-onset schizophrenia (EOS) group ($p < 0.05$, FWE corrected).

the abnormal brain structure of individuals with EOS is not associated with cortical surface area.

We found decreased GMV and reduced cortical thickness in the EOS group. However, no significant differences in surface area were found in the EOS group. The abnormal brain regions identified by the two analysis methods were inconsistent, and further analyzes are needed to investigate associations between GMV and cortical thickness. In other words, the differences highlight the complementary effects of the combined analysis of the three indexes. If only one index is used, the characteristics

TABLE 4 | Reduced cortical thickness between the comparison of the early-onset schizophrenia (EOS) and healthy controls (HCs) groups.

	Cluster no.	Cluster-wise *p*	T	MNI coordinates (X,Y,Z)	Anatomical regions
EOS < HCs					
	1	0.026	−3.91	−52, −60, −6	Left inferior temporal gyrus
	2	0.03	−3.99	−49, −15, −5	Left superior temporal gyrus
	3	0.03	−4.07	−29, 48, 5	Left middle frontal gyrus
	4	0.003	−3.83	31, 50, 1	Right middle frontal gyrus
	5	0.009	−3.91	38, 33, 14	Right inferior frontal gyrus

MNI: The Montreal Neurological Institute; EOS: Early-onset schizophrenia; HCs: Healthy controls.
$p < 0.05$, FWE corrected.

of the lesions cannot be more comprehensively understood, and the causes of the lesions cannot be independently assessed. The results show that it is necessary to simultaneously analyze the three indexes in future studies.

Comparison of Grey Matter Volume, Cortical Thickness and Surface Area Between Subgroups

To the best of our knowledge, this is the first study to conduct an exploratory analysis of whether the presence of a family history of schizophrenia causes differences in brain structure in EOS.

The onset of EOS is closely related to environmental factors (55). Environmental factors such as parents? reproductive age, obstetric complications, childbirth season, behavioral biases or language retardation, exposure to adverse life events and drug use can all increase the risk of EOS (56–59). The above environmental factors are likely to induce molecular genetic changes, which may cause damage to the brain structure in those with SSP. Although we did not find differences between the FEOS and SEOS groups, we found decreased GMV in the SEOS group in the left MTG when compared with the HCs group. Our earlier studies in AOS reported the WM fiber bundles were more severely damaged in the SSP group than the FSP group (21). Using FreeSurfer, we found a decreased surface area in the left prefrontal lobe in the SSP group compared with the FSP and HC groups (22). These results suggesting that the two types of schizophrenia may have different pathogeneses, and showing a trend that brain changes in sporadic schizophrenia may be more pronounced than in familiar schizophrenia.

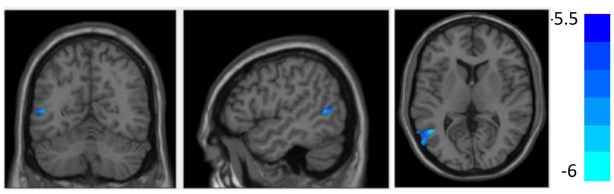

FIGURE 4 | Compared with the healthy controls (HCs), grey matter volume (GMV) reduced in the left middle temporal gyrus in sporadic early-onset schizophrenia (SEOS) group ($P < 0.05$, FDR corrected).

The genetic mutations play an important role in those with sporadic schizophrenia. Some phenotypes of people with SSP (such as abnormal brain structure and impaired WM integrity) may be affected by *de novo* copy number (CN) mutations and produce an independent phenotype than that of people with FSP (21, 60). Xu et al. (27) also mentioned that rare germline mutations lead to vulnerability in people with SSP, and rare genetic damage can explain (at least in part) the genetic heterogeneity of schizophrenia at many different genetic loci. However, the proportions of relatives at different levels may have influenced the results. Due to the small number of subjects in the FEOS group, we could not regroup them based on this factor. This study was only an exploratory analysis, and a larger sample size in the FEOS group is needed for further verification.

Our study had three major limitations. First, a small percentage of EOS were treated with antipsychotic drugs, and we cannot exclude the possibility that the drugs may have had an effect on the structure of the brain. However, the medication dosage and duration of administration were relatively small and short, and the medication time, drug dosage and types of drugs between the FEOS and SEOS groups were not significantly different. Second, the small sample size in the FEOS group may have resulted in insufficient power to find differences between subgroups. The results for the subgroup comparisons have to be interpreted with caution. Our findings may be regarded as preliminary and need to be confirmed by a larger sample size in the future. Third, there were no follow-up studies, and the results reflected structural differences in the brain at only one time point.

CONCLUSION

We confirmed abnormalities in GMV and cortical thickness, especially in the temporal lobe and frontal lobe, in the early stage of EOS by analyzing a relatively large sample from a Han Chinese population. The FEOS group and SEOS group showed different brain structure morphology.

DATA AVAILABILITY STATEMENT

The original contributions presented in this study are included in the article/supplementary material, further inquiries can be directed to the corresponding author.

ETHICS STATEMENT

The studies involving human participants were reviewed and approved by Medical Ethics Committee of West China Hospital of Sichuan University. Written informed consent to participate in this study was provided by the participants' legal guardian/next of kin.

AUTHOR CONTRIBUTIONS

JC, TL, and PS: designed the study. JC, WW, LZ, ML, XL, SL, WD, XD, QW, W-jG, and XM: recruited the participants, administered the assessment, and carried out data analysis. JC and WW: wrote the manuscript. TL: revised the manuscript. All authors contributed to the article and approved the submitted version.

FUNDING

This work was partly funded by the National Natural Science Foundation of China Key Project (TL, 81630030 and TL and PS, 81920108018), National Natural Science Foundation of China Project (WW, 82001410 and XL, 82001440), Project for Hangzhou Medical Disciplines of Excellence & Key Project for Hangzhou Medical Disciplines (TL, 202004A11), Introduction Project of Suzhou Clinical Expert Team (XD and TL, SZYJTD201715), Key R & D projects of Science and Technology Department of Sichuan Province (2021YFS0248), 1.3.5 Project for disciplines of excellence, West China Hospital of Sichuan University (ZY2016103, ZY2016203, and ZYGD20004), and Post Doctor Research Project, West China Hospital, Sichuan University (JC, 2021HXBH027).

ACKNOWLEDGMENTS

We thank all individuals who have participated in this study.

REFERENCES

1. Driver DI, Gogtay N, Rapoport JL. Childhood onset schizophrenia and early onset schizophrenia spectrum disorders. *Child Adolesc Psychiatr Clin N Am.* (2013) 22:539–55. doi: 10.1016/j.chc.2013.04.001
2. Cannon M, Jones P, Huttunen MO, Tanskanen A, Huttunen T, Rabe-Hesketh S, et al. School performance in Finnish children and later development of schizophrenia: a population-based longitudinal study. *Arch Gen Psychiatry.* (1999) 56:457–63. doi: 10.1001/archpsyc.56.5.457
3. Coulon N, Godin O, Bulzacka E, Dubertret C, Mallet J, Fond G, et al. Early and very early-onset schizophrenia compared with adult-onset schizophrenia: French FACE-SZ database. *Brain Behav.* (2020) 10:e01495. doi: 10.1002/brb3.1495
4. Gogtay N, Weisinger B, Bakalar JL, Stidd R, Fernandez de la Vega O, Miller R, et al. Psychotic symptoms and gray matter deficits in clinical pediatric populations. *Schizophr Res.* (2012) 140:149–54. doi: 10.1016/j.schres.2012.07.006
5. Reig S, Moreno C, Moreno D, Burdalo M, Janssen J, Parellada M, et al. Progression of brain volume changes in adolescent-onset psychosis. *Schizophr Bull.* (2009) 35:233–43. doi: 10.1093/schbul/sbm160
6. Taylor JL, Blanton RE, Levitt JG, Caplan R, Nobel D, Toga AW. Superior temporal gyrus differences in childhood-onset schizophrenia. *Schizophr Res.* (2005) 73:235–41. doi: 10.1016/j.schres.2004.07.023
7. Pagsberg AK, Baare WF, Raabjerg Christensen AM, Fagerlund B, Hansen MB, Labianca J, et al. Structural brain abnormalities in early onset first-episode psychosis. *J Neural Transm.* (2007) 114:489–98. doi: 10.1007/s00702-006-0573-8
8. Brent BK, Thermenos HW, Keshavan MS, Seidman LJ. Gray matter alterations in schizophrenia high-risk youth and early-onset schizophrenia: a review of structural MRI findings. *Child Adolesc Psychiatr Clin N Am.* (2013) 22:689–714. doi: 10.1016/j.chc.2013.06.003
9. Juuhl-Langseth M, Rimol LM, Rasmussen IA Jr, Thormodsen R, Holmen A, Emblem KE, et al. Comprehensive segmentation of subcortical brain volumes in early onset schizophrenia reveals limited structural abnormalities. *Psychiatry Res.* (2012) 203:14–23. doi: 10.1016/j.pscychresns.2011.10.005
10. Arango C, Moreno C, Martinez S, Parellada M, Desco M, Moreno D, et al. Longitudinal brain changes in early-onset psychosis. *Schizophr Bull.* (2008) 34:341–53. doi: 10.1093/schbul/sbm157
11. Greenstein D, Lerch J, Shaw P, Clasen L, Giedd J, Gochman P, et al. Childhood onset schizophrenia: cortical brain abnormalities as young adults. *J Child Psychol Psychiatry.* (2006) 47:1003–12. doi: 10.1111/j.1469-7610.2006.01658.x
12. Voets NL, Hough MG, Douaud G, Matthews PM, James A, Winmill L, et al. Evidence for abnormalities of cortical development in adolescent-onset schizophrenia. *Neuroimage.* (2008) 43:665–75. doi: 10.1016/j.neuroimage.2008.08.013
13. Janssen J, Aleman-Gomez Y, Schnack H, Balaban E, Pina-Camacho L, Alfaro-Almagro F, et al. Cortical morphology of adolescents with bipolar disorder and with schizophrenia. *Schizophr Res.* (2014) 158:91–9. doi: 10.1016/j.schres.2014.06.040
14. Crespo-Facorro B, Roiz-Santianez R, Perez-Iglesias R, Rodriguez-Sanchez JM, Mata I, Tordesillas-Gutierrez D, et al. Global and regional cortical thinning in first-episode psychosis patients: relationships with clinical and cognitive features. *Psychol Med.* (2011) 41:1449–60. doi: 10.1017/S003329171000200X
15. Epstein KA, Kumra S. Altered cortical maturation in adolescent cannabis users with and without schizophrenia. *Schizophr Res.* (2015) 162:143–52. doi: 10.1016/j.schres.2014.11.029
16. Mattai AA, Weisinger B, Greenstein D, Stidd R, Clasen L, Miller R, et al. Normalization of cortical gray matter deficits in nonpsychotic siblings of patients with childhood-onset schizophrenia. *J Am Acad Child Adolesc Psychiatry.* (2011) 50:697–704. doi: 10.1016/j.jaac.2011.03.016
17. Berman RA, Gotts SJ, McAdams HM, Greenstein D, Lalonde F, Clasen L, et al. Disrupted sensorimotor and social-cognitive networks underlie symptoms in childhood-onset schizophrenia. *Brain.* (2016) 139:276–91. doi: 10.1093/brain/awv306
18. Rijsdijk FV, van Haren NE, Picchioni MM, McDonald C, Toulopoulou T, Hulshoff Pol HE, et al. Brain MRI abnormalities in schizophrenia: same genes or same environment? *Psychol Med.* (2005) 35:1399–409. doi: 10.1017/S0033291705005167
19. Schulze K, McDonald C, Frangou S, Sham P, Grech A, Toulopoulou T, et al. Hippocampal volume in familial and nonfamilial schizophrenic probands and their unaffected relatives. *Biol Psychiatry.* (2003) 53:562–70. doi: 10.1016/s0006-3223(02)01910-8
20. Lui S, Deng W, Huang X, Jiang L, Ouyang L, Borgwardt SJ, et al. Neuroanatomical differences between familial and sporadic schizophrenia and their parents: an optimized voxel-based morphometry study. *Psychiatry Res.* (2009) 171:71–81. doi: 10.1016/j.pscychresns.2008.02.004
21. Wang Q, Deng W, Huang C, Li M, Ma X, Wang Y, et al. Abnormalities in connectivity of white-matter tracts in patients with familial and non-familial schizophrenia. *Psychol Med.* (2011) 41:1691–700. doi: 10.1017/S0033291710002412
22. Li Y, Deng W, Wang Q, Li M, Li N, Lei W, et al. Difference in brain surface area between first-episode familial and sporadic schizophrenia and its association with COMT gene polymorphisms. *Zhonghua Yi Xue Yi Chuan Xue Za Zhi.* (2015) 32:259–63. doi: 10.3760/cma.j.issn.1003-9406.2015.02.024
23. Ashburner J, Friston KJ. Voxel-based morphometry–the methods. *Neuroimage.* (2000) 11:805–21. doi: 10.1006/nimg.2000.0582
24. Wright IC, McGuire PK, Poline JB, Travere JM, Murray RM, Frith CD, et al. A voxel-based method for the statistical analysis of gray and white matter density

applied to schizophrenia. *Neuroimage.* (1995) 2:244–52. doi: 10.1006/nimg.1995.1032
25. Kay SR, Fiszbein A, Opler LA. The positive and negative syndrome scale (PANSS) for schizophrenia. *Schizophr Bull.* (1987) 12:261–76. doi: 10.1093/schbul/13.2.261
26. Annett M. A classification of hand preference by association analysis. *Br J Psychol.* (1970) 61:303–21. doi: 10.1111/j.2044-8295.1970.tb01248.x
27. Xu B, Roos JL, Levy S, van Rensburg EJ, Gogos JA, Karayiorgou M. Strong association of de novo copy number mutations with sporadic schizophrenia. *Nat Genet.* (2008) 40:880–5. doi: 10.1038/ng.162
28. Langer N, Benjamin C, Becker BLC, Gaab N. Comorbidity of reading disabilities and ADHD: structural and functional brain characteristics. *Hum Brain Mapp.* (2019) 40:2677–98. doi: 10.1002/hbm.24552
29. Diaz-Caneja CM, Schnack H, Martinez K, Santonja J, Aleman-Gomez Y, Pina-Camacho L, et al. Neuroanatomical deficits shared by youth with autism spectrum disorders and psychotic disorders. *Hum Brain Mapp.* (2019) 40:1643–53. doi: 10.1002/hbm.24475
30. James A, Hough M, James S, Winmill L, Burge L, Nijhawan S, et al. Greater white and grey matter changes associated with early cannabis use in adolescent-onset schizophrenia (AOS). *Schizophr Res.* (2011) 128:91–7. doi: 10.1016/j.schres.2011.02.014
31. Tang J, Liao Y, Zhou B, Tan C, Liu W, Wang D, et al. Decrease in temporal gyrus gray matter volume in first-episode, early onset schizophrenia: an MRI study. *PLoS One.* (2012) 7:e40247. doi: 10.1371/journal.pone.0040247
32. Brent BK, Rosso IM, Thermenos HW, Holt DJ, Faraone SV, Makris N, et al. Alterations of lateral temporal cortical gray matter and facial memory as vulnerability indicators for schizophrenia: an MRI study in youth at familial high-risk for schizophrenia. *Schizophr Res.* (2016) 170:123–9. doi: 10.1016/j.schres.2015.11.013
33. Hu M, Li J, Eyler L, Guo X, Wei Q, Tang J, et al. Decreased left middle temporal gyrus volume in antipsychotic drug-naive, first-episode schizophrenia patients and their healthy unaffected siblings. *Schizophr Res.* (2013) 144:37–42. doi: 10.1016/j.schres.2012.12.018
34. Goldman AL, Pezawas L, Mattay VS, Fischl B, Verchinski BA, Zoltick B, et al. Heritability of brain morphology related to schizophrenia: a large-scale automated magnetic resonance imaging segmentation study. *Biol Psychiatry.* (2008) 63:475–83. doi: 10.1016/j.biopsych.2007.06.006
35. Cabeza R, Nyberg L. Imaging cognition II: an empirical review of 275 PET and fMRI studies. *J Cogn Neurosci.* (2000) 12:1–47. doi: 10.1162/08989290051137585
36. Sato W, Toichi M, Uono S, Kochiyama T. Impaired social brain network for processing dynamic facial expressions in autism spectrum disorders. *BMC Neurosci.* (2012) 13:99. doi: 10.1186/1471-2202-13-99
37. Zhang W, Deng W, Yao L, Xiao Y, Li F, Liu J, et al. Brain structural abnormalities in a group of never-medicated patients with long-term schizophrenia. *Am J Psychiatry.* (2015) 172:995–1003. doi: 10.1176/appi.ajp.2015.14091108
38. Cui Y, Liu B, Song M, Lipnicki DM, Li J, Xie S, et al. Auditory verbal hallucinations are related to cortical thinning in the left middle temporal gyrus of patients with schizophrenia. *Psychol Med.* (2018) 48:115–22. doi: 10.1017/S0033291717001520
39. Xu J, Wang C, Xu Z, Li T, Chen F, Chen K, et al. Specific functional connectivity patterns of middle temporal gyrus subregions in children and adults with autism spectrum disorder. *Autism Res.* (2020) 13:410–22. doi: 10.1002/aur.2239
40. Gogtay N, Giedd JN, Lusk L, Hayashi KM, Greenstein D, Vaituzis AC, et al. Dynamic mapping of human cortical development during childhood through early adulthood. *Proc Natl Acad Sci U S A.* (2004) 101:8174–9. doi: 10.1073/pnas.0402680101
41. Binney RJ, Parker GJ, Lambon Ralph MA. Convergent connectivity and graded specialization in the rostral human temporal lobe as revealed by diffusion-weighted imaging probabilistic tractography. *J Cogn Neurosci.* (2012) 24:1998–2014. doi: 10.1162/jocn_a_00263
42. Fraguas D, Diaz-Caneja CM, Pina-Camacho L, Janssen J, Arango C. Progressive brain changes in children and adolescents with early-onset psychosis: a meta-analysis of longitudinal MRI studies. *Schizophr Res.* (2016) 173:132–9. doi: 10.1016/j.schres.2014.12.022
43. Janssen J, Reig S, Aleman Y, Schnack H, Udias JM, Parellada M, et al. Gyral and sulcal cortical thinning in adolescents with first episode early-onset psychosis. *Biol Psychiatry.* (2009) 66:1047–54. doi: 10.1016/j.biopsych.2009.07.021
44. Thormodsen R, Rimol LM, Tamnes CK, Juuhl-Langseth M, Holmen A, Emblem KE, et al. Age-related cortical thickness differences in adolescents with early-onset schizophrenia compared with healthy adolescents. *Psychiatry Res.* (2013) 214:190–6. doi: 10.1016/j.pscychresns.2013.07.003
45. Haller S, Borgwardt SJ, Schindler C, Aston J, Radue EW, Riecher-Rossler A. Can cortical thickness asymmetry analysis contribute to detection of at-risk mental state and first-episode psychosis? A pilot study. *Radiology.* (2009) 250:212–21. doi: 10.1148/radiol.2501072153
46. Buchy L, Makowski C, Malla A, Joober R, Lepage M. Longitudinal trajectory of clinical insight and covariation with cortical thickness in first-episode psychosis. *J Psychiatr Res.* (2017) 86:46–54. doi: 10.1016/j.jpsychires.2016.11.008
47. Zalesky A, Pantelis C, Cropley V, Fornito A, Cocchi L, McAdams H, et al. Delayed development of brain connectivity in adolescents with schizophrenia and their unaffected siblings. *JAMA Psychiatry.* (2015) 72:900–8. doi: 10.1001/jamapsychiatry.2015.0226
48. Gutierrez-Galve L, Chu EM, Leeson VC, Price G, Barnes TR, Joyce EM, et al. A longitudinal study of cortical changes and their cognitive correlates in patients followed up after first-episode psychosis. *Psychol Med.* (2015) 45:205–16. doi: 10.1017/S0033291714001433
49. Mitelman SA, Buchsbaum MS, Brickman AM, Shihabuddin L. Cortical intercorrelations of frontal area volumes in schizophrenia. *Neuroimage.* (2005) 27:753–70. doi: 10.1016/j.neuroimage.2005.05.024
50. Wong TY, Radua J, Pomarol-Clotet E, Salvador R, Albajes-Eizagirre A, Solanes A, et al. An overlapping pattern of cerebral cortical thinning is associated with both positive symptoms and aggression in schizophrenia *via* the ENIGMA consortium. *Psychol Med.* (2019) 50:2034–45. doi: 10.1017/S0033291719002149
51. Sisk CL, Foster DL. The neural basis of puberty and adolescence. *Nat Neurosci.* (2004) 7:1040–7. doi: 10.1038/nn1326
52. Keshavan MS, Anderson S, Pettegrew JW. Is schizophrenia due to excessive synaptic pruning in the prefrontal cortex? The Feinberg hypothesis revisited. *J Psychiatr Res.* (1994) 28:239–65. doi: 10.1016/0022-3956(94)90009-4
53. Hakak Y, Walker JR, Li C, Wong WH, Davis KL, Buxbaum JD, et al. Genome-wide expression analysis reveals dysregulation of myelination-related genes in chronic schizophrenia. *Proc Natl Acad Sci U S A.* (2001) 98:4746–51. doi: 10.1073/pnas.081071198
54. Rakic P. A small step for the cell, a giant leap for mankind: a hypothesis of neocortical expansion during evolution. *Trends Neurosci.* (1995) 18:383–8. doi: 10.1016/0166-2236(95)93934-p
55. Mortensen PB, Pedersen CB, Westergaard T, Wohlfahrt J, Ewald H, Mors O, et al. Effects of family history and place and season of birth on the risk of schizophrenia. *N Engl J Med.* (1999) 340:603–8. doi: 10.1056/NEJM199902253400803
56. Kollias C, Dimitrakopoulos S, Xenaki LA, Stefanis N, Papageorgiou C. Evidence of advanced parental age linked to sporadic schizophrenia. *Psychiatriki.* (2019) 30:24–31. doi: 10.22365/jpsych.2019.301.24
57. Scherr M, Hamann M, Schwerthoffer D, Frobose T, Vukovich R, Pitschel-Walz G, et al. Environmental risk factors and their impact on the age of onset of schizophrenia: comparing familial to non-familial schizophrenia. *Nord J Psychiatry.* (2012) 66:107–14. doi: 10.3109/08039488.2011.605171
58. DeQuardo JR, Goldman M, Tandon R. VBR in schizophrenia: relationship to family history of psychosis and season of birth. *Schizophr Res.* (1996) 20:275–85. doi: 10.1016/0920-9964(95)00003-8
59. Riglin L, Hammerton G, Heron J, Collishaw S, Arseneault L, Thapar AK, et al. Developmental contributions of schizophrenia risk alleles and childhood peer victimization to early-onset mental health trajectories. *Am J Psychiatry.* (2019) 176:36–43. doi: 10.1176/appi.ajp.2018.18010075
60. Rees E, Han J, Morgan J, Carrera N, Escott-Price V, Pocklington AJ, et al. De novo mutations identified by exome sequencing implicate rare missense

variants in SLC6A1 in schizophrenia. *Nat Neurosci*. (2020) 23:179–84. doi: 10.1038/s41593-019-0565-2

Conflict of Interest: The authors declare that the research was conducted in the absence of any commercial or financial relationships that could be construed as a potential conflict of interest.

Publisher's Note: All claims expressed in this article are solely those of the authors and do not necessarily represent those of their affiliated organizations, or those of the publisher, the editors and the reviewers. Any product that may be evaluated in this article, or claim that may be made by its manufacturer, is not guaranteed or endorsed by the publisher.

frontiers | Frontiers in Psychiatry

TYPE Original Research
PUBLISHED 11 August 2022
DOI 10.3389/fpsyt.2022.967941

OPEN ACCESS

EDITED BY
João Valente Duarte,
University of Coimbra, Portugal

REVIEWED BY
Otília C. d'Almeida,
University of Coimbra, Portugal
Serdar M. Dursun,
University of Alberta, Canada
Philip D. Harvey,
University of Miami, United States

*CORRESPONDENCE
Uzma Zahid
uzma.zahid@kcl.ac.uk

SPECIALTY SECTION
This article was submitted to Neuroimaging and Stimulation, a section of the journal Frontiers in Psychiatry

RECEIVED 13 June 2022
ACCEPTED 19 July 2022
PUBLISHED 11 August 2022

CITATION
Zahid U, McCutcheon RA, Borgan F, Jauhar S, Pepper F, Nour MM, Rogdaki M, Osugo M, Murray GK, Hathway P, Murray RM and Howes OD (2022) The effect of antipsychotics on glutamate levels in the anterior cingulate cortex and clinical response: A ^{1}H-MRS study in first-episode psychosis patients.
Front. Psychiatry 13:967941.
doi: 10.3389/fpsyt.2022.967941

The effect of antipsychotics on glutamate levels in the anterior cingulate cortex and clinical response: A ^{1}H-MRS study in first-episode psychosis patients

Uzma Zahid[1]*, Robert A. McCutcheon[1], Faith Borgan[1], Sameer Jauhar[1], Fiona Pepper[1,2,3], Matthew M. Nour[1,4,5], Maria Rogdaki[1,6], Martin Osugo[1], Graham K. Murray[7], Pamela Hathway[1], Robin M. Murray[1] and Oliver D. Howes[1,8,9]

[1]Department of Psychosis Studies, Institute of Psychiatry, Psychology and Neuroscience, King's College London, London, United Kingdom, [2]Department of Neuroimaging, Institute of Psychiatry, Psychology and Neuroscience, King's College London, London, United Kingdom, [3]Department of Clinical and Movement Neurosciences, Queen Square Institute of Neurology, University College London Centre, London, United Kingdom, [4]Max Planck University College London Centre for Computational Psychiatry and Ageing Research, London, United Kingdom, [5]Wellcome Trust Centre for Neuroimaging, University College London, London, United Kingdom, [6]Department of Child and Adolescent Psychiatry, Institute of Psychiatry, Psychology and Neuroscience, King's College London, London, United Kingdom, [7]Department of Psychiatry, University of Cambridge, Cambridge, United Kingdom, [8]Institute of Clinical Sciences, Faculty of Medicine, Imperial College London, London, United Kingdom, [9]H. Lundbeck UK, Valby, Denmark

Introduction: Glutamatergic dysfunction is implicated in the pathophysiology of schizophrenia. It is unclear whether glutamatergic dysfunction predicts response to treatment or if antipsychotic treatment influences glutamate levels. We investigated the effect of antipsychotic treatment on glutamatergic levels in the anterior cingulate cortex (ACC), and whether there is a relationship between baseline glutamatergic levels and clinical response after antipsychotic treatment in people with first episode psychosis (FEP).

Materials and methods: The sample comprised 25 FEP patients; 22 completed magnetic resonance spectroscopy scans at both timepoints. Symptoms were assessed using the Positive and Negative Syndrome Scale (PANSS).

Results: There was no significant change in glutamate [baseline 13.23 ± 2.33; follow-up 13.89 ± 1.74; t(21) = −1.158, p = 0.260], or Glx levels [baseline 19.64 ± 3.26; follow-up 19.66 ± 2.65; t(21) = −0.034, p = 0.973]. There was no significant association between glutamate or Glx levels at baseline and the change in PANSS positive (Glu r = 0.061, p = 0.777, Glx r = −0.152, p = 0.477), negative (Glu r = 0.144, p = 0.502, Glx r = 0.052, p = 0.811), general (Glu r = 0.110, p = 0.607, Glx r = −0.212, p = 0.320), or total scores (Glu r = 0.078, p = 0.719 Glx r = −0.155, p = 0.470).

Conclusion: These findings indicate that treatment response is unlikely to be associated with baseline glutamatergic metabolites prior to antipsychotic treatment, and there is no major effect of antipsychotic treatment on glutamatergic metabolites in the ACC.

KEYWORDS

spectroscopy, NMDA, imaging and schizophrenia, CSF-correction, longitudinal, glutamate

Introduction

Psychotic illnesses such as schizophrenia are characterised by positive symptoms such as delusions and hallucinations, negative symptoms such as anhedonia and blunted affect, and cognitive deficits (1). The disruption of dopaminergic signalling has been identified as a core component of the neurobiology of psychosis (2, 3). In support of this, previous studies have shown an association between antipsychotic striatal D_2 occupancy and clinical response (4).

Glutamatergic dysfunction has also been implicated in the pathophysiology of schizophrenia (5). Glutamate is an excitatory neurotransmitter, with two prominent classes of receptors: ionotropic and metabotropic. There is a growing body of evidence suggesting that hypofunction of the ionotropic glutamate receptor *N*-methyl-D-aspartate (NMDA) plays a role in the pathophysiology of schizophrenia (5, 6). For example, the NMDA receptor antagonist ketamine has been shown to induce negative symptoms and cognitive deficits, paralleling deficits seen in schizophrenia (7, 8). NMDA antagonists may reduce GABAergic interneuron functioning, leading to an increased release of neurotransmitters such as dopamine and glutamate (9–11). Thus, striatal dopaminergic hyperactivity in schizophrenia may be secondary to alterations in the glutamatergic system (12).

Proton magnetic resonance spectroscopy (^{1}H-MRS) enables the *in vivo* quantification of brain glutamate levels (13). Using this technique, ketamine has been shown to increase glutamate measures in the anterior cingulate cortex (ACC) in healthy volunteers (14). Findings from cross-sectional ^{1}H-MRS studies in patients with schizophrenia have shown that glutamate levels vary depending on whether patients demonstrate a clinical response to antipsychotic treatment. Demjaha et al. found that glutamate levels in the ACC were elevated in the treatment resistant (n = 6) but not treatment responsive patients (n = 8) with non-affective psychosis (15). Similarly, Mouchlianitis et al. (16) compared patients with non-affective psychosis that were either treatment responsive or treatment resistant. They found increased glutamate levels in the ACC of treatment resistant patients (n = 21) relative to treatment responsive patients (n = 20) (16). Egerton et al. found that ACC glutamate levels were elevated in patients with non-affective psychosis who were treatment resistant (n = 44) relative to those who were treatment responsive (n = 48) (17). However, Goldstein et al. Showed no group differences in ACC glutamate or Glx (combined signal of glutamate and glutamine) levels when comparing non-affective psychosis patients who were treatment responsive (n = 15), clozapine-responsive (n = 16), and clozapine-resistant (n = 11) (18). More recently, Tarumi et al. (19) showed no group difference in dorsal ACC (dACC) and caudate Glx levels between patients with non-affective psychosis who were either severely treatment resistant (n = 28) or treatment responsive (n = 31). Interestingly dACC Glx levels were higher in the treatment resistant group than in the healthy volunteer group (n = 29) (18). But, as these studies were cross-sectional in design, the outcome and exposure variables were measured at the same time, making it difficult to establish causal relationships. Cross-sectional studies also make it difficult to determine the stability of response and resistance status. Finally, these studies have included patients who have had prolonged antipsychotic exposure, which might have influenced brain glutamate levels (20).

To address these issues, several longitudinal ^{1}H-MRS studies have investigated the effect of antipsychotic treatment on glutamate and Glx levels in schizophrenia (21, 22). De la Fuente-Sandoval et al. found reduced glutamate levels in the striatum of antipsychotic naïve patients during their first non-affective psychosis episode after 4 weeks of antipsychotic treatment (n = 24) (23). Egerton et al. reported a reduction in ACC glutamate levels of minimally treated patients during their first non-affective psychosis episode after 4 weeks of antipsychotic treatment (n = 46) (24). Conversely, Kraguljac et al. reported no change in ACC or hippocampal glutamate levels in unmedicated non-affective psychosis patients (n = 61), after 6 weeks of antipsychotic treatment (25). A limitation of the majority these longitudinal studies, which could explain the heterogeneity in results, is that they report glutamate scaled to creatine (Cr) (25–30). The Cr peak is often used as a concentration reference in human ^{1}H-MRS studies, where metabolites are reported as ratios to Cr (31). Recently, however, Merritt et al., in a mega-analysis of schizophrenia studies, reported a trend toward lower Cr levels in patients with schizophrenia in the

medial frontal cortex, including the ACC, suggesting that the use of Cr as a reference in schizophrenia research could yield inaccurate findings and that scaling to water and correcting for cerebrospinal fluid (CSF) are preferable to avoid this bias (20).

Considering these methodological limitations, we aimed to investigate in a FEP sample whether there is a relationship between baseline glutamate and Glx levels scaled to water and corrected for CSF in the ACC and clinical response at follow-up after antipsychotic treatment. Our secondary aim was to investigate whether antipsychotics alter brain glutamate and Glx levels scaled to water and corrected for CSF, in the ACC at follow-up. We hypothesised that (1) glutamate and Glx levels at baseline would be directly associated with treatment response following antipsychotic medication; (2) glutamate and Glx levels will decrease after antipsychotic administration relative to baseline.

Materials and methods

This study was approved by the East of England-Cambridge East NHS Research Ethics Committee. All participants provided informed written consent prior to participation. The baseline ^{1}H-MRS data have been reported previously (13, 32).

Participants

Patients were recruited from early intervention psychosis services in London. Inclusion criteria were a diagnosis of schizophrenia or other psychotic disorders according to ICD-10 criteria (33), fulfilling criteria for having a first episode of psychosis [first treatment contact (34)] requiring treatment with antipsychotic medication, and being antipsychotic naive, antipsychotic free or minimally treated (taking antipsychotic medication for 2 weeks or less). Whilst other studies have used 3 weeks wash-out or oral antipsychotics (35) we defined subjects as being antipsychotic free if they had not taken any antipsychotic medication for at least 6 weeks (oral) or 6 months (depot, if relevant) to be conservative. Details of their prior antipsychotic medication and antipsychotic treatment between baseline and follow-up is available in **Table 1**. Chlorpromazine-equivalent doses were calculated for prior antipsychotic exposure using a previously described method (36). For lurasidone and amisulpride, we calculated the chlorpromazine-equivalent dose using the method described by Leucht et al. (37) and using data from the Maudsley Prescribing Guidelines, because these are not covered by Andreasen et al. (36). Exclusion criteria for all subjects were history of significant head trauma, dependence on illicit substances or alcohol, medical comorbidity (other than minor illnesses), current use of mood stabilisers–owing to effects on glutamate, and contraindications to MRI scanning. Ethnicity was self-reported, and level of education information collected using a sociodemographic schedule.

Clinical assessment

All patients were clinically assessed at baseline and reassessed after being compliant with antipsychotic treatment at a therapeutic dose as specified in the Maudsley Prescribing Guidelines (38) for a minimum of 4 weeks, before determining treatment response. Four weeks was chosen as the minimum duration of treatment based on evidence that most therapeutic responses to antipsychotic medication occur within 4 weeks (39, 40) including in first-episode psychosis (41). Moreover, non-response before 4 weeks is a predictor of subsequent non-response (40).

The choice of antipsychotic commenced was determined by the treating clinician in discussion with the patient as per standard clinical practice. Prior use of other psychotropic medication (e.g., antidepressants and benzodiazepines) was not an exclusion criterion for the study; however, current use of psychotropic medication (antidepressant or mood stabilizer medication) during the study period was an exclusion criterion. To assess concordance with antipsychotic medication, we used a multisource approach, requiring evidence of adequate adherence on at least two of the following: antipsychotic plasma levels, pharmacy, and electronic medical dispensing records, or reports from the patient and an independent source (family member/caregiver or health care professional) (42). Adequate concordance was defined as taking a minimum of 80% of prescribed doses, in line with consensus recommendations (43).

Symptoms were rated at baseline and follow-up using the Positive and Negative Syndrome Scale (PANSS) (44). The duration of illness was calculated from the onset of the first psychotic symptoms to the initiation of antipsychotic treatment as previously described (45).

Magnetic resonance spectroscopy (^{1}H-MRS)

^{1}H-MRS acquisition

All scans were acquired on a General Electric (Milwaukee, Wisconsin) Signa HDxt 3Tesla MRI scanner using an 8-coil head channel, as described previously (13). For the voxel placements, 3D coronal inversion recovery prepared spoiled gradient echo (IR-SPGR) scans were acquired, followed by auto pre-scans for optimisation of water suppression and shimming. ^{1}H-MRS spectra were acquired for the anterior cingulate (20 × 20 × 20 mm^{3}). The placement of the anterior cingulate voxel was based on the midline sagittal localizer with the centre of the 20 mm × 20 mm × 20 mm voxel placed

10.3389/fpsyt.2022.967941

TABLE 1 Socio-demographic and clinical characteristics of participants.

		Patients (n = 25)
Sex		
	Male	19
	Female	6
Years in Education, years (Mean [SD])	13.62 (3.33)	
Ethnicity		
	White	11
	Black	8
	Asian	2
	Mixed/Other	4
Medication Status at Baseline		
	Antipsychotic naive	12
	Minimally treated	6
	Amisulpride	2
	Risperidone	1
	Missing	3
	Antipsychotic free	7
	Risperidone	1
	Risperidone and pipothiazine	1
	Risperidone and paliperidone	1
	Aripiprazole	1
	Amisulpride and olanzapine	1
	Missing	2
Medication Between Baseline and Follow-Up		
Antipsychotic naïve		
	Amisulpride	3
	Aripiprazole	2
	Amisulpride and quetiapine	1
	Paliperidone, quetiapine, and olanzapine	1
	Risperidone	1
	Quetiapine	1
	Olanzapine	1
	Minimally treated	
	Amisulpride	2
	Aripiprazole	1
	Aripiprazole and risperidone	1
	Missing	1
	Antipsychotic free	
	Risperidone	3
	Amisulpride	1
	Aripiprazole and olanzapine	1
	Lurasidone	1
	Missing	1
Duration of Untreated Psychosis, months (Mean [SD])	18.63 (17.55)*	
PANSS Baseline (Mean [SD])		
	Positive	19.29 (5.88)
	Negative	16.17 (6.46)
	General	36.25 (10.66)
	Total	71.71 (19.71)
PANSS Follow-Up (Mean [SD])		
	Positive	13.00 (5.28)
	Negative	12.75 (5.97)
	General	27.00 (8.82)
	Total	52.75 (18.05)

*Mean duration of psychosis calculated from available data (n = 19).

13 mm above the anterior portion of the genu of the corpus callosum, perpendicular to the anterior commissure-posterior commissure line to minimize the inclusion of white matter and cerebral spinal fluid (CSF) (see **Supplementary Figure 1** for sample voxel placement). Finally, the ^{1}H-MRS spectra [Point RESolves Spectroscopy (PRESS), TE = 30 ms, TR = 2 s] were obtained through the PROton Brain Examination (PROBE) sequence by GE, which includes water suppression. The spectra were an average of 96 water suppressed acquisitions. Sixteen transients were also acquired without water suppression for use with water-referencing and eddy-current correction.

^{1}H-MRS quantification

Raw metabolite concentrations were estimated using LCModel version 6.3-0L,[1] which estimates the concentrations of 16 metabolites (L-alanine, aspartate, creatine, phosphocreatine, GABA, glucose, Glutamine, glutamate, glycerophosphocholine, glycine, myo-inositol, L-lactate, *N*-acetylaspartate, *N*-acetylaspartylglutamate, phosphocholine, and taurine) by fitting the output to a standard basis set acquired experimentally. As described previously (13), metabolite analyses were restricted to spectra with linewidth (full-width at half-maximum; FWHM) $\leq$ 0.1 ppm, Cramér-Rao lower bounds (CRLB) for glutamate $\leq$ 20%, signal to noise ratio $\geq$ 5. The data are not truncated. In-house scripts written in Python were used to identify the relative distribution of white matter, grey matter, and cerebrospinal fluid in the 8 cm^3 voxel prescribed to the anterior cingulate cortex. The following correction was subsequently applied to correct for cerebrospinal fluid within the 8 cm^3 voxel, where M = raw metabolite value, WM = white matter fraction and GM = grey matter fraction and CSF = cerebrospinal fluid fraction (46).

$$M\,corr = M\left(\frac{WM + (GM \times 1.21) + (CSF \times 1.55)}{(WM + GM)}\right)$$

In the equation, the numerator accounts for the fraction of each tissue type within the voxel, corrected by the water concentration in the tissue type. The denominator corrects for the assumption that CSF does not contain metabolites. No correction was applied for relaxation times, except for assuming the tissue water T2 = 80 ms. We report metabolite values scaled to water, as opposed to creatine, based on previous literature indicating that creatine levels are lower in patients with schizophrenia relative to healthy volunteers (47).

Statistical analysis

Statistical analyses were performed using SPSS, version 25, and significance set to $p < 0.05$ (two-tailed). Normality of distribution was assessed using Shapiro–Wilk test. To test the hypothesis glutamate and Glx levels at baseline would be associated with treatment response following antipsychotic medication, Pearson's correlation coefficient was calculated for glutamate and Glx levels at baseline and the percentage change in the PANSS score at follow-up. We carried out exploratory analyses investigating the association between the change in glutamate and Glx levels and the change in the PANSS score. Additionally, as cross-sectional studies report the association between endpoint glutamate and Glx levels and the PANSS score, we make available the results for this association in the present study. Pearson's correlation coefficient was calculated for both exploratory analyses. To test the hypothesis that glutamate and Glx levels will decrease after antipsychotic administration relative to baseline we conducted a paired samples *t*-test. Quantitative variables are presented as mean ± standard deviation (SD). Additionally, we carried out an exploratory analysis in participants who were antipsychotic-naïve and antipsychotic free, excluding minimally treated participants, to see whether antipsychotic treatment was associated with longitudinal change in glutamatergic measures. Finally, Bayesian statistical analyses were conducted using JASP (JASP Team, 2021) to help quantify the relative evidence of the null and alternative hypotheses and support inferences (48, 49). We used JASP default priors: for a paired *t*-test, the prior was determined by a Cauchy distribution centred on a zero-effect size and a width/scale of 0.707; for correlation, the prior was that any correlation between −1 and 1 was equally likely. Bayes Factor (BF_{10}) and corresponding credible intervals are provided.

Percentage changes for PANSS were calculated adjusting for minimum scores (7 for positive and negative symptom subscales, 30 for total symptoms) as shown here for the PANSS positive symptom subscale:

$$\%\ \text{change in positive PANSS} = \frac{\left(\left(\text{baseline score} - 7\right) - \left(\text{follow} - \text{up score} - 7\right)\right)}{\left(\text{baseline score} - 7\right)} \times 100$$

Results

Demographics

Demographic details of participants are given in **Table 1**. The sample comprised 25 first episode psychosis patients, 12 antipsychotic-naïve, 6 minimally treated, and 7 antipsychotic-free individuals. ICD-10 diagnoses at baseline were schizophrenia (n = 15) and bipolar disorder (n = 10). We acquired follow-up ^{1}H-MRS scans from 22 participants in our sample, these are included in the baseline vs. follow-up analysis. We make available the FWHM, CRLB, SNR, and tissue fractions for both baseline and follow-up in the **Supplementary Table 1**.

1 http://s-provencher.com/lcm-manual.shtml

Glutamate and Glx levels before and after antipsychotic administration

There was no significant change between baseline (13.23 ± 2.33) and follow-up glutamate levels ([13.89 ± 1.74]; t(21) = −1.158, p = 0.260) or between baseline (19.64 ± 3.26) and follow-up Glx levels ([19.66 ± 2.65]; t(21) = −0.034, p = 0.973, see **Figure 1**). Additionally, there was no significant change between baseline and follow-up glutamate and Glx levels when we excluded people who had been minimally treated. The results from this exploratory analysis are available in the **Supplementary material**. To quantify our null findings, we conducted Bayesian repeated measures t-tests. The resulting BF_{10} for baseline and follow up glutamate levels was 0.403 (95% CI: 0.623–0.178), indicating anecdotal evidence in favour of the null hypothesis of no change over time. The resulting BF_{10} for baseline and follow up Glx levels was 0.223 (95% CI: 0.397−0.384), indicating moderate evidence in favour of the null hypothesis of no change over time.

Association between baseline glutamate and Glx levels and the change in PANSS sub-scales scores

There was no significant association between glutamate levels at baseline and the change in PANSS positive scores (r = 0.061, n = 24, p = 0.777), the change in PANSS negative scores (r = 0.144, n = 24, p = 0.502) the change in PANSS general scores (r = 0.110, n = 24, p = 0.607) or the change in PANSS total scores (r = 0.078, n = 24, p = 0.719, see **Figure 2**). There was no significant association between Glx levels at baseline and the change in PANSS positive scores (r = −0.152, n = 24, p = 0.477), the change in PANSS negative scores (r = 0.052, n = 24, p = 0.811), the change in PANSS general scores (r = −0.212, n = 24, p = 0.320) or the change in PANSS total scores (r = −0.155, n = 24, p = 0.470, see **Figure 3**). As evident from the figures, an outlier value was present in the negative symptom scores; hence, we ran a sensitivity analysis excluding the observation containing the outlier. Findings show there was still no significant association between the change in PANSS negative scores and either glutamate levels (r = 0.127, n = 23, p = 0.563) or Glx levels (r = −0.101, n = 23, p = 0.647) at baseline. Furthermore, there was no significant association between the change in glutamate and Glx levels from baseline to follow-up and the change in PANSS scores from baseline to follow-up, and there was no significant association between glutamate levels at follow-up and the follow-up PANSS scores. The results from these exploratory analyses are available in the **Supplementary material**. To quantify our null findings, we conducted Bayesian correlations. The resulting BF_{10} for baseline glutamate levels and the change in PANSS positive (0.263), negative (0.313), general (0.287), and total (0.269) indicate moderate evidence in favour of the null hypothesis of no associations between glutamate levels and symptoms. The resulting BF_{10} for baseline Glx levels and the change in PANSS positive (0.322), negative (0.260), general (0.404), and total (0.324) indicate moderate to anecdotal evidence in favour of the null hypothesis of no association.

Cr levels before and after antipsychotic administration

There was no significant change between baseline (6.25 ± 0.57) and follow-up creatine levels ([6.39 ± 0.55]; t(21) = 1.121, p = 0.275).

Discussion

In a sample of FEP patients, we investigated whether there is a relationship between baseline ACC glutamate and Glx levels corrected for CSF and subsequent clinical response after antipsychotic treatment, and whether antipsychotics alter ACC glutamate and Glx levels corrected for CSF. No effect of antipsychotic treatment on glutamate and Glx levels in the ACC was found, and the therapeutic effects were not associated with glutamatergic levels measured before antipsychotic administration. Our findings are consistent with previous studies that have found no effect of antipsychotics on glutamate levels in the ACC (25) and no relationship between baseline glutamatergic metabolites and treatment response (18).

We hypothesised that glutamate and Glx levels at baseline would be directly associated with treatment response following antipsychotic medication. However, we found that therapeutic effects as measured by the PANSS sub-scales were not associated with glutamate compounds at baseline. Previous ^{1}H-MRS studies have shown glutamate metabolite levels vary depending on whether patients demonstrate a clinical response to antipsychotic treatment (15, 16, 21). However, these studies have been cross-sectional in design, which means it is not possible to determine whether a relationship with response suggests that glutamate levels are a predictor of response as opposed to a consequence of successful treatment. Our study was longitudinal in design and therefore addresses this limitation. The current study extends previous findings by reporting metabolites in ratio to CSF rather than Cr, a potential confounder in brain ^{1}H-MRS studies carried out in schizophrenia patients (47).

We hypothesized glutamate and Glx levels would decrease after antipsychotic treatment relative to baseline. However, we found no effect of antipsychotics on glutamate and Glx levels in the ACC. A recent meta-analysis and systematic review (22) summarised 32 longitudinal studies investigating the effect of treatment on brain glutamate levels in schizophrenia. Four longitudinal studies have looked at glutamatergic changes

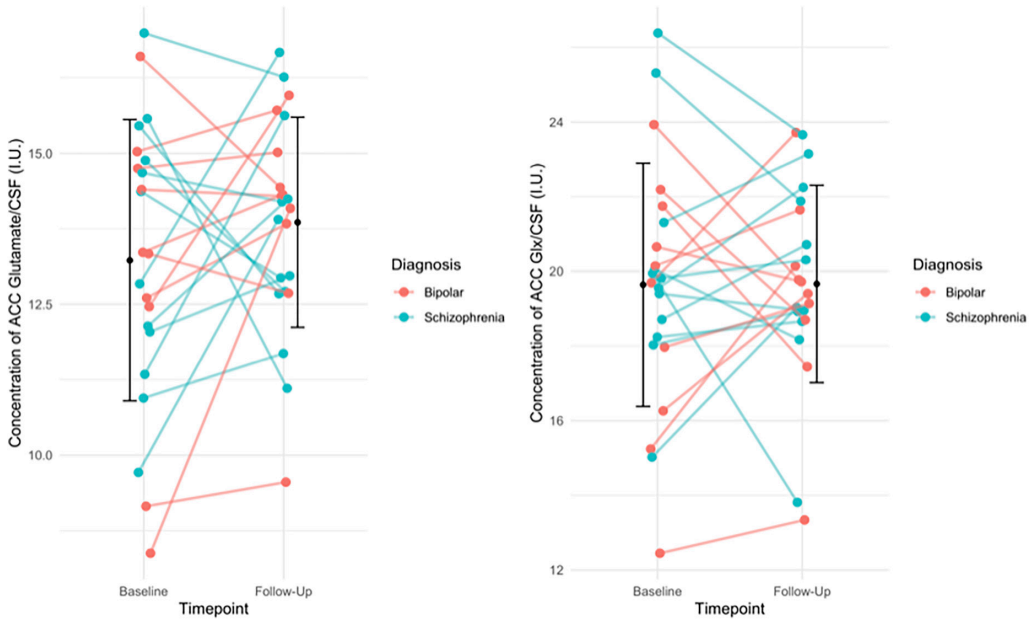

FIGURE 1
(Left) The individual change in glutamate levels from baseline to follow-up, with group mean (SD) of glutamate levels at baseline and follow-up (black circle and error bars). Individual change in the figure is stratified by diagnosis. Results of the paired *t*-test indicated no significant difference in glutamate levels over time (p = 0.260). **(Right)** The individual change in Glx levels from baseline to follow-up, with the group mean (SD) Glx levels at baseline and follow-up (black circles and error bars). Individual change in the figure is stratified by diagnosis. Results of the paired *t*-test indicated no significant difference in Glx levels over time (p = 0.973).

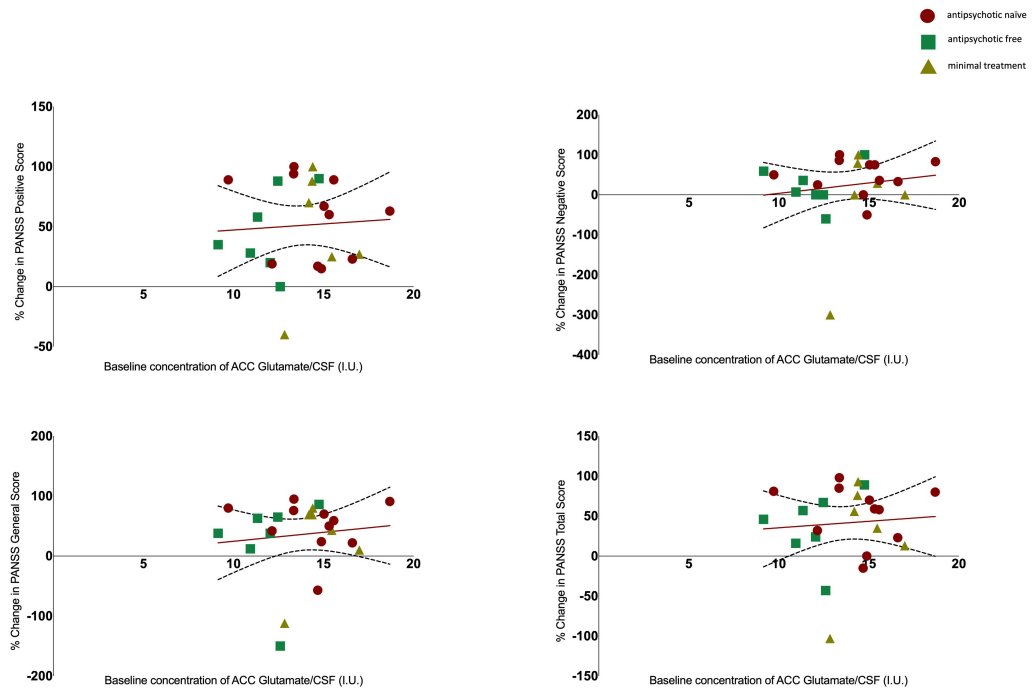

FIGURE 2
Relationship between glutamate levels and the percentage change in PANSS positive (r = 0.061, p = 0.777), negative (r = 0.144, p = 0.502), general (r = 0.110, p = 0.607), and total scores (r = 0.078, p = 0.719), with 95% confidence intervals derived from the line of best fit. Individuals are stratified by medication status, antipsychotic naïve (circle), antipsychotic free (square), minimal treatment (triangle).

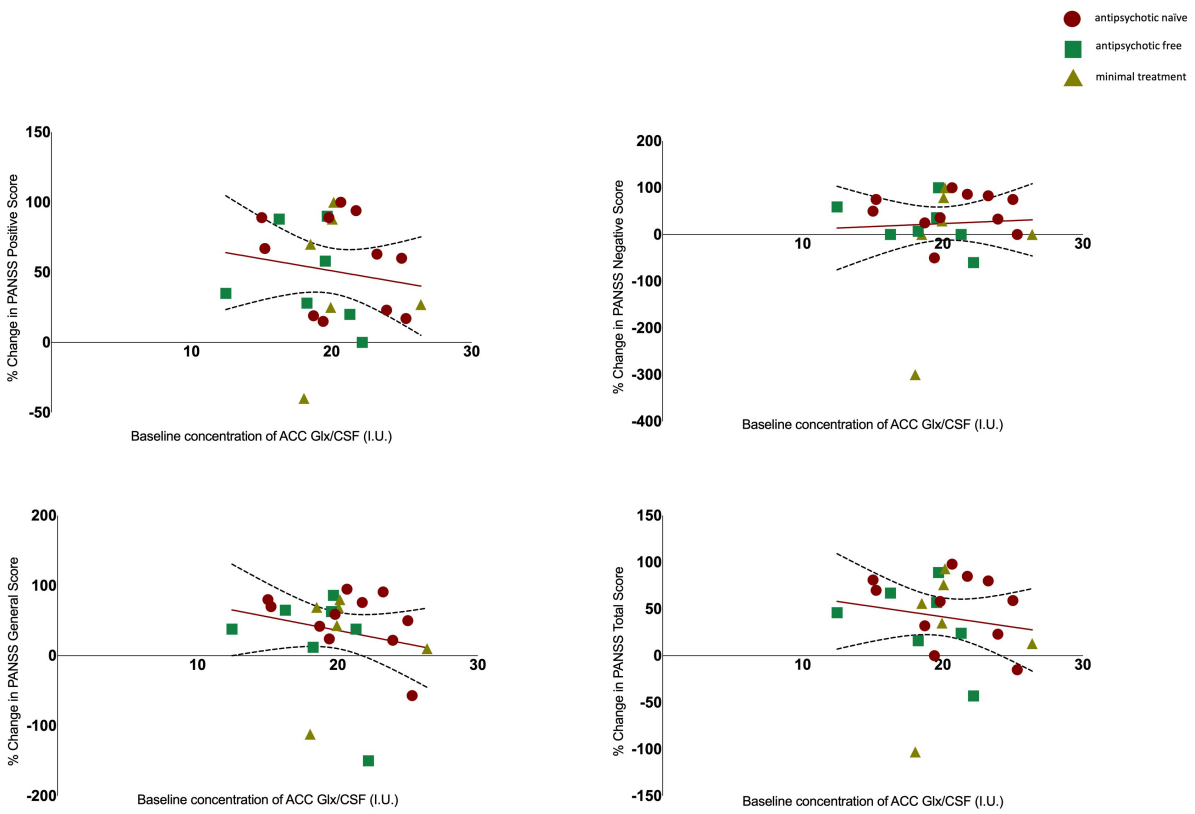

FIGURE 3
Relationship between Glx levels and the percentage change in PANSS positive (r = −0.152, p = 0.477), negative (r = 0.052, p = 0.811), general (r = −0.212, p = 0.320) and total scores (r = −0.155, p = 0.470) with 95% confidence intervals derived from the line of best fit. Individuals are stratified by medication status, antipsychotic naïve (circle), antipsychotic free (square), minimal treatment (triangle).

in the ACC, three of which have reported no change in metabolites (25, 50, 51) and one study has reported a reduction in glutamate levels (24). Bustillo et al. (51) investigated the effect of antipsychotic medication in the ACC in minimally treated schizophrenia patients, with follow-up scans repeated after 1 (n = 10), 6 (n = 8), and 12 (n = 7) months. They reported no effect of time on glutamate, glutamine and Glx levels (CSF corrected) after antipsychotic medication (51). Similarly, Aoyama et al. investigated the effect of antipsychotics on glutamate and glutamine (CSF corrected) in the ACC of medication naive schizophrenia patients at baseline and repeated scans at 10 months (n = 14) and 80 months (n = 16). They reported at the 10-month follow-up one patient was on no medication, and at the 80-month scan, four of the patients were not taking any medication (50). Our study extends the findings from these studies by reporting results in a larger sample, as well as having parameters in place to assess concordance with antipsychotic medication. Kraguljac et al. investigated the effect of risperidone on Glx levels scaled to creatine in the ACC after 6 weeks of treatment (n = 61) and reported no reduction of Glx levels (25). Our study extends the findings from this study by scaling to water and correcting for CSF, as well as reporting results for both glutamate and Glx levels. Conversely, Egerton et al. reported a reduction in glutamate levels in the ACC after treatment with antipsychotic medication for 4 weeks (n = 46), however again this study scaled to Cr, whereas the current study reports both glutamate and Glx levels and scales to water and corrects for CSF (24). Overall, the results from the current study are in line with most of the observations carried out in the ACC and extend these by showing the lack of relationships is not due to confounding by alterations in creatine.

Strengths and limitations

A strength of the study is the longitudinal design, and that metabolites were scaled to water and corrected for CSF content. We also use continuous scores for characterising symptom response to treatment, as opposed to dichotomising individuals in categories of responders and non-responders. The continuous symptom outcome has increased statistical power to detect a true relation with metabolite levels relative to a neat distinction between responders and non-responders, which could result in a loss of information.

A potential limitation is the heterogeneity in treatments administered to participants, as the differential effects of various antipsychotic medications on the glutamate system may have increased the variance in our data. However, all the antipsychotics were used at a dose that would block $D_{2/3}$ receptors, which is thought to be the common mode of therapeutic action of these drugs (52). Additionally, the treatment reflects clinical practice, increasing the generalisability of our findings. Another potential limitation is that some patients had received antipsychotic treatment prior to the baseline scan. However, we excluded these subjects from the analysis of the effect of antipsychotic treatment on glutamatergic measures. Though our study has a relatively modest sample size, Bayesian statistical analyses provided moderate to anecdotal evidence in favour of the null findings. A further limitation is that using the PANSS for patients with bipolar disorder could have induced a floor effect, showing no change in negative symptoms after treatment. However, we chose the PANSS as it is a standardised scale for measuring psychopathology in a transdiagnostic sample of psychotic disorders. For example, PANSS indexes both positive and manic items. Furthermore, time to response has been subject to debate, with some studies suggesting non-response before 4 weeks is a predictor of subsequent non-response (40) and other suggesting treatment response at 4 weeks may be too early an interval in first-episode psychosis patients (53). However, it is unknown how generalizable the findings are from Gallego et al. as their participants were assigned to treatment with either olanzapine or risperidone (53). Whereas in our study the choice of antipsychotic commenced was determined by the treating clinician in discussion with the patient as per standard clinical practice. Another limitation of the current study is that there is no control group, although we would expect no changes in the PANSS scores of healthy volunteers, as they would not be treated with antipsychotic medication. However, a control group would be important to evaluate glutamatergic changes over time and this would be useful to investigate in a further study. Finally, macromolecules were not described in the basis set used for the ^{1}H-MRS quantification and given that they represent a significant contamination source to the glutamate and Glx signal, future studies need to account for this to improve the accuracy of results (23, 54).

Implications

Although glutamate has been implicated in the pathophysiology of schizophrenia, our findings indicate that the mechanism of action of antipsychotic medications does not have a marked effect on glutamatergic function in the ACC. Whilst we cannot exclude modest effects or an effect on other aspects of the glutamate system, this suggests that antipsychotics' actions on other systems underlie their therapeutic effects (52). Moreover, the findings from the current study are not consistent with hypotheses that glutamate abnormalities underlie poor treatment response (55, 56) and further studies are needed to clarify this relationship.

Conclusion

Using a longitudinal design, we report no effect of antipsychotics on ACC glutamate and Glx levels and no association between baseline ACC glutamate and Glx levels and clinical response in FEP patients. These data extend previous literature to indicate that antipsychotic efficacy is not primarily due to modulation of the glutamatergic system. Notably, other studies have used samples of exclusively non-affective psychosis patients, but ours includes a great proportion of bipolar disorder patients, which could cause discrepancies with prior findings. However, we think that using a transdiagnostic approach is more appropriate in the field of psychosis. For example, our group showed that dopamine dysregulation in psychotic disorders as well as determinants of treatment response cut across the traditional categories of affective and non-affective psychosis (32, 57). The present study may serve as an important reference for other studies which will likewise examine a sample encompassing affective and non-affective psychotic disorders. Finally, more studies are needed to clarify the relationship between antipsychotics, glutamate, and treatment response.

Data availability statement

The raw data supporting the conclusions of this article will be made available by the authors, without undue reservation.

Ethics statement

The studies involving human participants were reviewed and approved by the East of England-Cambridge East NHS Research Ethics Committee. The patients/participants provided their written informed consent to participate in this study.

Author contributions

OH contributed to conception and design of the study. RAM, FB, SJ, FP, MN, MR, and PH contributed to organisation of the study, recruitment, and data collection. UZ performed the statistical analysis and wrote the first draft of the manuscript. MO and GM contributed to the statistical analysis. All authors contributed to manuscript revision, read, and approved the submitted version.

Funding

This study was funded by Medical Research Council-UK (no. MC_U120097115), Maudsley Charity (no. 666), and Wellcome Trust (no. 094849/Z/10/Z) grants to OH and the National Institute for Health Research (NIHR) Biomedical Research Centre at South London and Maudsley NHS Foundation Trust and King's College London. UZ was supported by funding from the Lord Leverhulme Charitable Trust. MN was funded by a UCL Welcome Ph.D. Fellowship for Clinicians (102186/B/13/Z). MN was pre-doctoral fellow of the International Max Planck Research School on Computational Methods in Psychiatry and Ageing Research (https://www.mps-ucl-centre.mpg.de/en/comp2psych. Participating institutions: Max Planck Institute for Human Development, Berlin and UCL). The Max Planck UCL Centre was supported by UCL and the Max Planck Society.

Acknowledgments

We would like to thank Emily P. Hedges for support and guidance on data visualisation.

Conflict of interest

OH was a part-time employee of H. Lundbeck A/S and has received investigator-initiated research funding from and/or participated in advisory/speaker meetings organised by Angellini, Autifony, Biogen, Boehringer-Ingelheim, Eli Lilly, Heptares, Global Medical Education, Invicro, Jansenn, Lundbeck, Neurocrine, Otsuka, Sunovion, Rand, Recordati, Roche, and Viatris/Mylan. Neither OH or his family have holdings/a financial stake in any pharmaceutical company. OH has a patent for the use of dopaminergic imaging. RM has received honoraria for non-promotional talks for Janssen, Sunovian, Otsuka, Lundbeck.

The remaining authors declare that the research was conducted in the absence of any commercial or financial relationships that could be construed as a potential conflict of interest.

Publisher's note

All claims expressed in this article are solely those of the authors and do not necessarily represent those of their affiliated organizations, or those of the publisher, the editors and the reviewers. Any product that may be evaluated in this article, or claim that may be made by its manufacturer, is not guaranteed or endorsed by the publisher.

Author disclaimer

The views expressed are those of the author(s) and not necessarily those of the NHS, the NIHR or the Department of Health.

Supplementary material

The Supplementary Material for this article can be found online at: https://www.frontiersin.org/articles/10.3389/fpsyt.2022.967941/full#supplementary-material

References

1. McCutcheon RA, Marques TR, Howes OD. Schizophrenia–An overview. *JAMA Psychiatry.* (2019) 77:201–10. doi: 10.1001/jamapsychiatry.2019.3360

2. Howes OD, Kambeitz J, Kim E, Stahl D, Slifstein M, Abi-Dargham A, et al. The nature of dopamine dysfunction in schizophrenia and what this means for treatment: Meta-analysis of imaging studies. *Arch Gen Psychiatry.* (2012) 69:776–86. doi: 10.1001/archgenpsychiatry.2012.169

3. van Rossum JM. The significance of dopamine-receptor blockade for the mechanism of action of neuroleptic drugs. *Arch Int Pharmacodyn Ther.* (1966) 160:492–4.

4. Kapur S, Zipursky R, Jones C, Remington G, Houle S. Relationship between dopamine D2 occupancy, clinical response, and side effects: A double-blind PET study of first-episode schizophrenia. *Am J Psychiatry.* (2000) 157:514–20. doi: 10.1176/appi.ajp.157.4.514

5. McCutcheon RA, Krystal JH, Howes OD. Dopamine and glutamate in schizophrenia: Biology, symptoms and treatment. *World Psychiatry.* (2020) 19:15–33. doi: 10.1002/wps.20693

6. Coyle JT. Glutamate and schizophrenia: Beyond the dopamine hypothesis. *Cell Mol Neurobiol.* (2006) 26:363–82. doi: 10.1007/s10571-006-9062-8

7. Beck K, Hindley G, Borgan F, Ginestet C, McCutcheon R, Brugger S, et al. Association of ketamine with psychiatric symptoms and implications for its therapeutic use and for understanding schizophrenia: A systematic review and meta-analysis. *JAMA Netw Open.* (2020) 3:e204693–204693. doi: 10.1001/jamanetworkopen.2020.4693

8. Moghaddam B, Javitt D. From revolution to evolution: The glutamate hypothesis of schizophrenia and its implication for treatment. *Neuropsychopharmacology.* (2012) 37:4–15. doi: 10.1038/npp.2011.181

9. Homayoun H, Moghaddam B. NMDA receptor hypofunction produces opposite effects on prefrontal cortex interneurons and pyramidal neurons. *J Neurosci.* (2007) 27:11496–500. doi: 10.1523/JNEUROSCI.2213-07.2007

10. Howes O, McCutcheon R, Stone J. Glutamate and dopamine in schizophrenia: An update for the 21st century. *J Psychopharmacol.* (2015) 29:97–115. doi: 10.1177/0269881114563634

11. Olney JW, Farber NB. Glutamate receptor dysfunction and schizophrenia. *Arch Gen Psychiatry.* (1995) 52:998–1007. doi: 10.1001/archpsyc.1995.03950240016004

12. Kokkinou M, Irvine EE, Bonsall DR, Natesan S, Wells LA, Smith M, et al. Reproducing the dopamine pathophysiology of schizophrenia and approaches to ameliorate it: A translational imaging study with ketamine. *Mol Psychiatr.* (2020) 26:2562–76. doi: 10.1038/s41380-020-0740-6

13. Borgan FR, Jauhar S, McCutcheon RA, Pepper FS, Rogdaki M, Lythgoe DJ, et al. Glutamate levels in the anterior cingulate cortex in un-medicated first episode psychosis: A proton magnetic resonance spectroscopy study. *Sci Rep.* (2019) 9:1–10. doi: 10.1038/s41598-019-45018-0

14. Stone JM, Dietrich C, Edden R, Mehta MA, De Simoni S, Reed LJ, et al. Ketamine effects on brain GABA and glutamate levels with 1H-MRS: Relationship to ketamine-induced psychopathology. *Mol Psychiatry.* (2012) 17:664–5. doi: 10.1038/mp.2011.171

15. Demjaha A, Egerton A, Murray RM, Kapur S, Howes OD, Stone JM, et al. Antipsychotic treatment resistance in schizophrenia associated with elevated glutamate levels but normal dopamine function. *Biol Psychiatry.* (2014) 75:e11–3. doi: 10.1016/j.biopsych.2013.06.011

16. Mouchlianitis E, Bloomfield MA, Law V, Beck K, Selvaraj S, Rasquinha N, et al. Treatment-resistant schizophrenia patients show elevated anterior cingulate cortex glutamate compared to treatment-responsive. *Schizophr Bull.* (2015) 42:744–52. doi: 10.1093/schbul/sbv151

17. Egerton A, Murphy A, Donocik J, Anton A, Barker GJ, Collier T, et al. Dopamine and glutamate in antipsychotic-responsive compared with antipsychotic-nonresponsive psychosis: A multicenter positron emission tomography and magnetic resonance spectroscopy study (STRATA). *Schizophr Bull.* (2021) 47:505–16. doi: 10.1093/schbul/sbaa128

18. Goldstein ME, Anderson VM, Pillai A, Kydd RR, Russell BR. Glutamatergic neurometabolites in clozapine-responsive and-resistant schizophrenia. *Int J Neuropsychopharmacol.* (2015) 18:yu117. doi: 10.1093/ijnp/pyu117

19. Tarumi R, Tsugawa S, Noda Y, Plitman E, Honda S, Matsushita K, et al. Levels of glutamatergic neurometabolites in patients with severe treatment-resistant schizophrenia: A proton magnetic resonance spectroscopy study. *Neuropsychopharmacology* (2020) 45:632–40. doi: 10.1038/s41386-019-0589-z

20. Merritt K, McGuire PK, Egerton A, Aleman A, Block W, Bloemen OJ, et al. Association of age, antipsychotic medication, and symptom severity in schizophrenia with proton magnetic resonance spectroscopy brain glutamate level: A mega-analysis of individual participant-level data. *JAMA Psychiatry.* (2021) 78:667–81.

21. Egerton A, Bhachu A, Merritt K, McQueen G, Szulc A, McGuire P. Effects of antipsychotic administration on brain glutamate in schizophrenia: A systematic review of longitudinal 1H-MRS studies. *Front Psychiatry.* (2017) 8:66. doi: 10.3389/fpsyt.2017.00066

22. Kubota M, Moriguchi S, Takahata K, Nakajima S, Horita N. Treatment effects on neurometabolite levels in schizophrenia: A systematic review and meta-analysis of proton magnetic resonance spectroscopy studies. *Schizophr Res.* (2020) 222:122–32. doi: 10.1016/j.schres.2020.03.069

23. de la Fuente-Sandoval C, León-Ortiz P, Azcárraga M, Stephano S, Favila R, Díaz-Galvis L, et al. Glutamate levels in the associative striatum before and after 4 weeks of antipsychotic treatment in first-episode psychosis: A longitudinal proton magnetic resonance spectroscopy study. *JAMA Psychiatry.* (2013) 70:1057–66. doi: 10.1001/jamapsychiatry.2013.289

24. Egerton A, Broberg B, Van Haren N, Merritt K, Barker G, Lythgoe D, et al. Response to initial antipsychotic treatment in first episode psychosis is related to anterior cingulate glutamate levels: A multicentre 1 H-MRS study (OPTiMiSE). *Mol Psychiatry.* (2018) 23:2145–55. doi: 10.1038/s41380-018-0082-9

25. Kraguljac NV, Morgan CJ, Reid MA, White DM, Jindal RD, Sivaraman S, et al. A longitudinal magnetic resonance spectroscopy study investigating effects of risperidone in the anterior cingulate cortex and hippocampus in schizophrenia. *Schizophr Res.* (2019) 210:239–44. doi: 10.1016/j.schres.2018.12.028

26. Choe B, Suh T, Shinn K, Lee C, Lee C, Paik I. Observation of metabolic changes in chronic schizophrenia after neuroleptic treatment by in vivo hydrogen magnetic resonance spectroscopy. *Invest Radiol.* (1996) 31:345–52. doi: 10.1097/00004424-199606000-00006

27. Goff DC, Hennen J, Lyoo IK, Tsai G, Wald LL, Evins AE, et al. Modulation of brain and serum glutamatergic concentrations following a switch from conventional neuroleptics to olanzapine. *Biol Psychiatry.* (2002) 51:493–7. doi: 10.1016/S0006-3223(01)01321-X

28. Goto N, Yoshimura R, Kakeda S, Nishimura J, Moriya J, Hayashi K, et al. Six-month treatment with atypical antipsychotic drugs decreased frontal-lobe levels of glutamate plus glutamine in early-stage first-episode schizophrenia. *Neuropsychiatr Dis Treat.* (2012) 8:119–22. doi: 10.2147/NDT.S25582

29. Szulc A, Galinska B, Tarasow E, Dzienis W, Kubas B, Konarzewska B, et al. The effect of risperidone on metabolite measures in the frontal lobe, temporal lobe, and thalamus in schizophrenic patients. A proton magnetic resonance spectroscopy (1H MRS) study. *Pharmacopsychiatry.* (2005) 38:214–9. doi: 10.1055/s-2005-873156

30. Szulc A, Galinska B, Tarasow E, Waszkiewicz N, Konarzewska B, Poplawska R, et al. Proton magnetic resonance spectroscopy study of brain metabolite changes after antipsychotic treatment. *Pharmacopsychiatry.* (2011) 44:148–57. doi: 10.1055/s-0031-1279739

31. Dager SR, Corrigan NM, Richards TL, Posse S. Research applications of magnetic resonance spectroscopy to investigate psychiatric disorders. *Top Magn Reson Imaging.* (2008) 19:81–96. doi: 10.1097/RMR.0b013e318181e0be

32. Jauhar S, McCutcheon R, Borgan F, Veronese M, Nour M, Pepper F, et al. The relationship between cortical glutamate and striatal dopamine in first-episode psychosis: A cross-sectional multimodal PET and magnetic resonance spectroscopy imaging study. *Lancet Psychiatry.* (2018) 5:816–23. doi: 10.1016/S2215-0366(18)30268-2

33. World Health Organization. *The ICD-10 classification of mental and behavioural disorders: Clinical descriptions and diagnostic guidelines*. Geneva: World Health Organization (1992).

34. Breitborde NJ, Srihari VH, Woods SW. Review of the operational definition for first-episode psychosis. *Early Interv Psychiatry.* (2009) 3:259–65. doi: 10.1111/j.1751-7893.2009.00148.x

35. Dazzan P, Morgan KD, Orr K, Hutchinson G, Chitnis X, Suckling J, et al. Different effects of typical and atypical antipsychotics on grey matter in first episode psychosis: The AESOP study. *Neuropsychopharmacology.* (2005) 30:765–74. doi: 10.1038/sj.npp.1300603

36. Andreasen NC, Pressler M, Nopoulos P, Miller D, Ho B. Antipsychotic dose equivalents and dose-years: A standardized method for comparing exposure to different drugs. *Biol Psychiatry.* (2010) 67:255–62. doi: 10.1016/j.biopsych.2009.08.040

37. Leucht S, Samara M, Heres S, Patel MX, Woods SW, Davis JM. Dose equivalents for second-generation antipsychotics: The minimum effective dose method. *Schizophr Bull.* (2014) 40:314–26. doi: 10.1093/schbul/sbu001

38. Taylor DM, Barnes TR, Young AH. *The Maudsley prescribing guidelines in psychiatry*. Hoboken, NJ: John Wiley & Sons (2018).

39. Agid O, Kapur S, Arenovich T, Zipursky RB. Delayed-onset hypothesis of antipsychotic action: A hypothesis tested and rejected. *Arch Gen Psychiatry.* (2003) 60:1228–35. doi: 10.1001/archpsyc.60.12.1228

40. Kinon BJ, Chen L, Ascher-Svanum H, Stauffer VL, Kollack-Walker S, Zhou W, et al. Early response to antipsychotic drug therapy as a clinical marker of subsequent response in the treatment of schizophrenia. *Neuropsychopharmacology.* (2010) 35:581. doi: 10.1038/npp.2009.164

41. Kahn RS, Fleischhacker WW, Boter H, Davidson M, Vergouwe Y, Keet IP, et al. Effectiveness of antipsychotic drugs in first-episode schizophrenia and schizophreniform disorder: An open randomised clinical trial. *Lancet.* (2008) 371:1085–97. doi: 10.1016/S0140-6736(08)60486-9

42. Sajatovic M, Velligan DI, Weiden PJ, Valenstein MA, Ogedegbe G. Measurement of psychiatric treatment adherence. *J Psychosom Res.* (2010) 69:591–9. doi: 10.1016/j.jpsychores.2009.05.007

43. Howes OD, McCutcheon R, Agid O, De Bartolomeis A, Van Beveren NJ, Birnbaum ML, et al. Treatment-resistant schizophrenia: Treatment response and resistance in psychosis (TRRIP) working group consensus guidelines on diagnosis and terminology. *Am J Psychiatry.* (2016) 174:216–29. doi: 10.1176/appi.ajp.2016.16050503

44. Kay SR, Fiszbein A, Opler LA. The positive and negative syndrome scale (PANSS) for schizophrenia. *Schizophr Bull.* (1987) 13:261–76. doi: 10.1093/schbul/13.2.261

45. Sarpal DK, Robinson DG, Fales C, Lencz T, Argyelan M, Karlsgodt KH, et al. Relationship between duration of untreated psychosis and intrinsic corticostriatal connectivity in patients with early phase schizophrenia. *Neuropsychopharmacology.* (2017) 42:2214. doi: 10.1038/npp.2017.55

46. Gasparovic C, Chen H, Mullins PG. Errors in 1H-MRS estimates of brain metabolite concentrations caused by failing to take into account tissue-specific signal relaxation. *NMR Biomed.* (2018) 31:e3914. doi: 10.1002/nbm.3914

47. Öngür D, Prescot AP, Jensen JE, Cohen BM, Renshaw PF. Creatine abnormalities in schizophrenia and bipolar disorder. *Psychiatry Res Neuroimaging.* (2009) 172:44–8. doi: 10.1016/j.pscychresns.2008.06.002

48. Merritt K, Catalan A, Cowley S, Demjaha A, Taylor M, McGuire P, et al. Glyceryl trinitrate in first-episode psychosis unmedicated with antipsychotics: A randomised controlled pilot study. *J Psychopharmacol.* (2020) 34:839–47. doi: 10.1177/0269881120922967

49. Quintana DS, Williams DR. Bayesian alternatives for common null-hypothesis significance tests in psychiatry: A non-technical guide using JASP. *BMC Psychiatry*. (2018) 18:178. doi: 10.1186/s12888-018-1761-4

50. Aoyama N, Theberge J, Drost DJ, Manchanda R, Northcott S, Neufeld RW, et al. Grey matter and social functioning correlates of glutamatergic metabolite loss in schizophrenia. *Br J Psychiatry*. (2011) 198:448–56. doi: 10.1192/bjp.bp.110.079608

51. Bustillo J, Rowland L, Mullins P, Jung R, Chen H, Qualls C, et al. 1 H-MRS at 4 tesla in minimally treated early schizophrenia. *Mol Psychiatry*. (2010) 15:629–36. doi: 10.1038/mp.2009.121

52. Kaar SJ, Natesan S, McCutcheon R, Howes OD. Antipsychotics: Mechanisms underlying clinical response and side-effects and novel treatment approaches based on pathophysiology. *Neuropharmacology*. (2020) 172:107704. doi: 10.1016/j.neuropharm.2019.107704

53. Gallego JA, Robinson DG, Sevy SM, Napolitano B, McCormack J, Lesser ML, et al. Time to treatment response in first-episode schizophrenia: Should acute treatment trials last several months? *J Clin Psychiatry*. (2011) 72:1691–6. doi: 10.4088/JCP.10m06349

54. Ramadan S, Lin A, Stanwell P. Glutamate and glutamine: A review of in vivo MRS in the human brain. *NMR Biomed*. (2013) 26:1630–46. doi: 10.1002/nbm.3045

55. Howes OD, Kapur S. A neurobiological hypothesis for the classification of schizophrenia: Type a (hyperdopaminergic) and type B (normodopaminergic). *Br J Psychiatry*. (2014) 205:1–3. doi: 10.1192/bjp.bp.113.138578

56. Potkin SG, Kane JM, Correll CU, Lindenmayer J, Agid O, Marder SR, et al. The neurobiology of treatment-resistant schizophrenia: Paths to antipsychotic resistance and a roadmap for future research. *NPJ Schizophr*. (2020) 6:1. doi: 10.1038/s41537-019-0090-z

57. Jauhar S, Nour MM, Veronese M, Rogdaki M, Bonoldi I, Azis M, et al. A test of the transdiagnostic dopamine hypothesis of psychosis using positron emission tomographic imaging in bipolar affective disorder and schizophrenia. *JAMA Psychiatry*. (2017) 74:1206–13. doi: 10.1001/jamapsychiatry.2017.2943

frontiers | Frontiers in Psychiatry

TYPE Original Research
PUBLISHED 06 September 2022
DOI 10.3389/fpsyt.2022.971105

OPEN ACCESS

EDITED BY
Wenbin Guo,
Second Xiangya Hospital, Central South University, China

REVIEWED BY
Xiao Chang,
King's College London, United Kingdom
Yongbin Wei,
Beijing University of Posts and Telecommunications (BUPT), China

*CORRESPONDENCE
Yuanjun Xie
xieyuanj@gmail.com
Peng Fang
fangpeng@fmmu.edu.cn

SPECIALTY SECTION
This article was submitted to Neuroimaging and Stimulation, a section of the journal Frontiers in Psychiatry

RECEIVED 16 June 2022
ACCEPTED 16 August 2022
PUBLISHED 06 September 2022

CITATION
Xie Y, Cai Y, Guan M, Wang Z, Ma Z, Fang P and Wang H (2022) The alternations of nucleus accumbent in schizophrenia patients with auditory verbal hallucinations during low-frequency rTMS treatment. *Front. Psychiatry* 13:971105. doi: 10.3389/fpsyt.2022.971105

The alternations of nucleus accumbent in schizophrenia patients with auditory verbal hallucinations during low-frequency rTMS treatment

Yuanjun Xie[1,2]*, Yun Cai[3], Muzhen Guan[4], Zhongheng Wang[5], Zhujing Ma[6], Peng Fang[7]* and Huaning Wang[5]

[1]School of Education, Xinyang College, Xinyang, China, [2]Department of Radiology, Xijing Hospital, Air Force Medical University, Xi'an, China, [3]Department of Neurodevelopment Psychology, School of Psychology, Army Medical University, Chongqing, China, [4]Department of Mental Health, Xi'an Medical University, Xi'an, China, [5]Department of Psychiatry, Xijing Hospital, Air Force Medical University, Xi'an, China, [6]Department of Clinical Psychology, Air Force Medical University, Xi'an, China, [7]Department of Military Medical Psychology, Air Force Medical University, Xi'an, China

Low-frequency repetitive transcranial magnetic stimulation (rTMS) has been shown to reduce the severity of auditory verbal hallucinations (AVH) and induce beneficial functional and structural alternations of the brain in schizophrenia patients with AVH. The nucleus accumbens (NAcc) as an important component of the ventral striatum is implicated with the pathology in AVH. However, the induced characteristic patterns of NAcc by low-frequency rTMS in schizophrenia with AVH are seldom explored. We investigated the functional and structural characteristic patterns of NAcc by using seed-based functional connectivity (FC) analysis and gray matter volume (GMV) measurement in schizophrenia patients with AVH during 1 Hz rTMS treatment. Although low-frequency rTMS treatment did not affect the volumetric changes of NAcc, the abnormal FC patterns of NAcc, including increased FC of NAcc with the temporal lobes and decreased FC of NAcc with the frontal cortices in the pretreatment patients compared to healthy controls, were normalized or reversed after treatment. These FC changes were associated with improvements in clinical symptoms and neurocognitive functions. Our findings may extend our understanding of the NAcc in the pathology of schizophrenia with AVH and might be a biomarker of clinical effect for low-frequency rTMS treatment in schizophrenia.

KEYWORDS

schizophrenia, auditory verbal hallucination, nucleus accumbent, functional connectivity, gray matter volume, repetitive transcranial magnetic stimulation

Introduction

Schizophrenia is a chronic and disabling disease that affects ∼0.7% of the population (1). Symptoms associated with schizophrenia can be divided into three domains: positive symptoms (e.g., hallucinations and delusions), negative symptoms (e.g., avolition and withdrawal), and cognitive symptoms (e.g., memory and executive function) (2). The etiology of schizophrenia is still poorly understood. However, the neurobiology of the psychotic symptoms has been associated with dopaminergic abnormality in the striatum (3). Abnormal dopaminergic regulation of striatal function could explain the mechanisms underlying the symptoms of schizophrenia (4, 5). Of particular interest is the nucleus accumbens (NAcc), a central component of the ventral striatum, which plays an important role in the pathology of schizophrenia (6). The modulation of the striatal circuit activity can reduce psychotic symptoms (7). Thus, NAcc has been proposed as the critical target for antipsychotic medications (8).

NAcc receives intensive excitatory afferents from the frontal cortex, hippocampus, and amygdala, closely associated with dopaminergic changes in schizophrenia pathology (9). Several studies have reported increased dopaminergic activity in the NAcc in schizophrenia (10, 11). Subsequent animal studies have confirmed similar findings (12–14). Structural abnormalities in the NAcc have been consistently illustrated in schizophrenia. There were significant reductions in gray matter volume (GMV)of the NAcc in schizophrenic brains from the structural magnetic resonance imaging data (15–17). In addition, resting-state functional magnetic resonance imaging (fMRI) studies have observed abnormal intrinsic functional connectivity (FC) of NAcc in schizophrenia (18–20), regions mainly located in the frontal, parietal, temporal, and limbic systems (e.g., the cingulate cortex, insula, parahippocampal gyrus, and ventral tegmental area). Therefore, NAcc is the primary region interacting with multiple areas of cortical and limbic systems and could provide a supplementary understanding of pathology in schizophrenia.

Current treatments of antipsychotics are thought to target the NAcc and can reduce a hyperdopaminergic state of the striatum (21, 22). However, antipsychotics are only responded to symptoms and are confined in their effectiveness, and frequently accompanied by side effects (23). Meta-analysis and system review studies have indicated that the application of low-frequency repetitive transcranial magnetic stimulation (rTMS) during schizophrenia can effectively reduce the severity of auditory verbal hallucinations (AVH) (24–28), although negative findings were reported (29, 30), probably because the heterogeneity of treatment protocols and placebo response (31). AVH are defined as perceptions in the absence of external verbal stimuli and are prominent among the core symptoms of schizophrenia (32). The activation of NAcc is associated with the vividness of hallucinations (33) and auditory verbal imagery in schizophrenia patients (34). Moreover, the abnormal FC (20, 35) and gray matter changes (36) of NAcc appeared to be associated with the presence of AVH and neurocognitive impairments. The results may indicate the unique role of NAcc in investigating the neural mechanisms of schizophrenia with AVH. Nevertheless, its underlying changes in schizophrenia with AVH during rTMS are seldom explored.

The purpose of the present study aimed to investigate the potential alternations of NAcc in schizophrenia patients with AVH during low-frequency rTMS treatment by using the seed-based FC analysis and GMV measurement. Correlation analyses were further done between the possible alternations of NAcc and clinical responses of patients after treatment. We hypothesized that low-frequency rTMS treatment could normalize or inverse the abnormal functional or structural patterns of NAcc and associated with the reduction of clinical symptom severity.

Materials and methods

Participants

Thirty-two patients with AVH were recruited from the Department of Psychiatry, Xijing Hospital of Fourth Military Medical University. The diagnosis of schizophrenia was made by experienced psychiatrists according to the Chinese version of the Structured Clinical Interview for Diagnosis and Statistical Manual of Mental Disorder (DSM-V). The inclusion criteria of the patient group were as follows: (1) AVH daily occurred with at least two antipsychotic medications, and (2) no less than five episodes of AVH per day over the past month. All patients who received a steady dose of antipsychotic medications remained unchanged during the study period. In addition, thirty-five healthy controls matched by age, sex, and education were recruited from the local community through advertising and had no history of psychiatric diseases. For all the participants, the exclusion criteria were as follows: (1) any past or current neurological diseases, (2) history of head injury, (3) alcohol or substance abuse, and (4) contraindications to MRI scans.

This study was approved by the Medical Ethics Committee of the Xijing Hospital and was conducted following the Declaration of Helsinki. Informed written consent was obtained from all the participants. The study was registered in the Chinese Clinical Trial Register (http://www.chictr.org/cn/, registration number: ChiCTR2100041876).

Clinical measurements

The severity of psychotic symptoms was assessed using the Positive and Negative Syndrome Scale (PANSS) (37). The AVH was assessed by the auditory Hallucination Rating Scale

(AHRS) (38). The Chinese version of the MATRICS Consensus Cognitive Battery (MCCB) was used to measure neurocognitive impairment in patients consisting of 10 tasks across seven cognitive domains (39): speed of processing test (SOPT), attention and vigilance test (AVT), working memory (WMT) test, verbal learning test (VERBLT), visual learning test (VISLT), reasoning and problem-solving test (RPST), and social cognition test (SCT). All clinical measures were performed by experienced psychiatrists at baseline and after treatment.

rTMS protocol

A type of 8-figure coil magnetic stimulator (YIRUIDE Inc., Wuhan, China) was used to perform 1 Hz rTMS treatment, and the left temporoparietal junction (TPJ) was selected as the stimulation target, which is referred to as the International 10–20 electrode location system (TP3). This stimulation target has been widely applied to treat AVH in schizophrenia by using low-frequency rTMS (40, 41). Patients were treated for 15 consecutive days at 15 min per day (once per second, 5 s interval) with a 110% resting motor threshold, generating 60 trains of 600 pulses.

MRI data acquisition

MRI data were obtained using a 3.0-Tesla scanner (GE Medical Systems, Milwaukee, WI) equipped with an 8-channel phased-array head coil. The patient group was scanned twice (before and after treatment), while the control group was scanned only once. During the entire scan, the participants were instructed to stay awake with their eyes closed and remain awake and keep their heads motionless. Resting-state functional images were obtained using a gradient-echo-planar imaging sequence with the following parameters: 45 axial slices, repetition time (TR) = 2,000 ms, echo time (TE) = 40 ms, matrix = 64 × 64, field of view (FOV) = 260 × 260 mm^2, flip angle = 90°; slice thickness = 3.5 mm (no gap), and 210 volumes were acquired. The T1-weighted structural images were obtained during the same scanning session by an MP-RAGE sequence as the following parameters: TR = 8.1 ms, TE = 3.2 ms, matrix size = 256 × 256, flip angle = 12°, FOV = 240 × 240 mm^2, 176 slices, and thickness=1.0 mm.

Neuroimaging data preprocessing

Resting-state functional imaging data were preprocessed using the SPM (https://www.fil.ion.ucl.ac.uk/spm/) and DPABI (http://rfmri.org/dpabi) toolbox. For each participant, the first ten functional volumes were removed to assure equilibration of the magnetic field. The remaining volumes were corrected for slice acquisition and head motion. Subsequently, the corrected images were normalized into the standard Montreal Neurological Institute (MNI) space by the Exponentiated Lie Algebra (DARTEL) algorithm (42) and then resampled to a 3 × 3 × 3 mm^3 resolution. Then, the normalized images were linearly detrended and regressed the nuisance covariates, including Friston 24 motion parameters (43), white matter signal, cerebrospinal fluid signal, and whole-brain global signal. Band-pass temporal filtering (0.01–0.1 Hz) was performed to reduce high-frequency physiological noise. Finally, spatial smoothing was conducted with a 6-mm Gaussian kernel for statistical analyses.

Structural imaging data were processed using SPM (https://www.fil.ion.ucl.ac.uk/spm/) and VBM (https://dbm.neuro.uni-jena.de/wordpress/vbm/) toolbox. The structural images were subjected to bias correction and tissue-classified into gray matter, white matter, and cerebrospinal fluid with the volume probability maps. The gray matter images were then normalized to standard Montreal Neurological Institute (MNI) space. Subsequently, intensity modulation and an 8 mm Gaussian kernel smoothing of the resulting images were completed.

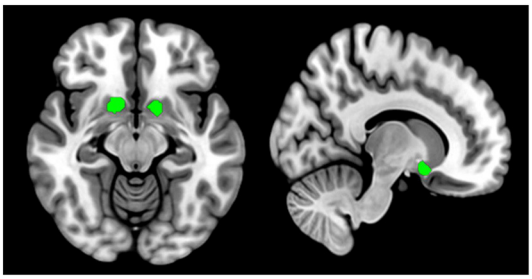

FIGURE 1
Nucleus accumbent seed regions of interest are defined by the Anatomical Automatic Labeling (AAL3) atlas (https://www.oxcns.org/aal3.html). Bilateral nucleus accumbent seeds are used in resting-state functional connectivity analysis and gray matter volume measure.

FC analysis

The bilateral NAcc were defined as seeds based on the Anatomical Automatic Labeling (AAL3) atlas (44), see Figure 1 for details. Subsequent procedures were executed in the left and right seed individually. Pearson correlation analyses were performed between the seed reference time course and time series of the whole brain. The resulting correlation coefficients were converted into z-scores using to enhance normality.

GMV analysis

The values of GMV from the NAcc were then extracted from the preprocessed gray matter images with the seed mask. The GMV differences of left and right NAcc were then compared between the patient and control groups or patients before and after treatment.

Statistical analysis

Statistical analysis of the demographic and clinical data was carried out using the SPSS (version 23.0; Chicago, IL, United States). Independent-sample *t*-test and chi-square test were conducted according to the characteristics of the data. In addition, the independent-sample *t*-tests were done to investigate group differences in FC and GMV between patients at baseline and controls with age, gender, education, and mean head motion (Framewise displacement, FD) parameter as covariates. These different brain regions were defined as a mask for subsequent analysis. A paired-sample *t*-test was used to examine the treatment effect of the two measures between patients after treatment and before treatment with the mask created above. Group statistical maps were thresholded at $p < 0.05$ and a voxel level of $p < 0.05$ with 30 voxel size using the Gaussian random field (GRF) method.

Finally, partial correlation coefficients were calculated between the altered measures and clinical responses in patients using the dosage of antipsychotics as a covariate. To explore the effect of antipsychotics on clinical symptoms and measure changes, correlations of the medication dosage with clinical response and measure changes were examined. For all correlation coefficients, a two-tailed p level of 0.05 was used as the criterion of statistical significance and corrected for multiple

TABLE 1 Demographic and clinical characteristics of the participants.

Variable	Patients ($n = 30$)	Controls ($n = 33$)	χ^2(t)	*p*-value
Age (year)	30.30 ± 4.46	32.03 ± 7.31	0.954	0.345
Sex (female/male)	17 (13)	20 (13)	0.101	0.751
Education (year)	13.20 ± 2.67	12.09 ± 2.04	1.708	0.094
Duration of illness (month)	21.36 ± 4.89	–	–	–
Medication dosage (CPED, mg/day)	584.8 ± 152.39	–	–	–
Medication duration (day)	15	–	–	–

CPED, Chlorpromazine equivalent doses (45).

TABLE 2 Comparisons of clinical responses between patients before and after treatment.

	Pretreatment ($n = 30$)	Posttreatment ($n = 30$)	*t*	*p*-value
PNASS				
Total scores	79.85 ± 10.55	67.50 ± 7.98	4.175	0.000
Positive symptoms	19.65 ± 4.60	14.45 ± 2.80	4.324	0.000
Negative symptoms	19.85 ± 4.53	17.85 ± 2.96	1.652	0.107
General symptoms	40.35 ± 6.65	35.20 ± 5.54	2.661	0.011
AHRS	27.45 ± 6.14	13.75 ± 7.07	6.542	0.000
MCCB				
SOPT	27.20 ± 14.61	34.15 ± 10.96	1.702	0.137
AVT	35.80 ± 13.00	42.20 ± 8.35	1.852	0.127
WMT	32.95 ± 12.34	39.75 ± 14.37	1.606	0.137
VERBLT	29.60 ± 12.60	39.80 ± 12.24	2.597	0.047
VISLT	34.55 ± 15.95	47.00 ± 10.54	2.912	0.042
RPST	35.45 ± 13.63	43.85 ± 12.38	2.040	0.114
SCT	31.95 ± 6.72	34.20 ± 7.49	1.000	0.327

PNASS, positive and negative syndrome scale; AHRS, auditory hallucination rating scale; MCCB, MATRICS Consensus Cognitive Battery; SOPT, speed of processing test attention; AVT, vigilance test; WMT, working memory test; VERBLT, verbal learning test; VISLT, visual learning test; RPST, reasoning and problem-solving test; SCT, social cognition test.

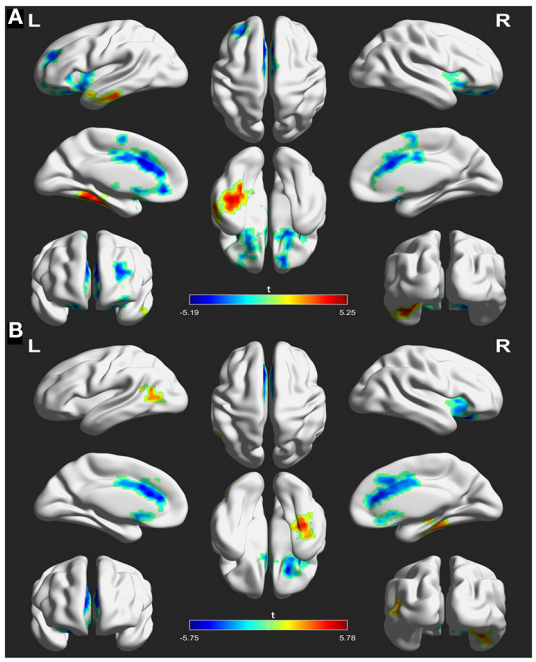

FIGURE 2
Differences in functional connectivity (FC) between patients at baseline and healthy controls using left nucleus accumbent **(A)** and right nucleus accumbent **(B)** seed regions. The warm color indicates an increased FC of seed with the whole brain and the cool color indicates a decreased FC of seed with the whole brain. The color scale is represented by the *t*-value of statistically significant clusters with the voxel-level statistical threshold of $p < 0.05$ and a cluster-level threshold of $p < 0.05$ corrected for the Gaussian random field (size >30).

comparisons with the false discovery rate correction (FDR) method.

Results

Demographic and clinical data comparisons

The demographic and clinical characteristics of the participants are displayed in Table 1. The difference in age ($t = 0.954$, $p = 0.345$), sex ($\chi^2 = 0.101$, $p = 0.751$), and educational years ($t = 1.708$, $p = 0.094$) distribution did not reach significance in the patients at baseline and controls.

But after rTMS treatment, the clinical responses, including positive symptoms (14.45 ± 2.80 vs. 19.65 ± 4.60, $t = 4.324$, $p = 0.000$), AVH (13.75 ± 7.07 vs. 27.45 ± 6.14, $t = 6.542$, $p = 0.000$), and certain neurocognitive functions such as verbal memory (29.60 ± 12.60 vs. 39.80 ± 12.24, $t = 2.597$, $p = 0.047$) and visual memory (34.55 ± 15.95 vs. 47.00 ± 10.54, $t = 2.912$, $p = 0.042$), were improved in patients compared to before treatment. Details are displayed in Table 2.

FC comparison of NAcc seeds

The analyses of FC in the NAcc seeds between patients at baseline and controls are shown in Figure 2 and Table 3. For the left NAcc seed, the patients exhibited significantly increased FC in the left inferior temporal gyrus and right fusiform gyrus, and decreased FC in the right superior frontal gyrus and left anterior cingulate gyrus when compared with the controls (GRF correction; voxel-level $p < 0.05$, cluster level $p < 0.05$, clusters size > 30 voxels). Similar, significantly increased FC of the right NAcc seed was seen in the left middle temporal gyrus and right fusiform gyrus, and decreased FC was seen in the right inferior frontal gyrus and left anterior cingulate gyrus in patients at baseline relative to the controls (GRF correction; voxel-level $p < 0.05$, cluster level $p < 0.05$, clusters size > 30 voxels). These abnormal FC regions were defined as mask for subsequent comparisons between patients before and after treatment.

However, these abnormal FC patterns did not persistent after rTMS treatment. Instead, initial FC of NACC with the left inferior temporal gyrus (posttreatment vs. pretreatment: -0.025 ± 0.089 vs. 0.023 ± 0.097, $t = 2.723$, $p = 0.011$) and right inferior frontal gyrus (posttreatment vs. pretreatment: 0.235 ± 0.108 vs. 0.180 ± 0.122, $t = 2.652$, $p = 0.013$) in patients before treatment was inversed after treatment. Details are displayed in Figure 3 and Table 4.

GMV comparison of NAcc seeds

The volumetric analysis showed that the patients at baseline had decreased GMV in left NAcc compared to the controls ($t = 2.18$, $p = 0.038$) (Figure 4), while the rTMS treatment did not affect the volumetric changes in the left or right NAcc in patients ($p > 0.05$) (Figure 4).

Correlation analysis

In the patient group, the changed FC value in the left NAcc seed with the left inferior temporal gyrus was positively correlated to the changed positive symptom score of PNASS ($r = -0.545$, $p = 0.024$, FDR correction). In addition, the changed FC value of the right NAcc seed with the right inferior frontal gyrus was negatively correlated to changed verbal memory score ($r = 0.526$, $p = 0.016$, FDR correction) in the patients. But the medication dosage was not significantly correlated with the clinical symptom score FC value changes (all $p > 0.05$, Supplementary Table 1). Details are displayed in Figure 5.

10.3389/fpsyt.2022.971105

TABLE 3 Functional connectivity differences of the nucleus accumbens seeds between patients at baseline and controls (patients > controls).

Brain regions	Side	BA	Cluster size	MNI coordinates			*t*-value
				x	*y*	*z*	
L NAcc seed							
Inferior temporal gyrus	L	37	242	−39	−33	−18	5.250
Fusiform gyrus	R	30	83	24	−30	−21	4.162
Superior frontal gyrus	R	48	77	24	12	−15	−4.797
Anterior cingulate gyrus	L	25	197	−9	27	18	−5.193
R NAcc seed							
Fusiform gyrus	R	20	95	36	−30	−18	5.776
Middle temporal gyrus	L	37	132	−54	−69	9	3.832
Inferior frontal gyrus	R	11	43	21	27	−21	−4.911
Anterior cingulate gyrus	L	24	188	−9	33	15	−5.750

NAcc, nucleus accumbens; L, left; R, right; BA, Brodmann area; MNI, Montreal Neurological Institute.

Discussion

In the present study, we investigated FC and GMV alternations of NAcc when schizophrenia patients with AVH received low-frequency rTMS treatment. Our findings demonstrated the patients at baseline had abnormal FC of NAcc with the temporal, frontal, and anterior cingulate cortices and decreased GMV in left NACC compared to controls. Although low-frequency rTMS did not affect the volumetric changes of NAcc, the abnormal FC patterns of NAcc with the temporal and frontal cortices were reversed in patients after treatment. The alternations of FC patterns were associated with clinical improvements in patients. These findings suggested that the NAcc may play an important role in the underlying pathology of schizophrenia and contribute to the effect of low-frequency rTMS on schizophrenia patients with AVH.

Our results indicated that patients at baseline had higher FC of NAcc with the temporal lobes (left middle temporal gyrus, left inferior temporal, and right fusiform gyrus) compared to control. These regions represent the speech processing areas (46, 47) and are known to be associated with AVH (48). Neuroimaging studies have indicated that auditory hallucinations are associated with hyperactivity in the auditory language cortex (49–51). Increased metabolism of temporal lobes has been reported in schizophrenia patients (52) and was related to positive symptoms (53). The hyperactive FC between NAcc and temporal lobes might be involved in an impaired function in speech perceptions and could be associated with the poor functional outcomes of patients with AVH. Higher FC between the NAcc and the temporal lobes appearing in schizophrenia patients with AVH was agreed with the previous report (19, 20), which might suggest a functional deficit of langue processing in the striatum-related circuits.

Decreased FC of NAcc with the frontal cortices (e.g., right superior frontal gyrus and inferior frontal gyrus) and anterior cingulate gyrus was also observed in patients at baseline relative to controls. The results are consistent with previous studies that reported hypoconnectivity of the frontostriatal loop in schizophrenia (18, 54). Specifically, Broca's region and its right hemisphere counterpart in the inferior frontal gyrus are involved in language processing (55, 56). There is common activation between the inferior frontal gyrus and NAcc during cognitive task processing (57) and decreased tract connections between them in schizophrenia (58, 59). In addition, the anterior cingulate gyrus is a critical area to integrate cognitive control processes (e.g., error monitoring) (60–62). Dysfunction of this region is found in schizophrenia (63) and may involve the

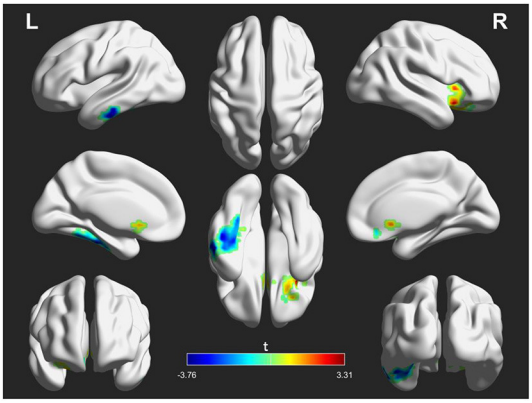

FIGURE 3
Differences in functional connectivity (FC) of the nucleus accumbens seeds between patients after treatment and before treatment. The warm color indicates an increased FC of seed with the whole brain and the cool color indicates a decreased FC of seed with the whole brain. The color scale is represented by the *t*-value of statistically significant clusters with the voxel-level statistical threshold of $p < 0.05$ and a cluster-level threshold of $p < 0.05$ corrected for the Gaussian random field (size >30).

TABLE 4 Functional connectivity differences of the nucleus accumbens seeds between patients after treatment and before treatment (after treatment > before treatment).

Brain regions	Side	BA	Cluster size	MNI coordinates			*t*-value
				x	*y*	*z*	
L NAcc seed							
Inferior temporal gyrus	L	20	90	−57	−18	−30	−3.759
R NAcc seed							
Inferior frontal gyrus	R	48	32	33	23	−7	3.314

NAcc, nucleus accumbens; L, left; R, right; MNI, Montreal Neurological Institute.

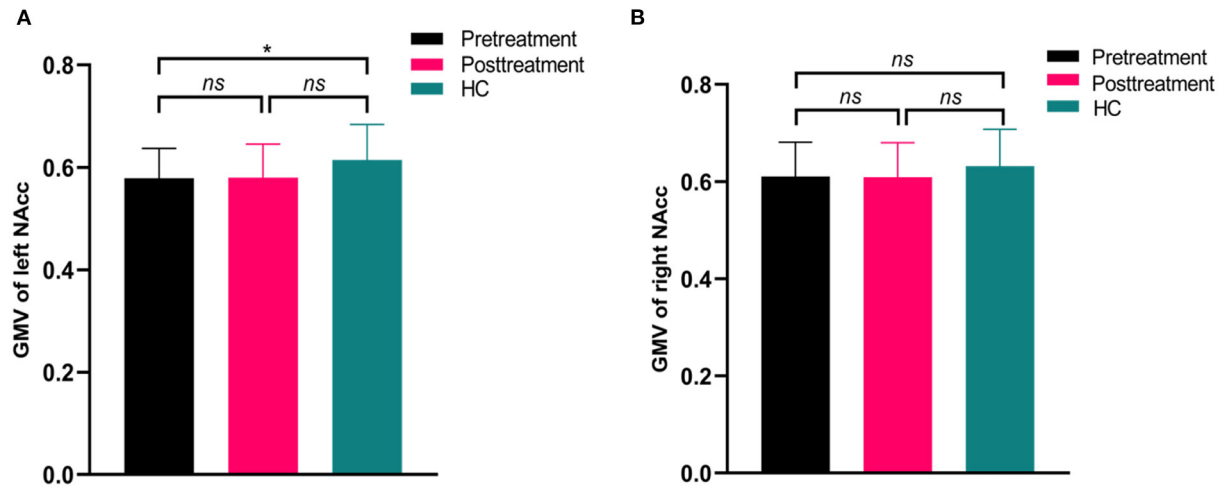

FIGURE 4
Differences in gray matter volume (GMV) of nucleus accumbens between patients (pretreatment and posttreatment) and healthy controls (HC). The pretreatment patients showed significantly decreased GMV in the left nucleus accumbent compared to HC **(A)**. While there were no significant differences in the right nucleus accumbens between patients (pretreatment and posttreatment) and HC **(B)**. *$p > 0.05$; ns, no significance.

misattribution of external sources of speech (64). The decreased FC of NAcc may partly explain the cognitive control deficits in patients that are characteristic of the clinical manifestations of schizophrenia, since the NAcc is implicated in cognitive functions, including memory, motivation, and decision-making (65) and is a virtual interface for information transmission between cortical and subcortical structures (66). Therefore, this hypoconnectivity of the NAcc circuit may lead to impairments of langue processing in schizophrenia.

However, these abnormal FC patterns of NAcc were normalized or inversed in patients after rTMS treatment. Several studies have indicated that low-frequency rTMS can increase the contribution of connected regions associated with auditory hallucinations (40, 41) due to long-lasting neuroplastic changes derived from the rTMS. Thus, the clinical effect of low-frequency rTMS on AVH may be associated with the reduction of hyperactivity in the auditory language cortex and relevant areas that propagate through remote pathways. Consistent with the hypothesis, we observed that initial increased FC between the NAcc and left inferior temporal gyrus in patients were inversed after treatment, which supports the long-term depression phenomenon induced by low-frequency rTMS (67). The inhibitory effect may shift from the target site to adjacent regions (e.g., NAcc) since there are well-established projections between them (68). This beneficial alternation may lead to the induced spread of the physiological effect in the auditory language circuit and may play an indirect modulatory effect on the NAcc connection loops, which could be associated with the reduction of clinical symptoms (e.g., positive symptom).

In addition, we found that the decreased FC of NAcc with the right inferior frontal gyrus was reversed in patients after rTMS treatment. Induced metabolic alternation in the frontal cortex by the low-frequency rTMS has been reported in schizophrenia with AVH (52). This alternation could be due to the induction of integration of frontotemporal disconnection that is documented in schizophrenia (69, 70). Studies have

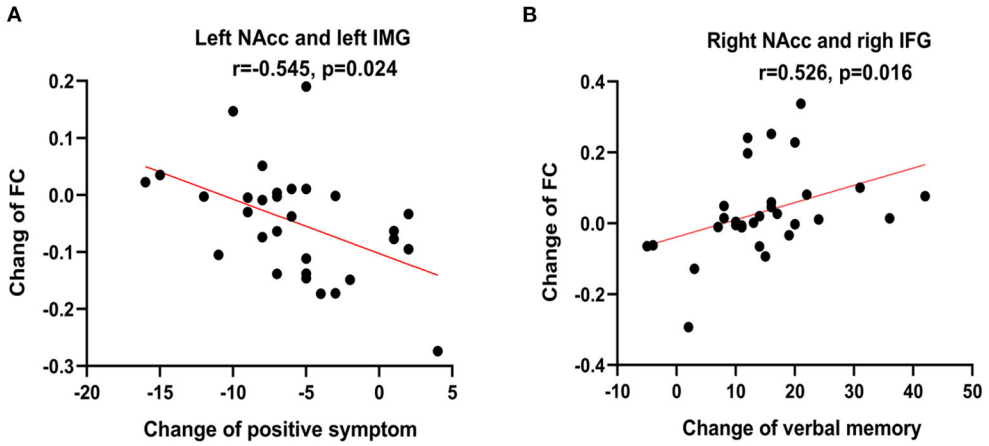

FIGURE 5
Correlations analysis showed that the changed functional connectivity (FC) value of left nucleus accumbens (NAcc) with the left inferior temporal gyrus (IMG) is negatively correlated with the change of positive symptom score of PNASS ($r = -0.545$, $p = 0.024$, False discovery rate correction) **(A)** and FC value of the right NAcc with the right inferior frontal gyrus (IFG) is positively correlated with the change of verbal memory score ($r = 0.526$, $p = 0.016$, False discovery rate correction) **(B)**.

indicated that the NAcc connected with the inferior frontal gyrus (20) and TMS over the frontal cortex can induce dopamine and glutamate changes in the NAcc (71). These findings suggest that low-frequency rTMS could have a modulatory effect on neurotransmitters released in the NAcc through the remote effects of stimulation at the interconnected regions and thus could be associated the neurocognitive improvements such as verbal learning and memory.

Structural abnormalities in NAcc have been consistently demonstrated in schizophrenia. Two meta-analyses studies showed significant reductions in NAcc volume in patients with schizophrenia (16, 72). There is evidence from studies in adolescents (73) and adults (74) that NACC volumes are larger in the left but not in the right hemisphere. However, we found a significantly smaller volume in the left NACC in patients compared to controls. This finding was consistent with the previous studies that deficit schizophrenia patients displayed smaller left NAcc volumes compared to controls (75) and may reflect the changes in structural asymmetries in the schizophrenia brain. Although we did not find any volumetric changes in NAcc in patients after rTMS treatment, the asymmetry of NAcc presented in schizophrenia may represent the alternations in specific deep gray matter nuclei associated with an endophenotype of schizophrenia with AVH.

Some limitations of the present stud should be considered. Firstly, the sample size was small and limited the statistical power. Future studies should consider collecting larger datasets to improve the statistical power. Secondly, patients enrolled in this study were under stable antipsychotic medication treatment, and the impact of antipsychotic medication on FC of the NAcc should be taken into account, although no correlations were found between medication and FC alterations of NAcc in patients. Finally, the absence of placebo sham stimuli may lead to caution about the efficacy of the stimulus paradigm.

Conclusions

In summary, our findings revealed abnormal FC and GMV changes of NAcc in patients and suggested an involvement of the striatal pathway in schizophrenia with AVH. Moreover, the abnormal FC patterns of the NAcc were inversed by low-frequency rTMS treatment and could be biomarkers of the clinical effectiveness of low-frequency rTMS treatment in schizophrenia with AVH.

Data availability statement

The original contributions presented in the study are included in the article/Supplementary material, further inquiries can be directed to the corresponding author/s.

Ethics statement

The studies involving human participants were reviewed and approved by the Medical Ethics Committee of the Xijing Hospital. The patients/participants provided their written informed consent to participate in this study.

Author contributions

YX, MG, and ZW design and organized the research. YX, YC, ZW, and PF collected the imaging and cognitive data. YX and PF analyzed the data. YX, YC, and MG wrote and revised the manuscript. PF and HW provided fund support. All authors contributed to the article and approved the submitted version.

Funding

This study was funded by the Natural Science Foundation of China (Nos. 81971255 and 81571651), Postdoctoral Science Foundation (2019M653963), and the Military Medical Science and Technology Youth Training Program of China (20QNPY049).

Conflict of interest

The authors declare that the research was conducted in the absence of any commercial or financial relationships that could be construed as a potential conflict of interest.

Publisher's note

All claims expressed in this article are solely those of the authors and do not necessarily represent those of their affiliated organizations, or those of the publisher, the editors and the reviewers. Any product that may be evaluated in this article, or claim that may be made by its manufacturer, is not guaranteed or endorsed by the publisher.

Supplementary material

The Supplementary Material for this article can be found online at: https://www.frontiersin.org/articles/10.3389/fpsyt.2022.971105/full#supplementary-material

References

1. Tandon R, Keshavan MS, Nasrallah HA. Schizophrenia, "just the facts" what we know in 2008. *Epidemiol Etiol Schizophr Res.* (2008) 102:1–18. doi: 10.1016/j.schres.2008.04.011

2. Mikell CB, McKhann GM, Segal S, McGovern RA, Wallenstein MB, Moore H. The hippocampus and nucleus accumbens as potential therapeutic targets for neurosurgical intervention in schizophrenia. *Stereotact Funct Neurosurg.* (2009) 87:256–65. doi: 10.1159/000225979

3. Miyake N, Thompson J, Skinbjerg M, Abi-Dargham A. Presynaptic dopamine in schizophrenia. *CNS Neurosci Ther.* (2011) 17:104–9. doi: 10.1111/j.1755-5949.2010.00230.x

4. Davis KL, Kahn RS, Ko G, Davidson M. Dopamine in schizophrenia: a review and reconceptualization. *Am J Psychiatry.* (1991) 148:1474–86. doi: 10.1176/ajp.148.11.1474

5. Kapur S. Psychosis as a state of aberrant salience: a framework linking biology, phenomenology, and pharmacology in schizophrenia. *Am J Psychiatry.* (2003) 160:13–23. doi: 10.1176/appi.ajp.160.1.13

6. Lum JS, Millard SJ, Huang X-F, Ooi L, Newell KA. A postmortem analysis of NMDA ionotropic and group 1 metabotropic glutamate receptors in the nucleus accumbens in schizophrenia. *J Psychiatry Neurosci.* (2018) 43:102–10. doi: 10.1503/jpn.170077

7. Abi-Dargham A, Rodenhiser J, Printz D, Zea-Ponce Y, Gil R, Kegeles Lawrence S, et al. Increased baseline occupancy of D2 receptors by dopamine in schizophrenia. *Proc Nat Acad Sci USA.* (2000) 97:8104–9. doi: 10.1073/pnas.97.14.8104

8. Xu S, Gullapalli RP, Frost DO. Olanzapine antipsychotic treatment of adolescent rats causes long term changes in glutamate and GABA levels in the nucleus accumbens. *Schizophr Res.* (2015) 161:452–7. doi: 10.1016/j.schres.2014.10.034

9. Britt JP, Benaliouad F, McDevitt RA, Stuber GD, Wise RA, Bonci A. Synaptic and behavioral profile of multiple glutamatergic inputs to the nucleus accumbens. *Neuron*. (2012) 76:790–803. doi: 10.1016/j.neuron.2012.09.040

10. Mackay AVP, Iversen LL, Rossor M, Spokes E, Bird E, Arregui A, et al. Increased brain dopamine and dopamine receptors in schizophrenia. *Arch Gen Psychiatry.* (1982) 39:991–7. doi: 10.1001/archpsyc.1982.04290090001001

11. Memo M, Kleinman Joel E, Hanbauer I. Coupling of dopamine D1 recognition sites with aenylate cyclase in nuclei accumbens and caudatus of schizophrenics. *Science.* (1983) 221:1304–7. doi: 10.1126/science.6310753

12. Hadar R, Soto-Montenegro ML, Götz T, Wieske F, Sohr R, Desco M, et al. Using a maternal immune stimulation model of schizophrenia to study behavioral and neurobiological alterations over the developmental course. *Schizophr Res.* (2015) 166:238–47. doi: 10.1016/j.schres.2015.05.010

13. Luchicchi A, Lecca S, Melis M, De Felice M, Cadeddu F, Frau R, et al. Maternal immune activation disrupts dopamine system in the offspring. *Int J Neuropsychopharmacol.* (2016) 19:1–10. doi: 10.1093/ijnp/pyw007

14. Meehan C, Harms L, Frost JD, Barreto R, Todd J, Schall U, et al. Effects of immune activation during early or late gestation on schizophrenia-related behaviour in adult rat offspring. *Brain Behav Immun.* (2017) 63:8–20. doi: 10.1016/j.bbi.2016.07.144

15. Bois C, Levita L, Ripp I, Owens DCG, Johnstone EC, Whalley HC, et al. Hippocampal, amygdala and nucleus accumbens volume in first-episode schizophrenia patients and individuals at high familial risk: a cross-sectional comparison. *Schizophr Res.* (2015) 165:45–51. doi: 10.1016/j.schres.2015.03.024

16. Okada N, Fukunaga M, Yamashita F, Koshiyama D, Yamamori H, Ohi K, et al. Abnormal asymmetries in subcortical brain volume in schizophrenia. *Mol Psychiatry.* (2016) 21:1460–6. doi: 10.1038/mp.2015.209

17. van Erp TGM, Hibar DP, Rasmussen JM, Glahn DC, Pearlson GD, Andreassen OA, et al. Subcortical brain volume abnormalities in 2028 individuals with schizophrenia and 2540 healthy controls via the ENIGMA consortium. *Mol Psychiatry.* (2016) 21:547–53. doi: 10.1038/mp.2015.63

18. Lin P, Wang X, Zhang B, Kirkpatrick B, Öngür D, Levitt JJ, et al. Functional dysconnectivity of the limbic loop of frontostriatal circuits in first-episode, treatment-naive schizophrenia. *Hum Brain Mapp.* (2018) 39:747–57. doi: 10.1002/hbm.23879

19. Potvin S, Dugre JR, Fahim C, Dumais A. Increased connectivity between the nucleus accumbens and the default mode network in patients with schizophrenia during cigarette cravings. *J Dual Diagn.* (2019) 15:8–15. doi: 10.1080/15504263.2018.1526432

20. Rolland B, Amad A, Poulet E, Bordet R, Vignaud A, Bation R, et al. Resting-state functional connectivity of the nucleus accumbens in auditory and visual hallucinations in schizophrenia. *Schizophr Bull.* (2015) 41:291–9. doi: 10.1093/schbul/sbu097

21. Deutch AY, Cameron DS. Pharmacological characterization of dopamine systems in the nucleus accumbens core and shell. *Neuroscience.* (1992) 46:49–56. doi: 10.1016/0306-4522(92)90007-O

22. Deutch AY, Lee MC, Iadarola MJ. Regionally specific effects of atypical antipsychotic drugs on striatal Fos expression: the nucleus accumbens shell as a locus of antipsychotic action. *Mol Cell Neurosci.* (1992) 3:332–41. doi: 10.1016/1044-7431(92)90030-6

23. Rummel-Kluge C, Komossa K, Schwarz S, Hunger H, Schmid F, Lobos CA, et al. Head-to-head comparisons of metabolic side effects of second generation antipsychotics in the treatment of schizophrenia: a systematic review and meta-analysis. *Schizophr Res.* (2010) 123:225–33. doi: 10.1016/j.schres.2010.07.012

24. He H, Lu J, Yang L, Zheng J, Gao F, Zhai Y, et al. Repetitive transcranial magnetic stimulation for treating the symptoms of schizophrenia: a PRISMA compliant meta-analysis. *Clin Neurophysiol.* (2017) 128:716–24. doi: 10.1016/j.clinph.2017.02.007

25. Kennedy NI, Lee WH, Frangou S. Efficacy of non-invasive brain stimulation on the symptom dimensions of schizophrenia: a meta-analysis of randomized controlled trials. *Eur Psychiatry.* (2018) 49:69–77. doi: 10.1016/j.eurpsy.2017.12.025

26. Li J, Cao X, Liu S, Li X, Xu Y. Efficacy of repetitive transcranial magnetic stimulation on auditory hallucinations in schizophrenia: a meta-analysis. *Psychiatry Res.* (2020) 290:113141. doi: 10.1016/j.psychres.2020.113141

27. Nathou C, Etard O, Dollfus S. Auditory verbal hallucinations in schizophrenia: current perspectives in brain stimulation treatments. *Neuropsychiatr Dis Treat.* (2019) 15:2105–17. doi: 10.2147/NDT.S168801

28. Slotema CW, Blom JD, van Lutterveld R, Hoek HW, Sommer IEC. Review of the efficacy of transcranial magnetic stimulation for auditory verbal hallucinations. *Biol Psychiatry.* (2014) 76:101–10. doi: 10.1016/j.biopsych.2013.09.038

29. Bais L, Vercammen A, Stewart R, van Es F, Visser B, Aleman A, et al. Short and long term effects of left and bilateral repetitive transcranial magnetic stimulation in schizophrenia patients with auditory verbal hallucinations: a randomized controlled trial. *PLoS ONE.* (2014) 9:e108828. doi: 10.1371/journal.pone.0108828

30. Slotema CW, Blom JD, de Weijer AD, Hoek HW, Sommer IE. Priming does not enhance the efficacy of 1 Hertz repetitive transcranial magnetic stimulation for the treatment of auditory verbal hallucinations: results of a randomized controlled study. *Brain Stimul.* (2012) 5:554–9. doi: 10.1016/j.brs.2011.10.005

31. Dollfus S, Lecardeur L, Morello R, Etard O. Placebo response in repetitive transcranial magnetic stimulation trials of treatment of auditory hallucinations in schizophrenia: a meta-analysis. *Schizophr Bull.* (2016) 42:301–8. doi: 10.1093/schbul/sbv076

32. Silbersweig DA, Stern E, Frith C, Cahill C, Holmes A, Grootoonk S, et al. A functional neuroanatomy of hallucinations in schizophrenia. *Nature.* (1995) 378:176–9. doi: 10.1038/378176a0

33. Raij TT, Valkonen-Korhonen M, Holi M, Therman S, Lehtonen J, Hari R. Reality of auditory verbal hallucinations. *Brain.* (2009) 132:2994–3001. doi: 10.1093/brain/awp186

34. Shergill SS, Bullmore E, Simmons A, Murray R, McGuire P. Functional anatomy of auditory verbal imagery in schizophrenic patients with auditory hallucinations. *Am J Psychiatry.* (2000) 157:1691–3. doi: 10.1176/appi.ajp.157.10.1691

35. Zhou C, Xue C, Chen J, Amdanee N, Tang X, Zhang H, et al. Altered functional connectivity of the nucleus accumbens network between deficit and non-deficit schizophrenia. *Front Psychiatry.* (2021) 12:704631. doi: 10.3389/fpsyt.2021.704631

36. Sampedro F, Roldán A, Alonso-Solís A, Grasa E, Portella MJ, Aguilar EJ, et al. Grey matter microstructural alterations in schizophrenia patients with treatment-resistant auditory verbal hallucinations. *J Psychiatr Res.* (2021) 138:130–8. doi: 10.1016/j.jpsychires.2021.03.037

37. Kay SR, Fiszbein A, Opler LA. The positive and negative syndrome scale (PANSS) for schizophrenia. *Schizophr Bull.* (1987) 13:261–76. doi: 10.1093/schbul/13.2.261

38. Hoffman RE, Hawkins KA, Gueorguieva R, Boutros NN, Rachid F, Carroll K, et al. Transcranial magnetic stimulation of left temporoparietal cortex and medication-resistant auditory hallucinations. *Arch Gen Psychiatry.* (2003) 60:49–56. doi: 10.1001/archpsyc.60.1.49

39. Shi C, Kang L, Yao S, Ma Y, Li T, Liang Y, et al. The MATRICS Consensus Cognitive Battery (MCCB): co-norming and standardization in China. *Schizophr Res.* (2015) 169:109–15. doi: 10.1016/j.schres.2015.09.003

40. Bais L, Liemburg E, Vercammen A, Bruggeman R, Knegtering H, Aleman A. Effects of low frequency rTMS treatment on brain networks for inner speech in patients with schizophrenia and auditory verbal hallucinations. *Progr Neuropsychopharmacol Biol Psychiatry.* (2017) 78:105–13. doi: 10.1016/j.pnpbp.2017.04.017

41. Vercammen A, Knegtering H, den Boer JA, Liemburg EJ, Aleman A. Auditory hallucinations in schizophrenia are associated with reduced functional connectivity of the temporo-parietal area. *Biol Psychiatry.* (2010) 67:912–8. doi: 10.1016/j.biopsych.2009.11.017

42. Ashburner J. A fast diffeomorphic image registration algorithm. *Neuroimage.* (2007) 38:95–113. doi: 10.1016/j.neuroimage.2007.07.007

43. Friston KJ, Williams S, Howard R, Frackowiak RSJ, Turner R. Movement-related effects in fMRI time-series. *Magn Reson Med.* (1996) 35:346–55. doi: 10.1002/mrm.1910350312

44. Rolls ET, Huang C-C, Lin C-P, Feng J, Joliot M. Automated anatomical labelling atlas 3. *Neuroimage.* (2020) 206:116189. doi: 10.1016/j.neuroimage.2019.116189

45. Woods SW. Chlorpromazine equivalent doses for the newer atypical antipsychotics. *J Clin Psychiatry.* (2003) 64:663–7. doi: 10.4088/JCP.v64n0607

46. Hickok G. The functional neuroanatomy of language. *Phys Life Rev.* (2009) 6:121–43. doi: 10.1016/j.plrev.2009.06.001

47. Turkeltaub PE, Eden GF, Jones KM, Zeffiro TA. Meta-analysis of the functional neuroanatomy of single-word reading: method and validation. *Neuroimage.* (2002) 16:765–80. doi: 10.1006/nimg.2002.1131

48. Diederen KMJ, Daalman K, de Weijer AD, Neggers SFW, van Gastel W, Blom JD, et al. Auditory hallucinations elicit similar brain activation in psychotic and nonpsychotic individuals. *Schizophr Bull.* (2012) 38:1074–82. doi: 10.1093/schbul/sbr033

49. Bohlken MM, Hugdahl K, Sommer IEC. Auditory verbal hallucinations: neuroimaging and treatment. *Psychol Med.* (2017) 47:199–208. doi: 10.1017/S003329171600115X

50. Cleghorn JM, Garnett ES, Nahmias C, Brown GM, Kaplan RD, Szechtman H, et al. Regional brain metabolism during auditory hallucinations in chronic schizophrenia. *Br J Psychiatry.* (1990) 157:562–70. doi: 10.1192/bjp.157.4.562

51. Copolov DL, Seal ML, Maruff P, Ulusoy R, Wong MTH, Tochon-Danguy HJ, et al. Cortical activation associated with the experience of auditory hallucinations and perception of human speech in schizophrenia: a PET correlation study. *Psychiatry Res Neuroimaging.* (2003) 122:139–52. doi: 10.1016/S0925-4927(02)00121-X

52. Horacek J, Brunovsky M, Novak T, Skrdlantova L, Klirova M, Bubenikova-Valesova V, et al. Effect of low-frequency rTMS on electromagnetic tomography (LORETA) and regional brain Metabolism (PET) in schizophrenia patients with auditory hallucinations. *Neuropsychobiology.* (2007) 55:132–42. doi: 10.1159/000106055

53. Paulman RG, Devous MD, Gregory RR, Herman JH, Jennings L, Bonte FJ, et al. Hypofrontality and cognitive impairment in schizophrenia: dynamic single-photon tomography and neuropsychological assessment of schizophrenic brain function. *Biol Psychiatry.* (1990) 27:377–99. doi: 10.1016/0006-3223(90)90549-H

54. Zhang B, Lin P, Wang X, Öngür D, Ji X, Situ W, et al. Altered functional connectivity of striatum based on the integrated connectivity model in first-episode schizophrenia. *Front Psychiatry.* (2019) 10:756. doi: 10.3389/fpsyt.2019.00756

55. Hagoort P, Levelt Willem JM. The speaking brain. *Science.* (2009) 326:372–3. doi: 10.1126/science.1181675

56. Saur D, Kreher Björn W, Schnell S, Kümmerer D, Kellmeyer P, Vry M-S, et al. Ventral and dorsal pathways for language. *Proc Nat Acad Sci USA.* (2008) 105:18035–40. doi: 10.1073/pnas.0805234105

57. Matthews SC, Simmons AN, Lane SD, and Paulus MP. Selective activation of the nucleus accumbens during risk-taking decision making. *Neuroreport.* (2004) 15:2123–7. doi: 10.1097/00001756-200409150-00025

58. de Leeuw M, Bohlken MM, Mandl RCW, Kahn RS, Vink M. Reduced fronto–striatal white matter integrity in schizophrenia patients and unaffected siblings: a DTI study. *npj Schizophrenia.* (2015) 1:15001. doi: 10.1038/npjschz.2015.1

59. James A, Joyce E, Lunn D, Hough M, Kenny L, Ghataorhe P, et al. Abnormal frontostriatal connectivity in adolescent-onset schizophrenia and its relationship to cognitive functioning. *Eur Psychiatry.* (2016) 35:32–8. doi: 10.1016/j.eurpsy.2016.01.2426

60. Kerns JG, Cohen JD, MacDonald AW, Johnson MK, Stenger VA, Aizenstein H, et al. Decreased conflict- and error-related activity in the anterior cingulate cortex in subjects with schizophrenia. *Am J Psychiatry.* (2005) 162:1833–9. doi: 10.1176/appi.ajp.162.10.1833

61. Paus T. Primate anterior cingulate cortex: where motor control, drive and cognition interface. *Nat Rev Neurosci.* (2001) 2:417–24. doi: 10.1038/35077500

62. Walton ME, Croxson PL, Behrens TEJ, Kennerley SW, Rushworth MFS. Adaptive decision making and value in the anterior cingulate cortex. *Neuroimage.* (2007) 36:T142–54. doi: 10.1016/j.neuroimage.2007.03.029

63. Fornito A, Yücel M, Dean B, Wood SJ, Pantelis C. Anatomical abnormalities of the anterior cingulate cortex in schizophrenia: bridging the

gap between neuroimaging and neuropathology. *Schizophr Bull.* (2009) 35:973–93. doi: 10.1093/schbul/sbn025

64. Mechelli A, Allen P, Amaro JrE, Fu CH, Williams SC, Brammer MJ. et al. Misattribution of speech and impaired connectivity in patients with auditory verbal hallucinations. *Hum. Brain Mapp.* (2007) 28:1213–22. doi: 10.1002/hbm.20341

65. West EA, Moschak TM, Carelli RM. Distinct functional microcircuits in the nucleus accumbens underlying goal-directed decision-making. In: Morris R, Bornstein A, Shenhav A, editors. *Goal-Directed Decision Making.* Cambridge, MA: Academic Press (2018). p. 199–219.

66. Dürschmid S, Zaehle T, Kopitzki K, Voges J, Schmitt F, Heinze H-J, et al. Phase-amplitude cross-frequency coupling in the human nucleus accumbens tracks action monitoring during cognitive control. *Front Hum Neurosci.* (2013) 7:635. doi: 10.3389/fnhum.2013.00635

67. Pascual-Leone A, Tarazona F, Keenan J, Tormos JM, Hamilton R, Catala MD. Transcranial magnetic stimulation and neuroplasticity. *Neuropsychologia.* (1998) 37:207–17. doi: 10.1016/S0028-3932(98)00095-5

68. Cauda F, Cavanna AE, D'Agata F, Sacco K, Duca S, Geminiani GC. Functional connectivity and coactivation of the nucleus accumbens: a combined functional connectivity and structure-based meta-analysis. *J Cogn Neurosci.* (2011) 23:2864–77. doi: 10.1162/jocn.2011.21624

69. Stevens AA, Goldman-Rakic PS, Gore JC, Fulbright RK, Wexler BE. Cortical dysfunction in schizophrenia during auditory word and tone working memory demonstrated by functional magnetic resonance imaging. *Arch Gen Psychiatry.* (1998) 55:1097–103. doi: 10.1001/archpsyc.55.12.1097

70. Yurgelun-Todd DA, Waternaux CM, Cohen BM, Gruber SA, English CD, Renshaw PF. Functional magnetic resonance imaging of schizophrenic patients and comparison subjects during word production. *Am J Psychiatry.* (1996) 153:200–5. doi: 10.1176/ajp.153.2.200

71. Zangen A, Hyodo K. Transcranial magnetic stimulation induces increases in extracellular levels of dopamine and glutamate in the nucleus accumbens. *Neuroreport.* (2002) 13:2401–5. doi: 10.1097/00001756-200212200-00005

72. Tang Y, Wang M, Zheng T, Yuan F, Yang H, Han F, et al. Grey matter volume alterations in trigeminal neuralgia: a systematic review and meta-analysis of voxel-based morphometry studies. *Progr Neuropsychopharmacol Biol Psychiatry.* (2020) 98:109821. doi: 10.1016/j.pnpbp.2019.109821

73. Dennison M, Whittle S, Yücel M, Vijayakumar N, Kline A, Simmons J, et al. Mapping subcortical brain maturation during adolescence: evidence of hemisphere- and sex-specific longitudinal changes. *Dev Sci.* (2013) 16:772–91. doi: 10.1111/desc.12057

74. Ahsan RL, Allom R, Gousias IS, Habib H, Turkheimer FE, Free S, et al. Volumes, spatial extents and a probabilistic atlas of the human basal ganglia and thalamus. *Neuroimage.* (2007) 38:261–70. doi: 10.1016/j.neuroimage.2007.06.004

75. De Rossi P, Dacquino C, Piras F, Caltagirone C, Spalletta G. Left nucleus accumbens atrophy in deficit schizophrenia: a preliminary study. *Psychiatry Re Neuroimaging.* (2016) 254:48–55. doi: 10.1016/j.pscychresns.2016.06.004

frontiers | Frontiers in Psychiatry

TYPE Original Research
PUBLISHED 10 October 2022
DOI 10.3389/fpsyt.2022.1003889

OPEN ACCESS

EDITED BY
Thomas Nickl-Jockschat,
The University of Iowa, United States

REVIEWED BY
Dusan Hirjak,
Heidelberg University, Germany
Yi Zhang,
Xidian University, China

*CORRESPONDENCE
Xiaoqi Huang
julianahuang@163.com
Qiyong Gong
qiyonggong@hmrrc.org.cn

†These authors have contributed equally to this work

SPECIALTY SECTION
This article was submitted to Neuroimaging and Stimulation, a section of the journal Frontiers in Psychiatry

RECEIVED 26 July 2022
ACCEPTED 16 September 2022
PUBLISHED 10 October 2022

CITATION
Hu X, Jiang P, Gao Y, Sun J, Zhou X, Zhang L, Qiu H, Li H, Cao L, Liu J, Gong Q and Huang X (2022) Brain morphometric abnormalities and their associations with affective symptoms in males with methamphetamine use disorder during abstinence. *Front. Psychiatry* 13:1003889. doi: 10.3389/fpsyt.2022.1003889

Brain morphometric abnormalities and their associations with affective symptoms in males with methamphetamine use disorder during abstinence

Xinyue Hu[1,2†], Ping Jiang[1,2,3†], Yingxue Gao[1,2], Jiayu Sun[4], Xiaobo Zhou[5], Lianqing Zhang[1,2], Hui Qiu[1,2], Hailong Li[1,2], Lingxiao Cao[1,2], Jing Liu[1,2], Qiyong Gong[1,2*] and Xiaoqi Huang[1,2*]

[1]Functional and Molecular Imaging Key Laboratory of Sichuan Province, Department of Radiology, Huaxi Magnetic Resonance Research Center (HMRRC), West China Hospital, Sichuan University, Chengdu, China, [2]Psychoradiology Research Unit of the Chinese Academy of Medical Sciences, West China Hospital of Sichuan University, Chengdu, China, [3]West China Medical Publishers, West China Hospital of Sichuan University, Chengdu, China, [4]Department of Radiology, West China Hospital of Sichuan University, Chengdu, China, [5]Department of Psychosomatics, Academy of Medical Sciences and Sichuan Provincial People's Hospital, Chengdu, China

Background: Methamphetamine (METH) use induces neurotoxic effects in brain structures and affective symptoms that persist during abstinence. However, the brain morphometry of individuals with METH use disorder (MUD) remains unclear, as well as their associations with affective symptoms during abstinence.

Methods: Forty-eight abstinent males with MUD and 66 age-, sex-, and education-matched healthy controls (HCs) underwent high-resolution T1-weighted magnetic resonance imaging. Cortical thickness, surface area, volume, local gyrification index (LGI), and subcortical volume were obtained with FreeSurfer software. Brain morphometry differences between groups and their associations with affective symptoms and drug abuse history within the males with MUD were examined, with intracranial volume, age, and years of education as covariates.

Results: Compared with the HCs, the individuals with MUD showed a significantly higher LGI in the right cuneus gyrus, left lingual gyrus, bilateral supramarginal gyrus, right inferior parietal gyrus (IPG), and right dorsal anterior cingulate cortex (clusterwise $p < 0.05$, Monte Carlo-corrected), as well as a smaller volume of the left nucleus accumbens (NAcc) ($p < 0.05$, FDR-corrected). However, there were no significant group differences in cortical thickness, area or volume. In addition, the LGI in the right IPG was positively associatedwith the severity of depression and anxiety symptoms in MUDs ($p < 0.05$, FDR-corrected).

Conclusion: Brain morphometric abnormalities in abstinent males with MUD were characterized by hypergyrification across multiple mid-posterior brain regions anda smaller volume of the left NAcc.Gyrification of the right IPG may be a potential neural substrate underlying the affective symptoms experienced by MUDs during abstinence.

KEYWORDS

methamphetamine use disorder, abstinence, cortical morphometry, subcortical volume, affective symptoms

Introduction

Methamphetamine (METH) is an amphetamine-type stimulant (ATS) that has high dopamine (DA)-related neurotoxicity in the mesocorticolimbic system (1). Chronic METH use can result in severe behavioral, cognitive, and memory impairments and symptoms of psychosis (2). Affective symptoms, including anxiety and depression, are frequently observed in individuals with methamphetamine use disorder (MUD) during abstinence (3). Affective symptoms have been shown to exacerbate relapse of METH use, craving and prolong treatment, especially in individuals with MUD early in the abstinence period (3–5). However, no medication-based interventions are available to effectively treat MUD and its related affective symptoms (2). A few brain structure studies have explored the relationships between brain structures and affective symptoms in individuals with MUD. For example, one study reported that decreased CT in the inferior temporal, orbitofrontal, and inferior frontal gyri was associated with dysfunction of affective regulation in individuals with MUD (6). However, the neuroanatomical basis of METH-related affective symptoms remains poorly understood, although it is critical for the development of treatment strategies for this population and thus for improving patient care and preventing relapse.

Converging evidence from pathological and neuroimaging studies in human drug users and animal models has suggested that chronic METH use can contribute to structural brain abnormalities (7–10). Structural brain abnormalities in individuals with MUD have been widely reported in the mesocorticolimbic system, including the regions of the prefrontal cortex (PFC), anterior cingulate cortex (ACC), hippocampus, amygdala, and nucleus accumbens (NAcc) (9, 11). Compared with healthy controls (HCs), abstinent MUDs displayed smaller gray matter volume (GMV) in the right lateral occipital cortex and decreased cortical thickness (CT) in the bilateral superior frontal cortex (12). Another study reported larger GMV in the striatum in MUDs than in HCs (13). However, there have not been sufficiently powered studies to comprehensively investigate sex differences in specific brain morphometric features in MUDs who only used METH (excluding multiple drug use).

To date, most previous studies of brain morphometric alterations in MUDs have focused on volumetric measures using voxel-based morphometry (VBM). However, a more comprehensive examination of abnormalities in brain morphometry in MUD individuals using surface-based morphometry (SBM), including CT, surface area (SA), cortical volume (CV), and local gyrification index (LGI), may advance our understanding of the effects of METH on the brain. These measures are influenced by distinct evolutionary, neurodevelopmental, and genetic factors in different ways (14–16). CT primarily reflects the number of neurons within a cortical column, starts to decreases from the age of 2–4 years and continues throughout the lifespan (17–19). SA is related to the number of cortical mini-columns, expands until about the age of 12 years, remains relatively stable and then shrinks with age (20). CV reflects the properties of both CT and SA, which is more closely related to SA rather than CT and follows a non-monotonic and non-linear developmental trajectory (17). The LGI reflects the degree of cortical gyrification, progressively increases in the first 2 years of life and then decreases throughout the lifespan (21–23).

Based on this background, our study aimed to investigate abnormal brain morphometry using multiple brain morphometric features, including CT, SA, CV, and the LGI, as well as subcortical volume in abstinent males with a history of METH abuse alone compared with age-, sex-, and education-matched HCs. The MUD participants recruited in the current study had a very low level of smoking (<1 cigarette per day), thereby eliminating the confounding effects of polysubstance abuse and assisting in the determination of the "pure" effect of METH on brain morphometry. In addition, we explored the relationships between abnormal brain morphometry and affective symptoms in MUDs. We hypothesized that the brain morphometric alterations would be observed in the PFC, ACC, and NAcc which are the key brain regions in the mesocorticolimbic system and that some of the abnormalities would be related to affective symptoms in the MUDs during abstinence.

Methods

Participants

This study was approved by the Research Ethics Committee of West China Hospital, Sichuan University, and fully informed written consent was obtained from all participants. Participation was entirely voluntary. Forty-eight male MUD participants during abstinence (mean age: 28.77 years, SD: 7.66 years) and 66 age-, sex-, and education-matched HCs (mean age: 30.85 years, SD: 7.97 years) were recruited for the study. All participants were native Han Chinese and right-handed. MUDs were recruited from Ziyang, a compulsory isolation and rehabilitation center in Sichuan Province, China. The MUDs eligible for our study were at least 16 years old and able to understand and complete the measurements. METH abuse was diagnosed based on the criteria of the Diagnostic and Statistical Manual of Mental Disorders, 4th edition (DSM-IV). The exclusion criteria were (1) a history of use of or dependence on any psychoactive substances other than METH or nicotine; (2) a history of mental disorders before METH abuse; (3) major systemic diseases or neurological disorders, including HIV and diabetes; or (4) any contraindications to magnetic resonance imaging (MRI).

HCs were recruited from the local community through posters and flyers distributed at West China Hospital of Sichuan University and through internet advertisements. The same exclusion criteria were applied to HCs except that individuals with any history of drug use were excluded.

Clinical assessment battery

METH abuse history and affective symptom assessments were recorded through a detailed interview by two experienced psychiatrists (XH and XZ) before the MRI scans.

In the MUD participants, the 17-item Hamilton Depression Scale (HAMD-17) and the 14-item Hamilton Anxiety Scale (HAMA-14) were used to evaluate the severity of depressive and anxiety symptoms, respectively. In both scales, a higher total score indicated more severe anxiety or depressive symptoms.

MRI data acquisition

High-resolution 3D T1-weighted images were acquired using a 3-T MR scanner (Trio Tim, Siemens Healthineers, Erlangen, Germany) with a 12-channel phase-array head coil. Foam padding and soft earplugs were used to reduce head motion and scanner noise, respectively. A magnetization-prepared rapid gradient-echo (MPRAGE) sequence was used with the following parameters: repetition time (TR) = 1,900 ms, echo time (TE) = 2.26 ms, flip angle = 9°, matrix = 256 × 256, field of view (FOV) = 256 × 256 mm^2, number of axial slices = 176, and slice thickness = 1.0 mm. All images were visually inspected by an experienced radiologist (J. Sun) during imaging, and those with head movement artifacts were immediately rescanned.

MRI data pre-processing

The T1-weighted images were analyzed using the mainstream recon-all process of FreeSurfer software (version 6.0) (http://surfer.nmr.mgh.harvard.edu/). The image processing pipeline included visual inspection of data for motion artifacts, removal of non-brain tissue, transformation to Talairach space, segmentation of subcortical gray/white matter (GM/WM), intensity normalization, tessellation of the GM/WM boundary, automated topology correction, and surface deformation (24–26). The cortical surface then underwent inflation, registration to a spherical atlas, and automatic identification of gyral and sulcal regions.

CT was defined as the shortest straight-line distance between the pial surface and the GM/WM boundary (27). SA was obtained by assigning an area to each vertex equal to the average of its surrounding triangles (28). CV was obtained by calculating the amount of GMV within the pial surface and the GM/WM boundary (17). The LGI was obtained by quantifying local cortical folding by calculating the ratio of the amount of cortex buried within the sulcal folds relative to the amount of cortex on the outer visible cortical hull in a 25-mm spherical region (16). Vertex-level CT, SA, CV, and LGI in each subject were projected onto a targeted and normalized surface ("fsaverage").

The volumes of subcortical nuclei, including the bilateral thalamus, caudate, putamen, pallidum, hippocampus, amygdala, and NAcc (Figure 2A), and the intracranial volume (ICV) were extracted from FreeSurfer's segmentation stream.

Statistical analysis

Group comparison of brain morphometry

We investigated group differences in demographic characteristics (age, years of education, and ICV) between the MUD and HC groups using an independent two-sample *t*-test. Statistical analyses of cortical morphometry were conducted with the FreeSurfer Query, Design, Estimate, Contrast (Qdec) program (http://www.freesurfer.net/fswiki/Qdec). First, the CT, SA, and CV maps were spatially smoothed with a full-width at half-maximum Gaussian kernel of 10 mm (the LGI map was not smoothed due to its intrinsic smoothness). Second, we used a general linear model (GLM) to test for group differences in CT, SA, CV, and the LGI in a vertex-by-vertex manner, with diagnosis as a fixed factor and age, years of education, and ICV as covariates. A Monte Carlo simulation was used to correct for multiple hypothesis testing, with 10,000 iterations,

cluster-forming $p < 0.01$ and clusterwise probability (CWP) < 0.05.

Analyses of group differences in the volumes of subcortical nuclei were tested using a multivariate analysis of covariance (MANCOVA), with age, years of education, and ICV as covariates. We used partial eta squared (η^2) to evaluate effect size (0.01 indicates a small effect size, 0.06 indicates a medium effect size and 0.14 indicates a large effect size). A false discovery rate (FDR) correction was applied to correct for multiple comparisons in the subcortical nuclei analyses.

Correlations with affective symptoms

To examine the relationship between brain regions with significant group differences and clinical features (abstinent days, usage duration, mean dose (g/time), mean dose (g/day), onset age of METH use, HAMD score, and HAMA score), mean measurements within each region were extracted, and partial rank correlation analyses were performed due to their non-normal distribution after controlling for age, years of education, and ICV. In addition, we used Spearman correlation analyses to examine correlations between METH abuse history [abstinent days, usage duration, mean dose (g/time), mean dose (g/day), and onset age of METH use] and affective symptoms (HAMD and HAMA scores). An FDR correction was applied to correct for multiple comparisons in the correlation analyses.

Result

Demographic and clinical characteristics

The demographic and clinical characteristics of the abstinent males with MUD and HCs are presented in Table 1. The MUDs and HCs did not differ significantly in terms of age, years of education, or ICV.

Group differences in brain morphometry

Compared with HCs, the MUDs showed higher LGI values mainly in the bilateral supramarginal gyrus (SMG), left lingual gyrus (LG), right inferior parietal gyrus (IPG), right cuneus (CU) and right dorsal anterior cingulate cortex (dACC) (CWP < 0.05, Monte Carlo-corrected, Table 2 and Figures 1A,B). Notably, these deficits were located primarily in the mid-posterior cortex. However, there were no significant differences in CT, SA, or CV between the MUDs and HCs.

Compared with HCs, the MUDs also showed a significantly smaller volume of the left NAcc ($F = 8.366$, FDR-corrected $p = 0.035$, $\eta^2 = 0.071$; Table 2 and Figure 2). Significant differences in other nuclei were not observed between the two groups (Figures 2B–D).

TABLE 1 Demographic and clinical data of the male abstinent MAs and HCs.

	MA ($N = 48$)	HC ($N = 66$)	t-value	p-value
Demographics				
Age (years)	28.77 ± 7.66	30.85 ± 7.97	1.464	0.146
Education (years)	8.27 ± 3.68	8.66 ± 3.21	0.732	0.466
Affective symptoms				
HAMA score	3.56 ± 5.09			
HAMD score	4.90 ± 5.25			
METH use				
Abstinent periods (days)	114.56 ± 116.20	–		
Duration of use (months)[a]	47.74 ± 39.62	–		
Mean dose (g/time)	0.39 ± 0.30	–		
Mean dose (g/day)	0.94 ± 1.49			
Age of first use (years)[a]	24.66 ± 8.20	–		

[a]N = 47. Data are presented as the means ± standard deviation. MA, methamphetamine abuser; HC, healthy control; METH: methamphetamine; HAMD: Hamilton depression scale; HAMA: Hamilton anxiety scale; g, gram.

Correlations with affective symptoms

HAMD scores were negatively correlated with the duration of abstinence ($r = -0.382$, FDR-corrected $p = 0.021$, Figure 3A), whereas both HAMD scores ($r = 0.455$, FDR-corrected $p = 0.012$, Figure 3B) and HAMA scores ($r = 0.397$, FDR-corrected $p = 0.021$, Figure 3C) were positively correlated with the LGI in the right IPG.

Discussion

In this study, we used multiple cortical and subcortical measures to investigate a comprehensive profile of morphometric abnormalities of the brain anatomy in the MUDs with several findings. First, comparing to HCs, we observed increased LGI in the bilateral SMG, left LG, right IPG, right CU, and right dACC. *Second*, we loated reduced volume of the left NAcc in the MUDs relative to HCs. *Second*, we found the LGI in the right IPG positively correlated with the severity of anxiety and depressed symptoms in the MUDs. Overall, these findings suggest that the gyrification of mid-posterior cortex are disrupted in the MUDs and that right IPG may serves as a neural substrate underlying affective symptoms in the MUDs.

TABLE 2 Significant group differences in brain morphometry between the abstinent males with methamphetamine use disorder and HCs.

Significant group differences in LGI with age, education years, and ICV as covariates

Brian morphometric	Anatomical location	Direction	MNI coordinates (peak vertex)			Size (mm^2)	CWP
			x	y	z		
LGI	Left supramarginal gyrus	MUD > HC	−51.4	−27.5	32.6	975.65	0.0012**
LGI	Left lingual gyrus	MUD > HC	−24.1	−51.0	−1.9	1,363.90	<0.001***
LGI	Right supramarginal gyrus	MUD > HC	54.1	36.7	40.6	1,694.14	<0.001***
LGI	Right inferior parietal gyrus	MUD > HC	47.1	−69.8	13.9	907.08	0.0012**
LGI	Right cuneus gyrus	MUD > HC	11.8	−74.9	27.3	1,044.67	<0.001***
LGI	Right dorsal anterior cingulate cortex	MUD > HC	13.6	−17.0	36.0	1,361.74	<0.001***

Significant group differences in volumes (mm^3) of subcortical nucleus with age, education years, and ICV as covariates

Volume	Volume in MUD (mm^3)	Volume in HC (mm^3)	*F*-value	η^2	FDR-corrected *p*-value
Left NAcc	446.47 ± 89.82	517.38 ± 53.25	8.336	0.071	0.035*

There were no significant differences in CT, SA, or CV between the MUDs and HCs. MUD, methamphetamine use disorder; HC, healthy control; MNI, Montreal neurological institute; LGI, local gyrification index; CWP, cluster-wise probability; NAcc, nucleus accumbens; CT, cortical thickness; SA, surface area; CV, cortical volume; FDR, false discovery rate. *p < 0.05, **p < 0.01; ***p < 0.001.

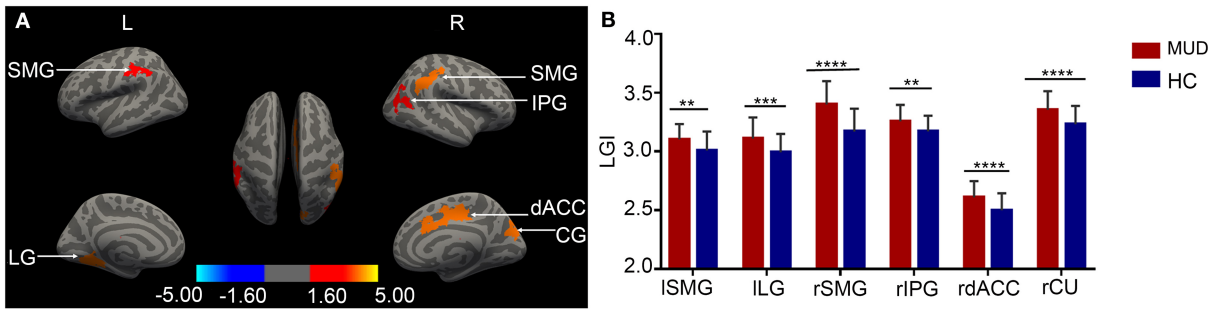

FIGURE 1
(A) Cortical clusters with significantly higher LGI values in MUD participants than HCs (CWP < 0.05, Monte Carlo-corrected). None of the significant clusters for cortical thickness, surface area or volume survived the correction. The color bar for p values is on a logarithmic scale (log_{10}) with a range of 1.6–5. **(B)** The group differences in LGI values are illustrated by representative bar plots. MUD, methamphetamine use disorder; HC, healthy control; LGI, local gyrification index; L/l, left; R/r, right; SMG, supramarginal gyrus; LG, lingual gyrus; IPG, inferior parietal gyrus; dACC, dorsal anterior cingulate cortex; CU, cuneus. CWP, clusterwise probability. **$p < 0.01$; ***$p < 0.001$, ****$p < 0.0001$.

Brain morphometric abnormalities in the MUDs

We found significant group differences in the LGI analyses; specifically, the MUDs showed significant hypergyrification in the right CU, left LG, bilateral SMG, right IPG, and right dACC regions compared with HCs. The LGI is a 3D metric used to quantify the degree of cortical gyrification, which reflects cortical complexity (16). A cortex with extensive gyrification has a high LGI, whereas a cortex with limited gyrification has a low LGI (16). Several factors influence cortical gyrification, including neuronal proliferation and migration, axonal connectivity, and mechanical constraints (29). Previous neuroimaging studies have reported that patterns of cortical gyrification are crucial for shaping different brain functions (30–32).

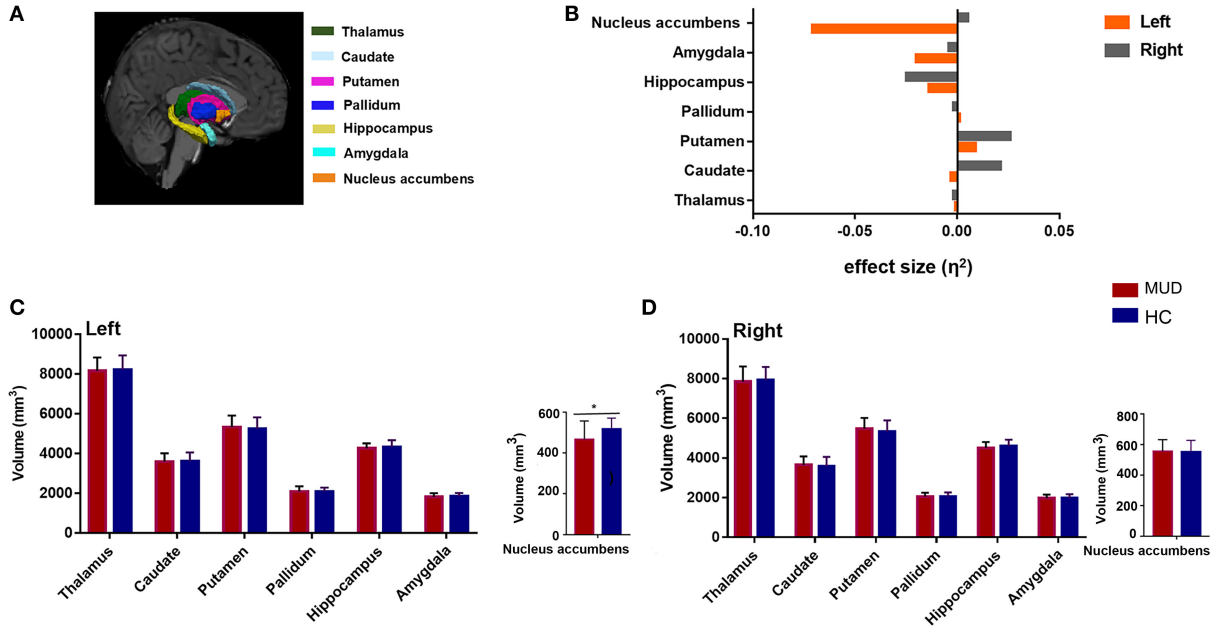

FIGURE 2
(A) An example of subcortical nucleus segmentation by FreeSurfer (version 6.0) in a healthy subject (right subcortical nucleus is shown). **(B)** Effect sizes for differences in left (gray) and right (orange) subcortical nuclei between the MUDs and HCs. **(C,D)** Bar plots of volumes (mm^3) of the bilateral subcortical nucleus in the MUD participants and HCs after controlling for age, years of education and ICV. *Indicates significance after FDR correction. MUD, methamphetamine use disorder; HCs, healthy control; ICV, intracranial volume; FDR, false discovery rate; L, left; R, right.

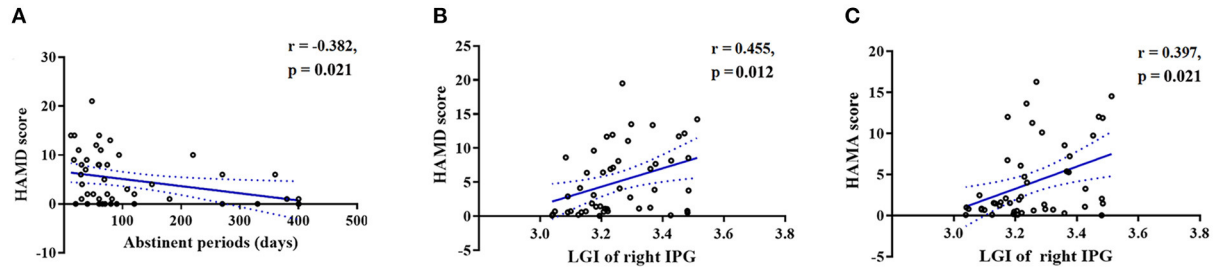

FIGURE 3
Scatterplots showing that the duration of abstinence was significantly negatively correlated with **(A)** HAMD scores in the MUDs. Scatterplots showing that the LGI in the right IPG was significantly positively correlated with the **(B)** HAMD and **(C)** HAMA scores in the MUDs. All of the abovementioned correlations, with the exception of those between the duration of abstinence and HAMA scores, remained significant after FDR correction. MUD, methamphetamine use disorder; HAMD, Hamilton depression scale; HAMA, Hamilton anxiety scale; LGI, local gyrification index; IPG, inferior parietal gyrus; FDR, false discovery rate.

Therefore, our observation of aberrant LGI values across the mid-posterior cortex may be related to corresponding cognitive and behavioral impairments.

Previous neuroimaging evidence has consistently demonstrated that METH abuse contributes to impairments in several neuropsychological functions, including executive functions, such as visual memory, verbal processing and cognitive control/response inhibition, and social cognition, such as empathy, communication, and facial-emotion recognition (33). In our study, the brain regions exhibiting hypergyrification in the MUDs have also been reported to play critical roles in executive function and social cognition. For example, the LG and CU are important for visual processing, and the IPG is associated with visual, auditory, and sensorimotor integration (34–36). The right SMG plays a key role in controlling empathy toward other people (37), and the left SMG is important in language perception and processing (38). In addition, the dACC plays a critical role in executive function, especially in reward-based decision making (39). Consistent with our morphological observations, dysfunctions in the SMG and

ACC during tasks that require executive function, and social cognition in early abstinent MUDs have also been reported (40). Therefore, hypergyrification in the mid-posterior brain regions reported here may be the neural-structural basis for impairments in executive function and cognition in MUDs. Moreover, as the neuronal development of gyrification is completed within the first 2 years of life, we boldly suggested that those identified regions with LGI alterations in the MUDs might be serve as vulnerability factors for METH abuse. Meanwhile, the relationship between gyrification in the dACC and executive function is still unclear, might be explored in future studies.

Our findings also showed a smaller volume of the left NAcc in the MUD s relative to HCs; similar findings have been reported by other neuroimaging studies with MUDs (11, 41). This observation supports our hypothesis that brain regions within the DA reward circuit are the main targets of the METH-induced neurotoxic effects. The NAcc is considered the main part of the ventral striatum (33), which receives rich dopaminergic input from the VTA and is an important component of the "reward circuit" of the brain, with functions related to the mediation of natural and drug rewards (42, 43). METH use leads to acute reward and reinforcement primarily *via* the release of massive amounts of DA in the reward circuit, including in the NAcc (33). Moreover, prolonged METH use results in neurotoxic effects, including declines in DA receptors and transporters as well as neurite degeneration (44–46). Since GMV correlated with DA receptor ligand binding (47), and reduced DA transporter density and DA receptors in the striatum had been detected in methamphetamine abusers in previous study (48), we postulated that volumetric alterations in the NAcc in MUDs probably reflect neuronal biochemical changes induced by METH.

Interestingly, among all four cortical parameters (CT, SA, CV, and the LGI), only the LGI showed significant group differences, suggesting that the LGI may be a more sensitive biomarker for abnormalities in cortical morphometry in MUDs during abstinence. Therefore, understanding the complex changes in cortical gyrification may contribute to current understanding of the effects of METH abuse on brain structure. However, our observations are inconsistent with some previous brain morphometric studies on METH abuse (12, 49). One study reported reduced CT in posterior cingulate gyrus in MUDs with including histories of marijuana abuse or dependence, compared with HCs (50). Another study reported increased CT in the parietal cortex in MUDs with a long-term (14–25 months) compulsory abstinence relative to HCs (51). Nie et al. (12) reported increased CT in the bilateral superior frontal gyri in MUDs compared to those in HCs. We hypothesis the discrepancies on CT alterations in our study with previous ones maybe due to the demographic and clinical characteristic difference (such as polysubstance abuse, duration of abstinence, and different sample sizes) among studies. And our study bears the advantage of single drug abuse.

Associations between brain morphometric abnormalities and affective symptoms in MUDs

Our exploratory analysis found that the LGI in the right IPG was positively associated with HAMD and HAMA scores in the MUDs. Previous studies have reported that aberrant changes in the LGI are related to emotion regulation in several psychiatric disorders, including major depression disorder, generalized anxiety disorder, and bipolar disorder (31, 52, 53).

One of the most influential perspectives posits that cortical gyrification is, to a large extent, induced by axonal tension between local brain regions that pull on the nearby cortex (21), influencing the formation of functional connectivity between these regions (54, 55). Therefore, a higher LGI may reflect long-range hypoconnectivity between brain regions (30); our observation of a higher LGI in the right IPG may imply hypoconnectivity between the right IPG and other brain regions in MUDs. The IPG is an important node in the default mode network (DMN) that is critically involved in the rumination process, and its dysfunction is a well-documented risk factor for the onset of depressive and anxiety symptoms (56). Therefore, aberrant gyrification in the IPG as described by this study may induce dysfunction of the DMN that is associated with depressive and anxiety symptoms, which is in line with our previous finding that intranetwork functional connectivity determines the severity of affective symptoms in MUDs (57). This result also suggests that the abnormal LGI in the right IPG in our MUDs may be a potential neural mechanism for METH use-induced affective symptoms.

The current study has several limitations. First, the cross-sectional design prevents the drawing of a causal relationship between brain morphometric abnormalities drug abuse as well as associated affective symptoms in MUDs. Longitudinal studies are encouraged to address these issues. Second, our sample was comprised of only male MUDs and thus cannot represent brain morphometric differences in female MUD participants. Since sex hormones may be an important factor in brain morphometric differences (41, 58), future work with female MUDs and investigations of sex differences are needed. Third, the MUDs were recruited from a compulsory isolation and rehabilitation center, which might limit the generalization of our findings. Future research with MUDs recruited from local communities is necessary to obtain generalizable results.

In summary, we found that the brains of abstinent males with MUD appeared to be characterized by

hypergyrification across multiple mid-posterior brain regions involved in processing language, vision and emotion; the MUDs possessed significantly smaller left NAcc volumes, an area involved in reward processing. In addition, gyrification in the right IPG was positively associated with the severity of affective symptoms in MUDs, suggesting that it may be a potential neural mechanism underlying the affective symptoms experienced by MUDs during abstinence.

Data availability statement

The raw data supporting the conclusions of this article will be made available by the authors, without undue reservation.

Ethics statement

The studies involving human participants were reviewed and approved by the Research Ethics Committee of West China Hospital, Sichuan University. The patients/participants provided their written informed consent to participate in this study.

Author contributions

XHu, PJ, XHua, and QG formulated the research questions. XHua and QG designed the study. JS, XZ, and HL acquired the data. XHu, LZ, YG, LC, and HQ analyzed the data. XHu, PJ, YG, XHua, and QG interpreted the data and wrote or revised the article. All authors approved the final version for publication.

Funding

This study was supported by grants from the 1.3.5 Project for Disciplines of Excellence, West China Hospital, Sichuan University (Grant No. ZYJC21041), the Clinical and Translational Research Fund of Chinese Academy of Medical Sciences (Grant No. 2021-I2M-C&T-B-097), and the Natural Science Foundation of Sichuan Province (Grant Nos. 2022NSFSC0052 and 2022NSFSC1454).

Acknowledgments

The authors thank all of the participants for participating in this study.

Conflict of interest

The authors declare that the research was conducted in the absence of any commercial or financial relationships that could be construed as a potential conflict of interest.

Publisher's note

References

1. Sambo DO, Lin M, Owens A, Lebowitz JJ, Richardson B, Jagnarine DA, et al. The sigma-1 receptor modulates methamphetamine dysregulation of dopamine neurotransmission. *Nat Commun.* (2017) 8:2228. doi: 10.1038/s41467-017-02087-x

2. Courtney KE, Ray LA. Methamphetamine: an update on epidemiology, pharmacology, clinical phenomenology, and treatment literature. *Drug Alcohol Depend.* (2014) 143:11–21. doi: 10.1016/j.drugalcdep.2014.08.003

3. Zorick T, Nestor L, Miotto K, Sugar C, Hellemann G, Scanlon G, et al. Withdrawal symptoms in abstinent methamphetamine-dependent subjects. *Addiction.* (2010) 105:1809–18. doi: 10.1111/j.1360-0443.2010.03066.x

4. Rawson RA, Chudzynski J, Gonzales R, Mooney L, Dickerson D, Ang A, et al. The impact of exercise on depression and anxiety symptoms among abstinent methamphetamine-dependent individuals in a residential treatment setting. *J Subst Abuse Treat.* (2015) 57:36–40. doi: 10.1016/j.jsat.2015.04.007

5. McGregor C, Srisurapanont M, Jittiwutikarn J, Laobhripatr S, Wongtan T, White JM. The nature, time course and severity of methamphetamine withdrawal. *Addiction.* (2005) 100:1320–9. doi: 10.1111/j.1360-0443.2005.01160.x

6. Uhlmann A, Fouche JP, Koen N, Meintjes EM, Wilson D, Stein DJ. Fronto-temporal alterations and affect regulation in methamphetamine dependence with and without a history of psychosis. *Psychiatry Res Neuroimaging.* (2016) 248:30–8. doi: 10.1016/j.pscychresns.2016.01.010

7. Kendrick KM, Daumann J, Wagner D, Koester P, Tittgemeyer M, Luo Q, et al. A prospective longitudinal study shows putamen volume is associated with moderate amphetamine use and resultant cognitive impairments. *Psychoradiology.* (2021) 1:3–12. doi: 10.1093/psyrad/kkab001

8. Morales AM, Kohno M, Robertson CL, Dean AC, Mandelkern MA, London ED. Gray-matter volume, midbrain dopamine D2/D3 receptors and drug craving in methamphetamine users. *Mol Psychiatry.* (2015) 20:764–71. doi: 10.1038/mp.2015.47

9. Koob GF, Volkow ND. Neurocircuitry of addiction. *Neuropsychopharmacology.* (2010) 35:217–38. doi: 10.1038/npp.2009.110

10. Kohno M, Morales AM, Ghahremani DG, Hellemann G, London ED. Risky decision making, prefrontal cortex, and mesocorticolimbic functional connectivity in methamphetamine dependence. *JAMA Psychiatry.* (2014) 71:812–20. doi: 10.1001/jamapsychiatry.2014.399

11. Mackey S, Allgaier N, Chaarani B, Spechler P, Orr C, Bunn J, et al. Mega-Analysis of gray matter volume in substance dependence: general and substance-specific regional effects. *Am J Psychiatry.* (2019) 176:119–28. doi: 10.1176/appi.ajp.2018.17040415

12. Nie L, Zhao Z, Wen X, Luo W, Ju T, Ren A, et al. Gray-matter structure in long-term abstinent methamphetamine users. *BMC Psychiatry.* (2020) 20:158. doi: 10.1186/s12888-020-02567-3

13. Chang L, Cloak C, Patterson K, Grob C, Miller EN, Ernst T. Enlarged striatum in abstinent methamphetamine abusers: a possible compensatory response. *Biol Psychiatry.* (2005) 57:967–74. doi: 10.1016/j.biopsych.2005.01.039

14. Rakic P. Specification of cerebral cortical areas. *Science.* (1988) 241:170–6. doi: 10.1126/science.3291116

15. Panizzon MS, Fennema-Notestine C, Eyler LT, Jernigan TL, Prom-Wormley E, Neale M, et al. Distinct genetic influences on cortical surface area and cortical thickness. *Cereb Cortex.* (2009) 19:2728–35. doi: 10.1093/cercor/bhp026

16. Schaer M, Cuadra MB, Tamarit L, Lazeyras F, Eliez S, Thiran JP. A surface-based approach to quantify local cortical gyrification.

IEEE Trans Med Imaging. (2008) 27:161–70. doi: 10.1109/TMI.2007.903576

17. Winkler AM, Kochunov P, Blangero J, Almasy L, Zilles K, Fox PT, et al. Cortical thickness or grey matter volume? The importance of selecting the phenotype for imaging genetics studies. *Neuroimage.* (2010) 53:1135–46. doi: 10.1016/j.neuroimage.2009.12.028

18. Rakic P. A small step for the cell, a giant leap for mankind: a hypothesis of neocortical expansion during evolution. *Trends Neurosci.* (1995) 18:383–8. doi: 10.1016/0166-2236(95)93934-P

19. Schmaal L, Hibar DP, Sämann PG, Hall GB, Baune BT, Jahanshad N, et al. Cortical abnormalities in adults and adolescents with major depression based on brain scans from 20 cohorts worldwide in the ENIGMA major depressive disorder working group. *Mol Psychiatry.* (2017) 22:900–9. doi: 10.1038/mp.2016.60

20. Wierenga LM, Langen M, Oranje B, Durston S. Unique developmental trajectories of cortical thickness and surface area. *Neuroimage.* (2014) 87:120–6. doi: 10.1016/j.neuroimage.2013.11.010

21. Van Essen DC. A tension-based theory of morphogenesis and compact wiring in the central nervous system. *Nature.* (1997) 385:313–8. doi: 10.1038/385313a0

22. Libero LE, Schaer M, Li DD, Amaral DG, Nordahl CW. A longitudinal study of local gyrification index in young boys with autism spectrum disorder. *Cereb Cortex.* (2019) 29:2575–87. doi: 10.1093/cercor/bhy126

23. Storsve AB, Fjell AM, Tamnes CK, Westlye LT, Overbye K, Aasland HW, et al. Differential longitudinal changes in cortical thickness, surface area and volume across the adult life span: regions of accelerating and decelerating change. *J Neurosci.* (2014) 34:8488–98. doi: 10.1523/JNEUROSCI.0391-14.2014

24. Fischl B, Salat DH, Busa E, Albert M, Dieterich M, Haselgrove C, et al. Whole brain segmentation: automated labeling of neuroanatomical structures in the human brain. *Neuron.* (2002) 33:341–55. doi: 10.1016/S0896-6273(02)00569-X

25. Dale AM, Fischl B, Sereno MI. Cortical surface-based analysis. I. Segmentation and surface reconstruction. *Neuroimage.* (1999) 9:179–94. doi: 10.1006/nimg.1998.0395

26. Fischl B, Sereno MI, Dale AM. Cortical surface-based analysis. II: Inflation, flattening, and a surface-based coordinate system. *Neuroimage.* (1999) 9:195–207. doi: 10.1006/nimg.1998.0396vspace*1pt

27. Fischl B, Dale AM. Measuring the thickness of the human cerebral cortex from magnetic resonance images. *Proc Natl Acad Sci USA.* (2000) 97:11050–5. doi: 10.1073/pnas.200033797

28. Winkler AM, Sabuncu MR, Yeo BT, Fischl B, Greve DN, Kochunov P, et al. Measuring and comparing brain cortical surface area and other areal quantities. *Neuroimage.* (2012) 61:1428–43. doi: 10.1016/j.neuroimage.2012.03.026

29. Striedter GF, Srinivasan S, Monuki ES. Cortical folding: when, where, how, and why? *Annu Rev Neurosci.* (2015) 38:291–307. doi: 10.1146/annurev-neuro-071714-034128

30. Nixon NL, Liddle PF, Nixon E, Worwood G, Liotti M, Palaniyappan L. Biological vulnerability to depression: linked structural and functional brain network findings. *Br J Psychiatry.* (2014) 204:283–9. doi: 10.1192/bjp.bp.113.129965

31. Han KM, Won E, Kang J, Kim A, Yoon HK, Chang HS, et al. Local gyrification index in patients with major depressive disorder and its association with tryptophan hydroxylase-2 (TPH2) polymorphism. *Hum Brain Mapp.* (2017) 38:1299–310. doi: 10.1002/hbm.23455

32. Jiang X, Zhang T, Zhang S, Kendrick KM, Liu T. Fundamental functional differences between gyri and sulci: implications for brain function, cognition, and behavior. *Psychoradiology.* (2021) 1:23–41. doi: 10.1093/psyrad/kkab002

33. Taylor SB, Lewis CR, Olive MF. The neurocircuitry of illicit psychostimulant addiction: acute and chronic effects in humans. *Subst Abuse Rehabil.* (2013) 4:29–43. doi: 10.2147/SAR.S39684

34. Bogousslavsky J, Miklossy J, Deruaz JP, Assal G, Regli F. Lingual and fusiform gyri in visual processing: a clinico-pathologic study of superior altitudinal hemianopia. *J Neurol Neurosurg Psychiatry.* (1987) 50:607–14. doi: 10.1136/jnnp.50.5.607

35. Caspers S, Schleicher A, Bacha-Trams M, Palomero-Gallagher N, Amunts K, Zilles K. Organization of the human inferior parietal lobule based on receptor architectonics. *Cereb Cortex.* (2013) 23:615–28. doi: 10.1093/cercor/bhs048

36. Crockford DN, Goodyear B, Edwards J, Quickfall J, el-Guebaly N. Cue-induced brain activity in pathological gamblers. *Biol Psychiatry.* (2005) 58:787–95. doi: 10.1016/j.biopsych.2005.04.037

37. Silani G, Lamm C, Ruff CC, Singer T. Right supramarginal gyrus is crucial to overcome emotional egocentricity bias in social judgments. *J Neurosci.* (2013) 33:15466–76. doi: 10.1523/JNEUROSCI.1488-13.2013

38. Yen M, DeMarco AT, Wilson SM. Adaptive paradigms for mapping phonological regions in individual participants. *Neuroimage.* (2019) 189:368–79. doi: 10.1016/j.neuroimage.2019.01.040

39. Bush G, Vogt BA, Holmes J, Dale AM, Greve D, Jenike MA, et al. Dorsal anterior cingulate cortex: a role in reward-based decision making. *Proc Natl Acad Sci USA.* (2002) 99:523–8. doi: 10.1073/pnas.012470999

40. Nestor LJ, Ghahremani DG, Monterosso J, London ED. Prefrontal hypoactivation during cognitive control in early abstinent methamphetamine-dependent subjects. *Psychiatry Res.* (2011) 194:287–95. doi: 10.1016/j.pscychresns.2011.04.010

41. Kogachi S, Chang L, Alicata D, Cunningham E, Ernst T. Sex differences in impulsivity and brain morphometry in methamphetamine users. *Brain Struct Funct.* (2017) 222:215–27. doi: 10.1007/s00429-016-1212-2

42. Alex KD, Pehek EA. Pharmacologic mechanisms of serotonergic regulation of dopamine neurotransmission. *Pharmacol Ther.* (2007) 113:296–320. doi: 10.1016/j.pharmthera.2006.08.004

43. Ikemoto S. Brain reward circuitry beyond the mesolimbic dopamine system: a neurobiological theory. *Neurosci Biobehav Rev.* (2010) 35:129–50. doi: 10.1016/j.neubiorev.2010.02.001

44. Cruickshank CC, Dyer KR. A review of the clinical pharmacology of methamphetamine. *Addiction.* (2009) 104:1085–99. doi: 10.1111/j.1360-0443.2009.02564.x

45. Sekine Y, Iyo M, Ouchi Y, Matsunaga T, Tsukada H, Okada H, et al. Methamphetamine-related psychiatric symptoms and reduced brain dopamine transporters studied with PET. *Am J Psychiatry.* (2001) 158:1206–14. doi: 10.1176/appi.ajp.158.8.1206

46. Wilson JM, Kalasinsky KS, Levey AI, Bergeron C, Reiber G, Anthony RM, et al. Striatal dopamine nerve terminal markers in human, chronic methamphetamine users. *Nat Med.* (1996) 2:699–703. doi: 10.1038/nm0696-699

47. Woodward ND, Zald DH, Ding Z, Riccardi P, Ansari MS, Baldwin RM, et al. Cerebral morphology and dopamine D2/D3 receptor distribution in humans: a combined [18F]fallypride and voxel-based morphometry study. *Neuroimage.* (2009) 46:31–8. doi: 10.1016/j.neuroimage.2009.01.049

48. Chang L, Alicata D, Ernst T, Volkow N. Structural and metabolic brain changes in the striatum associated with methamphetamine abuse. *Addiction.* (2007) 102 (Suppl. 1):16–32. doi: 10.1111/j.1360-0443.2006.01782.x

49. Ruan X, Zhong N, Yang Z, Fan X, Zhuang W, Du J, et al. Gray matter volume showed dynamic alterations in methamphetamine users at 6 and 12months abstinence: a longitudinal voxel-based morphometry study. *Prog Neuropsychopharmacol Biol Psychiatry.* (2018) 81:350–5. doi: 10.1016/j.pnpbp.2017.09.004

50. MacDuffie KE, Brown GG, McKenna BS, Liu TT, Meloy MJ, Tawa B, et al. Effects of HIV infection, methamphetamine dependence and age on cortical thickness, area and volume. *Neuroimage Clin.* (2018) 20:1044–52. doi: 10.1016/j.nicl.2018.09.034

51. Yang R, He L, Zhang Z, Zhou W, Liu J. The higher parietal cortical thickness in abstinent methamphetamine patients is correlated with functional connectivity and age of first usage. *Front Hum Neurosci.* (2021) 15:705863. doi: 10.3389/fnhum.2021.705863

52. Choi KW, Han KM, Kim A, Kang W, Kang Y, Tae WS, et al. Decreased cortical gyrification in patients with bipolar disorder. *Psychol Med.* (2020) 52:2232–44. doi: 10.1017/S0033291720004079

53. Molent C, Maggioni E, Cecchetto F, Garzitto M, Piccin S, Bonivento C, et al. Reduced cortical thickness and increased gyrification in generalized anxiety disorder: a 3 T MRI study. *Psychol Med.* (2018) 48:2001–10. doi: 10.1017/S003329171700352X

54. Yang DY, Beam D, Pelphrey KA, Abdullahi S, Jou RJ. Cortical morphological markers in children with autism: a structural magnetic resonance imaging study of thickness, area, volume, and gyrification. *Mol Autism.* (2016) 7:11. doi: 10.1186/s13229-016-0076-x

55. Palaniyappan L, Liddle PF. Diagnostic discontinuity in psychosis: a combined study of cortical gyrification and functional connectivity. *Schizophr Bull.* (2014) 40:675–84. doi: 10.1093/schbul/sbt050

56. Zhou HX, Chen X, Shen YQ, Li L, Chen NX, Zhu ZC, et al. Rumination and the default mode network: meta-analysis of brain imaging studies and implications for depression. *Neuroimage.* (2020) 206:116287. doi: 10.1016/j.neuroimage.2019.116287

57. Jiang P, Sun J, Zhou X, Lu L, Li L, Huang X, et al. Functional connectivity abnormalities underlying mood disturbances in male abstinent methamphetamine abusers. *Hum Brain Mapp.* (2021) 42:3366–78. doi: 10.1002/hbm.25439

58. Dluzen DE, McDermott JL. Estrogen, testosterone, and methamphetamine toxicity. *Ann N Y Acad Sci.* (2006) 1074:282–94. doi: 10.1196/annals.1369.025

frontiers | Frontiers in Psychiatry

TYPE Original Research
PUBLISHED 03 November 2022
DOI 10.3389/fpsyt.2022.1033918

OPEN ACCESS

EDITED BY
André Schmidt,
University of Basel, Switzerland

REVIEWED BY
Antonia New,
Icahn School of Medicine at Mount Sinai, United States
Yoji Hirano,
Kyushu University, Japan

*CORRESPONDENCE
Tsutomu Takahashi
tsutomu@med.u-toyama.ac.jp

SPECIALTY SECTION
This article was submitted to Neuroimaging and Stimulation, a section of the journal Frontiers in Psychiatry

RECEIVED 01 September 2022
ACCEPTED 20 October 2022
PUBLISHED 03 November 2022

CITATION
Takahashi T, Sasabayashi D, Velakoulis D, Suzuki M, McGorry PD, Pantelis C and Chanen AM (2022) Heschl's gyrus duplication pattern and clinical characteristics in borderline personality disorder: A preliminary study. *Front. Psychiatry* 13:1033918. doi: 10.3389/fpsyt.2022.1033918

Heschl's gyrus duplication pattern and clinical characteristics in borderline personality disorder: A preliminary study

Tsutomu Takahashi[1,2]*, Daiki Sasabayashi[1,2], Dennis Velakoulis[3,4], Michio Suzuki[1,2], Patrick D. McGorry[5,6], Christos Pantelis[3,7,8] and Andrew M. Chanen[5,6]

[1]Department of Neuropsychiatry, University of Toyama Graduate School of Medicine and Pharmaceutical Sciences, Toyama, Japan, [2]Research Center for Idling Brain Science, University of Toyama, Toyama, Japan, [3]Department of Psychiatry, Melbourne Neuropsychiatry Centre, The University of Melbourne and Melbourne Health, Carlton, VIC, Australia, [4]Neuropsychiatry Unit, Royal Melbourne Hospital, Melbourne Health, Melbourne, VIC, Australia, [5]Orygen, Melbourne, VIC, Australia, [6]Centre for Youth Mental Health, The University of Melbourne, Melbourne, VIC, Australia, [7]Florey Institute of Neuroscience and Mental Health, Parkville, VIC, Australia, [8]North Western Mental Health, Western Hospital Sunshine, St Albans, VIC, Australia

Inter-individual variations in the sulco-gyral pattern of Heschl's gyrus (HG) might contribute to emotional processing. However, it remains largely unknown whether borderline personality disorder (BPD) patients exhibit an altered HG gyrification pattern, compared with healthy individuals, and whether such a brain morphological feature, if present, might contribute to their clinical characteristics. The present study used magnetic resonance imaging to investigate the distribution of HG gyrification patterns (single or duplicated) and their relationship to clinical characteristics in teenage BPD patients with minimal treatment exposure. No significant difference was noted for the prevalence of HG patterns between 20 BPD and 20 healthy participants. However, the BPD participants with left duplicated HG were characterized by higher prevalence of comorbid disruptive behavior disorders, with higher externalizing score compared with those with left single HG. Our preliminary results suggest that neurodevelopmental pathology associated with gyral formation might be implicated in the neurobiology of early BPD, especially for emotional and behavioral control.

KEYWORDS

superior temporal gyrus, gyrification, sulco-gyral pattern, externalizing behavior, disruptive behavior disorders, magnetic resonance imaging

Introduction

Heschl's gyrus (HG), which is a convolution on the surface of superior temporal gyrus (STG), contains the primary auditory cortex and is central to auditory processing (1), while also having a prominent role in emotional information processing (2, 3). HG is known for its high inter-individual anatomical variability, potentially due to variations in cytoarchitectonic development during fetal life; about 30–50% of healthy adults have a partial split of the lateral part of the gyrus (i.e., partial duplication) or independent two gyri (complete duplication) (4, 5). Although the functional significance of different HG patterns remains unclear, HG duplication might be related to decreased HG activity during auditory processing (6) and learning impairment (7, 8). It is also reported that hyper-gyrification (i.e., extensive cortical folding) in the STG region is weakly associated with motor impulsivity (9) and irritability (10) in healthy young adults. However, the role of a HG duplication pattern on personality traits characterized by emotional dysregulation remains unknown.

Although the neurobiology of borderline personality disorder (BPD) has yet to be elucidated, abnormalities in neural networks, including the STG, have been implicated in their impulsive behaviors and emotional instability (11–13). Furthermore, previous magnetic resonance imaging (MRI) studies have reported that BPD patients exhibit brain morphological characteristics associated with fetal neurodevelopmental abnormalities (e.g., altered sulco-gyral patterns and hyper- or hypo-gyrification) at early stages of the illness (14–18). While our previous MRI study found no volume changes of HG in a BPD cohort and its clinical subgroups (e.g., with and without violent episodes) (19), no MRI studies have specifically investigated HG duplication patterns in BPD.

This MRI study examined the distribution of HG gyrification patterns in BPD teenagers who had received minimal treatment and in healthy control participants. Based on a possible role for the STG in emotional dysregulation in BPD (11) and structure-function relationships of HG gyrification patterns (6), we predicted that BPD patients would have an altered prevalence of HG duplication. We also explored whether the HG gyrification pattern was related to BPD phenomenology.

Materials and methods

Participants

The present study included 20 teenagers with BPD and 20 healthy controls (**Table 1**). Recruitment strategy and sample characteristics of this cohort have been detailed elsewhere (20). All participants in this study had no history of significant medical problems that could affect brain function and/or mental conditions (e.g., thyroid diseases, serious brain injury, seizure, neurological illness, or other).

Briefly, BPD teenagers meeting the Structured Clinical Interview for DSM-IV Axis II Disorders (SCID-II) criteria (21) but who had never received specific treatment for BPD, were recruited from the Helping Young People Early (HYPE) Clinic, an early intervention service for BPD in Melbourne, Australia (22). Major comorbid Axis I diagnoses were: disruptive behavior disorders (N = 10), mood disorder (N = 7), anxiety disorder (N = 9), and/or substance use disorders (N = 6). They were medication-free at scanning except for three patients who had received antidepressants. At intake, they were assessed for lifetime trauma exposure (physical, emotional, and/or sexual) and parasuicidal/violent episodes (**Table 1**) *via* a semi-structured interview.

The patients also completed the Young Adult Self-Report [YASR (23)] (age ≥18 years) or the Youth Self-Report [YSR (24)] (age <18 years).

Healthy comparison subjects were selected from a database of healthy volunteers who had no personal of family history of psychiatric disorders or substance abuse/dependence. The SCID-II derived checklist was used to confirm that they did not have any BPD symptoms. This study was approved by Melbourne Health Mental Health Research and Ethics Committee (MHREC2009.607). In accordance with the Declaration of Helsinki, Study participants or a parent or guardian gave written informed consent, prior to participating in the study.

Magnetic resonance imaging procedures

Magnetic resonance images were obtained using a 1.5T GE Signa scanner, with a three-dimensional volumetric spoiled gradient recalled echo sequence to provide 124 contiguous coronal slices of 1.5 mm thickness. Detailed imaging parameters were described elsewhere (17, 19).

As fully described previously (25–29), the HG gyrification patterns were classified into single or duplicated patterns on the reformatted MR images (i.e., 0.938 mm iso-voxel images) using Dr. View (Infocom, Tokyo, Japan); the duplicated HG patterns were subdivided into partial [i.e., common stem duplication (CSD)] or complete [i.e., complete posterior duplication (CPD)] patterns (**Figure 1**). All HG gyrification patterns were classified by one rater (TT) with no knowledge of the subjects' identities. A validation study of HG pattern classification in a randomly selected 20 hemispheres showed sufficient inter- (TT and DS) and intra-rater (TT) reliabilities (Cronbach's $\alpha > 0.80$).

TABLE 1 Demographic and clinical characteristics of the study participants.

Variable	Healthy controls	BPD patients	Group comparison
Age (years)	19 ± 2.2 (range, 16.2–23.8)	17.3 ± 1.1 (range, 15.4–19.2)	ANOVA: F (1, 38) = 2.97, p = 0.003
Gender (males/females)	5/15	5/15	χ^2 = 0.00, p = 1.000
Hand dominance (right/left/mixed)	18/2/0	18/1/1	Fisher's exact test: p = 0.513
NART-estimated IQ[a]	101.9 ± 9.1	100.9 ± 5.8	ANOVA: F (1, 37) = 0.20, p = 0.654
Life time trauma exposure (yes/no)[b]	–	10/9	
Parasuicidal episodes in 6 months (yes/no)	–	13/7	
Number of parasuicidal episode	–	11.0 ± 9.8 (N = 13)	–
Violent episodes in 6 months (yes/no)	–	9/11	
Number of violent episode	–	6.4 ± 9.2 (N = 9)	–
YASR or YSR subscale scores			
Internalizing	–	0.91 ± 0.49	–
Externalizing	–	0.76 ± 0.41	–
SCID-II total BPD score	–	21 ± 3.2	

Values represent means ± SDs. ANOVA, analysis of variance; BPD, borderline personality disorder; NART, National Adult Reading Test; SCID-II, Structured Clinical Interview for DSM-IV Axis II Disorders; YASR, Young Adult Self-Report; YSR, Youth Self-Report. [a]Data were not available for some participants. [b]Interview data were not available for one BPD patient.

Statistical analysis

Group differences in the HG pattern distribution (single, CSD, or CPD) were compared for each hemisphere using the χ^2 test or Fisher's exact test. Given that only four hemispheres in the BPD group had the CPD pattern (Table 2) and that partial and complete duplications likely have no differences in tonotopic organization of human auditory cortex (30), similar to a previous study examining the relationship between the HG patterns and HG activity (6), the CSD and CPD patterns were categorized together as "duplicated pattern" for subsequent analyses. Relationships between the HG gyrification patterns and BPD subgroups (i.e., with or without the trauma exposure, violent/parasuicidal behaviors, and comorbid DSM diagnoses) were also assessed by the χ^2 test or Fisher's exact test. Because of the small sample size, the non-parametric Mann–Whitney U test was used to evaluate the potential contribution of HG gyrification pattern to clinical variables (IQ, YSR/YASR subscale scores, number of suicidal and violent episodes, and SCID-II total BPD score). Statistical significance was set at $p < 0.05$.

Results

Sample characteristics

There were no significant group differences in gender ratio, height, handedness, and IQ, while BPD patients were younger than controls (Table 1). The BPD participants with comorbid disruptive behavior disorders had a higher YSR/YASR externalizing score (N = 10; mean = 1.04, SD = 0.37) than those without (N = 10; mean = 0.49, SD = 0.22) [F (1, 18) = 17.13], $p < 0.001$], but other demographic and clinical variables did not differ between these subgroups.

Heschl's gyrus pattern distributions

We found no significant differences in the prevalence of HG patterns bilaterally between the BPD and control groups (Table 2 and Figure 2), even when the CSD and CPD patterns were categorized together as the duplicated pattern (all $p > 0.197$).

Association between the Heschl's gyrus pattern and demographic/clinical characteristics

Gender and IQ were not related to the HG gyrification pattern for both BPD and healthy control groups.

The BPD patients with left duplicated HG were characterized by higher YSR/YASR externalizing scores (U = 79.0, p = 0.029) (Figure 3) and higher prevalence of comorbid disruptive behavior disorders (Fisher's exact test, p = 0.023) (Table 3), compared with those with left single HG. Other clinical variables and subgroups of the BPD patients were not related to HG gyrification patterns.

Discussion

To our knowledge, this is the first study examining the HG duplication pattern and its relationship to clinical characteristics in BPD. While the prevalence of HG duplication did not differ

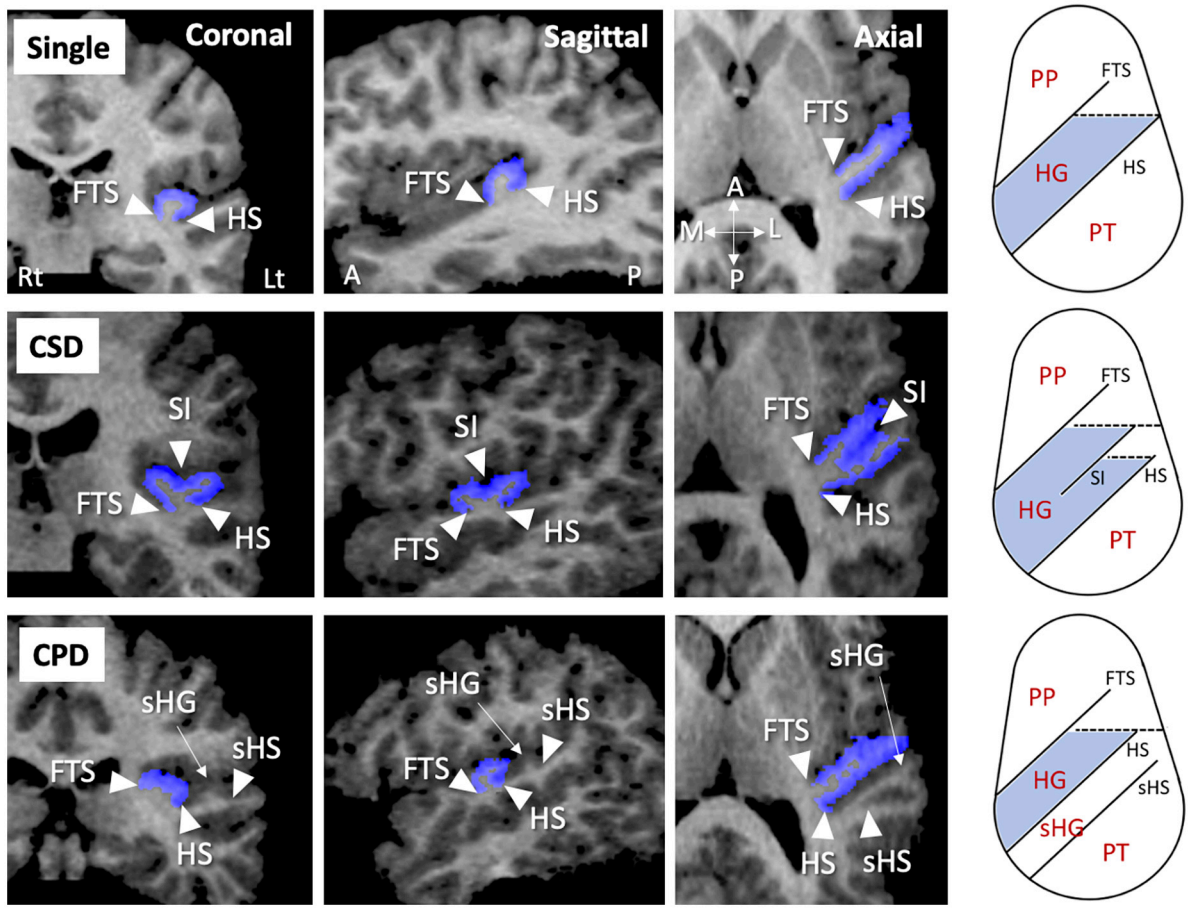

FIGURE 1
Sample MR images of different gyrification pattern in the Heschl's gyrus (HG) (colored in blue). These HG patterns have been demonstrated also in our previous publications (22–26). A, anterior; CPD, complete posterior duplication; CSD, common stem duplication; FTS, first transverse sulcus; HS, Heschl's sulcus; L, lateral; Lt, left; P, posterior; M, medial; PP, planum polare; Rt, right; sHG, second Heschl's gyrus; sHS, second Heschl's sulcus; SI, sulcus intermedius.

between the adolescent BPD patients and control subjects, the patients who had a duplicated HG on the left hemisphere were characterized by more severe aggressive behavior, compared with those with a single HG. The present results suggest that neurodevelopmental characteristics associated with fetal gyral formation might contribute to clinical subtypes and/or symptom severity early in the course of BPD.

Previous MRI studies in adolescent BPD demonstrated gray matter reduction and/or significant relationship with aggression/impulsivity predominantly in fronto-limbic brain regions (31, 32), which could not be explained by confounding factors associated with illness chronicity and treatment (33). Interestingly, a few diffusion tensor imaging studies in adolescent BPD (34–36) supported the notion that abnormalities in fronto-limbic networks are associated with emotional dysregulation and impulsivity early in the course of BPD (33). Further, recent MRI findings of gross anatomical features in BPD patients [e.g., altered cortical surface morphology (15, 17, 18)], which reflect prenatal brain development (37), may at least partly support their early neurodevelopmental pathology (33). However, there are discrepancies in previous cortical folding findings in BPD; Vatheuer et al. (18) demonstrated a parietal hyper-gyrification, while Depping et al. (15) reported a significant relationship between hypo-gyrification of the orbitofrontal region and impulsivity. Thus, potential role of early neurodevelopmental processes associated with cortical folding on the pathophysiology of BPD may have regional specificity.

The present findings of HG duplication pattern appear to reflect fetal neurodevelopment, because variations in the HG gyrification pattern are formed largely during the late gestation period along with neural development (38, 39) but remain rather stable after birth (40). Despite the small sample size, the prevalence and pattern (i.e., more frequent in right hemisphere) of HG duplication in our healthy subjects were comparable with previous reports in large samples (4, 5,

TABLE 2 Gyrification pattern of Heschl's gyrus (HG) in the study participants.

Healthy controls

		Right HG pattern [*N* (%)]			
		Single	**CSD**	**CPD**	**Total**
Left HG pattern [*N* (%)]	Single	6 (30.0)	6 (30.0)	2 (10.0)	14 (70.0)
	CSD	2 (10.0)	2 (10.0)	1 (5.0)	5 (25.0)
	CPD	1 (5.0)	0 (0.0)	0 (0.0)	1 (5.0)
	Total	9 (45.0)	8 (40.0)	3 (15.0)	20 (100.0)

BPD

		Right HG pattern [*N* (%)]			
		Single	**CSD**	**CPD**	**Total**
Left HG pattern [*N* (%)]	Single	5 (25.0)	5 (25.0)	0 (0.0)	10 (50.0)
	CSD	3 (15.0)	3 (15.0)	3 (15.0)	9 (45.0)
	CPD	0 (0)	1 (5.0)	0 (0.0)	1 (5.0)
	Total	8 (40.0)	9 (45.0)	3 (15.0)	20 (100.0)

CSD, common stem duplication; CPD, complete posterior duplication.

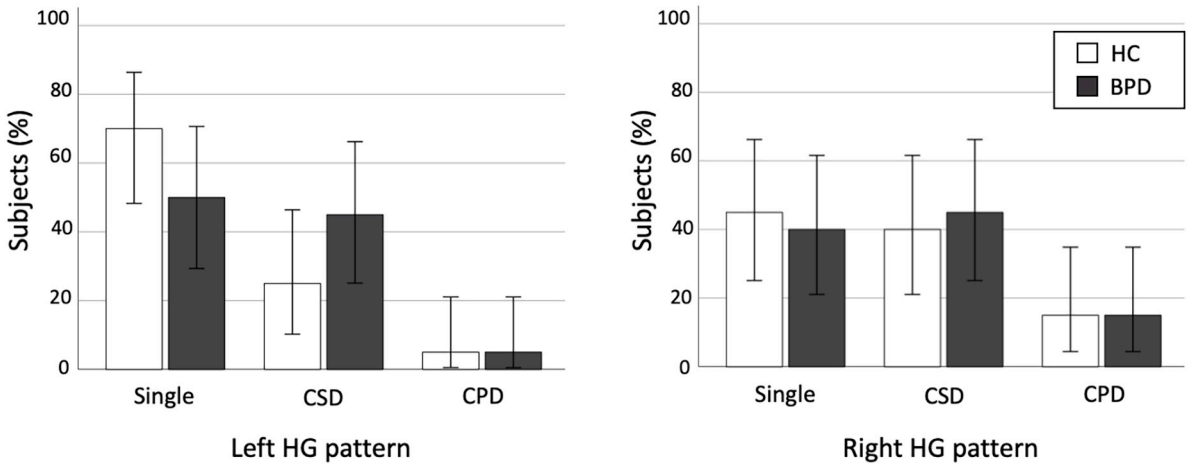

FIGURE 2
Distribution of Heschl's gyrus (HG) duplication patterns in the healthy control (HC) and borderline personality disorder (BPD) groups. CPD, complete posterior duplication; CSD, common stem duplication. Error bars show 95% confidence intervals.

41). The BPD group was characterized by higher prevalence of HG duplication on left hemisphere (50%) than healthy subjects (30%) [odds ratio = 2.33 (95% CI, 0.64–8.54)] with small-to-medium effect size (*Phi* = 0.204), but this difference was not statistically significant. This negative result might reflect the heterogeneity of the disorder (42), because the HG patterns were associated with specific subtypes and symptoms in our BPD cohort as detailed below. It is reported that antipsychotic medication (43) and adverse environmental factors [e.g., childhood maltreatment (44)] might also affect gyrification in the adult brain, but we found no effects of trauma exposure on HG patterns in our BPD cohort with minimal treatment exposure.

In the present study, our results suggested that left duplicated HG in BPD might contribute to higher score for delinquent and aggressive behavior (i.e., externalizing score) and higher prevalence of comorbid disruptive behavior disorders, supporting the notion that BPD is a heterogeneous disorder with different neurobiological underpinnings for core endophenotypes, such as emotional dysregulation and impulsive aggression (45). Although the present study cannot directly address the functional significance of HG patterns in the

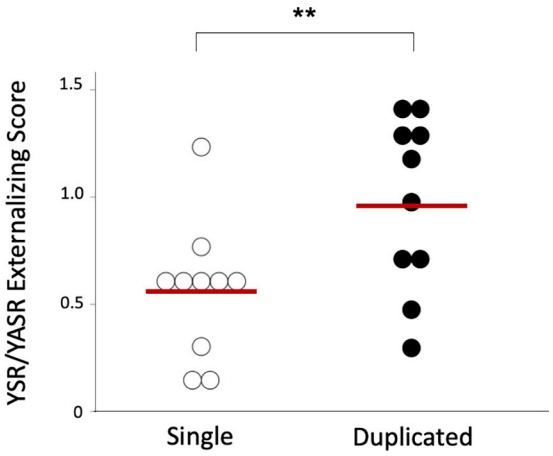

FIGURE 3
Youth Self-Report (YSR) or Young Adult Self-Report (YASR) externalizing scores in the borderline personality disorder patients with single and duplicated Heschl's gyrus patterns on the left hemisphere. Horizontal bars indicate means of each group. *$p < 0.05$.

neurobiology of BPD, our results are consistent with previous findings that the HG duplication is associated with impaired HG functioning (6) and that abnormal neural networks including the STG contribute to impulsive behaviors and emotional instability in BPD (11–13). These findings seem to support the early neurodevelopmental model of BPD that neurobiological vulnerability associated with fetal sulcal formation might contribute to specific clinical characteristics in early stages of BPD. However, further studies will be needed to clarify the role of environmental factors after birth that might further increase the risk of BPD in vulnerable individuals (33, 46).

There are several potential confounding factors in this study. First, the present study was clearly limited by a lack of statistical power to reliably detect group differences due to small sample size. Because the BPD group in this study had a somewhat higher prevalence of left HG duplication compared to controls (**Table 2** and **Figure 2**), the possibility exists that future investigation in a larger BPD cohort might be able to detect significant group differences. Similarly, potential gender differences in brain gyrification (47) could not be reliably examined in our small sample especially for male subjects. Second, younger age of the BPD patients (mean = 17.3 years), compared with control participants (mean = 19.0 years) in this study, might have biased our results. However, it is unlikely that this difference in a narrow age would have a major impact on gross sulco-gyral pattern, which is a rather stable neurodevelopmental marker (40). Indeed, we found no effect of age on the HG patterns (single vs. duplicated) in the present sample [left, F (1, 38) = 1.02, p = 0.320; right, F (1, 38) = 0.12, p = 0.744]. Furthermore, the effect of age alone could not explain our main finding of different prevalence of HG duplication between the BPD subgroups (with and without disruptive behavior disorders), since these subgroups did not differ for age. Third, the CSD and CPD patterns were categorized together in this study because only a few hemispheres had the CPD pattern. While the functional role of the HG duplication type (i.e., CPD vs. CSD) remains largely unknown, our previous study in schizophrenia suggested specific role of the CSD pattern on cognitive deficits (27). Thus, future studies should examine whether different HG duplication patterns play different roles in the pathophysiology of BPD. Finally, the present study cannot

TABLE 3 Gyrification pattern of Heschl's gyrus (HG) in borderline personality disorder (BPD) patients with and without comorbid disruptive behavior disorders.

BPD with disruptive behavior disorders

		Right HG pattern [*N* (%)]		
		Single	**Duplicated**	**Total**
Left HG pattern [*N* (%)]	Single	1 (10.0)	1 (10.0)	2 (20.0)
	Duplicated	3 (30.0)	5 (50.0)	8 (80.0)
	Total	4 (40.0)	6 (60.0)	10 (100.0)

BPD without disruptive behavior disorders

		Right HG pattern [*N* (%)]		
		Single	**Duplicated**	**Total**
Left HG pattern [*N* (%)]	Single	4 (40.0)	4 (40.0)	8 (80.0)
	Duplicated	0 (0.0)	2 (10.0)	2 (20.0)
	Total	4 (40.0)	6 (60.0)	10 (100.0)

address whether the relationship between the HG duplication and emotional/behavioral characteristics is specific to BPD, because of the lack of a clinical comparison group and because the healthy participants in this study were not comprehensively assessed for personality pathology or behavioral characteristics. It remains unanswered whether participants with disruptive behavior disorders, but without BPD features, have an altered HG pattern. Further, we have previously demonstrated the association between HG duplication and "lack" of emotional responsivity in schizophrenia (28), suggesting different contribution of HG patterns on clinical characteristics in different disorders/conditions. It should be noted that we examined only the HG patterns, but not other biological features, and their relationship with clinical and behavioral feature of our BPD cohort. Thus, the disease specificity of our HG findings and their functional significance should be further tested using larger samples of various clinical/non-clinical populations.

In summary, our preliminary results demonstrated a relationship between the HG duplication pattern and BPD phenomenology (especially aggressive behavior) in teenagers with first-presentation BPD. Thus, neurobiological vulnerability associated with fetal sulcal formation might increase the risk for impaired control of emotion and behavior in the early stages of BPD.

Data availability statement

The raw data supporting the conclusions of this article will be made available by the authors, without undue reservation.

Ethics statement

The studies involving human participants were reviewed and approved by the Melbourne Health Mental Health Research and Ethics Committee. Written informed consent to participate in this study was provided by the participants' legal guardian/next of kin.

Author contributions

AC, MS, CP, and PM conceived the idea and methodology of the study. TT conducted the statistical analyses and wrote the manuscript. AC and DV recruited subjects and involved in clinical and diagnostic assessments. TT and DS analyzed the MRI data. AC, CP, and MS contributed to the writing and editing of the manuscript. All authors contributed to the article and approved the submitted version.

Funding

This study was supported in part by JSPS KAKENHI grant numbers: JP18K07550 to TT, JP18K15509 to DS, and JP20H03598 to MS, and by the Health and Labor Sciences Research Grants for Comprehensive Research on Persons with Disabilities from the Japan Agency for Medical Research and Development (AMED) grant number: JP19dk0307029 to MS. CP was supported by a National Health and Medical Research Council (ID: NHMRC), L3 Investigator Grant (ID: 1196508), and a NHMRC Program Grant (ID: 1150083).

Conflict of interest

The authors declare that the research was conducted in the absence of any commercial or financial relationships that could be construed as a potential conflict of interest.

Publisher's note

References

1. Rademacher J, Caviness VS Jr, Steinmetz H, Galaburda AM. Topographical variation of the human primary cortices: implications for neuroimaging, brain mapping, and neurobiology. *Cereb Cortex.* (1993) 3:313–29. doi: 10.1093/cercor/3.4.313

2. Concina G, Renna A, Grosso A, Sacchetti B. The auditory cortex and the emotional valence of sounds. *Neurosci Biobehav Rev.* (2019) 98:256–64. doi: 10.1016/j.neubiorev.2019.01.018

3. Grosso A, Cambiaghi M, Concina G, Sacco T, Sacchetti B. Auditory cortex involvement in emotional learning and memory. *Neuroscience.* (2015) 299:45–55. doi: 10.1016/j.neuroscience.2015.04.068

4. Abdul-Kareem IA, Sluming V. Heschl gyrus and its included primary auditory cortex: structural MRI studies in healthy and diseased subjects. *J Magn Reson Imaging.* (2008) 28:287–99. doi: 10.1002/jmri.21445

5. Marie D, Jobard G, Crivello F, Perchey G, Petit L, Mellet E, et al. Descriptive anatomy of Heschl's gyri in 430 healthy volunteers, including 198 left-handers. *Brain Struct Funct.* (2015) 220:729–43. doi: 10.1007/s00429-013-0680-x

6. Tzourio-Mazoyer N, Marie D, Zago L, Jobard G, Perchey G, Leroux G, et al. Heschl's gyrification pattern is related to speech-listening hemispheric lateralization: fMRI investigation in 281 healthy volunteers. *Brain Struct Funct.* (2015) 220:1585–99. doi: 10.1007/s00429-014-0746-4

7. Leonard CM, Voeller KK, Lombardino LJ, Morris MK, Hynd GW, Alexander AW, et al. Anomalous cerebral structure in dyslexia revealed with magnetic resonance imaging. *Arch Neurol.* (1993) 50:461–9. doi: 10.1001/archneur.1993.00540050013008

8. Leonard CM, Eckert MA, Lombardino LJ, Oakland T, Kranzler J, Mohr CM, et al. Anatomical risk factors for phonological dyslexia. *Cereb Cortex.* (2001) 11:148–57. doi: 10.1093/cercor/11.2.148

9. Hirjak D, Thomann AK, Kubera KM, Wolf RC, Jeung H, Maier-Hein KH, et al. Cortical folding patterns are associated with impulsivity in healthy young adults. *Brain Imaging Behav.* (2017) 11:1592–603. doi: 10.1007/s11682-016-9618-2

10. Besteher B, Squarcina L, Spalthoff R, Bellani M, Gaser C, Brambilla P, et al. Brain structural correlates of irritability: findings in a large healthy cohort. *Hum Brain Mapp.* (2017) 38:6230–8. doi: 10.1002/hbm.23824

11. Koenigsberg HW, Siever LJ, Lee H, Pizzarello S, New AS, Goodman M, et al. Neural correlates of emotion processing in borderline personality disorder. *Psychiatry Res Neuroimaging.* (2009) 172:192–9. doi: 10.1016/j.pscychresns.2008.07.010

12. Leyton M, Okazawa H, Diksic M, Paris J, Rosa P, Mzengeza S, et al. Brainregional alpha-[11C]methyl-L-tryptophan trapping in impulsive subjects with borderline personality disorder. *Am J Psychiatry.* (2001) 158:775–82. doi: 10.1176/appi.ajp.158.5.775

13. Soloff PH, Meltzer CC, Greer PJ, Constantine D, Kelly TM. A fenfluramine-activated FDG-PET study of borderline personality disorder. *Biol Psychiatry.* (2000) 47:540–7. doi: 10.1016/s0006-3223(99)00202-4

14. de Araujo Filho GM, Abdallah C, Sato JR, de Araujo TB, Lisondo CM, de Faria ÁA, et al. Morphometric hemispheric asymmetry of orbitofrontal cortex in women with borderline personality disorder: a multi-parameter approach. *Psychiatry Res.* (2014) 223:61–6. doi: 10.1016/j.pscychresns.2014.05.001

15. Depping MS, Thomann PA, Wolf ND, Vasic N, Sosic-Vasic Z, Schmitgen MM, et al. Common and distinct patterns of abnormal cortical gyrification in major depression and borderline personality disorder. *Eur Neuropsychopharmacol.* (2018) 28:1115–25. doi: 10.1016/j.euroneuro.2018.07.100

16. Takahashi T, Chanen AM, Wood SJ, Walterfang M, Harding IH, Yücel M, et al. Midline brain structures in teenagers with first-presentation borderline personality disorder. *Prog Neuropsychopharmacol Biol Psychiatry.* (2009) 33:842–6. doi: 10.1016/j.pnpbp.2009.03.035

17. Takahashi T, Nishikawa Y, Velakoulis D, Suzuki M, McGorry PD, Pantelis C, et al. Olfactory sulcus morphology in teenagers with first-presentation borderline personality disorder. *Psychiatry Res Neuroimaging.* (2019) 292:1–4. doi: 10.1016/j.pscychresns.2019.08.006

18. Vatheuer CC, Dzionsko I, Maier S, Näher T, van Zutphen L, Sprenger A, et al. Looking at the bigger picture: cortical volume, thickness and surface area characteristics in borderline personality disorder with and without posttraumatic stress disorder. *Psychiatry Res Neuroimaging.* (2021) 311:111283. doi: 10.1016/j.pscychresns.2021.11128

19. Takahashi T, Chanen AM, Wood SJ, Yücel M, Kawasaki Y, McGorry PD, et al. Superior temporal gyrus volume in teenagers with first-presentation borderline personality disorder. *Psychiatry Res Neuroimaging.* (2010) 182:73–6. doi: 10.1016/j.pscychresns.2009.10.014

20. Chanen AM, Velakoulis D, Carison K, Gaunson K, Wood SJ, Yuen HP, et al. Orbitofrontal, amygdala and hippocampal volumes in teenagers with first-presentation borderline personality disorder. *Psychiatry Res.* (2008) 163:116–25. doi: 10.1016/j.pscychresns.2007.08.007

21. First MB, Gibbon M, Spitzer RL, Williams JBW, Benjamin LS. *User's Guide for the Structured Clinical Interview for DSM-IV Axis II Personality Disorders*. Washington, DC: American Psychiatric Press (1997).

22. Chanen AM, McCutcheon L, Germano D, Nistico H, Jackson HJ, McGorry PD. The HYPE Clinic: an early intervention service for borderline personality disorder. *J Psychiatr Pract.* (2009) 15:163–72. doi: 10.1097/01.pra.0000351876.51098.f0

23. Achenbach TM. *Manual for the Young Adult Self-report and Young Adult Behavior Checklist*. Burlington, VT: University of Vermont (1997).

24. Achenbach TM. *Manual for the Youth Self-report and 1991 Profiles*. Burlington, VT: University of Vermont (1991).

25. Takahashi T, Sasabayashi D, Takayanagi Y, Furuichi A, Kido M, Nakamura M, et al. Altered Heschl's gyrus duplication pattern in first-episode schizophrenia. *Schizophr Res.* (2021) 237:174–81. doi: 10.1016/j.schres.2021.09.011

26. Takahashi T, Sasabayashi D, Takayanagi Y, Furuichi A, Kido M, Pham TV, et al. Increased Heschl's gyrus duplication in schizophrenia spectrum disorders: a cross-sectional MRI study. *J Pers Med.* (2021) 11:40. doi: 10.3390/jpm11010040

27. Takahashi T, Sasabayashi D, Takayanagi Y, Higuchi Y, Mizukami Y, Nishiyama S, et al. Heschl's gyrus duplication pattern in individuals at risk of developing psychosis and patients with schizophrenia. *Front Behav Neurosci.* (2021) 15:647069. doi: 10.3389/fnbeh.2021.647069

28. Takahashi T, Sasabayashi D, Takayanagi Y, Furuichi A, Kobayashi H, Noguchi K, et al. Different Heschl's gyrus duplication patterns in deficit and non-deficit subtypes of schizophrenia. *Front Psychiatry.* (2022) 13:867461. doi: 10.3389/fpsyt.2022.867461

29. Takahashi T, Sasabayashi D, Yücel M, Whittle S, Lorenzetti V, Walterfang M, et al. Different frequency of Heschl's gyrus duplication patterns in neuropsychiatric disorders: an MRI study in bipolar and major depressive disorders. *Front Hum Neurosci.* (2022) 16:917270. doi: 10.3389/fnhum.2022.917270

30. Da Costa S, van der Zwaag W, Marques JP, Frackowiak RS, Clarke S, Saenz M. Human primary auditory cortex follows the shape of Heschl's gyrus. *J Neurosci.* (2011) 31:14067–75. doi: 10.1523/JNEUROSCI.2000-11.2011

31. Chu J, Zheng K, Yi J. Aggression in borderline personality disorder: a systematic review of neuroimaging studies. *Prog Neuropsychopharmacol Biol Psychiatry.* (2022) 113:110472. doi: 10.1016/j.pnpbp.2021.110472

32. Winsper C, Marwaha S, Lereya ST, Thompson A, Eyden J, Singh SP. A systematic review of the neurobiological underpinnings of borderline personality disorder (BPD) in childhood and adolescence. *Rev Neurosci.* (2016) 27:827–47. doi: 10.1515/revneuro-2016-0026

33. Chanen AM, Kaess M. Developmental pathways to borderline personality disorder. *Curr Psychiatry Rep.* (2012) 14:45–53. doi: 10.1007/s11920-011-0242-y

34. Maier-Hein KH, Brunner R, Lutz K, Henze R, Parzer P, Feigl N, et al. Disorder-specific white matter alterations in adolescent borderline personality disorder. *Biol Psychiatry.* (2014) 75:81–8. doi: 10.1016/j.biopsych.2013.03.031

35. New AS, Carpenter DM, Perez-Rodriguez MM, Ripoll LH, Avedon J, Patil U, et al. Developmental differences in diffusion tensor imaging parameters in borderline personality disorder. *J Psychiatr Res.* (2013) 47:1101–9. doi: 10.1016/j.jpsychires.2013.03.021

36. Sadek MN, Ismail ES, Kamel AI, Saleh AA, Youssef AA, Madbouly NM. Diffusion tensor imaging of corpus callosum in adolescent females with borderline personality disorder. *J Psychiatr Res.* (2021) 138:272–9. doi: 10.1016/j.jpsychires.2021.04.010

37. Zilles K, Palomero-Gallagher N, Amunts K. Development of cortical folding during evolution and ontogeny. *Trends Neurosci.* (2013) 36:275–84. doi: 10.1016/j.tins.2013.01.006

38. Chi JG, Dooling EC, Gilles FH. Gyral development of the human brain. *Ann Neurol.* (1977) 1:86–93. doi: 10.1002/ana.410010109

39. Van Essen DC. A tension-based theory of morphogenesis and compact wiring in the central nervous system. *Nature.* (1997) 385:313–8. doi: 10.1038/385313a0

40. Armstrong E, Schleicher A, Omran H, Curtis M, Zilles K. The ontogeny of human gyrification. *Cereb Cortex.* (1995) 5:56–63. doi: 10.1093/cercor/5.1.56

41. Tzourio-Mazoyer N, Mazoyer B. Variations of planum temporale asymmetries with Heschl's Gyri duplications and association with cognitive abilities: MRI investigation of 428 healthy volunteers. *Brain Struct Funct.* (2017) 222:2711–26. doi: 10.1007/s00429-017-1367-5

42. Skodol AE, Siever LJ, Livesley WJ, Gunderson JG, Pfohl B, Widiger TA, et al. The borderline diagnosis II: biology, genetics, and clinical course. *Biol Psychiatry.* (2002) 51:951–63. doi: 10.1016/s0006-3223(02)01325-2

43. Pham TV, Sasabayashi D, Takahashi T, Takayanagi Y, Kubota M, Furuichi A, et al. Longitudinal changes in brain gyrification in schizophrenia spectrum disorders. *Front Aging Neurosci.* (2021) 13:752575. doi: 10.3389/fnagi.2021.752575

44. Kelly PA, Viding E, Wallace GL, Schaer M, De Brito SA, Robustelli B, et al. Cortical thickness, surface area, and gyrification abnormalities in children exposed to maltreatment: neural markers of vulnerability? *Biol Psychiatry.* (2013) 74:845–52. doi: 10.1016/j.biopsych.2013.06.020

45. Siever LJ. Endophenotypes in the personality disorders. *Dialogues Clin Neurosci.* (2015) 7:139–51. doi: 10.31887/DCNS.2005.7.2/lsiever

46. Crowell SE, Beauchaine TP, Linehan MM. A biosocial developmental model of borderline personality: elaborating and extending Linehan's theory. *Psychol Bull.* (2019) 135:495–510. doi: 10.1037/a0015616

47. White T, Su S, Schmidt M, Kao CY, Sapiro G. The development of gyrification in childhood and adolescence. *Brain Cogn.* (2010) 72:36–45. doi: 10.1016/j.bandc.2009.10.009

frontiers | Frontiers in Psychiatry

TYPE Original Research
PUBLISHED 18 November 2022
DOI 10.3389/fpsyt.2022.1050712

OPEN ACCESS

EDITED BY
Yasuhiro Kawasaki,
Kanazawa Medical University, Japan

REVIEWED BY
Stefan Borgwardt,
University of Lübeck, Germany
Yoji Hirano,
Kyushu University, Japan

*CORRESPONDENCE
Tsutomu Takahashi
tsutomu@med.u-toyama.ac.jp

SPECIALTY SECTION
This article was submitted to Neuroimaging, a section of the journal Frontiers in Psychiatry

RECEIVED 22 September 2022
ACCEPTED 07 November 2022
PUBLISHED 18 November 2022

CITATION
Takahashi T, Sasabayashi D, Takayanagi Y, Furuichi A, Kobayashi H, Yuasa Y, Noguchi K and Suzuki M (2022) Gross anatomical features of the insular cortex in schizophrenia and schizotypal personality disorder: Potential relationships with vulnerability, illness stages, and clinical subtypes. *Front. Psychiatry* 13:1050712. doi: 10.3389/fpsyt.2022.1050712

Gross anatomical features of the insular cortex in schizophrenia and schizotypal personality disorder: Potential relationships with vulnerability, illness stages, and clinical subtypes

Tsutomu Takahashi[1,2]*, Daiki Sasabayashi[1,2], Yoichiro Takayanagi[1,3], Atsushi Furuichi[1,2], Haruko Kobayashi[1,2], Yusuke Yuasa[1,2], Kyo Noguchi[4] and Michio Suzuki[1,2]

[1]Department of Neuropsychiatry, University of Toyama Graduate School of Medicine and Pharmaceutical Sciences, Toyama, Japan, [2]Research Center for Idling Brain Science, University of Toyama, Toyama, Japan, [3]Arisawabashi Hospital, Toyama, Japan, [4]Department of Radiology, University of Toyama Graduate School of Medicine and Pharmaceutical Sciences, Toyama, Japan

Introduction: Patients with schizophrenia have a higher number of insular gyri; however, it currently remains unclear whether the brain characteristics of patients with schizotypal personality disorder (SPD), a mild form of schizophrenia, are similar. It is also unknown whether insular gross anatomical features are associated with the illness stages and clinical subtypes of schizophrenia.

Materials and methods: This magnetic resonance imaging study examined gross anatomical variations in the insular cortex of 133 patients with schizophrenia, 47 with SPD, and 88 healthy controls. The relationships between the insular gross anatomy and schizophrenia subgroups (71 first-episode and 58 chronic groups, 38 deficit and 37 non-deficit subtype groups) were also investigated.

Results: The number of insular gyri was higher in the schizophrenia and SPD patients than in the controls, where the patients were characterized by well-developed accessory, middle short, and posterior long insular gyri. The insular gross anatomy did not significantly differ between the first-episode and chronic schizophrenia subgroups; however, the relationship between the developed accessory gyrus and more severe positive symptoms was specific to the first-episode group. The prevalence of a right middle short gyrus was higher in the deficit schizophrenia group than in the non-deficit group.

Discussion: These findings suggest that schizophrenia and SPD patients may share an altered insular gross morphology as a vulnerability factor associated

with early neurodevelopmental anomalies, which may also contribute to positive symptomatology in the early illness stages and clinical subtypes of schizophrenia.

KEYWORDS

magnetic resonance imaging, schizotypal, deficit schizophrenia, insula, gyrification, early neurodevelopment

Introduction

The insular cortex is involved in a range of cognitive functions as a "limbic integration cortex" (1) and is characterized by large inter-individual variations in the gross gyral organization (2, 3). The anterior subdivision (short insular cortex) is typically composed of an accessory and three principal short gyri (anterior, middle, and posterior), while the accessory gyrus (AG) and middle short gyrus (MSG) are frequently underdeveloped or absent (up to 50–70%) in general population (4–6). The posterior subdivision (long insular cortex) consists of the anterior and posterior long insular gyri, where the posterior long gyrus (PLG) is missing in between 10 and 20% of human brains (4–6). The significance of the effects of these anatomical variations on the function of the insular cortex has not yet been established; however, we recently reported a higher number of insular gyri with a well-developed AG, MSG, and PLG in patients with first-episode schizophrenia than in controls (7). Since gross brain folding patterns do not markedly change after birth (8), this finding in schizophrenia potentially reflects anomalous neurodevelopment during the mid to late fetal period, during which insular cortical folds are formed (9, 10). Nevertheless, there is currently no evidence to show similar features of the insular gross anatomy in patients with schizophrenia spectrum disorders, who may share early neurodevelopmental pathologies associated with vulnerability to psychosis (11).

Schizotypal personality disorder (SPD) (12), or schizotypal disorder (13), is a milder form within the schizophrenia spectrum and is characterized by attenuated forms of schizophrenic features without overt psychosis. SPD patients are considered to share biological similarities with patients with full-blown schizophrenia, potentially reflecting a common vulnerability (11, 14). Schizophrenia spectrum disorders partly share brain abnormalities, such as diverse cortical hyper-gyrification (15, 16), which may reflect deviations in early neurodevelopment (17, 18). On the other hand, gray matter reductions in the insular cortex appear to be specific to schizophrenia among schizophrenia spectrum disorders (19–23). To the best of our knowledge, magnetic resonance imaging (MRI) studies have not yet specifically examined variations in the insular gross anatomy in SPD patients.

We previously demonstrated that the gross anatomical features of the insular cortex correlated with positive symptomatology in first-episode schizophrenia (7); however, their potential contribution to clinical characteristics at later illness stages and clinical subtypes was not examined. Patients with the deficit subtype of schizophrenia, who are found in approximately 15% of first-episode and 25–30% of more chronic patients, have a trait-like feature of primary and persistent negative symptoms even during remission periods (24, 25). Unlike the DSM/ICD subtypes of schizophrenia (12, 13) based on symptom profiles (e.g., paranoid, disorganized, and undifferentiated), the deficit/non-deficit categorization is highly stable over time and the patients with deficit subtype have rather homogeneous poor outcome as demonstrated in longitudinal clinical follow-up (25). Previous MRI studies on deficit schizophrenia revealed that the patients with this specific subtype may exhibit prominent abnormalities in neurodevelopment (26, 27), as suggested by gross brain changes, including an altered surface morphology in the fronto-temporal regions (28, 29). To obtain a more detailed understanding of the role of insular gross anatomical features in the pathophysiology of schizophrenia, further studies in different illness stages and in specific clinical subtypes, particularly those with a prominent neurodevelopmental pathology (i.e., deficit schizophrenia), are warranted.

We herein used MRI to examine the insular gross anatomy of SPD patients and patients with schizophrenia of different illness stages (first-episode and chronic) and subtypes (deficit and non-deficit). Due to shared neurodevelopmental pathologies in the schizophrenia spectrum and prominent neurodevelopmental abnormalities in deficit schizophrenia as described above, we expected SPD patients to have an elevated number of insular gyri, similar to schizophrenia, and this change to be prominent in the deficit schizophrenia subgroup. We also investigated whether the insular gross anatomy affects clinical characteristics even in the chronic stages of schizophrenia.

Materials and methods

Participants

Participants in the present study comprised 133 patients with schizophrenia, 47 with SPD, and 88 healthy controls (**Table 1**). Their physical condition was good at the time of MRI and they had no previous history of serious illnesses requiring medical treatment (e.g., hypertension, seizure, head injury, diabetes, and thyroid diseases), oral steroid use, or substance use disorders. Among 268 participants, the insular gross anatomy of 66 first-episode schizophrenia patients and 66 healthy controls was reported elsewhere (7). This study aimed to examine the insular anatomy in our SPD sample as well as in an expanded schizophrenia sample with different illness duration (i.e., first-episode vs. chronic patients) and clinical characteristics (i.e., deficit *vs.* non-deficit subtypes) to explore the role of vulnerability to psychosis, illness stages, and subtypes. The recruitment strategies and inclusion criteria of participants were fully described in previous studies (16, 23, 30, 31).

Briefly, we enrolled schizophrenia and SPD patients at the Department of Neuropsychiatry, Toyama University Hospital and they were diagnosed by experienced psychiatrists based on a structured interview using the Comprehensive Assessment of Symptoms and History (32) and the Scale for the Assessment of Negative Symptoms and the Scale for the Assessment of Positive Symptoms (SANS/SAPS) (33). The schizophrenia group was also assessed using the Brief Psychiatric Rating Scale (BPRS) (34) for the purpose of clinical subgrouping.

Schizophrenia patients fulfilling the ICD-10 research criteria (13) were operationally categorized into first-episode [illness duration $\leq$ 1 year (N = 54) or under psychiatric hospitalization for the first time (N = 17)] and chronic [illness duration $\geq$ 3 years (N = 58)] subgroups (35, 36). As previously described in detail (28, 29, 37), we divided the patients into deficit and non-deficit schizophrenia subgroups based on scores for Proxy for the Deficit Syndrome (PDS) (38), which were obtained as follows using BPRS scores: blunted affect – (anxiety + guilt feelings + depressive mood + hostility items). To reduce false classification, patients with the top and bottom 25% of PDS scores among the whole schizophrenia sample were categorized into the deficit and non-deficit subgroups, respectively (39).

All schizotypal patients met the DSM Axis II diagnosis of SPD, with 13 having a history of transient quasi-psychotic episodes fulfilling the DSM Axis I diagnosis of brief psychotic disorder (12). They also fulfilled the ICD-10 research criteria of schizotypal disorder (13). None of these patients had developed schizophrenia during clinical follow-ups for at least 2 years. **Table 1** shows the status of medication and clinical data on schizophrenia and SPD patients.

Following screening by a questionnaire on personal and family medical histories (40), healthy controls were enrolled from the community, hospital staff, and university students. None had a personal or family history of psychiatric illness among first-degree relatives. The Committee of Medical Ethics of the University of Toyama approved this study (ID: I2013006). In accordance with the Declaration of Helsinki, written informed consent was obtained from all participants after a full description of the study protocol. If a participant was younger than 20 years old, written consent was also obtained from a parent/guardian.

MR image acquisition and processing

One-millimeter-thick T1-weighted images were obtained in the sagittal plane with the three-dimensional gradient-echo sequence FLASH (fast low-angle shots) using a 1.5T Magnetom Vision MR scanner (Siemens Medical System, Inc., Erlangen, Germany) under the following imaging conditions: TR = 24 ms, TE = 5 ms, flip angle = 40°, field of view = 256 mm, matrix = 256 × 256 pixels, and voxel size = 1 × 1 × 1 mm.

Using Dr. View software (Infocom, Tokyo, Japan), MR images were reconstructed into 1-mm-thick coronal images perpendicular to the inter-commissural line after three-dimensional tilt correction.

Assessment of anatomical variations in the insula

As described in detail elsewhere (7), one rater who was blinded to the identities of subjects assessed the insular gross anatomy primarily using the sagittal view (**Figure 1**). Briefly, the AG and MSG were classified as absent, underdeveloped (i.e., identifiable, but does not extend to the convex surface of the insula), or developed based on the criteria reported by Wysiadecki et al. (6). The PLG was classified as present or absent because it is developed in most hemispheres (> 85%) and hypoplasia is rarely observed (4, 6). The anterior short gyrus (ASG), posterior short gyrus (PSG), and anterior long gyrus (ALG) were well-developed in all participants in this study. Regarding the number of insular gyri, only well-developed gyri were counted.

The classification reliabilities of insular gyri were examined in a subset of 10 brains that were randomly selected (20 hemispheres); intra- (TT) and inter-rater (TT and DS) reliabilities were > 0.89 for the number (intraclass correlation coefficients) and development classification (Cronbach's α).

Statistical analysis

Group differences in demographic and clinical data were assessed by the χ^2-test or an analysis of variance (ANOVA).

The developmental patterns of the AG, MSG, and PLG were exploratory compared between 3 groups (controls, SPD, and

10.3389/fpsyt.2022.1050712

TABLE 1 Sample characteristics and gross insular morphology of participants.

	Controls (N = 88)	SPD (N = 47)	Sz (N = 133)	Group differences
M/F	49/39	29/18	67/66	Chi-square = 1.93, p = 0.382
Age (years)	24.1 ± 6.0	25.0 ± 5.4	26.8 ± 6.3	$F(2, 265)$ = 5.45, p = 0.005; Controls < Sz
Handedness (Right/left/mixed)	88/0/0	47/0/0	126/1/6	Fisher's exact test, p = 0.095
Height (cm)	166.3 ± 7.8	165.9 ± 8.7	164.2 ± 7.9	$F(2, 265)$ = 1.57, p = 0.209
Education (years)	15.7 ± 3.0	13.1 ± 2.0	13.5 ± 2.0	$F(2, 265)$ = 27.22, p < 0.001; SPD, Sz < Controls
Parental education (years)[a]	13.0 ± 2.3	12.3 ± 1.7	12.5 ± 2.1	$F(2, 255)$ = 1.75, p = 0.176
Onset age (years)	–	–	22.6 ± 5.4	–
Duration of illness (years)	–	–	4.0 ± 4.4	–
Medication dose (HPD equivalent, mg/day)	–	4.8 ± 5.7	9.9 ± 8.4	$F(1, 178)$ = 15.09, p < 0.001; SPD < Sz
Duration of medication (years)	–	1.5 ± 3.0	2.8 ± 3.8	$F(1, 178)$ = 4.20, p = 0.042; SPD < Sz
Medication type (Atypical/typical/mixed)	–	26/14/0	78/45/6	Fisher's exact test, p = 0.503
Total SAPS scores[b]	–	16.0 ± 9.2	29.3 ± 22.8	$F(1, 169)$ = 14.46, p < 0.001; SPD < Sz
Total SANS scores[b]	–	41.9 ± 21.7	50.5 ± 22.6	$F(1, 169)$ = 4.90, p = 0.028; SPD < Sz
Number of short gyri				$F(2, 262)$ = 38.89, p < 0.001; Controls < SPD, Sz
Left	2.78 ± 0.58	3.32 ± 0.66	3.35 ± 0.69	
Right	2.70 ± 0.59	3.36 ± 0.67	3.18 ± 0.61	
Number of long gyri				$F(2, 262)$ = 9.56, p < 0.001; Controls < SPD, Sz in M
Left	1.85 ± 0.42	2.04 ± 0.20	2.01 ± 0.40	
Right	1.85 ± 0.44	1.98 ± 0.33	2.03 ± 0.37	
AG (Absent/underdeveloped/developed)				
Left	36/33/19	17/16/14	44/28/61	Chi-square = 15.79, p = 0.003
Right	44/32/12	13/15/19	56/36/41	Chi-square = 14.85, p = 0.005
MSG (Absent/underdeveloped/developed)				
Left	16/25/47	1/3/43	7/15/111	Chi-square = 34.28, p < 0.001
Right	11/31/46	2/3/42	9/17/107	Chi-square = 29.95, p < 0.001
PLG (Absent/present)				
Left	15/73	0/47	10/123	Chi-square = 11.55, p = 0.003
Right	16/72	3/44	9/124	Chi-square = 8.38, p = 0.015

Values represent means ± SDs unless otherwise stated.
AG, accessory gyrus; ALG, anterior long gyrus; F, female; HPD, haloperidol; M, male; MSG, middle short gyrus; PLG, posterior long gyrus; SANS, scale for the assessment of negative symptoms; SAPS, scale for the assessment of positive symptoms; SPD, schizotypal personality disorder; Sz, schizophrenia.
[a]Data not available for one control, four SPD, and five Sz subjects.
[b]Data not available for two SPD and seven Sz patients.

schizophrenia) using the χ^2-test or Fisher's exact test, where Benjamini-Hochberg procedure was used to decrease the false discovery rate. Lower-order comparisons (e.g., between two groups), which were not corrected for multiple comparisons due to prior hypothesis that both patient groups would similarly have well-developed insular gyri, were performed when significant group differences were found. The number of short (AG, ASG, MSG, and PSG) and long (ALG and PLG) gyri was log-transformed because of a skewed distribution (tested by Kolmogorov–Smirnov tests) and then compared between groups by ANOVA, with diagnosis and sex as between-subject factors and hemisphere as a within-subject variable.

Spearman's correlation analysis with the Bonferroni correction was used to investigate relationships between the number of short insular gyri and clinical variables (age at disease onset in schizophrenia, the dose of medication and total

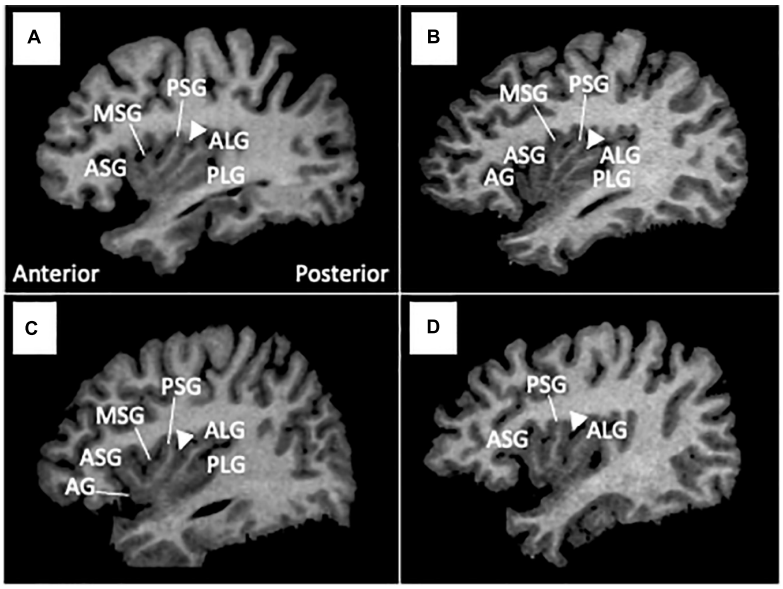

FIGURE 1
Insular gross anatomical variations in sample MR images in sagittal views. Coronal and axial views were simultaneously referred to in assessments of gyral development. Arrowheads indicate the location of the central insular sulcus, which subdivides the short (anterior) and long (posterior) insular cortices. The ASG, PSG, and ALG were well-developed in all participants in this study, while the AG and MSG were absent [subject **(D)**], underdeveloped [subject **(C)**], or well-developed [subject **(B)**]. The PLG was present in most subjects **(A–C)**, but was not observed in subject **(D)**. AG, accessory gyrus; ALG, anterior long gyrus; ASG, anterior short gyrus; MSG, middle short gyrus, PLS, posterior long gyrus; PSG, posterior short gyrus.

SANS/SAPS scores in both patient groups). We did not use the durations of illness and medication here, because these variables were unlikely to be related to the insular gross anatomy, a stable brain characteristic. The first-episode and chronic schizophrenia groups were separately treated to explore the role of illness stages. Long gyri were not used in correlation analyses because there were two in most hemispheres (87.2%). The potential effects of insular gyral development on these clinical variables were examined by ANOVA, with the development pattern (developed *vs.* underdeveloped or absent) as a between-subject factor. Clinical variables were log-transformed, except for the total SAPS score in the schizotypal group and the SANS score, due to their non-normal distributions (Kolmogorov–Smirnov tests). *Post hoc* Scheffé's tests were employed. The significance level was defined as $p < 0.05$.

Results

Demographic and clinical characteristics

No significant differences were observed in sex, handedness, or parental education between the groups; however, schizophrenia patients were older than healthy controls (Table 1). The education level was higher in healthy controls than in patient groups. The schizophrenia group was more symptomatic and received more medication than the SPD group (Table 1).

No significant differences were observed in age, handedness, personal or parental education, age at disease onset, illness duration, or medication (dose, type, and duration) between the deficit and non-deficit schizophrenia subgroups (27–29); however, a difference was noted in the sex ratio (Table 2). The deficit subgroup was characterized by a prominent blunted affect with less severe positive symptoms (Table 2).

Gross variations in insular gyri

The degree of gyral development for the AG, MSG, and PLG significantly differed between healthy controls and patient groups (i.e., schizophrenia and SPD groups), but not between patient groups (Table 1 and Figure 2). The AG (left, $\chi^2 = 13.51$, $p < 0.001$; right, $\chi^2 = 8.58$, $p = 0.003$), MSG (left, $\chi^2 = 19.99$, $p < 0.001$; right, $\chi^2 = 19.74$, $p < 0.001$), and PLG (left, $\chi^2 = 4.79$, $p = 0.029$; right, $\chi^2 = 6.88$, $p = 0.009$) were significantly more well-developed bilaterally in schizophrenia patients than in healthy controls. The right AG ($\chi^2 = 12.43$, $p < 0.001$), bilateral MSG (left, Fisher's exact test, $p < 0.001$; right, $\chi^2 = 18.57$, $p < 0.001$), and left PLG (Fisher's exact test, $p = 0.001$) were significantly more well-developed in the SPD group than in healthy controls. Among schizophrenia patients,

10.3389/fpsyt.2022.1050712

TABLE 2 Sample characteristics and gross insular morphology of first-episode (FE) and chronic (C) schizophrenia.

	FE-Sz (N = 71)	C-Sz (N = 58)	Group differences
M/F	40/31	25/33	Chi-square = 2.24, p = 0.094
Age (Years)	24.3 ± 5.5	29.8 ± 6.3	$F(1, 127) = 28.74$, $p < 0.001$
Handedness (Right/left/mixed)	69/0/2	53/1/4	Fisher's exact test, p = 0.304
Height (cm)	164.7 ± 7.8	163.9 ± 7.5	$F(1, 127) = 0.35$, p = 0.554
Education (Years)	13.5 ± 1.9	13.5 ± 2.0	$F(1, 127) = 0.07$, p = 0.785
Parental education (Years)[a]	12.9 ± 2.1	12.5 ± 2.1	$F(1, 123) = 6.77$, p = 0.010
Onset age (years)	23.3 ± 5.3	21.6 ± 5.3	$F(1, 127) = 3.57$, p = 0.061
Duration of illness (years)	0.9 ± 1.0	8.0 ± 3.9	$F(1, 127) = 217.88$, $p < 0.001$
Medication dose (HPD equivalent, mg/day)	10.2 ± 8.5	9.9 ± 8.4	$F(1, 127) = 0.03$, p = 0.867
Duration of medication (years)	0.6 ± 1.0	5.5 ± 4.3	$F(1, 127) = 87.44$, $p < 0.001$
Medication type (atypical/typical/mixed)	50/18/1	26/25/5	Fisher's exact test, p = 0.005
Total SAPS scores[b]	27.3 ± 23.0	33.3 ± 22.2	$F(1, 121) = 2.10$, p = 0.150
Total SANS scores[b]	51.7 ± 24.8	48.9 ± 19.6	$F(1, 121) = 0.46$, p = 0.501
Number of short gyri			$F(1, 125) = 1.67$, p = 0.200
Left	3.43 ± 0.60	3.26 ± 0.76	
Right	3.24 ± 0.62	3.16 ± 0.59	
Number of long gyri			$F(1, 125) = 0.88$, p = 0.350
Left	1.97 ± 0.38	2.03 ± 0.42	
Right	2.01 ± 0.36	2.03 ± 0.37	
AG (Absent/underdeveloped/developed)			
Left	22/15/34	21/12/25	Chi-square = 0.42, p = 0.809
Right	29/19/23	24/16/18	Chi-square = 0.03, p = 0.986
MSG (Absent/underdeveloped/developed)			
Left	1/7/63	6/7/45	Fisher's exact test, p = 0.060
Right	5/10/56	3/6/49	Fisher's exact test, p = 0.736
PLG (Absent/present)			
Left	6/65	4/54	Fisher's exact test, p = 1.000
Right	4/67	5/53	Fisher's exact test, p = 0.730

Values represent means ± SDs unless otherwise stated.
AG, accessory gyrus; ALG, anterior long gyrus; F, female; HPD, haloperidol; M, male; MSG, middle short gyrus; PLG, posterior long gyrus; SANS, scale for the assessment of negative symptoms; SAPS, scale for the assessment of positive symptoms; Sz, schizophrenia.
[a]Data not available for four Sz patients.
[b]Data not available for six Sz patients.

the right MSG was more developed in males than in females (χ^2 = 4.97, p = 0.026), while no other significant effects were noted involving sex and hemisphere for the degree of insular gyral development.

The number of short gyri was higher in the schizophrenia and SPD groups (Scheffé's test, $p < 0.001$) than in healthy controls (Table 1). A significant group-by-sex interaction [$F(2, 262) = 6.36$, p = 0.002] was observed for long gyri, with male schizophrenia (Scheffé's test, p = 0.005) and SPD (Scheffé's test, p = 0.001) patients having a higher number than healthy male controls. These results remained the same even when age and medication (dose/duration) were used as covariates.

No significant differences were noted in the number or development patterns of insular gyri between the first-episode and chronic subgroups (Table 2). Because the results of a largely overlapping (N = 66/71) first-episode schizophrenia cohort have been reported elsewhere (7), we also demonstrate the results excluding the first-episode schizophrenia patients as Supplementary Table 1; the results remained essentially the same as the original results using whole schizophrenia sample (N = 133).

No significant differences were observed in the number of insular gyri between the deficit and non-deficit schizophrenia subgroups, whereas the prevalence of a well-developed right MSG was higher in the deficit subgroup than in the non-deficit subgroup (χ^2 = 4.79, p = 0.029) (Table 3).

Relationships between the insular anatomy and clinical variables

A higher number of left short gyri was associated with a younger onset age (rho = –0.366, p = 0.002) and higher

10.3389/fpsyt.2022.1050712

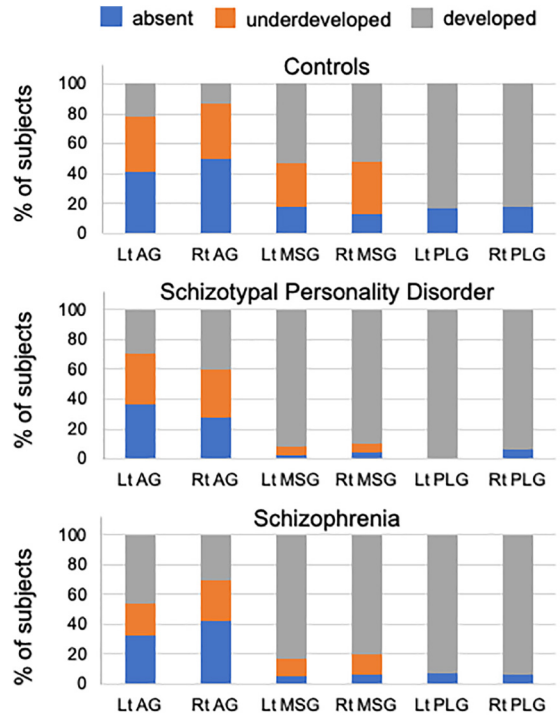

FIGURE 2
Percentage of insular gyral development in healthy controls, schizotypal patients, and schizophrenia patients. AG, accessory gyrus; MSG, middle short gyrus; PLG, posterior long gyrus.

medication dose (*rho* = 0.288, $p = 0.015$) in first-episode schizophrenia patients, but not in chronic schizophrenia patients. The number of right short gyri in SPD patients was also related to a higher SANS score (*rho* = 0.214, $p = 0.013$). Among these results, the relationship with onset age in first-episode schizophrenia patients remained after the Bonferroni correction for multiple comparisons [22 comparisons, $p < 0.0023$ (0.05/22)].

Schizophrenia patients with a left developed AG had a younger onset age than those without in the first-episode subgroup [$F(1, 69) = 9.47$, $p = 0.003$], but not in the chronic subgroup. Similarly, schizophrenia patients with a right developed AG had a higher SAPS score than those without only for the first-episode subgroup [$F(1, 67) = 4.43$, $p = 0.039$]. A developed right AG was also related to a higher SANS score in the SPD group [$F(1, 43) = 4.11$, $p = 0.049$].

Discussion

To the best of our knowledge, this is the first MRI study to demonstrate that patients with established schizophrenia (both first-episode and chronic stages) and SPD had a higher number of short and long insular gyri than healthy controls, potentially representing a common neurodevelopmental pathology within the schizophrenia spectrum. We also showed that a well-developed AG in schizophrenia was associated with an earlier onset and severe positive symptoms in first-episode, but not chronic patients. Furthermore, a well-developed MSG in schizophrenia was related to a subgroup with primary and persistent negative symptoms (i.e., deficit schizophrenia). Therefore, the gross anatomy of the insular cortex appears to contribute to vulnerability to psychosis, clinical features in early illness stages, and the clinical subtype of schizophrenia.

The present results showing an increased number of insular gyri in SPD, similar to schizophrenia, is considered to reflect common insults in the process of fetal insular gyration that predominantly occur between 17 and 35 weeks of gestation (9, 10). Previous MRI studies on shared abnormalities in early neurodevelopmental markers, such as the small adhesio interthalamica (41), an altered surface morphology in the orbitofrontal region (42, 43), and diverse cortical hyper-gyrification (16), support common neurodevelopmental pathologies among schizophrenia spectrum disorders (11, 14). Since aberrant neurodevelopmental processes associated with gyral formation *in uteri* may lead to neural dysconnectivity (17, 18), our results showing gross insular changes and their contribution to negative symptoms in SPD patients are partly consistent with the diffusion tensor imaging findings of schizotypal subjects with altered connectivity involving the insular cortex, which is associated with clinical symptoms and cognitive impairments (44, 45). The insular gray matter volume, which exhibits a progressive decline in the early stages of schizophrenia (20, 21), is preserved in SPD (19, 23); therefore, the results obtained in the present study appear to support the insular morphology in schizophrenia spectrum disorders having multiple pathological processes. Gross anatomical features may represent a vulnerability to psychosis that is attributable to prenatal neurodevelopment, while the gray matter volume more reflects dynamic brain pathologies related to the onset of overt psychosis. Interestingly, clinical high-risk individuals for psychosis (20, 46, 47), but not genetic high-risk subjects (48–50), likely exhibit gray matter reduction of the insular cortex especially for those who later develop psychosis. However, as far as we know, no MRI studies to date have specifically examined the insular gross anatomy in these high-risk groups. Thus, future studies will be warranted to examine whether the insular morphology is associated with vulnerability or genetic liability to psychosis and later psychosis onset.

The present study replicated our previous findings (7) in an expanded schizophrenia sample in which patients had an altered gyral organization with well-developed insular gyri (AG, MSG, and PLG), and also revealed no significant differences in the gross anatomical features of the insular cortex between the first-episode and chronically medicated subgroups. Previous gyrification studies in schizophrenia have demonstrated both hyper- and hypo-gyrification depending on the illness stages and brain regions (18); the patients

10.3389/fpsyt.2022.1050712

TABLE 3 Sample characteristics and gross insular morphology of deficit and non-deficit subtypes of schizophrenia.

	D-Sz (N = 38)	ND-Sz (N = 37)	Group differences
M/F	22/16	12/25	Chi-square = 4.90, p = 0.027
Age (Years)	27.1 ± 6.2	27.1 ± 7.5	$F(1, 73) < 0.01$, p = 0.984
Total BPRS score	36.5 ± 9.5	49.5 ± 12.0	$F(1, 73)$ = 27.45, $p < 0.001$; D-Sz < ND-Sz
PDS score	−1.8 ± 1.4	−10.1 ± 1.8	$F(1, 73)$ = 504.04, $p < 0.001$; ND-Sz < D-Sz
SAPS			Group-by-subscore interaction; $F(3, 219)$ = 12.58, $p < 0.001$
Hallucinations	5.3 ± 7.5	13.5 ± 8.2	*Post hoc* comparison, $p < 0.001$; D-Sz < ND-Sz
Delusions	8.1 ± 8.0	19.0 ± 9.6	*Post hoc* comparison, $p < 0.001$; D-Sz < ND-Sz
Bizarre behavior	4.5 ± 4.0	5.5 ± 4.4	–
Positive formal thought disorder	3.7 ± 5.6	6.8 ± 8.9	–
SANS			Group-by-subscore interaction; $F(4, 292)$ = 5.25, $p < 0.001$
Blunted affect	16.0 ± 8.8	12.7 ± 10.3	*Post hoc* comparison, p = 0.004; ND-Sz < D-Sz
Alogia	8.0 ± 5.6	6.9 ± 4.3	–
Avolition-apathy	10.8 ± 5.0	10.7 ± 4.8	–
Anhedonia-asociality	10.6 ± 5.8	12.8 ± 7.9	–
Attention deficit	7.5 ± 4.7	10.4 ± 4.1	*Post hoc* comparison, p = 0.011; D-Sz < ND-Sz
Number of short gyri			$F(1, 71)$ = 2.31, p = 0.133
Left	3.39 ± 0.68	3.32 ± 0.71	
Right	3.26 ± 0.55	3.16 ± 0.60	
Number of long gyri			$F(1, 71)$ = 1.68, p = 0.200
Left	2.05 ± 0.40	1.95 ± 0.33	
Right	1.97 ± 0.28	2.03 ± 0.29	
AG (absent/underdeveloped/developed)			
Left	12/8/18	10/10/17	Chi-square = 0.42, p = 0.811
Right	18/10/10	14/8/15	Chi-square = 1.71, p = 0.425
MSG (absent/underdeveloped/developed)			
Left	2/3/33	2/5/30	Fisher's exact test, p = 0.799
Right	2/1/35	2/8/27	Fisher's exact test, p = 0.028
PLG (absent/present)			
Left	2/36	3/34	Fisher's exact test, p = 0.674
Right	3/35	1/36	Fisher's exact test, p = 0.615

Values represent means ± SDs unless otherwise stated.
AG, accessory gyrus; ALG, anterior long gyrus; BPRS, Brief Psychiatric Rating Scale; D-Sz, deficit schizophrenia; F, female; M, male; MSG, middle short gyrus; ND-Sz, non-deficit schizophrenia; PDS, Proxy for the Deficit Syndrome; PLG, posterior long gyrus; SANS, scale for the assessment of negative symptoms; SAPS, scale for the assessment of positive symptoms.

likely have hyper-gyrification of diverse cortical regions in early stages (15, 51) but exhibit a progressive decline in brain gyrification predominantly in the fronto-temporal regions during the course of the illness (52). On the other hand, the present results appear to support insular gross anatomical features representing a stable neurodevelopmental marker regardless of illness stages. However, their contribution to clinical characteristics differed with the illness stage, with a developed AG being associated with an early illness onset, which implies prominent early developmental abnormalities (53), and severe positive symptoms specifically in the first-episode subgroup. We also demonstrated that a higher number of left short gyri was associated with a higher medication dose specifically in first-episode schizophrenia patients, supporting that gross anatomical features of the insular cortex may contribute to severe symptomatology that requires higher dose of medication at early illness stages. Interestingly, previous studies on first-episode schizophrenia also supported hyper-gyrification (15) and dysfunctional connectivity (54) in the anterior insular subdivision being associated with the severity of positive symptoms, implicating the contribution of early developmental processes associated with gyral formation in the anterior insula to the later production of psychotic symptoms. On the other hand, the relationships between the insular gross anatomy, a stable brain feature, and clinical features in chronic patients need to be interpreted with caution because the latter

may be affected by a number of factors (e.g., medication and the chronicity of illness). However, it is possible that the insular gross morphology also contributes to the clinical course (e.g., treatment response) and stable clinical characteristics associated with specific subtypes.

Indeed, the present results suggest that the insular gross anatomy is associated with a persistent trait-like clinical feature of schizophrenia. No significant differences were observed in the number of insular gyri between the deficit and non-deficit subtypes of schizophrenia; however, the deficit subgroup was characterized by a more well-developed right MSG than the non-deficit subgroup. While etiological factors related to deficit schizophrenia have yet to be identified, the relationships between deficit schizophrenia and premorbid maladjustment (25, 55), general cognitive impairments (56), and neurological anomalies (27) appear to support pervasive abnormalities in neurodevelopment in this specific subtype (26, 27). The present results are consistent with previous MRI findings showing enhanced interregional cortical coupling, which may reflect reduced network differentiation during early neurodevelopment (39), and alterations in the gross brain morphology (e.g., gyrification patterns) (28, 30) specifically in deficit schizophrenia. Although the exact role of the MSG in the human brain remains unclear, the present result showing its relationship with persistent negative symptoms in schizophrenia supports functional neuroimaging evidence showing the crucial involvement of the regional functional organization within the insular cortex of the short insula (incl. the MSG) in social-emotional networks, particularly on the right hemisphere (1, 3, 57).

There are several potential limitations in this study that need to be addressed. Although the insular cortex has a number of functions in a range of cognitive domains (57) that are impaired in schizophrenia (e.g., emotional, auditory processing, and language-related functions) (58), the present study did not systematically assess cognition in participants. Therefore, it remains unclear whether the insular gross anatomy in schizophrenia spectrum disorders is associated with cognitive impairments. Furthermore, since insular gross anatomical diversity itself is widely observed in healthy subjects, its relationship with brain function warrants further study, for example, using functional/connectivity neuroimaging. Another limitation in the present study is that the deficit and non-deficit schizophrenia subgroups were not matched for sex, potentially reflecting the general tendency that male sex is associated with deficit schizophrenia (59). Since male schizophrenia patients had a higher prevalence of a developed right MSG than female patients, our results on the schizophrenia subtype need to be replicated in a larger and/or more sex-balanced cohort. Moreover, schizophrenia patients were older than healthy controls. However, the present results did not change even when we statistically controlled for the age difference. In addition, because altered brain gyrification is also observed in other neuropsychiatric disorders, such as bipolar disorder [reviewed by Sasabayashi et al. (18)], the disease specificity of our gross insular findings in schizophrenia spectrum disorders needs to be examined in further studies.

In summary, the present MRI study on gross anatomical features in the insular cortex support schizophrenia and SPD patients having similar brain characteristics possibly on the basis of common vulnerability associated with early neurodevelopmental anomalies. In schizophrenia, the insular gross anatomy appears to be associated with symptom severity, particularly in the early illness stages, as well as persistent traits associated with the deficit syndrome. However, the functional significance of this gross anatomical variation needs to be investigated in more detail in patients with neuropsychiatric disorders and healthy controls.

Data availability statement

The raw data supporting the conclusions of this article will be made available by the authors, without undue reservation.

Ethics statement

The studies involving human participants were reviewed and approved by the Committee of Medical Ethics of the University of Toyama. Written informed consent to participate in this study was provided by the participants' legal guardian/next of kin.

Author contributions

MS and TT conceived the idea and methodology of the study. TT conducted the statistical analyses and wrote the manuscript. DS, YT, and HK recruited subjects and were involved in clinical and diagnostic assessments. TT and DS analyzed the MRI data. KN provided technical support for MRI scanning and data processing. AF and YY managed the MRI and clinical data. MS and YT contributed to the writing and editing of the manuscript. All authors contributed to the article and approved the submitted version.

Funding

This work was supported by JSPS KAKENHI (Grant Nos. JP18K07550 to TT, JP18K15509 to DS, and JP20H03598 to MS) and Health and Labour Sciences Research Grants for Comprehensive Research on Persons with Disabilities from the Japan Agency for Medical Research and Development (AMED) (Grant Nos. JP19dk0307029 to MS and JP22dk0307103h0002 to TT).

Conflict of interest

The authors declare that the research was conducted in the absence of any commercial or financial relationships that could be construed as a potential conflict of interest.

Publisher's note

All claims expressed in this article are solely those of the authors and do not necessarily represent those of their affiliated organizations, or those of the publisher, the editors and the reviewers. Any product that may be evaluated in this article, or claim that may be made by its manufacturer, is not guaranteed or endorsed by the publisher.

Supplementary material

The Supplementary Material for this article can be found online at: https://www.frontiersin.org/articles/10.3389/fpsyt.2022.1050712/full#supplementary-material

References

1. Augustine JR. Circuitry and functional aspects of the insular lobe in primates including humans. *Brain Res Brain Res Rev.* (1996) 22:229–44. doi: 10.1016/S0165-0173(96)00011-2

2. Türe U, Yasargil DCH, Al-Mefty O, Yasargil MG. Topographic anatomy of the insular region. *J Neurosurg.* (1999) 90:720–33. doi: 10.3171/jns.1999.90.4.0720

3. Uddin LQ, Nomi JS, Hébert-Seropian B, Ghaziri J, Boucher O. Structure and function of the human insula. *J Clin Neurophysiol.* (2017) 34:300–6. doi: 10.1097/WNP.0000000000000377

4. Cunha-Cabral D, Silva SM, Alves H, Vaz RP, Pereira PA, Andrade JP. Neurosurgical anatomy of the insular cortex. *Clin Neurol Neurosurg.* (2019) 186:105530. doi: 10.1016/j.clineuro.2019.105530

5. Rosen A, Chen DQ, Hayes DJ, Davis KD, Hodaie M. Neuroimaging strategy for the three-dimensional in vivo anatomical visualization and characterization of insular gyri. *Stereotact Funct Neurosurg.* (2015) 93:255–64. doi: 10.1159/000380826

6. Wysiadecki G, Małkiewicz A, Rożniecki J, Polguj M, Haładaj R, żytkowski A, et al. Anatomical variations of the insular gyri: a morphological study and proposal of unified classification. *Clin Anat.* (2018) 31:347–56. doi: 10.1002/ca.23060

7. Takahashi T, Sasabayashi D, Takayanagi Y, Furuichi A, Kobayashi H, Yuasa Y, et al. *Gross Anatomical Variations in the Insular Cortex in First-episode Schizophrenia* (in submission).

8. Armstrong E, Schleicher A, Omran H, Curtis M, Zilles K. The ontogeny of human gyrification. *Cereb Cortex.* (1995) 5:56–63. doi: 10.1093/cercor/5.1.56

9. Afif A, Bouvier R, Buenerd A, Trouillas J, Mertens P. Development of the human fetal insular cortex: study of the gyration from 13 to 28 gestational weeks. *Brain Struct Funct.* (2007) 212:335–46. doi: 10.1007/s00429-007-0161-1

10. Chi JG, Dooling EC, Gilles FH. Gyral development of the human brain. *Ann Neurol.* (1977) 1:86–93. doi: 10.1002/ana.410010109

11. Siever LJ, Davis KL. The pathophysiology of schizophrenia disorders: perspectives from the spectrum. *Am J Psychiatry.* (2004) 161:398–413. doi: 10.1176/appi.ajp.161.3.398

12. American Psychiatric Association [APA]. *Diagnostic and Statistical Manual of Mental Disorders*. 4th ed. Washington DC: American Psychiatric Association Press (1994).

13. World Health Organization [WHO]. *The ICD-10 Classification of Mental and Behavioural Disorders: Diagnostic Criteria for Research*. Geneva: World Health Organization (1993).

14. Siever LJ, Kalus OF, Keefe RSE. The boundaries of schizophrenia. *Psychiatr Clin N Am.* (1993) 16:217–44.

15. Sasabayashi D, Takayanagi Y, Nishiyama S, Takahashi T, Furuichi A, Kido M, et al. Increased frontal gyrification negatively correlates with executive function in patients with first-episode schizophrenia. *Cereb Cortex.* (2017) 27:2686–94. doi: 10.1093/cercor/bhw101

16. Sasabayashi D, Takayanagi Y, Takahashi T, Nemoto K, Furuichi A, Kido M, et al. Increased brain gyrification in the schizophrenia spectrum. *Psychiatry Clin Neurosci.* (2020) 74:70–6.

17. Zilles K, Palomero-Gallagher N, Amunts K. Development of cortical folding during evolution and ontogeny. *Trends Neurosci.* (2013) 36:275–84.

18. Sasabayashi D, Takahashi T, Takayanagi Y, Suzuki M. Anomalous brain gyrification patterns in major psychiatric disorders: a systematic review and transdiagnostic integration. *Transl Psychiatry.* (2021) 11:176. doi: 10.1038/s41398-021-01297-8

19. Takahashi T, Suzuki M, Zhou SY, Hagino H, Tanino R, Kawasaki Y, et al. Volumetric MRI study of the short and long insular cortices in schizophrenia spectrum disorders. *Psychiatry Res.* (2005) 138:209–20. doi: 10.1016/j.pscychresns.2005.02.004

20. Takahashi T, Wood SJ, Yung AR, Phillips LJ, Soulsby B, McGorry PD, et al. Insular cortex gray matter changes in individuals at ultra-high-risk of developing psychosis. *Schizophr Res.* (2009) 111:94–102. doi: 10.1016/j.schres.2009.03.024

21. Takahashi T, Wood SJ, Soulsby B, McGorry PD, Tanino R, Suzuki M, et al. Follow-up MRI study of the insular cortex in first-episode psychosis and chronic schizophrenia. *Schizophr Res.* (2009) 108:49–56. doi: 10.1016/j.schres.2008.12.029

22. Takahashi T, Wood SJ, Soulsby B, Tanino R, Wong MT, McGorry PD. Diagnostic specificity of the insular cortex abnormalities in first-episode psychotic disorders. *Prog Neuropsychopharmacol Biol Psychiatry.* (2009) 33:651–7. doi: 10.1016/j.pnpbp.2009.03.005

23. Takahashi T, Kido M, Sasabayashi D, Nakamura M, Furuichi A, Takayanagi Y, et al. Gray matter changes in the insular cortex during the course of the schizophrenia spectrum. *Front Psychiatry.* (2020) 11:659. doi: 10.3389/fpsyt.2020.00659

24. Carpenter WT Jr., Heinrichs DW, Wagman AM. Deficit and nondeficit forms of schizophrenia: the concept. *Am J Psychiatry.* (1988) 145:578–83. doi: 10.1176/ajp.145.5.578

25. Kirkpatrick B, Galderisi S. Deficit schizophrenia: an update. *World Psychiatry.* (2008) 7:143–7. doi: 10.1002/j.2051-5545.2008.tb00181.x

26. Galderisi S, Maj M, Mucci A, Cassano GB, Invernizzi G, Rossi A, et al. Historical, psychopathological, neurological, and neuropsychological aspects of deficit schizophrenia: a multicenter study. *Am J Psychiatry.* (2002) 159:983–90. doi: 10.1176/appi.ajp.159.6.983

27. Peralta V, Moreno-Izco L, Sanchez-Torres A, García de Jalón E, Campos MS, Cuesta MJ. Characterization of the deficit syndrome in drug-naive schizophrenia patients: the role of spontaneous movement disorders and neurological soft signs. *Schizophr Bull.* (2014) 40:214–24. doi: 10.1093/schbul/sbs152

28. Takahashi T, Takayanagi Y, Nishikawa Y, Nakamura M, Komori Y, Furuichi A, et al. Brain neurodevelopmental markers related to the deficit subtype of schizophrenia. *Psychiatry Res Neuroimaging.* (2017) 266:10–8. doi: 10.1016/j.pscychresns.2017.05.007

29. Takahashi T, Sasabayashi D, Takayanagi Y, Furuichi A, Kobayashi H, Noguchi K, et al. Different Heschl's gyrus Duplication patterns in deficit and non-deficit subtypes of schizophrenia. *Front Psychiatry.* (2022) 13:867461. doi: 10.3389/fpsyt.2022.867461

30. Suzuki M, Zhou SY, Takahashi T, Hagino H, Kawasaki Y, Niu L, et al. Differential contributions of prefrontal and temporolimbic pathology to mechanisms of psychosis. *Brain.* (2005) 128:2109–22. doi: 10.1093/brain/awh554

31. Takayanagi Y, Sasabayashi D, Takahashi T, Furuichi A, Kido M, Nishikawa Y, et al. Reduced cortical thickness in schizophrenia and schizotypal disorder. *Schizophr Bull.* (2020) 46:387–94. doi: 10.1093/schbul/sbz051

32. Andreasen NC, Flaum M, Arndt S. The comprehensive assessment of symptoms and history (CASH): an instrument for assessing diagnosis and psychopathology. *Arch Gen Psychiatry*. (1992) 49:615–23. doi: 10.1001/archpsyc.1992.01820080023004

33. Andreasen NC. *Scale for the Assessment of Negative Symptoms/Scale for the Assessment of Positive Symptoms*. Iowa City: The University of Iowa (1984).

34. Rhoades HM, Overall JE. The semistructured BPRS interview and rating guide. *Psychopharmacol Bull.* (1988) 24:101–4.

35. Hirayasu Y, McCarley RW, Salisbury DF, Tanaka S, Kwon JS, Frumin M, et al. Planum temporale and Heschl gyrus volume reduction in schizophrenia: a magnetic resonance imaging study of first-episode patients. *Arch Gen Psychiatry*. (2000) 57:692–9. doi: 10.1001/archpsyc.57.7.692

36. Schooler N, Rabinowitz J, Davidson M, Emsley R, Harvey PD, Kopala L, et al. Risperidone and haloperidol in first-episode psychosis: a long-term randomized trial. *Am J Psychiatry*. (2005) 162:947–53. doi: 10.1176/appi.ajp.162.5.947

37. Takayanagi Y, Sasabayashi D, Takahashi T, Komori Y, Furuichi A, Kido M, et al. Altered brain gyrification in deficit and non-deficit schizophrenia. *Psychol Med*. (2019) 49:573–80. doi: 10.1017/S0033291718001228

38. Kirkpatrick B, Buchanan RW, Breier A, Carpenter WT Jr. Case identification and stability of the deficit syndrome of schizophrenia. *Psychiatry Res.* (1993) 47:47–56. doi: 10.1016/0165-1781(93)90054-k

39. Wheeler AL, Wessa M, Szeszko PR, Foussias G, Chakravarty MM, Lerch JP, et al. Further neuroimaging evidence for the deficit subtype of schizophrenia: a cortical connectomics analysis. *JAMA Psychiatry*. (2015) 72:446–55. doi: 10.1001/jamapsychiatry.2014.3020

40. Takahashi T, Suzuki M, Tsunoda M, Kawamura Y, Takahashi N, Maeno N, et al. The association of genotypic combination of the DRD3 and BDNF polymorphisms on the adhesio interthalamica and medial temporal lobe structures. *Prog Neuropsychopharmacol Biol Psychiatry*. (2008) 32:1236–42. doi: 10.1016/j.pnpbp.2008.03.014

41. Takahashi T, Suzuki M, Zhou SY, Nakamura K, Tanino R, Kawasaki Y, et al. Prevalence and length of the adhesio interthalamica in schizophrenia spectrum disorders. *Psychiatry Res.* (2008) 164:90–4. doi: 10.1016/j.pscychresns.2008.03.001

42. Nishikawa Y, Takahashi T, Takayanagi Y, Furuichi A, Kido M, Nakamura M. Orbitofrontal sulcogyral pattern and olfactory sulcus depth in the schizophrenia spectrum. *Eur Arch Psychiatry Clin Neurosci.* (2016) 266:15–23. doi: 10.1007/s00406-015-0587-z

43. Takahashi T, Nakamura M, Nishikawa Y, Takayanagi Y, Furuichi A, Kido M, et al. Decreased number of orbital sulci in schizophrenia spectrum disorders. *Psychiatry Res Neuroimaging.* (2016) 250:29–32. doi: 10.1016/j.pscychresns.2016.03.005

44. Gurrera RJ, Nakamura M, Kubicki M, Dickey CC, Niznikiewicz MA, Voglmaier MM, et al. The uncinate fasciculus and extraversion in schizotypal personality disorder: a diffusion tensor imaging study. *Schizophr Res.* (2007) 90:360–2. doi: 10.1016/j.schres.2006.10.003

45. Nakamura M, McCarley RW, Kubicki M, Dickey CC, Niznikiewicz MA, Voglmaier MM, et al. Fronto-temporal disconnectivity in schizotypal personality disorder: a diffusion tensor imaging study. *Biol Psychiatry*. (2005) 58:468–78. doi: 10.1016/j.biopsych.2005.04.016

46. Fusar-Poli P, Radua J, McGuire P, Borgwardt S. Neuroanatomical maps of psychosis onset: voxel-wise meta-analysis of antipsychotic-naive VBM studies. *Schizophr Bull.* (2012) 38:1297–307. doi: 10.1093/schbul/sbr134

47. Smieskova R, Fusar-Poli P, Allen P, Bendfeldt K, Stieglitz RD, Drewe J, et al. Neuroimaging predictors of transition to psychosis–a systematic review and meta-analysis. *Neurosci Biobehav Rev*. (2010) 34:1207–22. doi: 10.1016/j.neubiorev.2010.01.016

48. Fusar-Poli P, Smieskova R, Serafini G, Politi P, Borgwardt S. Neuroanatomical markers of genetic liability to psychosis and first episode psychosis: a voxelwise meta-analytical comparison. *World J Biol Psychiatry*. (2014) 15:219–28. doi: 10.3109/15622975.2011.630408

49. Lin B, Li XB, Ruan S, Wu YX, Zhang CY, Wang CY, et al. Convergent and divergent gray matter volume abnormalities in unaffected first-degree relatives and ultra-high risk individuals of schizophrenia. *Schizophrenia*. (2022) 8:55. doi: 10.1038/s41537-022-00261-9

50. Smieskova R, Marmy J, Schmidt A, Bendfeldt K, Riecher-Rössler A, Walter M. Do subjects at clinical high risk for psychosis differ from those with a genetic high risk?–A systematic review of structural and functional brain abnormalities. *Curr Med Chem*. (2013) 20:467–81. doi: 10.2174/09298673113200030018

51. Sasabayashi D, Takayanagi Y, Takahashi T, Koike S, Yamasue H, Katagiri N, et al. Increased occipital gyrification and development of psychotic disorders in individuals with an at-risk mental state: a multicenter study. *Biol Psychiatry*. (2017) 82:737–45. doi: 10.1016/j.biopsych.2017.05.018

52. Pham TV, Sasabayashi D, Takahashi T, Takayanagi Y, Kubota M, Furuichi A, et al. Longitudinal changes in brain gyrification in schizophrenia spectrum disorders. *Front Aging Neurosci.* (2021) 13:752575. doi: 10.3389/fnagi.2021.752575

53. Chen BY, Tsai IN, Lin JJ, Lu MK, Tan HP, Jang FL, et al. Risk model assessment in early-onset and adult-onset schizophrenia using neurological soft signs. *J Clin Med.* (2019) 8:1443. doi: 10.3390/jcm8091443

54. Schmidt A, Palaniyappan L, Smieskova R, Simon A, Riecher-Rössler A, Lang UE, et al. Dysfunctional insular connectivity during reward prediction in patients with first-episode psychosis. *J Psychiatry Neurosci.* (2016) 41:367–76. doi: 10.1503/jpn.150234

55. Bucci P, Mucci A, Piegari G, Nobile M, Pini S, Rossi A, et al. Characterization of premorbid functioning during childhood in patients with deficit vs. non-deficit schizophrenia and in their healthy sibling. *Schizophr Res.* (2016) 174:172–6. doi: 10.1016/j.schres.2016.01.032

56. Mucci A, Merlotti E, Üçok A, Aleman A, Galderisi S. Primary and persistent negative symptoms: concepts, assessments and neurobiological bases. *Schizophr Res.* (2007) 186:19–28. doi: 10.1016/j.schres.2016.05.014

57. Nieuwenhuys R. The insular cortex: a review. *Prog Brain Res.* (2012) 195:123–63. doi: 10.1016/B978-0-444-53860-4.00007-6

58. Jauhar S, Johnstone M, McKenna PJ. Schizophrenia. *Lancet.* (2022) 399:473–86. doi: 10.1016/S0140-6736(21)01730-X

59. Roy MA, Maziade M, Labbé A, Mérette C. Male gender is associated with deficit schizophrenia: a meta-analysis. *Schizophr Res.* (2001) 47:141–7. doi: 10.1016/s0920-9964(99)00231-5

frontiers | Frontiers in Psychiatry

TYPE Original Research
PUBLISHED 19 January 2023
DOI 10.3389/fpsyt.2022.1086038

OPEN ACCESS

EDITED BY
Nuno Madeira,
University of Coimbra, Portugal

REVIEWED BY
Sandra Vieira,
Institute of Psychiatry, Psychology and Neuroscience, King's College London, United Kingdom
Marco Simoes,
University of Coimbra, Portugal
João Valente Duarte,
University of Coimbra, Portugal

*CORRESPONDENCE
Diana Prata
✉ diana.prata@kcl.ac.uk

SPECIALTY SECTION
This article was submitted to Neuroimaging, a section of the journal Frontiers in Psychiatry

RECEIVED 31 October 2022
ACCEPTED 29 December 2022
PUBLISHED 19 January 2023

CITATION
Tavares V, Vassos E, Marquand A, Stone J, Valli I, Barker GJ, Ferreira H and Prata D (2023) Prediction of transition to psychosis from an at-risk mental state using structural neuroimaging, genetic, and environmental data.
Front. Psychiatry 13:1086038.
doi: 10.3389/fpsyt.2022.1086038

Prediction of transition to psychosis from an at-risk mental state using structural neuroimaging, genetic, and environmental data

Vânia Tavares[1,2], Evangelos Vassos[3,4], Andre Marquand[5,6], James Stone[7], Isabel Valli[8,9], Gareth J. Barker[10], Hugo Ferreira[1] and Diana Prata[1,11]*

[1]Instituto de Biofísica e Engenharia Biomédica, Faculdade de Ciências, Universidade de Lisboa, Lisbon, Portugal, [2]Faculdade de Medicina, Universidade de Lisboa, Lisbon, Portugal, [3]Social, Genetic and Developmental Psychiatry Centre, Institute of Psychiatry, Psychology and Neuroscience, King's College London, London, United Kingdom, [4]National Institute for Health Research Maudsley Biomedical Research Centre, South London and Maudsley National Health System Trust, London, United Kingdom, [5]Donders Centre for Cognitive Neuroimaging, Donders Institute for Brain, Cognition and Behaviour, Radboud University, Nijmegen, Netherlands, [6]Department of Cognitive Neuroscience, Radboud University Medical Centre, Nijmegen, Netherlands, [7]Brighton and Sussex Medical School, University of Sussex, Brighton, United Kingdom, [8]Department of Psychosis Studies, Institute of Psychiatry, Psychology and Neuroscience, King's College London, London, United Kingdom, [9]Institut d'Investigacions Biomèdiques August Pi i Sunyer, University of Barcelona, Barcelona, Spain, [10]Department of Neuroimaging, Institute of Psychiatry, Psychology and Neuroscience, King's College London, London, United Kingdom, [11]Department of Old Age Psychiatry, Institute of Psychiatry, Psychology and Neuroscience, King's College London, London, United Kingdom

Introduction: Psychosis is usually preceded by a prodromal phase in which patients are clinically identified as being at in an "At Risk Mental State" (ARMS). A few studies have demonstrated the feasibility of predicting psychosis transition from an ARMS using structural magnetic resonance imaging (sMRI) data and machine learning (ML) methods. However, the reliability of these findings is unclear due to possible sampling bias. Moreover, the value of genetic and environmental data in predicting transition to psychosis from an ARMS is yet to be explored.

Methods: In this study we aimed to predict transition to psychosis from an ARMS using a combination of ML, sMRI, genome-wide genotypes, and environmental risk factors as predictors, in a sample drawn from a pool of 246 ARMS subjects (60 of whom later transitioned to psychosis). First, the modality-specific values in predicting transition to psychosis were evaluated using several: (a) feature types; (b) feature manipulation strategies; (c) ML algorithms; (d) cross-validation strategies, as well as sample balancing and bootstrapping. Subsequently, the modalities whose at least 60% of the classification models showed an balanced accuracy (BAC) statistically better than chance level were included in a multimodal classification model.

Results and discussion: Results showed that none of the modalities alone, i.e., neuroimaging, genetic or environmental data, could predict psychosis from an ARMS statistically better than chance and, as such, no multimodal classification model was trained/tested. These results suggest that the value of structural MRI data and genome-wide genotypes in predicting psychosis from an ARMS, which has been fostered by previous evidence, should be reconsidered.

KEYWORDS

machine learning, biomarker, schizophrenia, ARMS, prognosis

1. Introduction

Psychosis is a severe condition usually within the context of a mental disorder such as a schizophrenia, some neurological disorders (e.g., Alzheimer's disease) or other medical conditions (e.g., induced by drugs or illicit substances), characterized by a disconnection from reality (1). The onset of psychosis, when in the context of a mental disorder, is typically preceded by a prodromal phase that lasts months to years (2); and usually starts early during adolescence and precedes the onset of psychotic symptoms by 10 or more years (3). In this prodromal phase, subtle and subjectively experienced disturbances in mental processes emerge (basic symptoms). These are the first manifestations of the neurobiological processes underlying psychosis and are mainly distinguished from other symptoms (i.e., positive or negative symptoms) by their self-experience nature (4). As the course of the psychotic illness evolves, increasingly disabling behavioral symptoms start to emerge, generally called negative symptoms, in particular a reduction of motivation and/or expressiveness (5). Additionally, cognitive deficits in attention, memory, reasoning, lack of concentration and executive functioning appear (6). Lastly, positive symptoms emerge, such as hallucinations, delusions, disorganized speech, and behavior (1).

A patient may be clinically identified as being at a late prodromal phase of psychosis or having an "At Risk Mental State" (hereinafter: ARMS) if they present a functional decline in association with one or more of the following commonly used criteria (2, 7): (1) attenuated psychotic symptoms (APS), such as delusions, hallucinations, or disorganized speech with a frequency of at least once per week in the past month; (2) a brief limited intermittent psychotic (BLIP) episode lasting less than 1 week which resolves without antipsychotic medication; or (3) a genetic liability to psychosis or schizotypal traits, i.e., having either a first-degree relative with psychosis or a schizotypal personality disorder.

Transition to psychosis from an ARMS may be evaluated based on the severity, frequency, and total duration of the psychotic symptoms, i.e., when the subject experiences a first episode of psychosis (FEP). Subjects with an ARMS and seeking help have a transition rate to psychosis of about 9% in the first 6 months and 25% in the first 3 years (8) and, in particular, an increased risk of transition to schizophrenia of 15.7% within an average period of 2.35 years, as shown by a meta-analysis (9). Thus, most of the people with an ARMS who later develop a psychotic illness will be diagnosed with schizophrenia. Furthermore, since about 70% of subjects diagnosed with an ARMS never develop a full-blown psychotic illness (9), these people may benefit from a less intensive treatment to ameliorate symptoms or need no treatment at all. Such increase in treatment cost-effectiveness would represent a substantial decrease in healthcare costs, and treatment burden to patients, including pharmacological side effects. However, there is no method for distinguishing between individuals with an ARMS who will subsequently develop a psychotic illness from those who will not (i.e., before a FEP onset).

Given the above need, an effective, precise, and quantitative tool for the prediction of transition to psychosis from an ARMS has been sought by several studies employing machine learning (ML) methods and structural magnetic resonance imaging (sMRI). Indeed, several studies have consistently showed prediction of transition to psychosis from as ARMS with accuracies ranging between 74 and 84% (10–15). Transition to psychosis from an ARMS using only sMRI and ML was first predicted using whole-brain gray matter volume metrics with an accuracy of 82% [(15 ARMS who transitioned to psychosis (ARMS-T) and 18 who did not (ARMS-NT)] (10). This finding was later replicated: (a) in an independent sample by the same group [balanced accuracy (BAC) = 84%, 16 ARMS-T and 21 ARMS-NT] (11); (b) combining both these samples (BAC = 80%, 33 ARMS-T and 33 AMRS-NT) (12); (c) using also one of the above samples for graph-extracted network metrics from cortical gyrification (BAC = 81%, 16 ARMS-T and 63 ARMS-NT) (15), and regional gray matter metrics (BAC = 74%, 16 ARMS-T and 19 ARMS-NT) (14); and (d) using regional gray matter metrics in an independent sample (BAC = 77%, 17 ARMS-T and 17 ARMS-NT; specificity of a replication sample of individuals with an ARMS who did not develop psychosis = 68%, 40 ARMS-NT) (13). To date, only two, relatively small, ARMS samples have been used for sMRI and ML analysis: FETZ (10, 12, 15) and FePsy (11, 12, 14). Thus, the robustness and generalizability of the above findings are still unclear due to possible specific sample characteristics, i.e., small sample sizes (from 33 individuals to at most 79 individuals with ARMS), with several studies stemming from a single site (10, 11, 13–15) or a combination of previously studied sites (12), which makes them not actual replications, with one exception (13).

Interestingly, to the best of our knowledge, genetic data has been explored for the prediction of the transition to psychosis from an ARMS only once (16). In this study, a schizophrenia polygenic risk score (PRS) was able to predict transition to psychosis in individuals with an European [area under the curve (AUC) = 0.65; 32 ARMS-T and 92 ARMS-NT] and with a Non-European (AUC = 0.59; 48 ARMS-T and 156 ARMS-NT) ancestry, respectively. This is despite there being several classification studies showing that genetic markers can predict schizophrenia (17–22), FEP (23) or ARMS (23), both of individual polymorphisms (18, 19, 21, 23) or, composite polygenic scores (20–22), and gene expression profiles (24). From an environmental exposure perspective, and to the best of our knowledge, environmental data have never been explored for predicting individual transition to psychosis from an ARMS.

The combination of neuroimaging measures and genetics or environmental measures, using ML, has, to the best of our knowledge, been explored once to predict ARMS prognosis (i.e., transition to psychosis from an ARMS) in a study running in parallel to ours (25). Therein, a large sample from the PRONIA project (26 ARMS-T and 308 ARMS-NT from 7 sites) was used to build a sequential stacked multimodal model using clinical-neurocognitive (including environmental data), genetic (in the form of a PRS for schizophrenia) and neuroimaging (in the form of voxel-based gray matter volume maps) data and - unlike the present study–human prognostic ratings, showing a final balanced accuracy in predicting transition to psychosis of 86%.

In the present longitudinal prognostic biomarker study, we aimed to explore the use of ML models trained with sMRI, genetic, and environmental baseline data to predict the individual-level transition to psychosis from an ARMS within a 2-year follow up. While providing such preliminary (given the unprecedented data combinations/features and a limited sample size) evidence at the multimodal level, we took the opportunity to attempt to replicate previous promising sMRI-ML findings of studies using similar or smaller sample size (10–15). Methods-wise, we used naturalistically diverse samples but balanced them for demographic (age and sex) and imaging (scan acquisition sMRI protocol) variables. We set out to train and test modality-specific models first and then, provided

TABLE 1 Socio-demographic and clinical information of the At Risk Mental State (ARMS) sample with structural MRI data.

	Protocol 1		Protocol 2		Protocol 3		Group comparison
	ARMS-T (n = 14)	ARMS-NT (n = 19)	ARMS-T (n = 3)	ARMS-NT (n = 16)	ARMS-T (n = 6)	ARMS-NT (n = 41)	
Age at baseline (years)	23.2 ± 3.4 [15.6 26.9]	24.5 ± 4.8 [19.2 34.5]	26.2 ± 7.0 [20.1 33.8]	24.5 ± 5.2 [17.8 35.3]	23.4 ± 4.5 [17.5 29.2]	21.8 ± 4.3 [17.1 33.1]	Protocol: p = 0.271 Transition: p = 0.592 Protocol × Transition: p = 0.447
Age at follow-up or transition (years)	25.6 ± 4.2 [17.3 33.4]	32.7 ± 5.2 [22.6 43.9]	29.2 ± 5.4 [20.2 38.8]	28.8 ± 5.6 [22.9 43.1]	25.2 ± 4.8 [18.3 31.0]	25.6 ± 4.8 [20.3 41.2]	Protocol: p = 0.027* Transition: p = 0.099 Protocol × Transition: p = 0.025*
Age at scan (years)	23.0 ± 3.6 [17.5 27.8]	23.9 ± 4.8 [18.5 34.8]	27.0 ± 8.2 [20.2 36.1]	25.1 ± 5.4 [18.6 37.4]	24.1 ± 4.8 [18.3 30.8]	22.4 ± 4.6 [17.7 38.3]	Protocol: p = 0.261 Transition: p = 0.499 Protocol × Transition: p = 0.541
Interval between baseline and scan age (years)	−0.2 ± 1.4 [−2.3 1.9]	−0.5 ± 1.1 [−2.3 2.1]	0.9 ± 1.3 [0.1 2.4]	0.5 ± 0.5 [0.1 2.1]	0.6 ± 0.5 [0.2 1.6]	0.6 ± 1.0 [0.0 5.1]	Protocol: $p < 0.001$*** Transition: p = 0.419 Protocol × Transition: p = 0.795
Sex (male/female)	11/3	9/10	2/1	14/2	3/3	19/22	Protocol × Transition: Protocol 1: p = 0.070 Protocol 2: p = 0.422 Protocol 3: p = 1
Handedness[a] (right/left/ambidextrous)	12/0/1	16/0/0	3/0/0	13/1/0	4/0/0	36/4/0	Protocol × Transition: Protocol 1: p = 0.448 Protocol 2: p = 1 Protocol 3: p = 1
Self-reported ethnicity (White/Black/Asian/other)	7/5/1/1	11/5/1/2	2/1/0/0	13/1/1/1	4/1/1/0	19/19/1/2	Protocol × Transition: Protocol 1: p = 0.933 Protocol 2: p = 0.530 Protocol 3: p = 0.212
Years of education	13.4 ± 2.1 [10 18]	13.1 ± 1.9 [10 17]	11.7 ± 2.3 [9 13]	14.1 ± 2.6 [11 20]	15.2 ± 2.5 [11 18]	13.0 ± 2.2 [9 20]	Protocol: p = 0.298 Transition: p = 0.966 Protocol × Transition: p = 0.024*
IQ (z-standardized)[b]	−1.1 ± 1.1 [−2.1 1.0]	0.0 ± 1.1 [−2.1 1.8]	0.1 ± 0.1 [0.0 0.2]	0.5 ± 0.9 [−1.3 1.6]	−0.1 ± 1.3 [−2.1 1.6]	0.1 ± 1.1 [−2.1 3.5]	Protocol: p = 0.427 Transition: p = 0.252 Protocol × Transition: p = 0.923
GAF at baseline	52.9 ± 16.0 [35 90]	57.8 ± 11.4 [35 75]	58.7 ± 3.2 [55 61]	58.6 ± 9.9 [41 75]	50.3 ± 11.4 [35 65]	53.6 ± 14.8 [0 75]	Protocol: p = 0.402 Transition: p = 0.475 Protocol × Transition: p = 0.877
GAF at follow-up[c]	49.3 ± 18.6 [10 69]	58.5 ± 17.9 [20 94]	27.3 ± 6.8 [22 35]	62.3 ± 13.5 [46 93]	52.5 ± 20.0 [30 78]	66.2 ± 13.6 [33 87]	Protocol: p = 0.064 Transition: $p < 0.001$*** Protocol × Transition: p = 0.095
CAARMS at baseline[d]	33.2 ± 13.0 [9 56]	28.4 ± 15.3 [8 58]	29.3 ± 21.9 [12 54]	23.2 ± 14.3 [0 51]	39.7 ± 24.1 [0 69]	28.5 ± 16.7 [0 81]	Protocol: p = 0.505 Transition: p = 0.153 Protocol × Transition: p = 0.824
CAARMS at follow-up[e]	19.6 ± 23.0 [0 63]	11.6 ± 10.9 [0 31]	42.0 ± 43.3 [6 90]	14.7 ± 18.4 [0 54]	42.7 ± 42.1 [0 102]	15.5 ± 17.2 [0 60]	Protocol: p = 0.082 Transition: p = 0.001*** Protocol × Transition: p = 0.262

Data format: mean ± standard deviation [min max]. Information not available for [a]1 ARMS-T and 3 ARMS-NT (Protocol 1), 2 ARMS-NT (Protocol 2), 2 ARMS-T and 1 ARMS-NT (Protocol 3); [b]1 ARMS-T and 1 ARMS-NT (Protocol 2), 1 ARMS-NT (Protocol 3); [c]2 ARMS and 5 ARMS-NT (Protocol 1), 4 ARMS-NT (Protocol 2), 8 ARMS-NT (Protocol 3); [d]2 ARMS-T and 7 ARMS-NT (Protocol 1), 3 ARMS-NT (Protocol 2), 2 ARMS-NT (Protocol 3); [e]3 ARMS-T and 6 ARMS-NT (Protocol 1), 3 ARMS-NT (Protocol 2), 8 ARMS-NT (Protocol 3). ARMS, at-risk mental state; ARMS-T, individuals at ARMS that did not transition to psychosis; ARMS-NT, individual [illegible] it did not transitioned to psychosis. *$p < 0.05$; ***$p < 0.001$.

10.3389/fpsyt.2022.1086038

these performed above chance-level, a multimodal one. For the sMRI data, we used state-of-the-art preprocessing and ML pipelines; and explored several unprecedented combinations of brain structural measures, feature manipulation and cross-validation (CV) strategies. For the genetic data, we explored several approaches: a schizophrenia PRS (26), individual GWA-implicated SNPs (27), and a brain-specific expression Quantitative Trait Loci (eQTL) score. For the environmental data, we employed a schizophrenia environmental risk score (ERS) (28), and individual risk factors.

2. Materials and methods

2.1. Sample description

The total sample consisted of 246 individuals with an ARMS, recruited at first presentation from consecutive referrals to the Outreach and Support in South London (OASIS) high-risk service, South London and Maudsley NHS Foundation Trust (29). The presence of ARMS was assessed using the CAARMS, a detailed clinical assessment (30). When the subjects were first diagnosed as having an ARMS (i.e., baseline) a set of data were acquired: (a) a sMRI scan; (b) genome-wide genotypes; and (c) assessment of environmental risk exposures. Subjects were labeled as transitioned to psychosis (ARMS-T) if they later presented a FEP or as not-transitioned to psychosis (ARMS-NT) if they did not present a FEP within a period of at least 2 years. For a detailed description of the recruitment, inclusion and exclusion criteria please refer to the **Supplementary material**. Additional socio-demographic and clinical measures were also assessed at baseline, including: age; sex; handedness; self-reported ethnicity; full scale intelligence quotient measured by the National Adult Reading Test (31); years of education; and global assessment of function using the GAF instrument tool at baseline and at follow-up (32), and CAARMS (at baseline and follow-up) (30). Regarding the sMRI, genetic and environmental sub-samples: 99, 135 and all the 246 individuals with an ARMS had a baseline sMRI scan (**Table 1**), genome-wide genotyped data (**Table 2**), and environmental risk factors assessment data (**Table 3**), respectively (more details in the **Supplementary material**). Over the 2-years follow-up period, 23, 41, and 60 individuals at an ARMS from each of the previous sub-samples developed psychosis (AMRS-T) and the remaining 15, 94, and 186 did not (ARMS-NT), respectively. Moreover, part of the study's data collection occurred under the Genetic and Psychosis (GAP) umbrella project (33). Ethics approval was obtained by the NHS South East London Research Ethics Committee (Project GAP; Ref. 047/04), consistent with the Helsinki Declaration of 1975 (as revised in 2008) and all subjects gave written informed consent.

TABLE 2 Socio-demographic and clinical information of the At Risk Mental State (ARMS) sample with genetic data and an European ancestry.

	ARMS-T (n = 21)	ARMS-NT (n = 54)	Group comparison
Age at baseline (years)	23.8 ± 5.3 [15.6 33.8]	22.5 ± 4.0 [14.6 34.5]	p = 0.284
Age at follow-up or transition (years)	25.3 ± 5.9 [17.3 38.8]	27.9 ± 5.1 [18.5 43.9]	p = 0.069
Sex (male/female)	14/7	30/24	p = 0.380
Years of education	13.0 ± 2.2 [10.0 18.0]	12.0 ± 4.4 [0 18.0]	p = 0.292
IQ (z-standardized)[a]	0.1 ± 1.0 [−2.1 2.2]	0.2 ± 1.0 [−2.1 1.8]	p = 0.678
GAF at baseline	54.0 ± 15.7 [0 80]	53.6 ± 16.0 [0 78]	p = 0.923
GAF at follow-up[b]	47.8 ± 24.3 [0 79]	59.2 ± 21.0 [0 94]	p = 0.050
CAARMS at baseline[c]	37.6 ± 17.5 [6 69]	29.9 ± 16.2 [0 81]	p = 0.097
CAARMS at follow-up[d]	24.4 ± 27.9 [0 90]	12.4 ± 14.0 [0 60]	p = 0.019*

Data format: mean ± standard deviation [min max]. Information not available for [a]2 ARMS-T and 9 ARMS-NT; [b]4 ARMS-NT; [c]1 ARMS and 9 ARMS-NT; [d]1 ARMS-T and 3 ARMS-NT. ARMS, at-risk mental state; ARMS-T, individuals at ARMS that did not transition to psychosis; ARMS-NT, individuals at ARMS that did not transitioned to psychosis.
*$p < 0.05$.

Socio-demographic and clinical variables were analyzed using a two-tailed independent t-test or a Univariate Analysis of Variance (ANOVA) for continuous data and a chi-square test or Fisher's exact test (if there were less than 5 subjects in one group) for ordinal data (**Tables 1–3**). These statistical analyses were performed using the Statistical Package for the Social Sciences 26 (SPSS 26 for Windows, Chicago, IL, USA).

2.2. Structural neuroimaging data

2.2.1. Structural magnetic resonance imaging acquisition

Structural magnetic resonance imaging (sMRI) scans were acquired with one of two scanners (one with a field strength of 1.5T, the other 3T) using one of three 3-Dimensional enhanced fast gradient echo protocols (detailed description in **Supplementary material**).

2.2.2. Image processing

High spatial resolution volumetric T1-weighted images were processed with the Computational Anatomy Toolbox for Statistical Parametric Mapping (SPM) –12 (CAT12; v1092[1]), an SPM12 add-on (v6909[2]) using default settings and MATLAB (9.3) as we have described elsewhere (34) (detailed description in **Supplementary material**). In summary, gray and white matter volumes for 64 regions-of-interest (ROIs; description of each ROI is in the **Supplementary Table 1**) were extracted using the Hammers atlas (35). Additionally, regional-based cortical thickness and surface measures (i.e., folding measures)–gyrification index, the depth of sulci and the measurement of local surface complexity were extracted for 68 ROIs (description of each ROI is in the **Supplementary Table 2**) defined by the Desikan–Killiany atlas (36).

2.2.3. Image quality control

The quality of each processed image was empirically assessed using the quality assurance framework of CAT12 (detailed description in the **Supplementary material**). We set the subject's image inclusion threshold at D (sufficient), i.e., only subjects whose

1 http://www.neuro.uni-jena.de/cat/

2 http://www.fil.ion.ucl.ac.uk/spm/

images had an image quality rate of A (excellent) to D (sufficient) (in a scale that goes up to F–unacceptable/failed) were included in the final sample, as it has been shown that typical scientific (clinical) data get good-to-satisfactory ratings (37). All this study's images passed the above criteria and thus were included in all analyses (see **Supplementary material** for more details).

2.3. Genetic data

Genotyping procedures have been previously described (26, 38). In summary, samples were genotyped at two different sites with two distinct chips (Illumina HumanCore Exome BeadChip and Genome-wide Human SNP Array 6.0). A standard quality control screening (exclusion of SNPs with low minor allele frequency, high genotypic failure and not in Hardy Weinberg equilibrium) followed by imputation procedures were conducted. Then, samples from both sites were merged by keeping only the overlapped imputed SNPs followed by a second quality control screening. Finally, a population stratification analysis was conducted with principal component analysis (PCA) to select only subjects with a European ancestry (the number of subjects per self-reported ethnicity is in the **Supplementary Table 3**). For a detailed description see the **Supplementary material**.

2.4. Environmental data

Each subject was assessed on at least one of eight environmental risk factors: (1) tobacco and (2) cannabis consumption; (3) being migrant; (4) belonging to an ethnic minority; (5) the upbringing urbanicity level; (6) the parental age at birth; (7) the presence of childhood trauma; and (8) the season of birth (detailed description of how the risk for psychosis was assessed in each factor is in **Supplementary material**).

TABLE 3 Socio-demographic and clinical information of the At Risk Mental State (ARMS) sample with environmental data (with less than 20% of the environmental risk factors missing).

	ARMS-T (n = 37)	ARMS-NT (n = 97)	Group comparison
Age at baseline (years)	23.6 ± 4.8 [15.6 33.6]	21.9 ± 3.7 [14.6 33.1]	p = 0.027*
Age at follow-up or transition (years)[a]	25.6 ± 5.6 [17.3 39.2]	27.1 ± 4.7 [18.5 41.2]	p = 0.131
Sex (male/female)	22/15	50/47	p = 0.411
Years of education[b]	13.2 ± 2.7 [8 18]	13.3 ± 2.0 [9 18]	p = 0.686
IQ (z-standardized)[c]	−0.3 ± 1.0 [−2.1 2.2]	0.1 ± 1.0 [−2.1 3.5]	p = 0.049*
GAF at baseline[d]	55 ± 12.5 [35 90]	56.7 ± 8.6 [40 80]	p = 0.523
GAF at follow-up[e]	50.4 ± 19.9 [10 88]	63.2 ± 14.2 [20 94]	p =< 0.001*
CAARMS at baseline[f]	30.9 ± 19.4 [0 78]	28.3 ± 16.0 [0 81]	p = 0.478
CAARMS at follow-up[g]	29.7 ± 31.2 [0 102]	13.3 ± 14.2 [0 60]	p =<0.001*

Data format: mean ± standard deviation [min max]. Information not available for [a]1 ARMS-T; [b]5 ARMS-T and 6 ARMS-NT; [c]7 ARMS-T and 13 ARMS-NT; [d]5 ARMS-T and 4 ARMS-NT; [e]5 ARMS-T and 8 ARMS-NT; [f]6 ARMS-T and 13 ARMS-NT; [g]4 ARMS-T and 8 ARMS-NT; subject. ARMS, at-risk mental state; ARMS-T, individuals at ARMS that did not transition to psychosis; ARMS-NT, individuals at ARMS that did not transition to psychosis.
*$p < 0.05$.

2.5. Machine learning approach

Several ML strategies to generate prediction models for transition to psychosis from sMRI data using our ARMS sample were investigated (**Figures 1**, **2**). These include: (a) sample balancing and bootstrapping; and testing several: (b) feature types; (c) feature manipulation approaches; and (d) CV approaches. The analyses were conducted using the neuroimaging ML tool NeuroMiner v1.0 ELESSAR[3] for sMRI data, chosen given that it was used in the previous above-mentioned ARMS prognosis studies and provided therein high accuracy results (12, 39, 40), and R software 4.0.5 (41) for genetic (16) and environmental data. As detailed below, we have used SVM on the neuroimaging data since that is the approach which not only is more often employed with sMRI data but also that which has shown higher accuracies in psychiatric diagnostic classifications using sMRI data including in the ARMS population (10–14) which we herein attempt to replicate. We have used elastic-net algorithm for the genetic data (SNPs and eQTL scores) and environmental risk factors as it a well-suited method for dealing with high-dimensional data and possibly correlated data; and it performs an embedded feature selection and model fitting at once. The PRS and the environmental risk score were analyzed with logistic regression, given that only one feature was used.

2.5.1. Sample balancing and bootstrapping

The final sample used in the ML analyses was defined by all the ARMS-T subjects available (23 subjects for the sMRI predictors, 19 for the PRS predictor, 21 for the SNP's alleles predictors, 21 for eQTL scores predictors, 37 for the ERS predictor, and 17 for the individual environmental predictors), and the same number of ARMS-NT subjects randomly selected to match the ARMS-T for age and sex (for each data modality), and for scan acquisition protocol (for sMRI data). The matching criteria for age and sex were based on the non-rejection of the null hypothesis (i.e., $p > 0.05$) that the ARMS-T and ARMS-NT groups had the same median age (tested with a two-sided Mann–Whitney U-test) and sex proportions (tested with a two-sided chi-square statistic). The matching for the scan acquisition protocol was done in a one-to-one manner, i.e., the number of ARMS-NT subjects within each protocol is the same as the number of ARMS-T. Of note, we have considered the approach of applying a class-weighted support vector machine for our neuroimaging measures and have detected that differences in terms of accuracies between a model with weights vs. no-weights (considering the full unbalanced samples) were practically null (results not shown)–and therefore we did not pursue that approach. Then, each subsampling was repeated five times, i.e., 5 bootstrapped samples were created, and the subsequent ML analyses were conducted for each of the bootstrapped sample.

3 http://proniapredictors.eu/neurominer/index.html

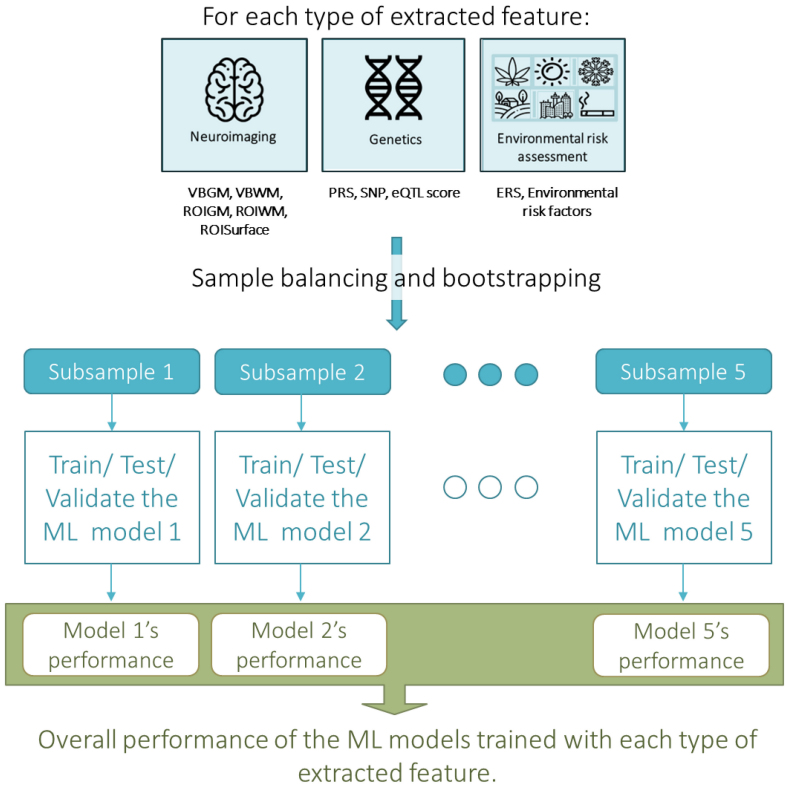

FIGURE 1
Overall machine learning approach taken for assessing the predictive value, i.e., the accuracy, of each type of extracted neuroimaging, genetic or environmental feature in predicting transition to psychosis from an At Risk Mental State (ARMS). ERS, environmental risk score; eQTL score, expression quantitative trait loci; PRS, polygenic risk score; ROIGM, regional-based gray matter volumes; ROISurface, surface-based regional cortical thickness, and gyrification, sulci, and complexity indexes; ROIWM, regional-based white matter volumes; SNP, single nucleotide polymorphism; VMGM, voxel-based gray matter volume maps; VMWM, voxel-based white matter volume maps.

2.5.2. Feature types

2.5.2.1. Structural magnetic resonance imaging data

Individual ML models were trained and validated for each of the following brain measures: (a) voxel-based gray matter (VBGM) maps (297,811 initial features); (b) voxel-based white matter (VBWM) maps (204,706 initial features); (c) regional-based gray (ROIGM) and (d) white (ROIWM) matter volumes (each with 64 initial features) scaled to the total intracranial volume (TIV); and (e) surface-based regional cortical thickness, and gyrification, sulci, and complexity indexes (ROISurface; 272 initial features). Each feature is scaled between 0 and 1 before entering a support vector machine (SVM) classification algorithm.

2.5.2.2. Genetic data

We tested whether a PRS which we have previously found to predict (R^2 = 0.94) a cross-sectional diagnosis of FEP (vs. healthy controls) would be a good longitudinal predictor for ARMS prognosis. Following the same methodology (26), this PRS was computed as the sum of SNPs alleles statistically associated with schizophrenia in a GWAS meta-analysis study (42) weighted by the effect size of that association (more details in **Supplementary material**). In addition, two other novel prediction models using the present ARMS sample were trained and tested. One used SNPs' alleles (79,247 SNPs) as predictors and the other used eQTL scores of genes expressed in brain tissue (141 genes across several brain tissues). Both SNPs and genes' eQTL scores were chosen as the ones most associated with psychosis as ascertained in a recent meta-analysis (27). The eQTL score of each gene was extracted with the eGenScore which we developed and published previously (43) and it was computed as the sum of the alleles of SNPs showing a statistically significant association with the brain gene expression in a standard genomic and transcriptomic sample weighted by the size of that effect (further details available in **Supplementary material**).

2.5.2.3. Environmental data

We tested whether an ERS for psychosis which we have previously developed (28) would be a good longitudinal predictor for ARMS prognosis. Only subjects with less than 20% of missing information (i.e., missing data for less than 2 environmental risk factors) were considered for the ERS-based ML analysis. Therefore, the final sample included 37 ARMS-T subjects and 97 ARMs-NT subjects. Then, each environmental risk factor (see Section "2.4. Environmental data") was used as an individual feature in the model. For this ML analysis only subjects with information for all the environmental risk factors (i.e., with no missing information) were considered (i.e., 17 ARMS-T and 49 ARMS-NT subjects). Further details available in **Supplementary material**.

2.5.3. Feature manipulation

Feature manipulation was performed only in ML analyses using sMRI data. In particular, feature dimensionality reduction was performed for VBGM and VBWM features using robust PCA (44,

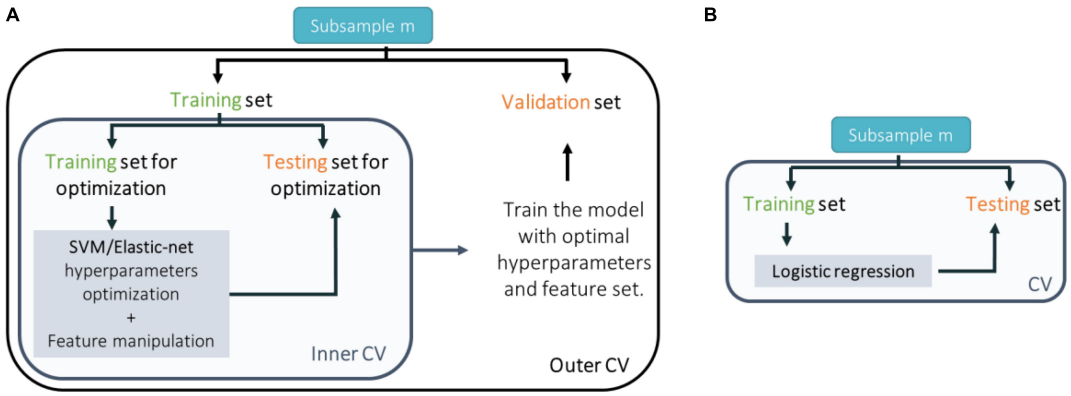

FIGURE 2
Scheme of the cross-validation (CV) approach taken to train, test, and validate classification models trained with **(A)** neuroimaging data and support vector machines (SVM); genetic (single nucleotide polymorphisms or expression quantitative trait loci) or environmental (environmental risk factors) data and elastic-net; or **(B)** genetic (polygenic risk score) or environmental (environmental risk score) data and logistic regression.

45). Here the robust PCA was applied during the inner CV cycle (see Section "2.5.5. Cross-validation"). The number of principal components that were retained explained up to 80% of the variance in the data and were limited by the inner CV cycle's sample size, n, i.e., a maximum of only $n/2$ components could indeed be extracted. Supplementary Table 5 shows the maximum number of principal components that can be extracted for each inner CV cycle in each CV scheme that was used (see also Section "2.5.5. Cross-validation") (for detailed description see the Supplementary material).

Feature selection was performed on regional brain features (i.e., ROIGM, ROIWM, and ROISurface) using a greedy forward search feature selection algorithm. This is a stepwise algorithm that starts with an empty set of features and then tests the predictive value of every single feature, selecting the ones improving the overall accuracy across the inner CV cycle folds (see Section "2.5.5. Cross-validation"). The final set of features is, then, composed by the 10% most predictive variables. Additionally, no feature selection, i.e., using the total number regional brain features, was also tested.

2.5.4. Machine learning algorithm

Binary classification of transition to psychosis from an ARMS (i.e., ARMS-T vs. ARMS-NT) was performed using linear SVM for sMRI data, and logistic regression and elastic net for both genetic and environmental data.

2.5.4.1. Support vector machine classification

Binary classification of transition to psychosis from an ARMS (i.e., ARMS-T vs. ARMS-NT) using sMRI data was performed using linear SVM (46, 47). In this study we exclusively used a linear kernel SVM to reduce the risk of overfitting the data (given our final sample size being relatively small). Furthermore, the linear SVM classifier has a penalty parameter C that controls the trade-off between having zero training error and allowing misclassification. Herein, a parameter search was carried out to identify the optimal C value (i.e., 2^l, l $[-5:1:4]$) in the inner CV cycle (see Section "2.5.5. Cross-validation").

2.5.4.2. Logistic regression for classification

Binary classification of transition to psychosis from an ARMS (i.e., ARMS-T vs. ARMS-NT) using genetic (PRS) or environmental (ERS) data was performed using simple logistic regression. A threshold of 0.5 was applied to the probability of observing the outcome, i.e., an ARMS-T (see Supplementary material for more details).

2.5.4.3. Elastic net for classification

Binary classification of transition to psychosis from an ARMS (i.e., ARMS-T vs. ARMS-NT) using genetic (psychosis-associated SNPs or eQTL scores of psychosis-associated genes) or environmental (environmental risk factors) data was performed using logistic regularized regression with elastic net (48) using hyperparameters search to identify the optimal l_1 and λ values (regression weights shrinkage) (i.e., l_1 $0:0.1:1$; λ $0.01:0.01:1$) in the inner CV cycle (see Section "2.5.5. Cross-validation") (for detailed description see the Supplementary material). The elastic net was implemented using the "glmnet" v4.0 R package.

2.5.5. Cross-validation

Each model (trained with sMRI, psychosis-associated SNPs or eQTL scores of psychosis-associated genes and environmental risk factors) was trained in a nested-CV scheme for hyperparameter tuning (in the inner CV cycle) and to estimate the generalizability of the trained prediction model and its performance (in the outer CV cycle) (Figure 2A). For more details see the Supplementary material. For sMRI models, we tested three different nested-CV schemes: (a) leave-one scan acquisition protocol-out (LSO); (b) leave-one per group from the same scan acquisition protocol-out (LPO); and (c) classic 5-fold CV. For the remaining sMRI, genetic (trained with psychosis-associated SNPs or eQTL scores of psychosis-associated genes data) and environmental (trained with environmental risk factors data) models, nested-CV was defined with an inner 5-fold and an outer leave-one per group-out (LPO) CV schemes. Furthermore, the logistic regression (trained with genetic–PRS–and environmental–ERS–data) was trained and tested in a simple LPO CV scheme (Figure 2B).

2.5.6. Performance measures

Each model's performance was evaluated using measures derived from the confusion matrix: sensitivity; specificity; BAC; positive likelihood ratio; negative likelihood ratio; and diagnostic odds ratio

(DOR). Moreover, permutation testing was used to test if the BAC was higher than chance–50%–with a statistical significance of 5% (For a detailed description of each measure see the **Supplementary material**).

The prediction ability of each tested combination of feature type, feature manipulation, and CV scheme was defined as significant if the BAC was higher than chance–50% in at least 3 out of 5 bootstrapped samples. evaluated by testing the statistical significance of the median BAC across bootstrapped samples using a one-tailed Wilcoxon signed rank test (i.e., to test if the median BAC across bootstrapped samples is higher than chance– 50%, with a statistical significance level of 5%). *P*-values were not adjusted for multiple comparisons due to non-independence of the samples used in each statistical test.

3. Results

Overall, the BAC of the classification models trained and validated using each combination of feature type (i.e., ROIGM, ROIWM, ROISurface, VBGM, or VBWM–for sMRI data; PRS, psychosis-associated SNPs or psychosis-associated brain eQTL score genes scores–for genetic data; or ERS or individual environmental risk factors–for environmental data), feature manipulation (i.e., feature dimensionality reduction through PCA; no feature selection; or forward feature selection), CV scheme (i.e., LSO CV; LPO CV; or 5-fold CV), and bootstrapped sample (i.e., one of the 5 samples) ranged from 37 to 67% for the classification models trained with sMRI (**Tables 4**, **5** and **Figures 3**, **4**), from 26 to 62% for the models trained with genetic data (**Table 6** and **Figure 5**) and from 38 to 61% for models trained with environmental data (**Table 6** and **Figure 6**). The prediction ability of each model was not significant as less than 3 bootstrapped samples per each feature type showed a BAC statistically higher than chance–50%.

4. Discussion

This study aimed to predict transition to psychosis from an ARMS using ML applied to quantitative data across modalities–i.e., neuroimaging (sMRI), genetics (genome-wide genotypes), and environment–collected when subjects first sought clinical help (i.e., at baseline) and were identified with an ARMS. This is, to the best of our knowledge, the first study: (1) of longitudinal design exploring sMRI, genetic and environmental data to predict the development of a psychotic disorder from a prodromal stage; and (2) when considering each modality individually, exploring a range of approaches (for genetics and environmental data) and/or feature combinations (for sMRI data).

4.1. Prediction of transition to psychosis using structural neuroimaging data

In this study we applied ML to structural neuroimaging data using a relatively larger sample and an ML approach, improved to the best of our ability, to detect transition to psychosis from an ARMS and to replicate previous positive findings of accuracies 74 to 84% of six studies, which together used 3 independent samples (10–15). For this, we decided: to: (1) use only the most recent versions of the image processing tools (i.e., CAT12) and ML tools (i.e., NeuroMiner); (2) replicate as accurately as possible the methods that were described in the abovementioned MRI papers since it was not possible to access their processing and ML pipelines; (3) add a layer of ML generalizability by bootstrapping and fitting a model to each subsample; and (4) overcome previous studies' limitations (e.g., sample unbalancing for demographics). Furthermore, we explored, for the first time, the use of whole brain white matter volume and regional white matter volume, cortical thickness, and surface-based brain gyrification, sulci depth, and complexity indexes with ML to predict transition to psychosis.

Unexpectedly, we did not replicate previous findings. After balancing the samples for binary classification of transition to psychosis accounting for age, sex, and the three different scan acquisition protocols to avoid overoptimistic results, the performance of all tested combinations (i.e., of feature type–ROIGM, ROIWM, ROISurface, VBGM, or VBWM; feature manipulation–feature dimensionality reduction through PCA, no feature selection, or forward feature selection; and CV scheme–LSO CV, LPO CV, or 5-fold CV) were not significantly better than chance level.

Compared to the previous studies reporting high balanced accuracies (74 to 84%) in predicting transition to psychosis from sMRI maps (10–15), the current study has some advantages. First, this study's sample is drawn from a more naturalistic ARMS population as it includes subjects whose sMRI images were acquired using three different scan acquisition protocols. Training a classification model with data from different centers potentially increases its generalizability. Only one of the previous transition to psychosis prediction studies used a two-site group balanced sample (12), combining the samples reported in two previous studies by the same authors (10, 11). The main differences between this report and our study are the following: (a) Their sample was larger than our balanced bootstrapped samples (i.e., 36% larger than ours, measured as the absolute value of the change in sample size, divided by the average of the size of the two samples). However, we tested our ML models on five balanced subsamples (i.e., through bootstrapping), allowing us to obtain a measure of generalizability of these models' performance. Moreover, they do not present a measure of the statistical significance of the model's BAC, which we do herein. (b) They controlled the effect of site on the classification using partial correlations during the training phase of the CV cycle, whereas we controlled it by keeping the same proportion of subjects at an ARMS that transitioned to psychosis and those who did not in each scan protocol during the training phase of the CV cycle (i.e., when using the LPO CV scheme as the previous study did). Additionally, we also guaranteed that the pair of subjects left out for testing/validation were from the same site. This potentially increases the generalizability of the classification model by training it with a more heterogeneous sample (and, as explained above, more naturalistic) and diminishing the effect of site on the testing/validation classification accuracy, which is not taken into account in the previous report (12).

Second, we trained our classification models with samples balanced for group (subjects at an ARMS who later transitioned to psychosis and who did not), age at scan and sex. Balancing for group is important to avoid biasing the classification model to the most represented group and it was not taken into account by three out of six previous reports (10, 11, 14). Moreover, the effects of age (49) and sex (50) on brain structure, rate of transition to psychosis from ARMS (2), and prevalence of psychosis (3, 51), have been consistently reported and, therefore, should be taken into

10.3389/fpsyt.2022.1086038

TABLE 4 Performance measures of each structural magnetic resonance imaging (sMRI) classification model based on brain regional features across bootstrapped samples.

	ROIGM		ROIWM		ROISurface	
	No-FS	FFS	No-FS	FFS	No-FS	FFS
LSO CV scheme						
SE (%)	55.7 ± 6.4 [47.8, 65.2]	59.1 ± 11.7 [47.8, 78.3]	57.4 ± 19.1 [30.4, 82.6]	62.6 ± 13.3 [52.2, 82.6]	41.7 ± 14.6 [26.1, 60.9]	39.1 ± 20.6 [17.4, 65.2]
SP (%)	55.7 ± 10.4 [43.5, 69.6]	40.9 ± 10.5 [26.1, 52.2]	46.1 ± 14 [21.7, 56.5]	27.8 ± 22.3 [0.0, 56.5]	61.7 ± 17.8 [34.8, 82.6]	63.5 ± 12.1 [43.5, 73.9]
BAC (%)	55.7 ± 5.5 [47.8, 63.0]	50.0 ± 3.8 [43.5, 52.2]	51.7 ± 5.6 [43.5, 58.7]	45.2 ± 6.6 [37.0, 54.3]	51.7 ± 7.4 [43.5, 63.0]	51.3 ± 9.8 [43.5, 67.4]
PLR	1.3 ± 0.3 [0.9, 1.9]	1.0 ± 0.1 [0.8, 1.1]	1.1 ± 0.2 [0.7, 1.4]	0.9 ± 0.2 [0.7, 1.2]	1.2 ± 0.4 [0.8, 1.8]	1.1 ± 0.6 [0.6, 2.1]
NLR	0.8 ± 0.2 [0.6, 1.1]	1.0 ± 0.2 [0.8, 1.4]	0.9 ± 0.2 [0.7, 1.2]	1.5 ± 0.7 [0.8, 2.5]	1.0 ± 0.3 [0.6, 1.4]	1.0 ± 0.3 [0.5, 1.2]
DOR	1.7 ± 0.8 [0.8, 3.0]	1.0 ± 0.3 [0.6, 1.3]	1.3 ± 0.5 [0.6, 2.0]	0.6 ± 0.5 [0.0, 1.4]	1.4 ± 0.9 [0.6, 2.9]	1.5 ± 1.6 [0.5, 4.3]
Significant models	1	0	0	0	1	1
LPO CV scheme						
SE (%)	47.8 ± 6.1 [43.5, 56.5]	67.0 ± 7.9 [56.5, 73.9]	49.6 ± 8.5 [39.1, 60.9]	39.1 ± 9.2 [26.1, 47.8]	53.9 ± 6.6 [43.5, 60.9]	52.2 ± 6.9 [43.5, 60.9]
SP (%)	54.8 ± 6.6 [47.8, 60.9]	44.3 ± 10.8 [34.8, 60.9]	52.2 ± 5.3 [43.5, 56.5]	50.4 ± 12.5 [34.8, 69.6]	54.8 ± 5.0 [47.8, 60.9]	54.8 ± 12.9 [39.1, 69.6]
BAC (%)	51.3 ± 4.8 [45.7, 58.7]	55.7 ± 7.1 [45.7, 65.2]	50.9 ± 5.2 [43.5, 56.5]	44.8 ± 6.6 [37.0, 54.3]	54.3 ± 4.3 [50.0, 60.9]	53.5 ± 7.5 [43.5, 60.9]
PLR	1.1 ± 0.2 [0.8, 1.4]	1.3 ± 0.3 [0.9, 1.8]	1.0 ± 0.2 [0.8, 1.3]	0.8 ± 0.3 [0.5, 1.3]	1.2 ± 0.2 [1.0, 1.6]	1.2 ± 0.3 [0.8, 1.6]
NLR	1.0 ± 0.2 [0.7, 1.2]	0.8 ± 0.3 [0.5, 1.3]	1.0 ± 0.2 [0.8, 1.3]	1.3 ± 0.3 [0.9, 1.5]	0.8 ± 0.1 [0.6, 1.0]	0.9 ± 0.3 [0.6, 1.3]
DOR	1.2 ± 0.5 [0.7, 2]	1.9 ± 1.1 [0.7, 3.6]	1.1 ± 0.4 [0.6, 1.7]	0.7 ± 0.4 [0.3, 1.5]	1.5 ± 0.6 [1.0, 2.4]	1.5 ± 0.8 [0.6, 2.4]
Significant models	0	0	0	0	1	0
5-fold CV scheme						
SE (%)	42.6 ± 3.6 [39.1, 47.8]	40.9 ± 5.8 [34.8, 47.8]	59.1 ± 6.6 [52.2, 69.6]	45.2 ± 8.5 [34.8, 56.5]	53.0 ± 10.4 [39.1, 65.2]	57.4 ± 8.4 [47.8, 69.6]
SP (%)	54.8 ± 12.5 [34.8, 65.2]	40.9 ± 7.3 [30.4, 47.8]	40.9 ± 8.5 [30.4, 52.2]	53 ± 11.3 [34.8, 65.2]	54.8 ± 6.6 [47.8, 60.9]	53 ± 11.7 [39.1, 65.2]
BAC (%)	48.7 ± 6.6 [39.1, 56.5]	40.9 ± 2.4 [37.0, 43.5]	50.0 ± 5.1 [45.7, 56.5]	49.1 ± 2.5 [45.7, 52.2]	53.9 ± 5.2 [47.8, 60.9]	55.2 ± 9.3 [47.8, 67.4]
PLR	1.0 ± 0.3 [0.7, 1.4]	0.7 ± 0.1 [0.6, 0.8]	1.0 ± 0.2 [0.9, 1.2]	1.0 ± 0.1 [0.9, 1.1]	1.2 ± 0.2 [0.9, 1.6]	1.3 ± 0.5 [0.9, 2.0]
NLR	1.1 ± 0.3 [0.8, 1.6]	1.5 ± 0.2 [1.3, 1.9]	1.0 ± 0.3 [0.7, 1.3]	1.1 ± 0.1 [0.9, 1.3]	0.9 ± 0.2 [0.6, 1.1]	0.9 ± 0.3 [0.5, 1.1]
DOR	1.0 ± 0.5 [0.4, 1.7]	0.5 ± 0.1 [0.3, 0.6]	1.1 ± 0.5 [0.7, 1.8]	0.9 ± 0.2 [0.7, 1.2]	1.5 ± 0.6 [0.8, 2.4]	2.0 ± 1.6 [0.8, 4.3]
Significant models	0	0	0	0	0	1

Measures for each tested combination of brain regional feature type [i.e., regional-based gray (ROIGM) and white (ROIWM) matter volume; and surface-based regional cortical thickness, gyrification, sulci, and complexity indexes (ROISurface)], feature selection [i.e., no feature selection (No-FS); and forward feature selection (FFS)], and cross-validation (CV) scheme [i.e., leave-one scan acquisition protocol-out (LSO) CV; leave-one per group-out (LPO) CV; and 5-fold CV] are presented. Statistical significance of the balanced accuracy (BAC) for each bootstrapped sample was tested using permutation testing with a significance level of 5%. Data format: mean ± standard deviation [min max]. DOR, diagnostic odds ratio; NLR, negative likelihood ratio; PLR, positive likelihood ratio; SE, sensitivity; SP, specificity. Significant models: number of models with statistically significant BAC higher than 50%.

account in these studies. All previous reports (and the current study) matched transition proportion for age and sex (10–14), except for one (15). Das and colleagues reported a statistically significant and better than chance level BAC in predicting transition to psychosis using a sample unbalanced for both group and sex. Although they used a ML algorithm with class (i.e., group) weighing–which in summary increases the influence of the minority class when training the model by assigning higher weights to rare cases, the authors

10.3389/fpsyt.2022.1086038

TABLE 5 Performance measures of each structural magnetic resonance imaging (SMRI) classification model based on voxel-wise features across bootstrapped samples.

	LSO CV scheme		LPO CV scheme		5-fold CV scheme	
	VBGM	VBWM	VBGM	VBWM	VBGM	VBWM
SE (%)	20.9 ± 34.8 [0, 82.6]	46.1 ± 38.2 [4.3, 78.3]	47.0 ± 10.4 [34.8, 60.9]	50.4 ± 11.3 [34.8, 60.9]	30.4 ± 10.2 [21.7, 43.5]	41.7 ± 8.5 [34.8, 56.5]
SP (%)	72.2 ± 35.7 [8.7, 91.3]	53 ± 35.4 [21.7, 95.7]	55.7 ± 8.4 [43.5, 65.2]	53.0 ± 7.1 [47.8, 65.2]	51.3 ± 7.8 [43.5, 60.9]	52.2 ± 6.1 [43.5, 60.9]
BAC (%)	46.5 ± 3.6 [43.5, 52.2]	49.6 ± 2.4 [45.7, 52.2]	51.3 ± 7.5 [45.7, 63.0]	51.7 ± 2.8 [47.8, 54.3]	40.9 ± 2.4 [37.0, 43.5]	47.0 ± 6.8 [41.3, 58.7]
PLR	0.6 ± 0.6 [0.0, 1.5]	0.9 ± 0.3 [0.3, 1.1]	1.1 ± 0.4 [0.8, 1.8]	1.1 ± 0.1 [0.9, 1.2]	0.6 ± 0.1 [0.5, 0.8]	0.9 ± 0.3 [0.7, 1.4]
NLR	1.3 ± 0.4 [1.0, 2.0]	1.0 ± 0.1 [0.9, 1.1]	1.0 ± 0.3 [0.6, 1.2]	0.9 ± 0.1 [0.8, 1.1]	1.4 ± 0.1 [1.3, 1.5]	1.1 ± 0.3 [0.7, 1.4]
DOR	0.7 ± 0.9 [0.0, 2.2]	0.8 ± 0.4 [0.1, 1.1]	1.3 ± 1.0 [0.7, 3.1]	1.1 ± 0.2 [0.8, 1.4]	0.4 ± 0.1 [0.2, 0.6]	0.9 ± 0.7 [0.5, 2.1]
Significant models	0	1	0	0	0	0

Measures for each tested combination of voxel-wise feature type [i.e., voxel-based gray (VBGM) and white (VBWM) matter volume maps], feature dimensionality reduction through principal component analysis and cross-validation (CV) scheme [i.e., leave-one scan acquisition protocol-out (LSO) CV; leave-one per group-out (LPO) CV; and 5-fold CV] are presented. Statistical significance of the balanced accuracy (BAC) for each bootstrapped sample was tested using permutation testing with a significance level of 5%. Data format: mean ± standard deviation [min max]. DOR, diagnostic odds ratio; NLR, negative likelihood ratio; PLR, positive likelihood ratio; SE, sensitivity; SP, specificity. Significant models: number of models with statistically significant BAC higher than 50%.

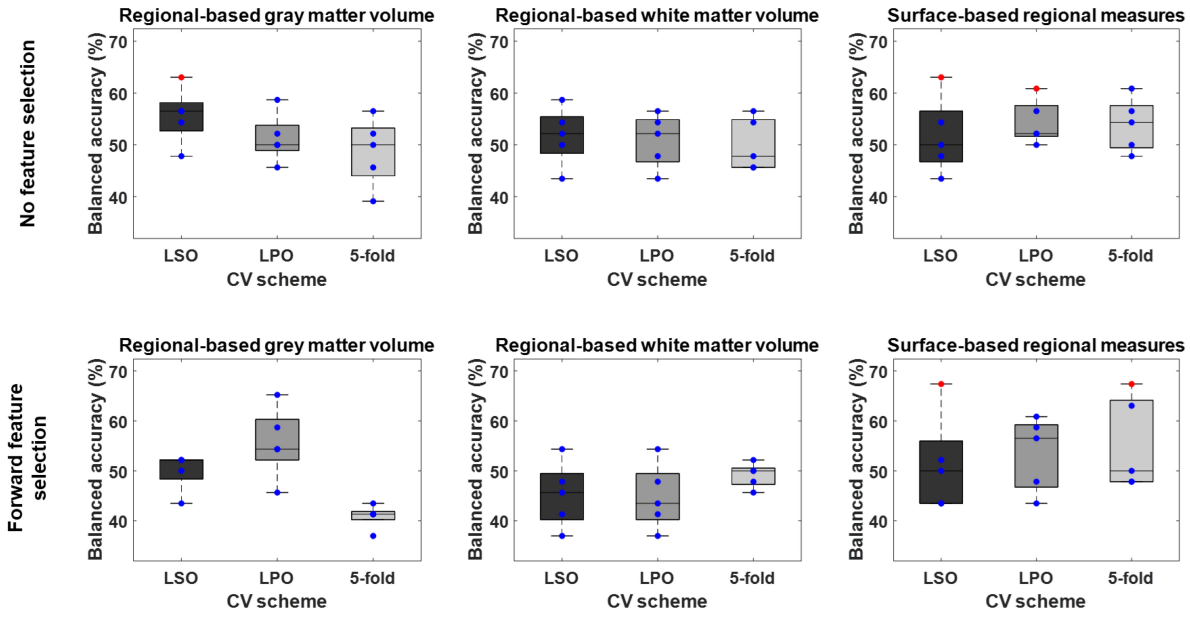

FIGURE 3
Balanced accuracy across bootstrapped samples for each tested combination of regional feature type [i.e., regional-based gray and white matter volume; and surface-based regional cortical thickness, gyrification, sulci, and complexity indexes (surface-based regional measures)], feature selection [i.e., no feature selection; and forward feature selection (FFS)], and cross-validation (CV) scheme [i.e., leave-one scan acquisition protocol-out (LSO) CV; leave-one per group-out (LPO) CV; and 5-fold CV]. Dots represent the balanced accuracy value in each of the five bootstrapped samples and are red colored if the balanced accuracy is statistically significant (i.e., $p < 0.05$) or blue colored if it is not (i.e., $p > 0.05$). The statistical significance of the balanced accuracy in each bootstrapped sample was evaluated through permutation testing.

performed an unspecified correction for sex effect (as well as for age and TIV effects) to the data during the training CV cycle. This approach may not be the most appropriate given the known effect of sex on brain structure (50) and the, abovementioned, empirically tested association between sex and group (i.e., transition to psychosis from an ARMS vs. no transition) (15), which makes sex a potential confounder in this analysis. Furthermore, in three of the six previous reports, the effects of age and sex were corrected before entering the ML analysis (10), and during the training CV cycle (11, 15) using partial correlations (10, 11) or an unspecified method (15)–which we did not perform. Correction for age effects in ML analysis has been previously shown to increase classification accuracy in Alzheimer's disease, when it is estimated from healthy subjects (52). Correction for effects of no interest in ML analyses should be done with extreme caution as it can easily remove relevant subject-specific information (53). This is especially important when the correction

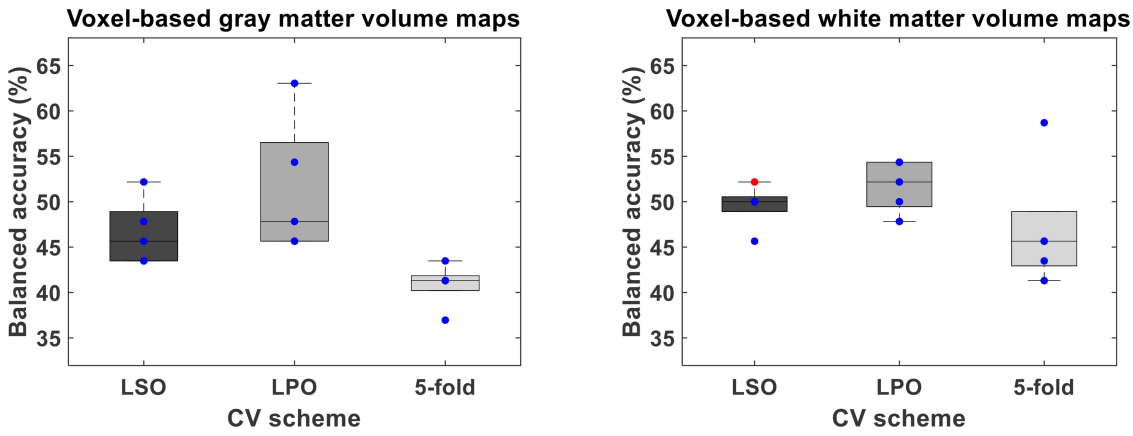

FIGURE 4
Balanced accuracy across bootstrapped samples for each tested combination of voxel-wise feature type [i.e., voxel-based gray (VBGM) and white (VBWM) matter volume maps], feature dimensionality reduction through principal component analysis and cross-validation (CV) scheme [i.e., leave-one scan acquisition protocol-out (LSO) CV; leave-one per group-out (LPO) CV; and **5**-fold CV. Dots represent the balanced accuracy value in each of the five bootstrapped samples and are red colored if the balanced accuracy is statistically significant (i.e., $p < 0.05$) or blue colored if it is not (i.e., $p > 0.05$). The statistical significance of the balanced accuracy in each bootstrapped sample was evaluated through permutation testing.

TABLE 6 Performance measures of: (1) a genetic schizophrenia polygenic risk score (PRS), (2) a list of psychosis-associated single nucleotide polymorphisms (SNPs), (3) expression quantitative trait loci (eQTL) scores (43) of a list of psychosis-associated genes expressed in the brain; (4) an environmental schizophrenia risk score (ERS), and (5) a list of schizophrenia-associated environmental risk factors, classification models across bootstrapped samples.

	PRS	SNP	eQTL score	ERS	Environmental risk factors
SE (%)	42.1 ± 20.0 [21.1, 63.2]	41.9 ± 13.6 [23.8, 61.9]	61.0 ± 17.0 [47.6, 85.7]	44.9 ± 5.1 [29.7, 56.8]	10.6 ± 4.9 [5.9, 17.6]
SP (%)	46.3 ± 11.4 [31.6, 57.9]	50.5 ± 16.4 [28.6, 66.7]	31.4 ± 23.2 [4.8, 57.1]	50.8 ± 8.2 [45.9, 64.9]	70.6 ± 7.2 [64.7, 82.4]
BAC (%)	44.2 ± 15.3 [26.3, 60.5]	46.2 ± 10.7 [33.3, 61.9]	46.2 ± 4.9 [40.5, 52.4]	47.8 ± 8.8 [37.8, 60.8]	40.6 ± 2.5 [38.2, 44.1]
PLR	0.9 ± 0.5 [0.3, 1.5]	0.9 ± 0.4 [0.5, 1.6]	0.9 ± 0.1 [0.8, 1.1]	1.0 ± 0.4 [0.6, 1.6]	0.4 ± 0.1 [0.2, 0.5]
NLR	1.4 ± 0.8 [63.6, 2.5]	1.3 ± 0.6 [0.6, 2.2]	1.9 ± 1.1 [0.9, 3.0]	1.1 ± 0.3 [0.7, 1.5]	1.3 ± 0.1 [1.1, 1.4]
DOR	1.0 ± 1.0 [0.1, 2.4]	1.0 ± 1.0 [0.2, 2.6]	0.7 ± 0.4 [0.3, 1.2]	1.0 ± 0.8 [0.4, 2.4]	0.3 ± 0.1 [0.2, 0.4]
Significant models	0	0	1	0	0

Statistical significance of the balanced accuracy (BAC) for each bootstrapped sample was tested using permutation testing with a significance level of 5%. Data format: mean ± standard deviation [min max]. DOR, diagnostic odds ratio; NLR, negative likelihood ratio; PLR, positive likelihood ratio; SE, sensitivity; SP, specificity. Significant models: number of models with statistically significant BAC higher than 50%.

is being performed in a non-healthy (i.e., non-standard) population, because the effect of external variables such as age and sex might be modulated by the presence of the disease (e.g., being at ARMS or having schizophrenia).

Third, this study's sample is composed of subjects whose clinical diagnosis of an ARMS was based on having a schizotypal personality disorder or on the subject's familial-high risk coupled with functioning decline and on the CAARMS (54), which mainly evaluates positive symptoms. These were not the same criteria as those used in the previous studies predicting transition to psychosis from an ARMS. These previous studies all used samples of subjects clinically assessed with tools that evaluate not only positive symptoms, but also basic and negative symptoms (10–12, 14, 15), except one (13), which included only familial-high risk subjects in its sample. This potentially increases the inclusion of subjects in the early phase of the psychosis prodrome (characterized by the presence of basic and negative symptoms), whereas our sample includes mainly subjects in the late prodromal phase of psychosis (characterized mainly by the presence of positive symptoms) (2). Therefore, our results suggest that previously reported accuracies in predicting transition to psychosis may be population-specific, poorly generalizable to differently clinically characterized populations (as ours herein).

4.2. Prediction of transition to psychosis using genetic data

In this study we applied ML to genetic data and used three types of genetic features to detect transition to psychosis from an ARMS: (a) a schizophrenia PRS that we have previously shown to distinguish

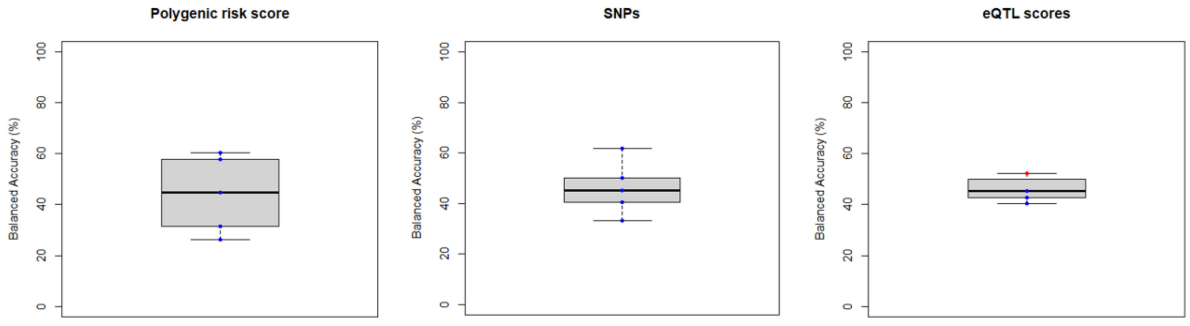

FIGURE 5
Balanced accuracy across bootstrapped samples for each model trained with the polygenic risk score, the list of psychosis-associated single nucleotide polymorphism (SNPs) or with the list of psychosis-associated genes for which an expression quantitative trait loci (eQTL) score was extracted. Dots represent the balanced accuracy value in each of the 5 bootstrapped samples and are red colored if the balanced accuracy is statistically significant (i.e., $p < 0.05$) or blue colored if it is not (i.e., $p > 0.05$). The statistical significance of the balanced accuracy in each bootstrapped sample was evaluated through permutation testing.

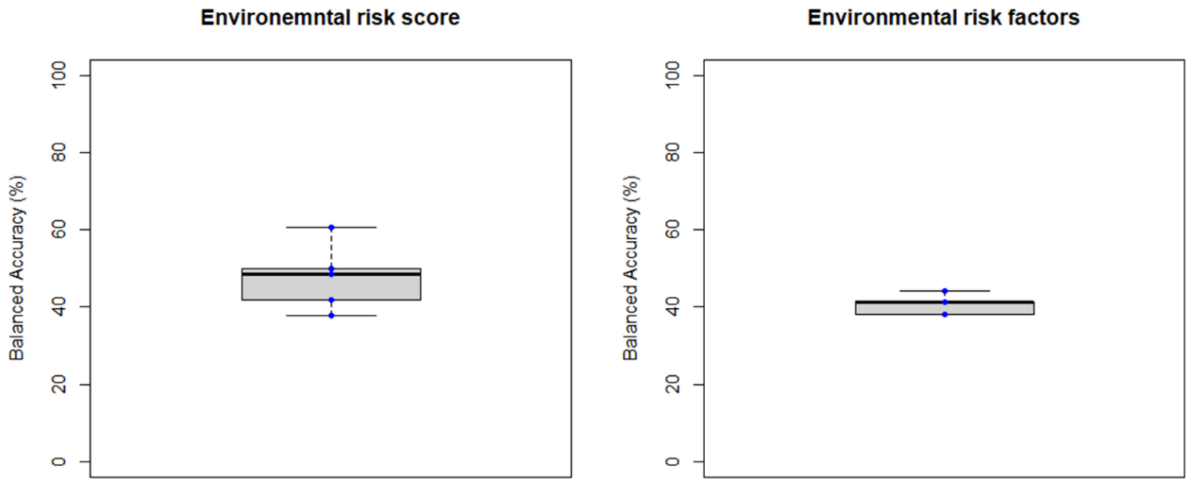

FIGURE 6
Balanced accuracy across bootstrapped samples for each model trained with the environmental risk score or with each environmental risk factors as features. Dots represent the balanced accuracy value in each of the 5 bootstrapped samples and are red colored if the balanced accuracy is statistically significant (i.e., $p < 0.05$) or blue colored if it is not (i.e., $p > 0.05$). The statistical significance of the balanced accuracy in each bootstrapped sample was evaluated through permutation testing.

FEP patients from healthy controls (26) and ARMS-T from ARMS-NT (16), (b) a set of psychosis-associated SNPs previously associated with schizophrenia in a recent GWAS meta-analysis (27), and (c) a brain-specific expression Quantitative Trait Loci (eQTL) score including the latter genes.

Genetic data showed a poor performance in predicting transition to psychosis from an ARMS. SNPs-based classification models have been previously shown to classify schizophrenia (18, 19, 21), and FEP patients (23) (vs. healthy controls) better than chance level, but not subjects at an ARMS vs. healthy controls or FEP patients (23). Furthermore, one of these studies has selected a list of SNPs from the Psychiatric Genomics Consortium 2 (PGC2) (21, 42), which potentially overlaps with the ones selected in this study (27).

Despite the (scarce) evidence of the potential of PRS for schizophrenia (20–22) to classify schizophrenia patients (vs. healthy controls) and the one report showing the schizophrenia PRS's ability to predict transition to psychosis (16) we were not able to predict transition to psychosis from an ARMS using this type of genetic feature. Although the latter study (16) used a larger sample (i.e., 106% higher than ours, measured as the absolute value of the change in sample size, divided by the average of the size of the two samples) to train the PRS-based model, sample balancing in terms of group and age or sex were not taken into account or that was unclear, respectively. Furthermore, herein we applied a bootstrapped sample approach to estimate generalizability of the PRS-based model by assuring that each bootstrapped sample met the balancing conditions for group, age, and sex–which does not seem to be the case in that study (16). Furthermore, another possible explanation for the PRS negative results is that although the genetic architecture, conveyed through a PRS, has been shown to differ between patients with schizophrenia and healthy controls, one cannot exclude the possibility that it is specific to schizophrenia (a fully developed psychotic disorder), and might even be present in all subjects at an ARMS, i.e., those who later transition to psychosis and those who do not. The constellation of genetic variations (i.e., SNPs) that might confer susceptibility to transition to psychosis already from a prodromal stage is not necessarily the same as the one for schizophrenia (when drawn in comparison to healthy controls). This

may justify the advantage of using a less hypothesis-based approach for the selection of genetic features (as we did by pre-selecting a large list of SNPs and performing an embedded feature selection using elastic net regression). Lastly, using a PRS formula made specifically for transition to psychosis from an ARMS would require a larger and independent sample to estimate SNP effect sizes, which might be better provided by multicenter projects, such as NAPLS 2 (55) and PRONIA[4] over the next years.

Expression Quantitative Trait Loci (eQTL) scores for psychosis associated genes expressed in the brain were also not able to predict transition to psychosis from an ARMS. Only one previous study has shown the predictive value of gene expression profiling in the frontal brain region in classifying schizophrenia patients (vs. healthy controls) (17). In the present study, instead of actual gene expression measures we used a proxy for a-genetically regulated component of the expression of genes, the eQTL scores. Although we have computed eQTL scores only for the genes having a validated eQTL score model (43), this does not guarantee that the estimated gene expression represents (or correlates perfectly with) the real levels of the expression. Furthermore, although we have selected the initial list of genes as the ones most associated with schizophrenia (vs. healthy controls), this selection did not take into account the expression profile of these genes in the brain, and we have computed an eQTL score for several brain tissues. A future improvement of this step would be to test an eQTL scores-based model with a selection of genes that: (a) are highly expressed in the brain in healthy subjects, and (b) their expression is associated to a schizophrenia diagnosis, or even better with the transition to psychosis from an ARMS.

4.3. Prediction of transition to psychosis using environmental data

In this study we applied, for the first time, ML to environmental data using two types of features to detect transition to psychosis from an ARMS: (a) a schizophrenia ERS which we have previously reported (28), and (b) a set of environmental risk factors as predictors. Overall, neither environmental risk assessment, could predict transition to psychosis from an ARMS with an averaged accuracy, i.e., across bootstrapped samples, better than chance level. Although we know of no similar longitudinal ARMS transition study, the closest other report using ML and environmental data to diagnose schizophrenia (vs. healthy controls) (22) also found a BAC not statistically better than chance level, even having included features such as the presence of obstetric complications and of developmental anomalies, the parental socio-economic status; and –without feature selection– trained and tested the model in a 13 times larger, albeit age, sex, and group -unbalanced, sample (103 patients and 337 controls) than ours (22). However, due to the still poorly understood environmental risk mechanisms one cannot exclude the lack of statistical power as a potential explanation for these negative findings including ours.

The ML model trained with the ERS for schizophrenia, which we have tested as an (admittedly limited) exploratory predictor of the transition to psychosis from an ARMS, showed a poor performance, i.e., a BAC similar to chance level. Indeed, ERS is a composite score of individual risk factors computed under the assumption that the risk factors are completely independent (28), which has been shown not to be the case (56)–i.e., intercorrelated risk factors may inflate the ERS estimation. This crude approach may limit the ability of the ERS to capture the detailed environmental architecture underlying psychosis. Moreover, just as for a PRS, an ERS for schizophrenia may not be a good substitute of a potential ERS for transition to psychosis from an ARMS (57).

Lastly, our criterion for training and testing a fully multimodal ML model with modalities that would show an ML model performance statistically better than chance (i.e., 50%) predicting transition to psychosis from an ARMS in at least 3 of 5 bootstrapped samples was not fulfilled given that none of the modality-based ML models survived that threshold. This conservative criterion was chosen given the already small sample size available for the training of the multimodal ML model, i.e., only 6 ARMS-T and 23 ARMS-NT (only this subset of subjects had data for the three data modalities, simultaneously). The decrease in sample size, remarkably impairs the prediction power of the model, i.e., its accuracy. Without previous evidence of the ability to predict transition to psychosis from an ARMS by modality supporting its integration in a multimodal ML model, negative results from this multimodal model would be highly difficult to explain, as they could theoretically be explained by the increase of noise in the model due to the inclusion of features that did show previous predictive ability or by the lack of predictive power due to the very small sample size. Moreover, the parallel-to-ours, multi-site study, albeit very group-unbalanced (only 26 ARMS-T patients vs. 308 ARMS-NT), from the PRONIA project, showed that a stacked model combining similar data to our study's plus human prognostic ratings could predict transition to psychosis with a balanced accuracy of 86% and a good geographical generalizability (25). This multimodal approach was showed to improve biological-based unimodal models by 15% (VBGM volume maps-based model) and 20% (PRS for schizophrenia-based model). As such, the replication of this promising finding, following the same multimodal approach as that study, using in our study's sample and data features co-existing in both samples, would be interesting as an additional method to ascertain whether our negative findings are due to lack of power or to no discriminability with our feature sets.

4.4. Limitations

This study was limited by several factors. First, and foremost, the small sample size may have limited the performance of classification models, even though our sample size was informed by previous ML studies showing 74–84% accuracies in predicting transition to psychosis from an ARMS (10–15). Indeed, this is a critical limitation when dealing with high dimensional data, such as neuroimaging and genetics–which we have used herein. Although we have taken measures to avoid overfitting and an overestimation of the classification models' performance such as artificially increasing the sampling through bootstrapping and employing CV strategies, this might not be enough to overcome this limitation. Indeed, our complementary analysis comparing the models' training and testing performance (results in the **Supplementary material**) is indicative that some of the tested classification models (mainly trained with neuroimaging or with SNPs) might suffer from some degree of overfitting. Ultimately, we cannot determine whether our negative findings were due to lack of power to obtain a good performance or due to a true lack of association between the predictors and the transition to psychosis from an ARMS (and hence inflated findings

4 http://pronia.eu

from previous studies). This is one of the reasons why replication studies in independent datasets are essential in ML literature. As a final note, a power analysis for this study design would have been the most informative way to define the sample size needed to achieve an accuracy in predicting transition to psychosis from an ARMS better than chance level. However, this is not a trivial task in ML analysis and there is no established method to perform this analysis as there is for univariate analysis [for examples of studies exploring innovative ways of computing sample size for classification problems see Refs. (58, 59)] and, therefore, it was not performed.

Second, in order to dilute possible confounding effects in the developed classification models we have restricted the samples used to train the models to: (a) be class-balanced, i.e., with the same number of ARMS-T and ARMS-NT subjects; (b) be matched for age, sex, scanning acquisition protocols for neuroimaging data; (c) include subjects with European ancestry only for genetic data; and (d) limit the proportion of missing data for the environment data. Although this has artificially homogenized the study sample thus avoiding the presence of statistical confounders, it has deemed the sample to be less representative of the ARMS population. Third, overall, the findings of this study are only valid to young help-seeking individuals, i.e., that are clinically screened for ARMS criteria, and whose ARMS diagnosis was based on having a schizotypal personality disorder or on the subject's familial-high risk coupled with functioning decline and on the CAARMS (54), which mainly evaluates positive symptoms.

5. Conclusion and future directions

In this study, we explored the value of using exclusively quantitative and multimodal data (i.e., as predictors) to predict transition to psychosis from an ARMS. Overall, we found that, contrary to what has been previously reported, sMRI could not predict transition to psychosis from an ARMS. We have employed several ML strategies aiming to replicate the highly promising previous positive sMRI findings (74–84%) (10–15). This is even though our sample was larger than four of the above 6 studies (10, 11, 13, 14), respectively (Conversely, our sample was smaller than two of the above studies [Das et al. (15); Koutsouleris et al. (12), respectively]. This points to the need for a cautious interpretation of small sample size studies. Also, we could not replicate the one previous evidence of the value of the schizophrenia PRS in predicting transition to psychosis. Moreover, and to the best of our knowledge, we explored for the first time the value of environment in the prediction of psychosis already from a prodromal stage. Lastly, the genetic and the environmental data used could not predict transition to psychosis from an ARMS. In summary, the present study should serve as a call for caution and skepticism regarding the currently achievable prognostic and diagnostic biomarker development goals, with the existing modeling tools and data measurement tools. Additionally, our study's methodological approaches tailored to each data modality, may serve as suggestive proofs-of-concept for the exploration of future multimodal datasets, either for novel discovery or replication of previous promising findings, across psychiatric disorders, not exclusive to ARMS. We further suggest larger samples (in the several hundreds) should be employed for both model training and testing, given the inherent high data dimensionality (specially of neuroimaging and genetics) and the still little established relevance of individual features. Although heterogeneity in phenotypic measurements is increased in larger samples, they bring not only statistical power but ecological generalizability, and thus carry a higher potential to be clinically useful. This is best achieved with consortia multi-center studies which are increasingly common albeit not without challenges (60). Alternatively, methods for synthetic generation of data such as the Generative Adversarial Networks (GAN)-based are also a promising avenue for sample size augmentation, now starting to be applied in the clinical research field (61). Last, but not least, we recommend the use of objective and quantitative criteria-based tools for the assessment of a ML biomarker's clinical applicability, once high effect size and accuracy estimates are achieved, such as one we have previously proposed (62).

Data availability statement

The datasets presented in this article are not readily available because ethics approval did not include public data sharing. Requests to access the datasets should be directed to the corresponding author.

Ethics statement

The studies involving human participants were reviewed and approved by NHS South East London Research Ethics Committee. The patients/participants provided their written informed consent to participate in this study.

Author contributions

VT ran most data preprocessing and statistical analyses and drafted the manuscript. EV coordinated genotyping and advised the genetic and environmental data analysis. AM and HF provided advise on imaging data processing and machine learning analysis. JS and IV collected imaging data. GB provided advise on imaging data processing. DP collected genetic and environmental data, co-designed the study, ran preliminary data preprocessing and machine learning analyses, and supervised the study. All authors revised the manuscript and agreed with its final version.

Funding

This study, VT received support from Fundação para a Ciência e a Tecnologia (FCT) Ph.D. fellowship PD/BD/114460/2016 and DSAIPA/DS/0065/2018 grants; DP received primary support from National Institute for Health Research (NIHR) PDF-2010-03-047 grant, and additionally from FCT FCT-IF/00787/2014, LISBOA-01–0145-FEDER-030907, and DSAIPA/DS/0065/2018 grants, and a European Commission (EC) Marie Curie Career Integration Grant (FP7-PEOPLE-2013-CIG 631952). EV was part-funded by the NIHR Maudsley Biomedical Research Centre at South London and Maudsley NHS Foundation Trust and King's College London. IV was supported by EC's Horizon 2020 Marie Skłodowska-Curie grant (Ref. 754550, project BITRECS) and "La Caixa" Foundation (LCF/PR/GN18/50310006).

Acknowledgments

We thank Prof. Philip McGuire for his invaluable guidance during data design and collection, the OASIS team, and all volunteers with an ARMS who made this study possible.

Conflict of interest

The authors declare that the research was conducted in the absence of any commercial or financial relationships that could be construed as a potential conflict of interest.

The reviewer SV declared a shared affiliation with the authors EV, IV, GB, and DP to the handling editor at the time of review.

Publisher's note

All claims expressed in this article are solely those of the authors and do not necessarily represent those of their affiliated organizations, or those of the publisher, the editors and the reviewers. Any product that may be evaluated in this article, or claim that may be made by its manufacturer, is not guaranteed or endorsed by the publisher.

Author disclaimer

The views expressed were those of the authors and not necessarily those of any of the above sponsors.

Supplementary material

The Supplementary Material for this article can be found online at: https://www.frontiersin.org/articles/10.3389/fpsyt.2022.1086038/full#supplementary-material

References

1. Schrimpf L, Aggarwal A, Lauriello J. Psychosis. *Contin Lifelong Learn Neurol.* (2018) 24:845–60. doi: 10.1212/CON.0000000000000602

2. Fusar-Poli P, Borgwardt S, Bechdolf A, Addington J, Riecher-Rössler A, Schultze-Lutter F, et al. The psychosis high-risk state. *JAMA Psychiatry.* (2013) 70:107. doi: 10.1001/jamapsychiatry.2013.269

3. Kahn R, Sommer I, Murray R, Meyer-Lindenberg A, Weinberger D, Cannon T, et al. Schizophrenia. *Nat Rev Dis Prim.* (2015) 1:15067. doi: 10.1038/nrdp.2015.67

4. Schultze-Lutter F, Ruhrmann S, Fusar-Poli P, Bechdolf AG, Schimmelmann B, Klosterkotter J. Basic symptoms and the prediction of first-episode psychosis. *Curr Pharm Des.* (2012) 18:351–7. doi: 10.2174/138161212799316064

5. Correll C, Schooler N. Negative symptoms in schizophrenia: A review and clinical guide for recognition, assessment, and treatment. *Neuropsychiatr Dis Treat.* (2020) 16:519–34. doi: 10.2147/NDT.S225643

6. Sheffield J, Karcher N, Barch D. Cognitive deficits in psychotic disorders: A lifespan perspective. *Neuropsychol Rev.* (2018) 28:509–33. doi: 10.1007/s11065-018-9388-2

7. Yung A, McGorry P, McFarlane C, Jackson H, Patton G, Rakkar A. Monitoring and care of young people at incipient risk of psychosis. *Schizophr Bull.* (1996) 22:283–303. doi: 10.1093/schbul/22.2.283

8. Salazar De Pablo G, Radua J, Pereira J, Bonoldi I, Arienti V, Besana F, et al. Probability of transition to psychosis in individuals at clinical high risk: An updated meta-analysis. *JAMA Psychiatry.* (2021) 78:970–8. doi: 10.1001/jamapsychiatry.2021.0830

9. Fusar-Poli P, Bechdolf A, Taylor M, Bonoldi I, Carpenter W, Yung A, et al. At risk for schizophrenic or affective psychoses? A meta-analysis of DSM/ICD diagnostic outcomes in individuals at high clinical risk. *Schizophr Bull.* (2013) 39:923–32. doi: 10.1093/schbul/sbs060

10. Koutsouleris N, Meisenzahl E, Davatzikos C, Bottlender R, Frodl T, Scheuerecker J, et al. Use of neuroanatomical pattern classification to identify subjects in at-risk mental states of psychosis and predict disease transition. *Arch Gen Psychiatry.* (2009) 66:700–12. doi: 10.1001/archgenpsychiatry.2009.62

11. Koutsouleris N, Borgwardt S, Meisenzahl E, Bottlender R, Möller H, Riecher-Rössler A. Disease prediction in the at-risk mental state for psychosis using neuroanatomical biomarkers: Results from the fepsy study. *Schizophr Bull.* (2012) 38:1234–46. doi: 10.1093/schbul/sbr145

12. Koutsouleris N, Riecher-Rössler A, Meisenzahl E, Smieskova R, Studerus E, Kambeitz-Ilankovic L, et al. Detecting the psychosis prodrome across high-risk populations using neuroanatomical biomarkers. *Schizophr Bull.* (2015) 41:471–82. doi: 10.1093/schbul/sbu078

13. Zarogianni E, Storkey A, Johnstone E, Owens D, Lawrie S. Improved individualized prediction of schizophrenia in subjects at familial high risk, based on neuroanatomical data, schizotypal and neurocognitive features. *Schizophr Res.* (2017) 181:6–12. doi: 10.1016/j.schres.2016.08.027

14. Zarogianni E, Storkey A, Borgwardt S, Smieskova R, Studerus E, Riecher-Rössler A, et al. Individualized prediction of psychosis in subjects with an at-risk mental state. *Schizophr Res.* (2019) 214:18–23. doi: 10.1016/j.schres.2017.08.061

15. Das T, Borgwardt S, Hauke D, Harrisberger F, Lang U, Riecher-Rössler A, et al. Disorganized gyrification network properties during the transition to psychosis. *JAMA Psychiatry.* (2018) 75:613–22. doi: 10.1001/jamapsychiatry.2018.0391

16. Perkins D, Loohuis L, Barbee J, Ford J, Jeffries C, Addington J, et al. Polygenic risk score contribution to psychosis prediction in a target population of persons at clinical high risk. *Am J Psychiatry.* (2020) 177:155–63. doi: 10.1176/appi.ajp.2019.18060721

17. Struyf J, Dobrin S, Page D. Combining gene expression, demographic and clinical data in modeling disease: A case study of bipolar disorder and schizophrenia. *BMC Genomics.* (2008) 9:531. doi: 10.1186/1471-2164-9-531

18. Yang H, Liu J, Sui J, Pearlson G, Calhoun V. A hybrid machine learning method for fusing fMRI and genetic data: Combining both improves classification of schizophrenia. *Front Hum Neurosci.* (2010) 4:192. doi: 10.3389/fnhum.2010.00192

19. Aguiar-Pulido V, Seoane J, Rabuñal J, Dorado J, Pazos A, Munteanu C. Machine learning techniques for single nucleotide polymorphism - disease classification models in schizophrenia. *Molecules.* (2010) 15:4875–89. doi: 10.3390/molecules15074875

20. Chen J, Wu J, Mize T, Shui D, Chen X. Prediction of schizophrenia diagnosis by integration of genetically correlated conditions and traits. *J Neuroimmune Pharmacol.* (2018) 13:532–40. doi: 10.1007/s11481-018-9811-8

21. Vivian-Griffiths T, Baker E, Schmidt K, Bracher-Smith M, Walters J, Artemiou A, et al. Predictive modeling of schizophrenia from genomic data: Comparison of polygenic risk score with kernel support vector machines approach. *Am J Med Genet Part B Neuropsychiatr Genet.* (2019) 180:80–5. doi: 10.1002/ajmg.b.32705

22. Antonucci L, Pergola G, Pigoni A, Dwyer D, Kambeitz-Ilankovic L, Penzel N, et al. A pattern of cognitive deficits stratified for genetic and environmental risk reliably classifies patients with schizophrenia from healthy control subjects. *Biol Psychiatry.* (2020) 87:697–707. doi: 10.1016/j.biopsych.2019.11.007

23. Pettersson-Yeo W, Benetti S, Marquand A, Dell'Acqua F, Williams S, Allen P, et al. Using genetic, cognitive and multi-modal neuroimaging data to identify ultra-high-risk and first-episode psychosis at the individual level. *Psychol Med.* (2013) 43:2547–62. doi: 10.1017/S003329171300024X

24. Fromer M, Roussos P, Sieberts S, Johnson J, Kavanagh D, Perumal T, et al. Gene expression elucidates functional impact of polygenic risk for schizophrenia. *Nat Neurosci.* (2016) 19:1442–53.

25. Koutsouleris N, Dwyer D, Degenhardt F, Maj C, Urquijo-Castro M, Sanfelici R, et al. Multimodal machine learning workflows for prediction of psychosis in patients with clinical high-risk syndromes and recent-onset depression. *JAMA Psychiatry.* (2021) 78:195–209.

26. Vassos E, Di Forti M, Coleman J, Iyegbe C, Prata D, Euesden J, et al. An examination of polygenic score risk prediction in individuals with first-episode psychosis. *Biol Psychiatry.* (2017) 81:470–7. doi: 10.1016/j.biopsych.2016.06.028

27. Pardiñas A, Holmans P, Pocklington A, Escott-Price V, Ripke S, Carrera N, et al. Common schizophrenia alleles are enriched in mutation-intolerant genes and in regions under strong background selection. *Nat Genet.* (2018) 50:381–9.

28. Vassos E, Sham P, Kempton M, Trotta A, Stilo S, Gayer-Anderson C, et al. The Maudsley environmental risk score for psychosis. *Psychol Med.* (2020) 50:2213–20. doi: 10.1017/S0033291719002319

29. Broome M, Woolley J, Johns L, Valmaggia L, Tabraham P, Gafoor R, et al. Outreach and support in south London (OASIS): implementation of a clinical service for prodromal psychosis and the at risk mental state. *Eur Psychiatry.* (2005) 20:372–8. doi: 10.1016/j.eurpsy.2005.03.001

30. Phillips L, Yung A, McGorry P. Identification of young people at risk of psychosis: validation of Personal Assessment and Crisis Evaluation Clinic intake criteria. *Aust N Z J Psychiatry.* (2000) 34Suppl:S164–9. doi: 10.1046/j.1440-1614.2000.00798.x

31. Nelson H. The National Adult Reading Test (NART): Test Manual. *Wind UK NFER-Nelson.* (1982) 124:0–25.

32. American Psychiatric Association. *Diagnostic and Statistical Manual of Mental Disorders, Text Revision (DSM-IV-TR).* Fourth ed. (Vol. 1). Arlington, VA: American Psychiatric Association (2000).

33. Murray R, Mondelli V, Stilo S, Trotta A, Sideli L, Ajnakina O, et al. The influence of risk factors on the onset and outcome of psychosis: What we learned from the GAP study. *Schizophr Res.* (2020) 225:63–8. doi: 10.1016/j.schres.2020.01.011

34. Tavares V, Prata D, Ferreira H. Comparing SPM12 and CAT12 segmentation pipelines: a brain tissue volume-based age and Alzheimer's disease study. *J Neurosci Methods.* (2020) 334:108565. doi: 10.1016/j.jneumeth.2019.108565

35. Hammers A, Allom R, Koepp M, Free S, Myers R, Lemieux L, et al. Three-dimensional maximum probability atlas of the human brain, with particular reference to the temporal lobe. *Hum Brain Mapp.* (2003) 19:224–47. doi: 10.1002/hbm.10123

36. Desikan R, Ségonne F, Fischl B, Quinn B, Dickerson B, Blacker D, et al. An automated labeling system for subdividing the human cerebral cortex on MRI scans into gyral based regions of interest. *Neuroimage.* (2006) 31:968–80. doi: 10.1016/j.neuroimage.2006.01.021

37. Dahnke, R, Ziegler G, Grosskreutz J, Gaser C. *Retrospective Quality Assurance of MR Images*. Seattle, WA: Human Brain Mapping (2013). Availale online at: http://dbm.neuro.uni-jena.de/HBM2013/Dahnke01.pdf

38. Bramon E, Pirinen M, Strange A, Lin K, Freeman C, Bellenguez C, et al. A genome-wide association analysis of a broad psychosis phenotype identifies three loci for further investigation. *Biol Psychiatry.* (2014) 75:386–97. doi: 10.1016/j.biopsych.2013.03.033

39. Kambeitz-Ilankovic L, Meisenzahl E, Cabral C, von Saldern S, Kambeitz J, Falkai P, et al. Prediction of outcome in the psychosis prodrome using neuroanatomical pattern classification. *Schizophr Res.* (2016) 173:159–65. doi: 10.1016/j.schres.2015.03.005

40. Koutsouleris N, Kambeitz-Ilankovic L, Ruhrmann S, Rosen M, Ruef A, Dwyer D, et al. Prediction models of functional outcomes for individuals in the clinical high-risk state for psychosis or with recent-onset depression: A multimodal, multisite machine learning analysis. *JAMA Psychiatry.* (2018) 75:1156–72. doi: 10.1001/jamapsychiatry.2018.2165

41. R Core Team. *R: A Language and Environment for Statistical Computing*. Vienna: R Foundation for Statistical Computing (2014).

42. Ripke S, Neale B, Corvin A, Walters J, Farh K, Holmans P, et al. Biological insights from 108 schizophrenia-associated genetic loci. *Nature.* (2014) 511:421–7. doi: 10.1038/nature13595

43. Tavares V, Monteiro J, Vassos E, Coleman J, Prata D. Evaluation of genotype-based gene expression model performance: A cross-framework and cross-dataset study. *Genes (Basel).* (2021) 12:1531. doi: 10.3390/genes12101531

44. Hubert M, Rousseeuw P, Verdonck T. Robust PCA for skewed data and its outlier map. *Comput Stat Data Anal.* (2009) 53:2264–74. doi: 10.1016/j.csda.2008.05.027

45. Hubert M, Rousseeuw P, Vanden Branden K. ROBPCA: A new approach to robust principal component analysis. *Technometrics.* (2005) 47:64–79. doi: 10.1198/004017004000000563

46. Cortes C, Vapnik V. Support-vector networks. *Mach Learn.* (1995) 20:273–97. doi: 10.1007/BF00994018

47. Burges C. A tutorial on support vector machines for pattern recognition. *Data Min Knowl Discov.* (1998) 2:121–67.

48. Zou H, Hastie T. Regularization and variable selection via the elastic net. *J R Stat Soc Ser B Stat Methodol.* (2005) 67:301–20. doi: 10.1111/j.1467-9868.2005.00503.x

49. Fjell A, Walhovd K. Structural brain changes in aging: courses, causes and cognitive consequences. *Rev Neurosci.* (2010) 21:187–221. doi: 10.1515/REVNEURO.2010.21.3.187

50. Ruigrok A, Salimi-Khorshidi G, Lai M, Baron-Cohen S, Lombardo MV, Tait R, et al. A meta-analysis of sex differences in human brain structure. *Neurosci Biobehav Rev.* (2014) 39:34–50. doi: 10.1016/j.neubiorev.2013.12.004

51. Castillejos M, Martín-Pérez C, Moreno-Küstner B. Incidence of psychotic disorders and its association with methodological issues. A systematic review and meta-analyses. *Schizophr Res.* (2019) 204:458–9. doi: 10.1016/j.schres.2018.07.031

52. Falahati F, Ferreira D, Soininen H, Mecocci P, Vellas B, Tsolaki M, et al. The effect of age correction on multivariate classification in Alzheimer's Disease, with a focus on the characteristics of incorrectly and correctly classified subjects. *Brain Topogr.* (2016) 29:296–307. doi: 10.1007/s10548-015-0455-1

53. Wachinger C, Rieckmann A, Pölsterl S. Detect and correct bias in multi-site neuroimaging datasets. *Med Image Anal.* (2021) 67:101879. doi: 10.1016/j.media.2020.101879

54. Yung A, Yung A, Pan Yuen H, Mcgorry P, Phillips L, Kelly D, et al. Mapping the onset of psychosis: The comprehensive assessment of at-risk mental states. *Aust New Zeal J Psychiatry.* (2005) 39:964–71. doi: 10.1080/j.1440-1614.2005.01714.x

55. Addington J, Cadenhead K, Cornblatt B, Mathalon D, McGlashan T, Perkins D, et al. North American Prodrome Longitudinal Study (NAPLS 2): Overview and recruitment. *Schizophr Res.* (2012) 142:77–82. doi: 10.1016/j.schres.2012.09.012

56. Guloksuz S, Rutten B, Pries L, Ten Have M, De Graaf R, Van Dorsselaer S, et al. The complexities of evaluating the exposome in psychiatry: A data-driven illustration of challenges and some propositions for amendments. *Schizophr Bull.* (2018) 44:1175–9. doi: 10.1093/schbul/sby118

57. Padmanabhan J, Shah J, Tandon N, Keshavan M. The "polyenviromic risk score": Aggregating environmental risk factors predicts conversion to psychosis in familial high-risk subjects. *Schizophr Res.* (2017) 181:17–22. doi: 10.1016/j.schres.2016.10.014

58. Figueroa R, Zeng-Treitler Q, Kandula S, Ngo L. Predicting sample size required for classification performance. *BMC Med Inform Decis Mak.* (2012) 12:8. doi: 10.1186/1472-6947-12-8

59. Dobbin K, Simon R. Sample size planning for developing classifiers using high-dimensional DNA microarray data. *Biostatistics.* (2007) 8:101–17. doi: 10.1093/biostatistics/kxj036

60. Tognin S, Van Hell H, Merritt K, Winter-Van Rossum I, Bossong M, Kempton M, et al. Towards precision medicine in psychosis: Benefits and challenges of multimodal multicenter studies - PSYSCAN: Translating neuroimaging findings from research into clinical practice. *Schizophr Bull.* (2020) 46:432–41.

61. Laino M, Cancian P, Politi L, Della Porta M, Saba L, Savevski V. Generative adversarial networks in brain imaging: A narrative review. *J Imaging.* (2022) 8:83. doi: 10.3390/jimaging8040083

62. Prata D, Mechelli A, Kapur S. Clinically meaningful biomarkers for psychosis: A systematic and quantitative review. *Neurosci Biobehav Rev.* (2014) 45:134–41. doi: 10.1016/j.neubiorev.2014.05.010

Frontiers in Psychiatry

Explores and communicates innovation in the field of psychiatry to improve patient outcomes

The third most-cited journal in its field, using translational approaches to improve therapeutic options for mental illness, communicate progress to clinicians and researchers, and consequently to improve patient treatment outcomes.

Discover the latest Research Topics

See more →

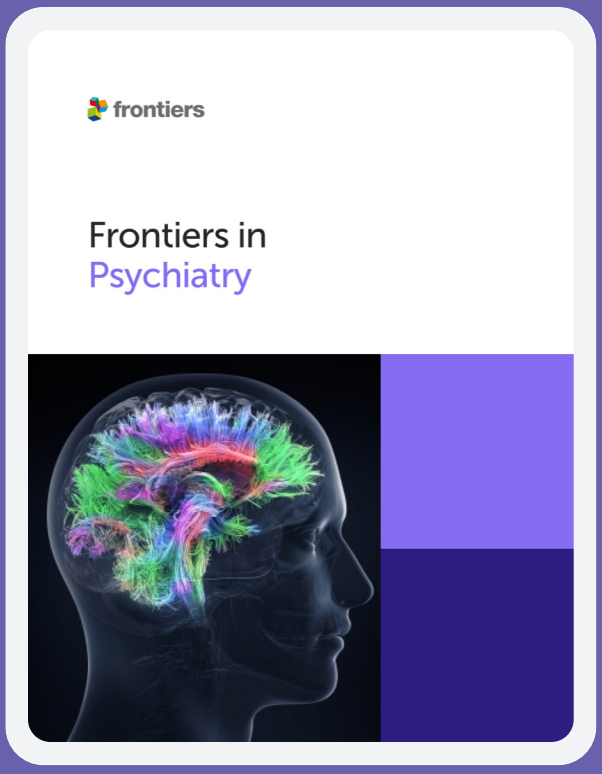

Frontiers

Avenue du Tribunal-Fédéral 34
1005 Lausanne, Switzerland
frontiersin.org

Contact us

+41 (0)21 510 17 00
frontiersin.org/about/contact